

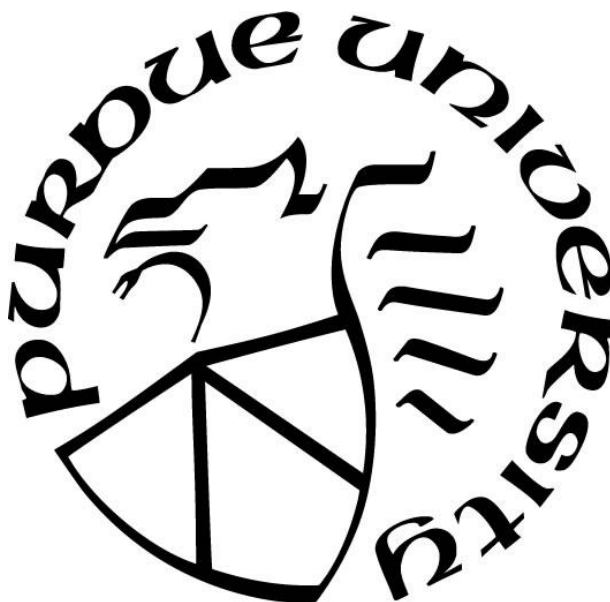
**SYNTHESIS OF ACYL-THIOESTER ANALOGS AND THEIR
APPLICATION IN KINETIC/STRUCTURE-FUNCTION STUDIES WITH
C-C BOND REMODELING ENZYMES**

by
Trevor Boram

A Dissertation

*Submitted to the Faculty of Purdue University
In Partial Fulfillment of the Requirements for the degree of*

Doctor of Philosophy



Department of Biochemistry
West Lafayette, Indiana
May 2022

THE PURDUE UNIVERSITY GRADUATE SCHOOL
STATEMENT OF COMMITTEE APPROVAL

Dr. Jeremy R. Lohman, Chair

School of Biochemistry

Dr. Frederick S. Gimble

School of Biochemistry

Dr. Mark C. Hall

School of Biochemistry

Dr. Carol B. Post

School of Medicinal Chemistry and Molecular Pharmacology

Approved by:

Dr. Andrew D. Mesecar

I dedicate this work to all the friends and family who have supported me on this academic journey.

ACKNOWLEDGMENTS

The work I conducted in the following pages was made possible through funding from the Purdue Department of Biochemistry from Bird Stair fellowships, the Beach Travel Award, the Bilsland Dissertation Award, the Andrews Assistantship, and the Outstanding Teaching Assistant Award. I am very appreciative of all of the support I have received from the department. Additionally, this research was funded through the National Institute of General Medical Sciences (NIGMS) via Grant no. 1R01GM140290-01.

Additionally, I want to acknowledge my thesis committee members for having helpful conversations with me about my professional plans, and providing encouragement for me to overcome hurdles I faced. I also want to thank all of the friends I made during my time at Purdue, as well as the 18 rotation students/undergraduates I mentored. I think it is also critical to take a moment and thank my adviser, Jeremy Lohman, who mentored me, was patient with my mistakes, taught me an astonishing amount in under 5 years, and reassured me that I was doing well when I was stressed or didn't believe in myself. Speaking of advisers, I also want to thank my undergraduate research advisers, Hitesh Kathuria and Yu Kay Law, who gave me many opportunities to develop as a scientist early in my career.

Most importantly, I want to thank my family and friends. My brothers, Trent, Zack, Jordan, David, and DJ. My dad, Kelly, my step-mom, Patty, and my mom, Darla, who could only be here in spirit. Speaking of family, I am thankful to my aunts, uncles, cousins, and grandparents: Chris, Susan, Sherry, Mark, Freddy, Sammy, Alex, Jared, Bethany, Dakota, Lindsey, Mark, Hunter, Cooper, PJ, Chris, Sean, Burt, Sandy, Cori, Jeremy, Robin, Scott, Micah, Ethan, Gabe, Seth, Joshua, Karen, Jerry, Pam, Barry, Sharon, Ron, and Jan. I want to also thank my friends, Tony, Niemann, Jordan, Ashley, and Adam for always making long drives so we could hang out together, my longtime friends, Griffin, Mac, Julie, and Wilson for always believing in me, even when I was a hyper high school student, my amazing friends Michael, Joseph, Allen, Will, Steven, Dalton, Cody, Dustin, and Thomas for spending so many late nights playing games together on Discord when we lived 1,000 miles apart. Thank you to my long time mentors, Sifu Berry and Nate for their guidance. Lastly, I want to thank all of my other friends and family who have been there for me over the years – I would need so much more space on this page to name you all. Thank you for supporting me and making this achievement possible.

TABLE OF CONTENTS

LIST OF TABLES	8
LIST OF FIGURES	9
LIST OF SCHEMES	13
LIST OF ABBREVIATIONS	15
ABSTRACT	17
CHAPTER 1. DEVELOPMENT OF CoA ANALOGS AND THEIR ROLE IN PROBING ENZYME CATALYSIS	18
1.1 Historical context and relevance of CoA and CoA using enzymes	18
1.2 Fatty acid biosynthesis is essential in all kingdoms of life and revolves around acyl- thioester catalysis	19
1.2.1 Carboxylases provide the source of malonyl-thioesters used in fatty acid elongation through a C-C bond forming reaction	21
1.2.2 The wealth of fatty acid biosynthetic machinery provides abundant targets for medicine, herbicide, and biofuel production	23
1.3 Polyketide biosynthesis catalysis, complexity, and importance mirrors fatty acid biosynthesis, as polyketides have revolutionized the pharmaceutical industry	27
1.3.1 While polyketide synthases perform similar C-C bond extension reaction to FAS, diversity in their assembly line allows for a wide variety of products	27
1.3.2 Polyketide biosynthesis provides a vast variety of natural product pharmaceuticals with hopes to engineer many more	31
1.3.3 Shortcomings of PKS engineering are due to an underestimation of the complex effects of protein-protein interactions and conformational changes on catalysis	32
1.4 Mechanistic studies on fatty acid and polyketide biosynthesis components can provide critical missing information tackling drug discovery and engineering hurdles	33
1.5 Synthesis of CoA-thioester analogs has a long, slowly-evolving history, as probes for enzyme catalysis, conformational changes, and inhibition	36
1.5.1 Acyl-CoA analogs stable to hydrolysis emerged in the 1970s with application in enzyme mechanism experiments but featured difficult synthesis procedures	39

1.5.2 Structure-function studies of acyl-thioester analogs seek to elucidate key conformational changes.....	44
1.6 Our lab has applied acyl-CoA analogs as mechanistic probes to KS and carboxylase catalysis via kinetic and structure-function studies	48
1.7 References.....	49
CHAPTER 2. DESIGN, SYNTHESIS, AND IMPROVEMENTS OF ACYL-THIOESTER ANALOGS FOR USE IN PROBING C-C BOND CATALYSIS	54
2.1 Abstract.....	54
2.2 The strategy of acyl-thioester analog design involves mimicking the enzyme catalyzed transformations from substrate to product via atom substitutions that stabilize the molecule to enzyme chemistry while having minimal changes	54
2.3 Synthesis of malonyl-CoA analogs for use as mechanistic probes of C-C bond forming enzymes.....	56
2.4 Synthesis of stable acyl-CoA, enolate, and product analogs provides a means to probe enzyme catalysis for KS, carboxylases, and related acyl-CoA using enzymes	66
2.5 Synthesis of CoA isosteres as tools for monitoring analog stability in the presence of thioester cleaving enzymes	76
2.6 Materials and Methods.....	77
2.7 Synthetic Procedures and Results	78
2.8 References.....	99
CHAPTER 3. APPLICATION OF ACYL-COA ANALOGS TO MECHANISTIC AND DRUG DEVELOPMENT STUDIES WITH RESPECT TO ACYL-COA CARBOXYLASES	101
3.1 Abstract.....	101
3.2 While the BC reaction of YCCs is largely understood and well-studied, there are still missing details obscuring understanding of the CT catalytic mechanism	101
3.3 Optimization of YCC production is necessary to overcome difficulty in sample production for crystallography and protein crystal diffraction quality	110
3.4 Development of UV-vis assays for YCC enzymology for studying inhibitor induced futile-cycle activation	118
3.5 Conclusions.....	120
3.6 Materials and Methods.....	121

3.6.1	Cloning, expression, and purification of carboxylases	121
3.6.2	Crystallization and diffraction of EcACC CT and ScPCC CT	126
3.6.3	HPLC assay, UV-vis assay, and futile cycle development for EcACC.....	126
3.7	References	127
CHAPTER 4. APPLICATION OF ACYL-COA ANALOGS TO MECHANISTIC STUDIES WITH KETOSYNTHASES		129
4.1	Abstract	129
4.2	Synthesis and Application of Acyl-CoA analogs to FabH may serve as effective mechanistic probes	129
4.3	Synthetic Procedures and Characterization Data	143
4.4	Cloning and mutagenesis of FabH and AckA from <i>Escherichia coli</i>	152
4.5	Enzyme expression and purification	153
4.6	FabH enzymatic assay procedures	154
4.7	References	156
CHAPTER 5. CONCLUDING REMARKS		159
5.1	Analogues of acyl-thioesters have broader implications in the study of enzymes that are not C-C bond forming.....	159
5.2	Concluding remarks	161
5.3	References	162

LIST OF TABLES

Table 1.1 Non-exhaustive list of CoA analogs reported in the 1960's	38
Table 1.2 Representative methylene substituted acyl-CoA analogs reported in the 1980's.....	41
Table 1.3 Initially reported acyl-dithio-CoA analogs of the 1980's.	43
Table 1.4 Report of reaction intermediate analog, hydroxyethyl-CoA.	44
Table 2.1 Malonyl-CoA, methylmalonyl-CoA, and oxa, aza, and carba(dethia) thioester isosteres	57
Table 4.1 Rates of FabH or C112Q mutant reactivity with substrates and analogs.	138
Table 4.2 Inhibition constants of substrate and product analogs	141

LIST OF FIGURES

Figure 1.1 Organization and nomenclature of Coenzyme A	19
Figure 1.2 Overview of the iterative nature of fatty acid biosynthesis and divergent product fates. The ketosynthase (KS), ketoreductase (KR), dehydratase (DH), and enoyl reductase (ER) work in repeated sequence to produce the elongated fatty acid-thioester.	21
Figure 1.3 General reaction of ATP dependent acyl-CoA carboxylases. The YCC chemistry proceeds in two half reactions, the first of which is the biotin carboxylase (BC) catalyzed carboxylation of biotin. Afterward, the YCC undergoes a large conformational change to transfer the carboxyl group from biotin to an acyl-CoA via the carboxyltransferase (CT) activity, leading to a malonyl-CoA product.	23
Figure 1.4 Contrast of the organization of single polypeptide eukaryotic YCCs vs. multi-subunit prokaryotic YCCs. Eukaryotic YCCs are often homodimeric, with a molecular weight over 0.5 MDa. Prokaryotic YCC components can be more easily studied in high resolution structural studies due to their lower molecular weight.	24
Figure 1.5 Moiramide B (<i>black</i>) inhibits the CT (<i>red/teal</i>) of <i>E. coli</i> ACC at the interface of the α and β subunits via interactions of the succinimide warhead situated in the active site.	25
Figure 1.6 Cerulenin (<i>black</i>) irreversibly inhibits the catalytic cysteine residue of FabB (<i>teal</i>). 26	
Figure 1.7 Biosynthesis of the immunosuppressant drug, rapamycin, is performed by the sequential action of polyketide synthase modules and tailoring enzymes. Atoms donated by malonyl-CoA are shown in <i>blue</i> , while atoms donated by methylmalonyl-CoA are in <i>red</i> . Engineering of different PKS components could allow for substrate promiscuity in any of the extension reactions.	29
Figure 1.8 Variation of extender units used by polyketide synthases is route being researched to diversify polyketide products. Most PKS demonstrate little diversity in extender unit incorporation, using only malonyl- or methylmalonyl-CoA. However, PKS pathways exist that accept less common (or even synthetic) extender units.	31
Figure 1.9 Malonyl-thioesters and acyl-thioesters are both prone to enzyme catalyzed hydrolysis. Malonyl-thioesters may also be decarboxylated by enzymatic activity.	35
Figure 1.10 Structure of <i>E. coli</i> FabD (PDB: 2G2Z) solved at 2.8 Å with a malonyl-enzyme intermediate modeled. This structure models a malonyl-enzyme intermediate and CoA in the active site, though the density is sparse.	35
Figure 1.11 Chemical synthesis of CoA using 2',3'-phospho-AMP-morpholine synthon.	37
Figure 1.12 β -aletheine is composed of β -alanine and cysteamine.	39
Figure 1.13 Crystal structure of <i>E. coli</i> methylmalonyl-CoA decarboxylase with (2 <i>S</i>)-carboxypropyl-CoA (PDB: 1EF9) solved at 2.7 Å.	45

Figure 1.14 Crystal structure of <i>Streptomyces peucetius</i> DpsC with oxetane-PPANT analog bound (PDB: 5WGC) solved at 2.15 Å .	46
Figure 1.15 Crystal structure of <i>E. coli</i> MMCD with 2-sulfonate-propionyl-CoA bound (PDB: 6N95) solved at 1.8 Å.	47
Figure 1.16 Flattened schematic displaying: A) 2-sulfonate-propionyl-CoA bound to MMCD, B) (2 <i>R/S</i>)-methylmalonyl-CoA modeled with MMCD, C) (2 <i>S</i>)-carboxypropyl-CoA bound to MMCD.	48
Figure 2.1 Comparison of inhibition constants of different enolate isosteres with citrate synthase.	55
Figure 2.2 Proposed mechanism of Cys-His-Asn KS catalysis, with presentation of analogs to mimic catalytic states.	55
Figure 2.3 Comparison of 2-sulfinate-acetyl-CoA analog to malonyl-CoA. The single sulfur atom substitution closely mimics malonyl-CoA.	61
Figure 2.4 Thin-layer chromatography of different reaction states in producing phenyl- <i>O</i> -nitroacetate.	64
Figure 2.5 Tautomerization of an acetyl-CoA enolate intermediate.	74
Figure 3.1 Proposed catalytic strategies of YCC CTs in the product of malonyl-CoA products	103
Figure 3.2 Overall reaction of <i>P. shermanii</i> transcarboxylase.	104
Figure 3.3 Crystal structure of <i>P. shermanii</i> transcarboxylase 12 <i>S</i> subunit (1-507) with (2 <i>R/S</i>)-methylmalonyl-CoA bound (PDB: 1ON3), solved at 1.9 Å ¹⁰ .	106
Figure 3.4 Flattened schematic displaying the inferred orientation of propionyl-CoA and carboxy-biotin bound in the active site of PCCβ from <i>S. coelicolor</i> ¹¹	107
Figure 3.5 Crystal structure of PCCβ from <i>S. coelicolor</i> with propionyl-CoA and biotin modeled (PDB: 1XNY) solved at 2.2 Å. Top- Display of proposed oxyanion hole with the carbonyl group of propionyl-CoA oriented for catalysis. Bottom- Display of modeled biotin and propionyl-CoA ligands in PCCβ crystal structure ¹¹ .	108
Figure 3.6 Cryo-EM structure of biotinylated-ACC1 from <i>S. cerevisiae</i> with CoA bound (PDB: 5CSL), solved at 3.2 Å ¹² .	109
Figure 3.7 The malonyl-CoA:CT:biotin interaction could be mimicked by a stable malonyl-CoA analog, capturing the ternary complex.	110
Figure 3.8 Various prokaryotic and eukaryotic YCCs were studied in mechanistic investigations in this thesis work.	111
Figure 3.9 Cryo-EM negative stain of ScvACC1 in the following conditions: 1 mg/ml ACC1, 10 mM HEPES pH = 7.5, 150 mM NaCl, 20 mM sodium citrate, 0.9% glycerol	112
Figure 3.10 Protein crystals grown in various morphologies and sizes of <i>E. coli</i> ACC CT that led to low quality diffraction.	113

Figure 3.11 Representative X-ray diffraction image of EcACC CT crystals. Diffraction data shows severe twinning/multiple crystals.	114
Figure 3.12 SDS-PAGE gel demonstrating the successful purification of tagless-PCC β via non-affinity chromatography methods.	116
Figure 3.13 Protein crystals grown in various morphologies of <i>S. coelicolor</i> PCC β that led to low quality diffraction.	116
Figure 3.14 Representative X-ray diffraction image of PCC β (tagless).	117
Figure 3.15 Strategy of monitoring ACC ATP turnover using a continuous, coupled UV-vis assay to look for futile cycle producing small molecules.	118
Figure 3.16 HPLC traces demonstrating nonreactive acetyl-CoA analogs lead to equivalent of increased ACC catalyzed ATP turnover relative to acetyl-CoA incubated ACC.	120
Figure 4.1 Initiation of fatty acid biosynthesis and potential substrate analogs. A) FabH activity. B) FabH C \rightarrow Q mutant decarboxylation activity. C) FabH transthiolation reaction prevented by stable acetyl-CoA analogs. D) Decarboxylation reaction of FabH C \rightarrow Q prevented or slowed by stable malonyl-thioester analogs.	131
Figure 4.2 Analyses of FabH activity with substrates and analogs at pH 8.1. HPLC traces for A) acyl- and Coenzyme A standards, B) 1 , 3 , 5 , C) 2 , 4 , 6 standard HPLC traces for D-I) stability of 250 μ M acetyl- or malonyl-CoA and analogs with 10 μ M FabH over 24 hours at pH 8.1, D) acetyl-CoA, E) 1 , F) 2 , G) malonyl-CoA, H) 3 , I) 4 . J) HPLC traces for 10 μ M FabH with 250 μ M each acetyl- and malonyl-CoA at pH 8.1. K) Representative kinetic analysis of HPLC data from panel J) with malonyl-CoA (red squares and line) use and CoA (green circles and line) production fit to exponential decay or increase, with the acetyl-CoA substrate and acetoacetyl-CoA (black Xs and gold line) product peaks integrated together and shown with a smoothed trend line for visualization. Notice that the CoA production line and acetyl-CoA/acetoacetyl-CoA has a burst phase, while malonyl-CoA does not. L) Representative UV-Vis assay for acetoacetyl-CoA production by 0.5 μ M FabH with 30 μ M acetyl-CoA and 125 μ M malonyl-CoA, initiating the reaction with either FabH or malonyl-CoA. Notice that there is a significant lag phase when the reaction is initiated with FabH as compared to malonyl-CoA.	136
Figure 4.3 Analyses of FabH C112Q activity with substrates and analogs at pH 8.1. HPLC traces for A/C/D/E/G/H) stability of 250 μ M acetyl- or malonyl-CoA and analogs with 10 μ M FabH over 24 hours at pH 8.1, A) acetyl-CoA, C) 1 , D) 2 , E) malonyl-CoA, G) 3 , H) 4 . B) Kinetic analysis of HPLC data from panel A) with the acetyl-CoA substrate (gold Xs and line) and hydrolysis product CoA (green circles and line) fit to exponential decay or increase. F) Kinetic analysis of HPLC data from panel E) with the malonyl-CoA (red squares and line) substrate and acetyl-CoA (gold Xs and line) product or hydrolysis product CoA (green circles and line) fit to exponential decay or increase.	138
Figure 4.4 Kinetic analysis of FabH activity with acetyl- and malonyl-CoA. Panel A) is varying both substrates at the same concentration, Xs are data points for UV-Vis assay monitoring formation of acetoacetyl-CoA and circles are from the HPLC assay for the disappearance of malonyl-CoA. Panel B) varying acetyl-CoA while holding malonyl-CoA at 125 μ M. Panel C) varying malonyl-CoA while holding malonyl-CoA at 125 μ M.	140

Figure 4.5 Representative plot, fitting, and determination of initial rates of FabH with varying malonyl-CoA and acetyl-CoA concentrations. [E] = 0.5 μ M, [acetyl-CoA] = 15 μ M, [malonyl-CoA] = 125 μ M.....	155
Figure 5.1 Preparation of <i>crypto</i> -ACPs from acyl-CoA analogs using Sfp catalysis.	160
Figure 5.2 Proposed enzymatic synthesis of stereospecific methylmalonyl-CoA for kinetic characterization of LnmK and KS enzymes with stereochemical substrate preference.	161

LIST OF SCHEMES

Scheme 2.1 Comparison of differing synthetic routes for aza(dethia) and oxa(dethia) isosteres of malonyl-CoA and (2 <i>R/S</i>)-methylmalonyl-CoA.	58
Scheme 2.2 Comparison of our attempted synthetic route for malonyl-carba(dethia)CoA (left) vs. the previously reported synthesis of malonyl-carba(dethia)CoA ²	59
Scheme 2.3 Synthetic improvements (<i>green</i>) for 2-sulfonate bearing isosteres of malonyl-CoA compared to their previously synthesis (<i>black</i>) ⁷	60
Scheme 2.4 Attempted synthesis of 2-nitroacetyl-aza(dethia)CoA via 3 routes: A) nitration of 2-bromoacetyl intermediate, B) DCC coupling of nitroacetic acid to pantetheine acetonide, C) acylation and repeated oxidation of aza(dethia)-pantetheine acetonide.	62
Scheme 2.5 Synthesis of (2 <i>R/S</i>)-nitropropionyl-carba(dethia)CoA and attempted synthesis of 2-nitroacetyl-carba(dethia)CoA.	63
Scheme 2.6 Synthetic route to 2-phosphonate-acetyl-aza(dethia)CoA	65
Scheme 2.7 Our synthetic route to acetyl-aza(dethia)CoA (<i>left</i>) vs. previously reported synthesis of acetyl-aza(dethia)CoA (<i>right</i>).....	67
Scheme 2.8 Synthetic route and changes for acetyl-oxa(dethia)CoA. Steps exclusive to the original route are grayed out. Changes shown in the new route are shown in <i>green</i> text.....	68
Scheme 2.9 New synthetic route to acetyl-carba(dethia)CoA (<i>left</i>) and novel 2-sulfonate-acetyl-carba(dethia)CoA (<i>right</i>).	69
Scheme 2.10 Simplified synthesis of propionyl-aza(dethia)CoA and novel synthesis of propionyl-oxa(dethia)CoA. Our synthetic route is shown on the <i>left</i> , previous route in on the <i>right</i> ¹⁵	70
Scheme 2.11 Simplified synthesis of propionyl-carba(dethia)CoA. Our synthetic route is shown on the <i>left</i> , previous route in on the <i>right</i> ¹⁴	71
Scheme 2.12 Application of previous acyl-dithio-CoA synthesis to the production of novel hexanoyl-dithio-CoA.	72
Scheme 2.13 Modified synthesis of methylsulfoxide carba(dethia)-CoA. Reagents and purification strategies of this synthetic route were altered from previous work to improve the yield of this compound ¹	73
Scheme 2.14 Synthesis of thiocarbamate CoAs and a novel carbothionic CoA ester.	74
Scheme 2.15 Synthetic scheme for enolate-carba(dethia)CoA analogs.	75
Scheme 2.16 Synthetic scheme for acetoacetyl-aza/oxa(dethia)CoA analogs.	76
Scheme 2.17 Synthesis of oxa/carba(dethia)CoA and desulfo-CoA.	77
Scheme 4.1 Synthesis of acetyl- and malonyl-oxa/aza(dethia)CoA analogs.....	132

Scheme 4.2 Alternative synthetic routes of aza(dethia)CoA using different amine protecting strategies.	134
---	-----

LIST OF ABBREVIATIONS

2-PS – 2-pyrone synthase	DMF – dimethylformamide
ACC – acetyl-CoA carboxylase	DMAP – 4-dimethylaminopyridine
AckA – acetate kinase	DMP – Dess-Martin Periodinane
ACN – acetonitrile	DPCK – dephospho-CoA kinase
ACP – acyl carrier protein	DpsC – daunorubicin-doxorubicin
ACS – acetyl-CoA synthetase	polyketide synthase
Adk – adenylate kinase	DTNB - 5,5'-dithiobis(2-nitrobenzoic acid)
ADP – adenosine diphosphate	DTT - dithiothreitol
AMP – adenosine monophosphate	ECF – ethylchloroformate
ANL – Argonne National Labs	EDC – 1-Ethyl-3-(3-
APANT – pantetheine acetamide	dimethylaminopropyl)carbodiimide
APS – Advanced Photon Source	EML – Essential Medicines List
AT – acyltransferase	ESI-MS – electrospray ionization-mass
ATP – adenosine triphosphate	spectrometry
BC – biotin carboxylase	EtOAc – ethyl acetate
BCCP – biotin carboxy carrier protein	EtOH – ethanol
BPL1 – biotin-protein ligase	ER – enoyl-reductase
C-C – carbon-carbon bond	FA – formic acid
CHS – chalcone synthase	FabB - 3-oxoacyl-ACP synthase I
CoA – coenzyme A	FabD – malonyl-CoA-ACP transacylase
Cryo-EM – cryo electron microscopy	FabF - 3-oxoacyl-ACP synthase II
CT - carboxytransferase	FabH – 3-oxoacyl-ACP synthase III
DAD – diode array detector	FAS – fatty acid synthase
DC – decarboxylase	HATU – hexafluorophosphate
DCC – N,N'-dicyclohexylcarbodiimide	azabenzotriazole tetramethyl uronium
DCM – dichloromethane	HMG-CoA – 3-hydroxy-3-methylglutaryl-
DEBS – 6-deoxyerythronolide B synthase	CoA
DH – β -hydroxyacyl dehydratase	HPLC – high performance liquid
DIC – N,N'-diisopropylcarbodiimide	chromatography

ITC – isothermal titration calorimetry	PPAT – phosphopantetheine
KR – β -ketoacyl-ACP reductase	adenosyltransferase
KS – ketosynthase	PPANT – 4'-phosphopantetheine
LB – lysogeny broth	PDB – protein databank
LC-MS – liquid chromatography – mass spectrometry	PKS – polyketide synthase
MatB – malonyl-CoA synthetase	pTsOH – p-toluenesulfonic acid
MCM – methylmalonyl-CoA mutase	R _f – retention factor
MIC – minimum inhibitory concentration	SDS-PAGE – sodium dodecyl
MMCD – methylmalonyl-CoA decarboxylase	polyacrylamide gel electrophoresis
MMCE – methylmalonyl-CoA epimerase	SEC – size exclusion chromatography
MWCO – molecular weight cutoff	STS – stilbene synthase
m/z – mass to charge ratio	TAE – tris acetate EDTA
NADH – nicotinamide adenine dinucleotide (reduced form)	TB – terrific broth
n.d. – not detected	TC – transcarboxylase
NMR – nuclear magnetic resonance	TCEP – tris(2-carboxyethyl)phosphine
NRPS – non-ribosomal peptide synthetase	TE – thioesterase
OXONE – potassium peroxymonosulfate	TEA – triethylamine
PanK – pantetheine kinase	TEOA – triethanolamine
PANT – pantetheine	TEV – Tobacco Etch Virus
PCC – propionyl-CoA carboxylase	TFA – trifluoroacetic acid
PCR – polymerase chain reaction	TLC – thin layer chromatography
PEG – polyethylene glycol	TMS - tetramethylsilane
	UHP – urea-hydrogen peroxide adduct
	UV - ultraviolet
	WHO – World Health Organization
	YCC – acyl-CoA carboxylase

ABSTRACT

Biosynthesis of fatty acids and specialized metabolites, such as polyketides, is dependent on the C-C bond forming enzymatic activity of carboxylases and ketosynthases (KS). Carboxylases and KS perform complex carbon-carbon bond forming reactions via a ping-pong mechanism; the catalytic interactions of which are still unclear. The KS reaction involves the Claisen condensation of an acylated enzyme with a malonyl-thioester, driven forward by the energy of the malonyl-thioester decarboxylation. Similarly, the carboxylase proceeds via a carboxyl-biotin-enzyme intermediate, and a subsequent C-C bond forming reaction. Engineering the substrate specificity of these enzyme involved in producing polyketides is sought after for the purpose of producing novel, derivative polyketides. These derivative polyketides may have serve as effective new antibiotics, of which discovery has waned. Unfortunately, incomplete understanding of protein-protein interactions, conformational changes, and substrate orientation in catalysis leads to not well informed engineering attempts. A challenge in deducing the catalytic details of enzymes acting on malonyl-thioesters in general is the hyper-reactivity of their β -ketoacid and thioester substrates, which are prone to hydrolysis and decarboxylation. Many structures of malonyl-CoA bound enzymes feature hydrolysis of the thioester, preventing determination of enzyme:substrate interactions in structure-function studies. To work around this problem of innate reactivity, groups have synthesized a variety of acyl-thioester analogs for probing the details of enzyme catalysis with mixed success. The success of these enzyme:analog mechanistic studies appears to hinge upon the similarity of the analog to the natural substrate. Here, we demonstrate the synthesis of near-natural, acyl-thioester analogs, featuring single atom substitutions. Using a novel UV-vis assay, we have determined K_i values of our analogs with paradigmatic KSs *E. coli* FabH. These K_i values are marginally higher than the substrate K_m values, suggesting the KSs bind the analogs as they would natural substrates. Using this information, we have conducted preliminary X-ray crystallography experiments to determine the carboxylase:analog and KS:analog catalytic interactions, which will allow for new insight into debated C-C bond forming catalytic details. The information presented in this thesis and additional studies on protein-protein interactions can be leveraged into informed engineering studies of PKS enzymes.

CHAPTER 1. DEVELOPMENT OF COA ANALOGS AND THEIR ROLE IN PROBING ENZYME CATALYSIS

1.1 Historical context and relevance of CoA and CoA using enzymes

Coenzyme A (CoA) has a deep-rooted history entwined in the field of biochemistry. Since its initial discovery immediately post-World War II, CoA is now known to be a coenzyme for a plethora/multitude of enzymes¹. In fact, it is estimated that between 4-9% of all known enzymes employ CoA². What makes CoA so essential is its thiol functional group, which powers the reactions in which it partakes. This thiol group shuttles acyl functional groups around the cell by forming the labile thioester linkage (S-C=O-R). This thioester linkage allows for facile bond transfer due to its large ΔG of hydrolysis³. Additionally, CoA can be conveniently biosynthesized by the cell from the D-pantothenate, adenosine triphosphate (ATP), and cysteine – resulting in CoA - a phosphopantetheine thiol-containing arm linked to a 3',5'-adenosine-bisphosphate, Figure 1.1⁴. Similarly, acyll carrier proteins (ACPs) employ the same thiol-containing phosphopantetheine moiety to shuttle acyl groups to enzymes that recognize the ACP. Some of the most critical areas of acyl-thioester using enzymes include those involved in fatty acid biosynthesis, a process necessary for all living things on Earth, and polyketide biosynthesis, which is responsible for approximately a third of all natural product pharmaceuticals.

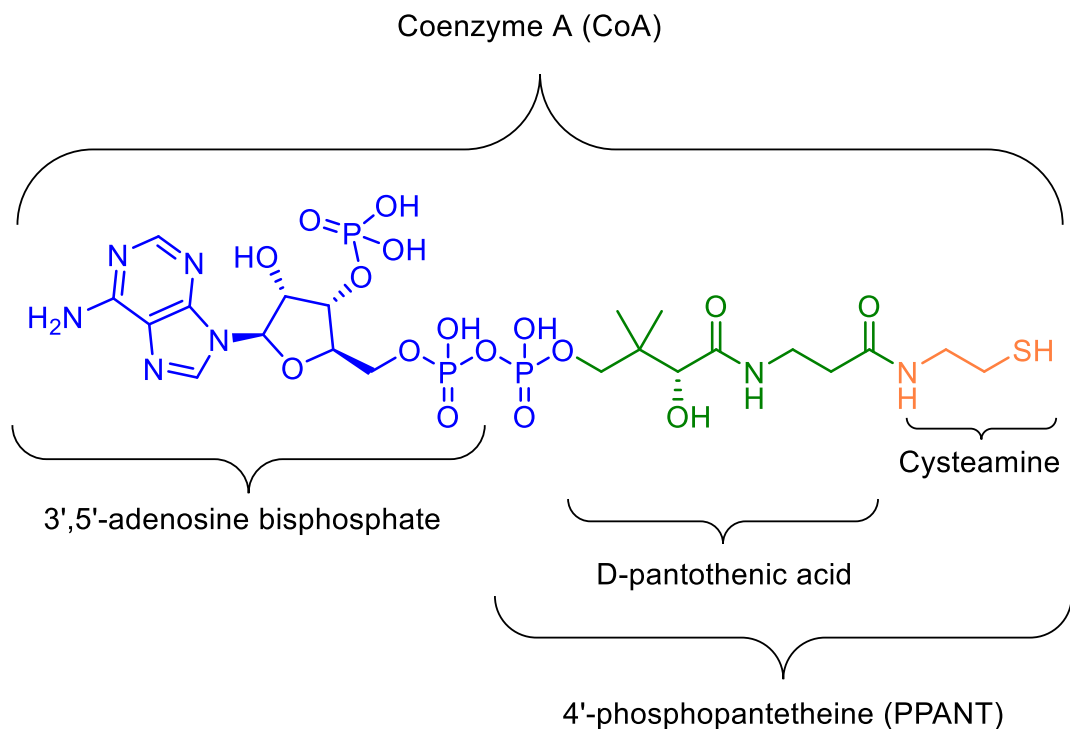


Figure 1.1 Organization and nomenclature of Coenzyme A

1.2 Fatty acid biosynthesis is essential in all kingdoms of life and revolves around acyl-thioester catalysis

Fatty acids consist of variable length hydrocarbon tails (occasionally with degrees of unsaturation), and a polar, carboxylate head. These relatively simple molecules are ubiquitous throughout eukaryotic and prokaryotic organisms, and are known to be essential. Looking at the structures of fatty acids, it would seem that they are neither complex nor remarkable. However, the construction of fatty acids is an incredibly sophisticated and assembly line-styled process. Fatty acids are constructed through the activity of fatty acid synthases (FASs), which contain many different enzymatic activities and active sites⁵. The prototypical fatty acid production is the result of the sequential action of several different enzyme chemistries operating on acyl-thioester substrates (either acyl-CoAs or acyl-ACPs). Canonical FAS chemistry begins with a short-chain acyl-thioester substrate, such as acetyl-CoA, propionyl-CoA, or isobutyryl-CoA⁶. This acyl-thioester substrate is then transthiolated via interaction with a ketosynthase (KS) active site cysteine residue. The acylated-KS can then bind and decarboxylate its second substrate – a malonyl-thioester, which then condenses the decarboxylated malonyl-thioester to the acyl group

linked to the KS. This reaction is described as decarboxylative Claisen condensation, which leads to the formation of a new bond between two carbon atoms, creating a β -ketoacyl-thioester⁷. Downstream of this elongated 3-oxoacyl-thioester produced by the KS, a ketoreductase (KR) activity leads to reduction of the ketone in the β -position to an alcohol. Subsequently, the alcohol group is eliminated by the action of a dehydratase (DH). Finally, an elongated acyl-thioester can be reduced again, leading to saturation of the fatty acid chain by the action of an enoyl-reductase (ER). At this point, the product appears very similar to the initial reactant before KS chemistry – but with the addition of two new methylene groups. This KS-KR-DH-ER cycle will repeat, growing the acyl-thioester an additional 2_n methylene groups in length, where n is the number of reaction cycles the substrate moves through. After n reaction cycles complete, the acyl-thioester will be cleaved from its acyl-carrier via the activity of a thioesterase (TE) activity, yielding a fatty acid product, Figure 1.2. Alternatively, the acyl-thioester may be directly transthiolated to CoA or transesterified to glycerol. In summary, fatty acid synthesis occurs via the action of an assembly line-like process which iteratively grows the hydrocarbon tail of the fatty acid by 2 carbon units after each step, before exiting the assembly line⁸.

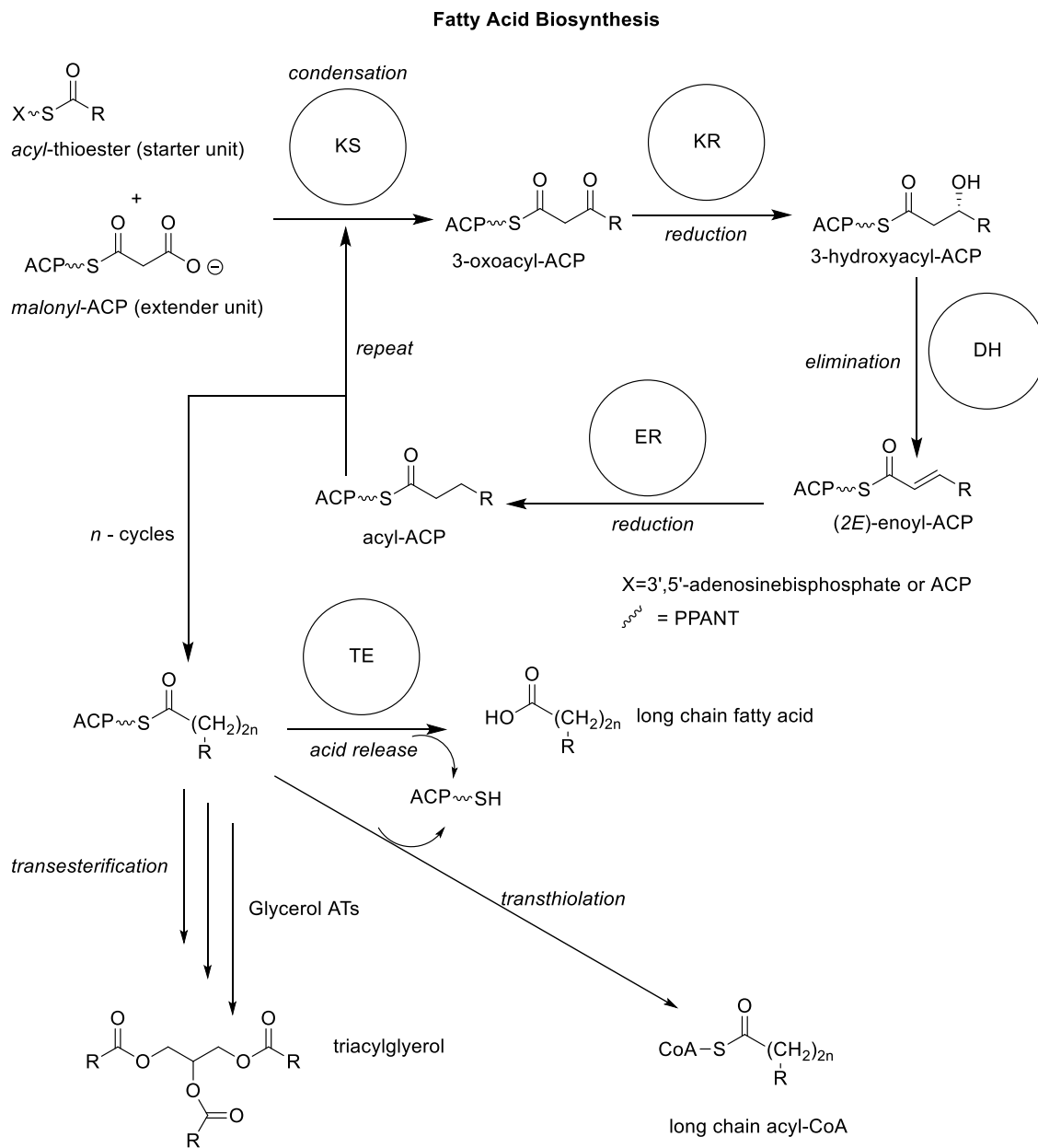


Figure 1.2 Overview of the iterative nature of fatty acid biosynthesis and divergent product fates. The ketosynthase (KS), ketoreductase (KR), dehydratase (DH), and enoyl reductase (ER) work in repeated sequence to produce the elongated fatty acid-thioester.

1.2.1 Carboxylases provide the source of malonyl-thioesters used in fatty acid elongation through a C-C bond forming reaction

At this point the reader may be wondering how all of these materials are being made to expand the growing fatty acid chain. We know that malonyl-thioesters are the source of the 2 carbon units that extend the nascent fatty acid, but where do they come from and how are they

provided to the FAS catalytic domains? These malonyl-thioesters are predominantly produced by an enzyme type discrete from the FAS known as carboxylases⁹. Carboxylases, while not part of the FAS, are understood to be the initial rate-limiting step in fatty acid production, as they have the crucial job of making malonyl-CoA¹⁰. The synthesis of malonyl-thioesters seems simple enough – turn an acyl-thioester into a β -ketothioester by ligating a carbon dioxide (CO_2) to the end of the substrate. However, as is a theme in this dissertation, we will see that this chemistry is the activity of a complex carbon-carbon (C-C) bond forming enzyme. Carboxylases function in two half-reactions – the first of which provides the energy for the second reaction. These two reactions are connected via a biotinylated subunit of the carboxylase known as a biotin carboxy carrier protein (BCCP), which moves CO_2 between reaction centers¹¹. In canonical fatty acid synthesis, acetyl-CoA carboxylase (ACC) hydrolyzes ATP in the first reaction with bicarbonate, generating a CO_2 -biotin-enzyme intermediate, catalyzed by the biotin carboxylase (BC) reaction center of ACC. This CO_2 -biotin-enzyme intermediate is a substrate, along with acetyl-CoA in the second ACC reaction center, the carboxyltransferase (CT), where the enzyme catalyzes condensation of the α -carbon on acetyl-CoA to the CO_2 on biotin, leading to the production of malonyl-CoA, Figure 1.3¹¹. This malonyl-CoA can be used for various cellular processes, such as malonyl-transfer by an AT onto a FAS ACP, where it can extend nascent acyl-thioesters.

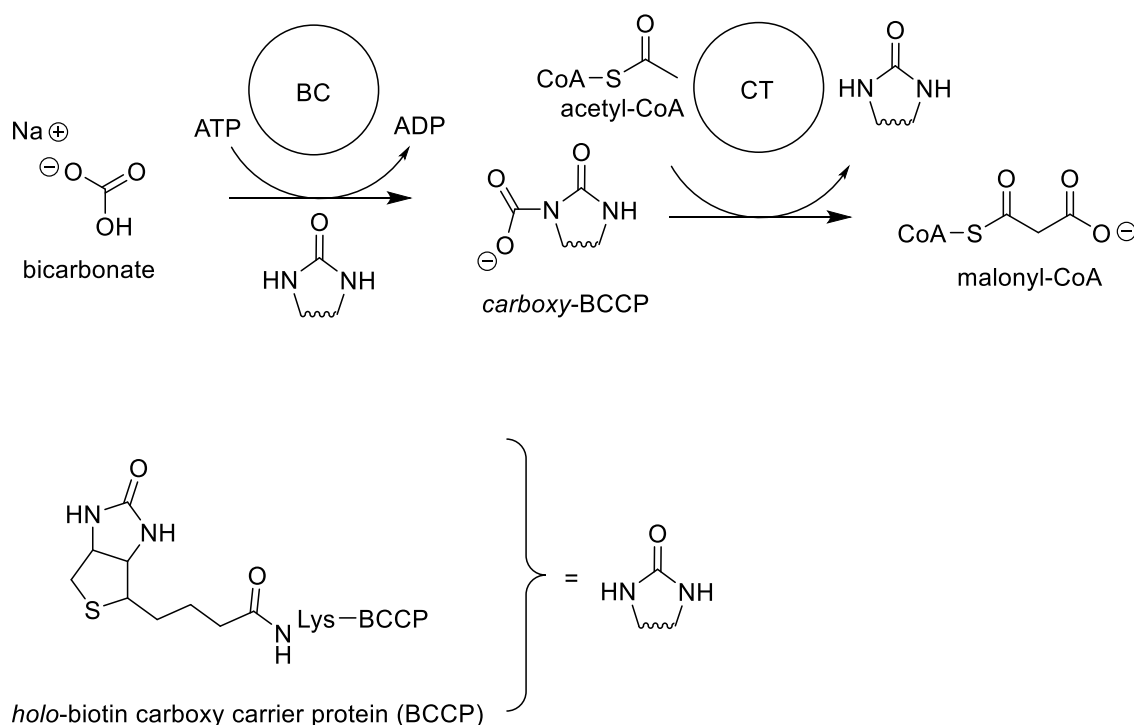


Figure 1.3 General reaction of ATP dependent acyl-CoA carboxylases. The YCC chemistry proceeds in two half reactions, the first of which is the biotin carboxylase (BC) catalyzed carboxylation of biotin. Afterward, the YCC undergoes a large conformational change to transfer the carboxyl group from biotin to an acyl-CoA via the carboxyltransferase (CT) activity, leading to a malonyl-CoA product.

1.2.2 The wealth of fatty acid biosynthetic machinery provides abundant targets for medicine, herbicide, and biofuel production

Due to the essential nature of fatty acid biosynthesis, a great deal of work has been put into targeting its machinery for drug development¹². Additionally, an added benefit of targeting fatty acid biosynthesis enzymes for drug discovery is their structural diversity between different types of organisms. For example, acetyl-CoA carboxylase in *Escherichia coli* consists of 4 discrete subunits that are separately translated, and come together to form a relatively weak heterotetrameric complex. This is in stark contrast to the *Homo sapiens* ACC, which is a single polypeptide, and contains a large, additional central domain for regulatory purposes, Figure 1.4^{10, 13}. As such, a potent inhibitor a prokaryotic ACC could shut down malonyl-CoA production in pathogenic bacteria, while not affecting human ACC. In this example, the proposed inhibitor could lead to a new class of antibiotics.

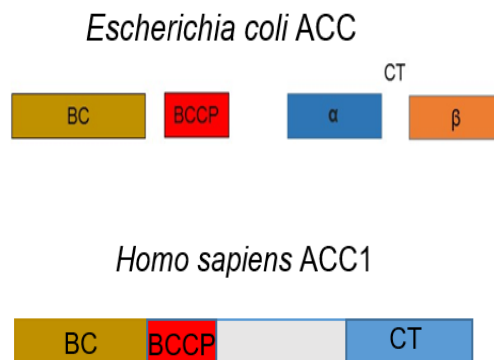


Figure 1.4 Contrast of the organization of single polypeptide eukaryotic YCCs vs. multi-subunit prokaryotic YCCs. Eukaryotic YCCs are often homodimeric, with a molecular weight over 0.5 MDa. Prokaryotic YCC components can be more easily studied in high resolution structural studies due to their lower molecular weight.

Through decades of research, other groups have discovered and characterized various inhibitors of carboxylases and fatty acid synthase modules with potential (or approval in some cases) to serve as medicines or agrochemicals¹⁴. In 2004, a group of researchers observed that the natural product moiramide B is a potent inhibitor of gram positive *Staphylococcus aureus* ACC, yielding a K_i via a radiometric assay of 5 nM¹⁵. Additionally, this group synthetically derivatized the molecule with different hydrophobic tails. Over a decade later, a study from 2016 deduced the structure-function relationship of moiramide B with *S. aureus* ACC, showing that the molecule binds via its methyl succinimide warhead at the interface of the α and β subunits of the carboxyltransferase (CT) reaction center, Figure 1.5¹⁶. The derivatized hydrophobic tail opposite of the warhead is suggested to be relevant in crossing the cell membrane. Through bacterial inhibition assays, it was learned that *E. coli*, *S. aureus*, and *Bacillus subtilis* minimum inhibitory concentrations (MICs) were found to be 4, 8, and 1 $\mu\text{g/ml}$, respectively^{15, 17}. These values indicate the concentration of moiramide B necessary to observe significant reduced bacterial growth of each strain, suggesting that moiramide B is a potent antibacterial.

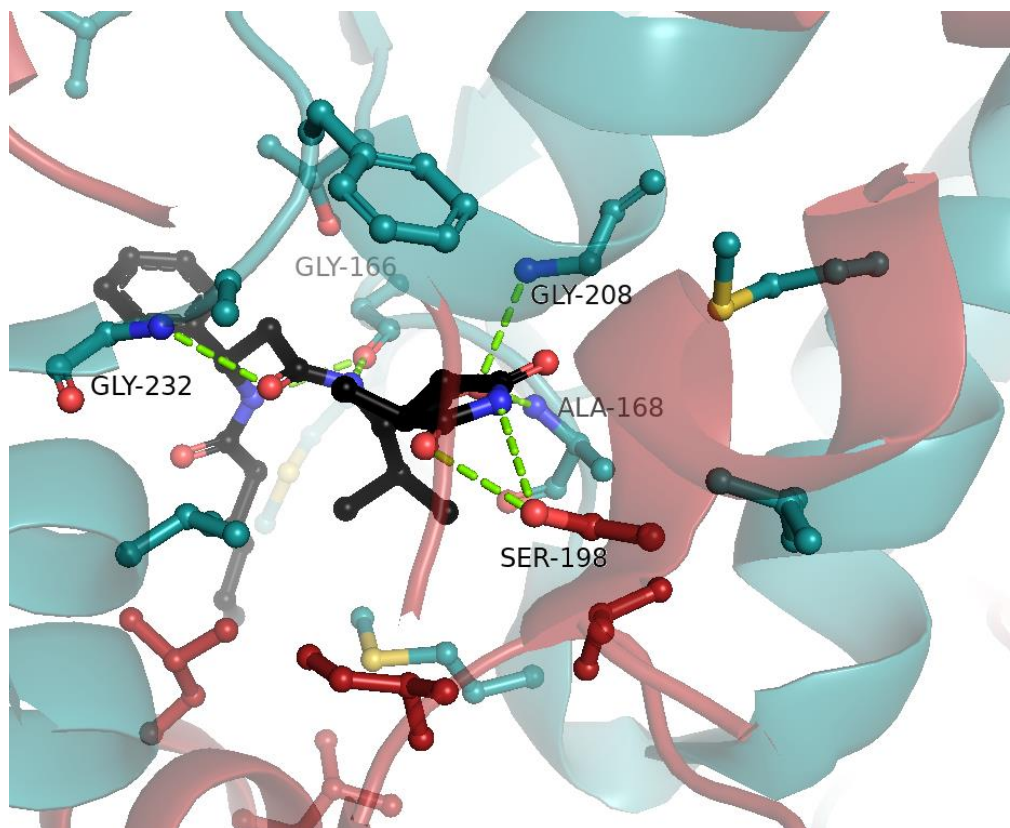


Figure 1.5 Moiramide B (*black*) inhibits the CT (*red/teal*) of *E. coli* ACC at the interface of the α and β subunits via interactions of the succinimide warhead situated in the active site.

In another case study of fatty acid biosynthesis targeting, it was found that three different herbicides in use, dichlofop, haloxyfop, and sethodim, both inhibit lipid and fatty acid biosynthesis in corn and other monocot plants¹⁸. Shortly after, another group deduced that these herbicides specifically targeted the plastid ACC. The group reported nearly 90% inhibition of *Zea mays* plastid ACC activity with 1 μ M haloxyfop and 10 μ M sethoxydim. In addition, it was found in the same study that while these herbicides were potent in corn in other monocots, they had no effect at 10-fold increased concentration in the model dicot plant, peas¹⁸.

To provide one more example of efficacy of targeting fatty acid biosynthetic machinery with inhibitors, consider the case of the natural product cerulenin. Cerulenin features an oxirane ring, flanked by carbonyl groups – one of which is bound to a short, unsaturated hydrocarbon tail. It has long been known that cerulenin is a potent inhibitor of fatty acid biosynthesis – specifically FabB – a critical KS enzyme that leads to iterative condensation of long-chain fatty acids. Rock and colleagues determined the structure of the bacterial fatty acid biosynthesizing KSs, FabB,

FabF, and FabH¹⁹. Furthermore, they elucidated the cerulenin-FabB structure, which illustrated that the enzyme catalyzed a covalent linkage with the oxirane ring amide carbonyl, leading to irreversible inhibition of the enzyme, Figure 1.6²⁰. Additionally, the amide carbonyl was situated in the proposed oxyanion hole used in catalysis to promote malonyl-ACP decarboxylation. Furthermore, this inhibitor was shown to have antineoplasia activity in mice, suggesting its potential as an anti-cancer drug.

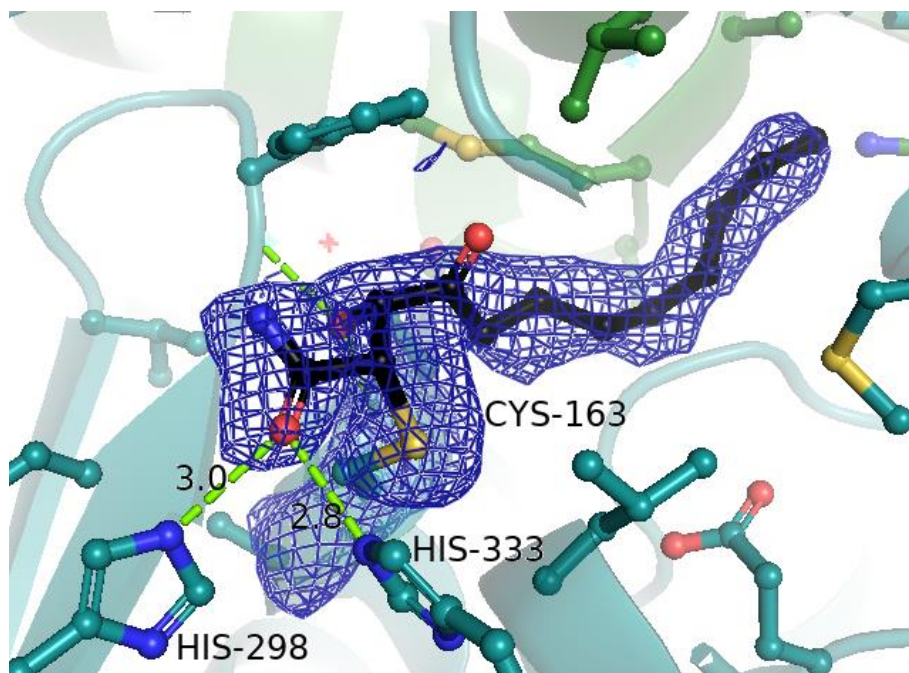


Figure 1.6 Cerulenin (*black*) irreversibly inhibits the catalytic cysteine residue of FabB (*teal*).

Many of these drugs that target fatty acid biosynthesis share a common theme of having been characterized as inhibitors for multiple decades; often having been discovered serendipitously. While further research has been conducted by academic groups to elucidate the mechanism of action of these inhibitors – there has been a lack of fatty acid synthesis inhibitor discovery in the past 15 years. Later on in this thesis, I will address a new plan to tackle the challenge of drug discovery targeting fatty acid biosynthesis. However, like two-sides of the same coin, while we have seen that fatty acid biosynthesis is a drug target, a source of many natural product drugs (e.g. lovastatin) is polyketide biosynthesis. Next, we will explore the origin of many of these natural product drugs through the analogous iterative activity of PKS.

1.3 Polyketide biosynthesis catalysis, complexity, and importance mirrors fatty acid biosynthesis, as polyketides have revolutionized the pharmaceutical industry

Like fatty acid biosynthesis, polyketide biosynthesis has a long, rich history of discovery of modular, assembly line-like enzymatic machinery producing lengthy C-C bond centered molecules²¹. However, in stark contrast to the production of fatty acids, polyketides are much more specialized, only being produced by some plants, bacteria, and fungi²². Additionally, in contrast to the simplicity of long, undecorated hydrocarbon chains of fatty acids, polyketides are much more diverse in nature, featuring a variety of functional groups, heterocycles, aromatics, and varying degrees of oxidation and unsaturation uncommon to fats²². Perhaps most interesting of all, is that polyketides are produced by virtually the same enzymatic reactions as fatty acids – via acyl-thioesters transthiolated by an AT and shuttled to KS-KR-DH-ER modules in succession. We will examine this concept as we dive into more decades of discovery, medicinal success stories, engineering attempts, and mechanistic observations, we will begin to unravel how these similarities and differences coexist.

1.3.1 While polyketide synthases perform similar C-C bond extension reaction to FAS, diversity in their assembly line allows for a wide variety of products

To first understand how polyketide synthases perform their complicated chemistry, let's compare them to fatty acid biosynthesis. Both types of enzymes employ similar modules for catalysis⁸. Thus, we begin polyketide biosynthesis via an acyl-thioester substrate, such as acetyl-CoA, propionyl-ACP, butanoyl-ACP, etc. This acyl-thioester substrate is known as the *starter unit*. This starter unit can then be transacylated to the ACP of a polyketide synthase (PKS), via the action of an AT, again similar to FAS²³. This starter unit will have a designated route to move through various modules of the PKS in the case of modular type I PKS, or move iteratively through a module in the case of type II and iterative type I PKS.

To illustrate representative type I PKS biosynthesis, consider the biosynthesis of the polyketide, rapamycin, a pharmaceutical used as an immunosuppressant to prevent organ transplant rejection, Figure 1.7. The biosynthesis of rapamycin begins via the action of three modular PKS – RapA, RapB, and RapC²⁴. These PKS contain, 4, 6, and 4 modules, respectively, and within each module, there is a KS, AT, and ACP, responsible for extending the bound nascent polyketide chain. Additionally, there is a variety of derivatized malonyl-thioesters used to extend

the nascent polyketide chain. These malonyl-thioesters, referred to as *extender units*, may contain different substituents at the α -carbon, leading to more diversity of the polyketide. In RapB, the module 5 KS uses a malonyl-thioester to extend the polyketide chain, whereas module 6 uses a methylmalonyl-thioester to extend the chain. After biosynthesis of the linear polyketide scaffold by RapA, RapB, and RapC, other enzymes, such as the nonribosomal peptide synthase (NRPS), RapP, further modify the growing molecule and cyclize it. Lastly, rapamycin synthesis is finished through modification by the *tailoring* enzymes RapI (*O*-methylation), RapJ (oxidation), RapM (*O*-methylation), RapN (hydroxylation), and RapQ (*O*-methylation)²⁴. As this representative polyketide biosynthesis demonstrates – the chemistry performed by the PKS is the same as in a FAS, however, the mix-and-match format of the enzymes in each module lead to a much more sophisticated product than a fatty acid.

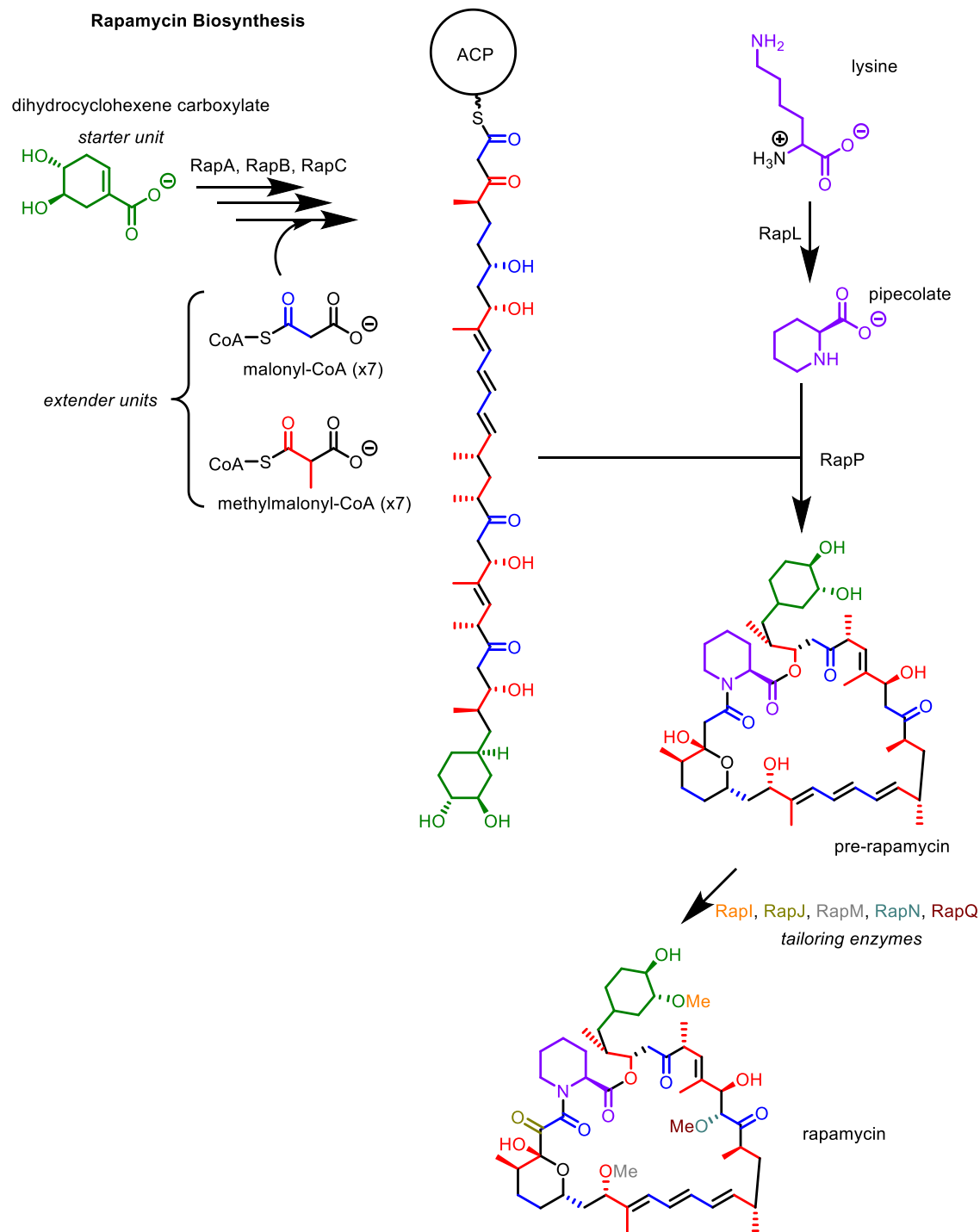


Figure 1.7 Biosynthesis of the immunosuppressant drug, rapamycin, is performed by the sequential action of polyketide synthase modules and tailoring enzymes. Atoms donated by malonyl-CoA are shown in *blue*, while atoms donated by methylmalonyl-CoA are in *red*. Engineering of different PKS components could allow for substrate promiscuity in any of the extension reactions.

While PKS are known have a great diversity in their starter units, they frequently only incorporate two types of extender units: malonyl-CoA and methylmalonyl-CoA²⁵. As observed by the 14 PKS catalyzed extension steps in rapamycin biosynthesis, there is a large opening for diversifying PKS products via use of different extender units. Within the past two decades PKS researchers gained some understanding of the usage of rarely used extender units that provide a means of incorporating diverse functional groups such as amines, halogens, alkenes, and aromatics, Figure 1.8²⁵. Additionally, research conducted by G. Williams' group demonstrated the potential to synthesize unnatural extender units via the activity of a mutant malonyl-CoA synthetase (MatB)²⁶. Furthermore, using both unnatural and uncommon extender units generated by MatB, they were able to incorporate these rare, α -substituted extender units into a polyketide by the action of the final PKS module from 6-deoxyerythronolide B synthase (DEBS). A noncomprehensive list of PKS extender units is shown below.

Various Extender Units Used by PKS

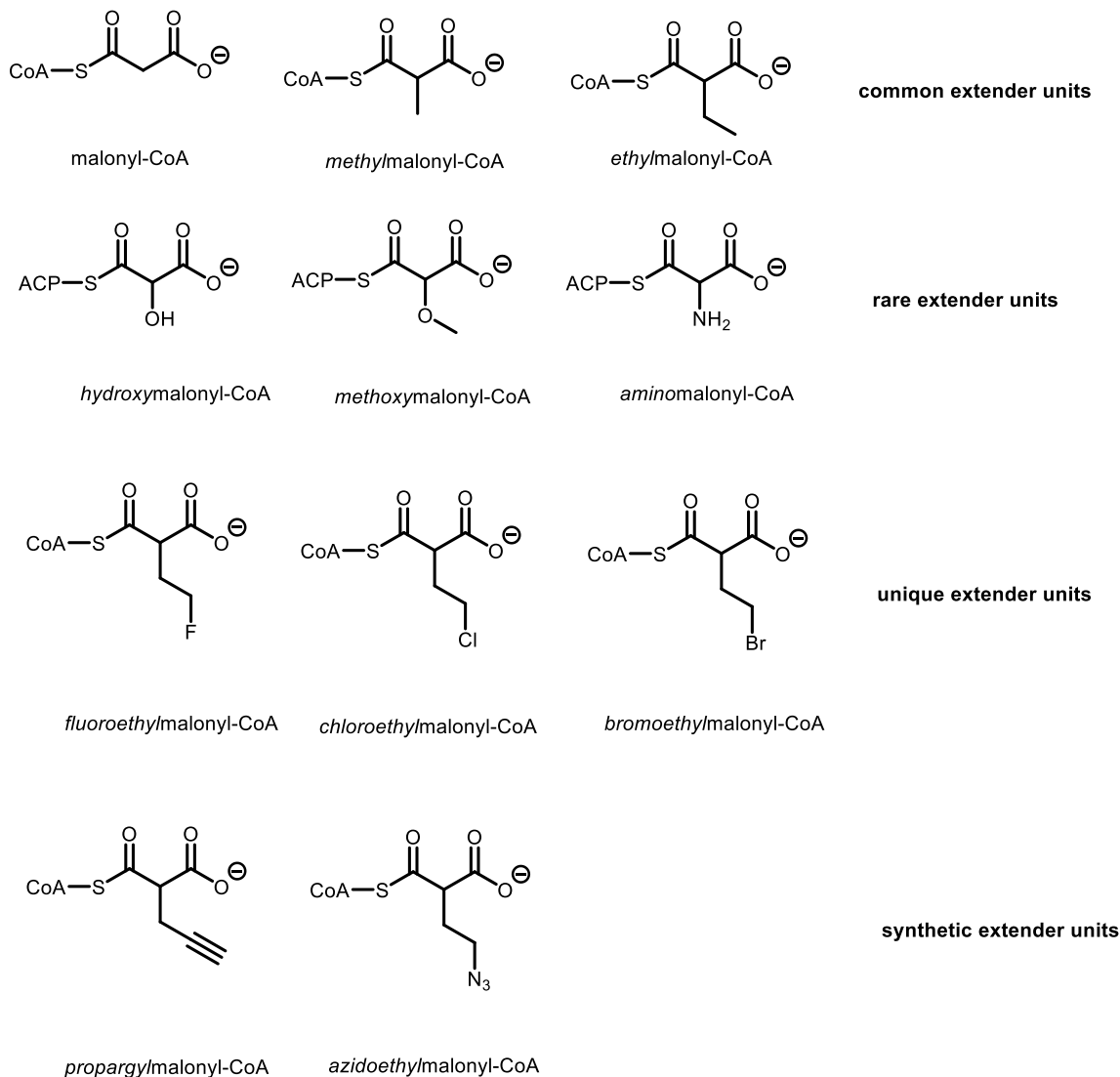


Figure 1.8 Variation of extender units used by polyketide synthases is route being researched to diversify polyketide products. Most PKS demonstrate little diversity in extender unit incorporation, using only malonyl- or methylmalonyl-CoA. However, PKS pathways exist that accept less common (or even synthetic) extender units.

1.3.2 Polyketide biosynthesis provides a vast variety of natural product pharmaceuticals with hopes to engineer many more

Whereas fatty acid biosynthesis is essential for organismal viability, making it an ideal drug target, PKS are nonessential. A PKS is an evolutionary advantage, not a necessity, as many organisms use their PKS to secrete toxins, such as maitotoxin, which will allow them to easily

fight off their neighbors and proliferate²⁷. Many of molecules produced (or partially produced) by the action of PKS sit on the World Health Organization (WHO) Essential Medicines List (EML) – a list of medications that are very safe and effective for treatment within a health system²⁸. Some medicines on this list that are produced in part by PKS are the antibiotics vancomycin, doxycycline, and erythromycin. In addition to these antibiotics, we also find the cholesterol lowering agent, lovastatin on this list. However, more recent drug candidates, such as the proposed anti-cancer drug neocarzinostatin, synthesized partially by a PKS may eventually find their way on this list.

Although polyketides have helped usher in a golden age of drug discovery in the 20th century, there has been a marked decrease in discovery and approval of natural product medicines in the past two decades²⁹. This may be due to a combination of factors including a paradigm shift in drug discovery to drug library screening, unmet promise in PKS engineering, and possibly a dried up pool of undiscovered natural products with pharmaceutical potential. While PKS engineering seems to be a logical idea to increase the amount of polyketide drugs going from discovery to clinical trials, this engineering has posed a challenge³⁰.

1.3.3 Shortcomings of PKS engineering are due to an underestimation of the complex effects of protein-protein interactions and conformational changes on catalysis

In late 2017, at the beginning of my Ph.D. work, I had the opportunity to attend a lecture by Professor David Sherman as part of the seminar series held by the Purdue Department of Biochemistry. On a slide near the beginning of Dr. Sherman's talk was a graphic from his 2005 *Nature Biotechnology* paper titled "The Lego-ization of polyketide biosynthesis". In this paper, Sherman had observed the work of many research groups engineering polyketide synthases by mixing and matching pieces of various PKS to generate systems that make new products³⁰. Here, Sherman described this concept as "Lego-ization", where different PKS components can be used in conjunction to make a new product, analogous to how different Lego pieces from different kits can be stuck together to make a Lego masterpiece. This idea was remarkable – that mixing and matching PKS components from different systems could take the number of polyketide products discovered from 10,000 to hundreds of millions, with that many new drug leads to evaluate. While some success has been demonstrated from this idea, shortly after this slide in Dr. Sherman's talk, he went on to talk about this conclusion being hasty, and that many details were missing to truly

realize the potential of PKS engineering. These missing details are what our lab and others in our field seek to elucidate³¹⁻³³. For example, what specific protein-protein interactions are mandated intra- and inter-module in a PKS to efficiently catalyze polyketide formation and these preserved during mixing-and-matching components? Next, how do we accommodate substrate promiscuity into our Lego-ized PKS? To elaborate, can downstream PKS modules perform chemistry on unnatural substrates produced by upstream modules? Lastly, what are the changes in conformation and substrate binding throughout catalysis of this highly dynamic system? Understanding the answer to these questions will help researchers in their goal of mass engineering PKS.

1.4 Mechanistic studies on fatty acid and polyketide biosynthesis components can provide critical missing information tackling drug discovery and engineering hurdles

As a result of these previously mentioned unknowns hampering PKS engineering studies, some researchers have taken a more mechanistic approach to understand PKS and FAS structure-function relationships³⁴⁻³⁶. The work of Professor Joe Noel and his research group conducted many important structure-function and kinetic studies on type III PKS, which are the smallest and simplest models for polyketide production. Some type III PKS, such as *Medicago sativa* chalcone synthase II (CHS), *Gerbera hybrida* 2-pyrone synthase (2-PS), and *Pinus sylvestris* stilbene synthase (STS), perform all of their chemistry in a single active site³⁷⁻³⁹. This is in stark contrast to the mega type I PKS from the previous section. Noel's group performed X-ray diffraction experiments on crystals grown of these enzymes, gaining high-resolution data of their structure in the presence of various ligands³⁴. These structures were effective at illustrating the general substrate binding pocket, allowing for some speculation about how catalysis might occur. However, this work did not share the details of conformational changes of different catalytic states, such as the acyl-enzyme intermediate of the PKS, malonyl-thioester binding, decarboxylation, or Claisen condensation. This work laid the foundation that other groups, including ours, would work to build upon⁴⁰.

Over a decade later, the collaborative effort of the Gorgio Skiniatis and David Sherman research groups would lead to solution of the first structure of an entire type I PKS module via cryo-electron microscopy (cryo-EM)^{41, 42}. This collaborative effort would lead to insights into how the ACP moved to interact with each reaction center in the module. The module being studied was module 5 of the pikromycin biosynthetic pathway, containing the ACP tethered acyl chain, and

three enzymatic activities – KS, AT, and KR. The group noted that the ACP of module 5 would be found interacting with different catalytic domains of the module based on the oxidation state of the acyl group appended to the ACP. This result suggests that substrates are efficiently recognized by each domain, which results in effective catalysis by the PKS assembly line. However, the group noted that while this study provided catalytic details, it meant that much more care than originally anticipated would need to be done to engineer the PKS system⁴². Additionally, while this study is groundbreaking, it also is just the beginning of many details to be uncovered about PKS catalysis. Due to the low resolution of the cryo-EM in 2014, fine conformational changes, such as residue movement shifts and substrate binding are unidentifiable from this work.

A longstanding challenge of capturing individual catalytic states and conformational changes that are often undetermined is the reactivity of the acyl-thioester substrates to enzyme chemistry. As discussed at the beginning of this thesis, CoA (and ACP) can effectively move acyl groups and transthiolate enzyme chemistry as a result of the facile cleavage of the thioester moiety. While this property of CoA is great for maintaining homeostasis of an organism, it complicates structure-function studies to a great degree, Figure 1.9. If we examine the protein data bank (PDB), many enzyme structures have been deposited with acyl-CoAs listed as ligands^{23, 43}. In the electron density map of many of these structures, the acyl-CoA is in a hydrolyzed state, with electron density becoming obscured after the thiol on CoA, Figure 1.10. Additionally, it is known that malonyl-thioesters are prone to decarboxylating from enzyme chemistry or in acidic conditions⁴⁴. As acyl/malonyl-thioesters are substrates for a vast number of enzymes, this becomes a major problem to overcome when conducting structure-function studies of these enzymes. This poses the question – how can unknown catalytic states be observed in structure-function studies of highly-reactive enzyme substrate pairs? One approach to answering this long standing question has been synthesis of nonreactive analogs that mimic the chemical properties of the reactants, intermediates, and products of different reactions⁴⁵.

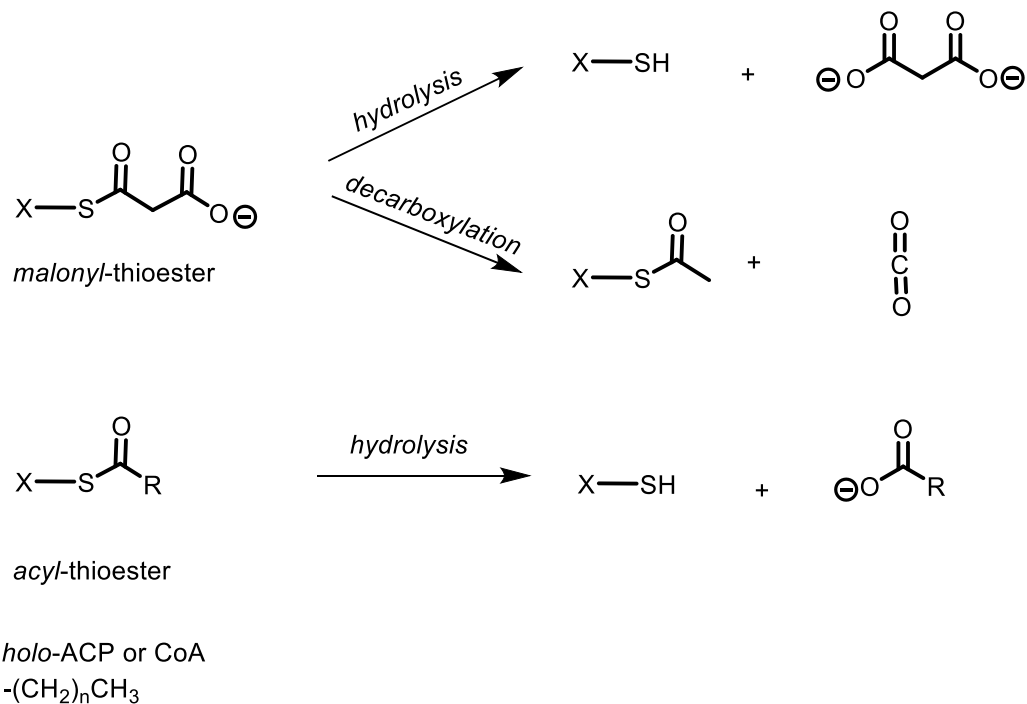


Figure 1.9 Malonyl-thioesters and acyl-thioesters are both prone to enzyme catalyzed hydrolysis. Malonyl-thioesters may also be decarboxylated by enzymatic activity.

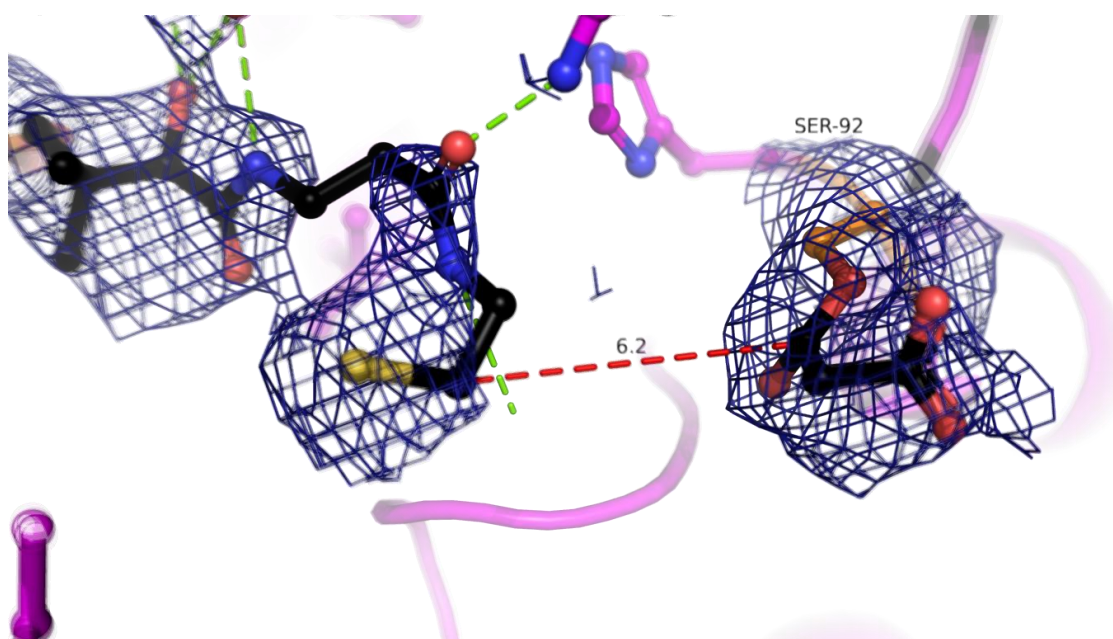


Figure 1.10 Structure of *E. coli* FabD (PDB: 2G2Z) solved at 2.8 Å with a malonyl-enzyme intermediate modeled. This structure models a malonyl-enzyme intermediate and CoA in the active site, though the density is sparse.

1.5 Synthesis of CoA-thioester analogs has a long, slowly-evolving history, as probes for enzyme catalysis, conformational changes, and inhibition

Not long after the initial discovery of CoA as a critical coenzyme in shuttling acyl groups were scientists working to determine the structure and chemically synthesize the molecule. These tasks were in part completed by the Nobel prize awarded Fritz Lipmann, who pieced together the structure of CoA in 1953, and synthesized one half of CoA, known as 4'-phosphopantetheine (PPANT)⁴. Finally, at the beginning of 1959, the research team of J.G. Moffatt and H.G. Khorana had accomplished the first recorded total synthesis of CoA⁴⁶. This synthesis was an impressive feat, using previously established information on the structure of CoA and synthesis of PPANT in conjunction with the new concept of developing the 2',3'-phospho-AMP-morpholine synthon, Figure 1.11. Fusion of this new synthon with PPANT in basic conditions, followed by acid cleavage of the cyclic phosphate ring yielded a mix of CoA and *iso*-CoA (where the 3'-phosphate of CoA is instead on the 2' position), which were separated via anion exchange chromatography. This reaction, unbeknownst to the researchers, would go on to pave the road for decades of CoA derivative and analog chemical synthesis.

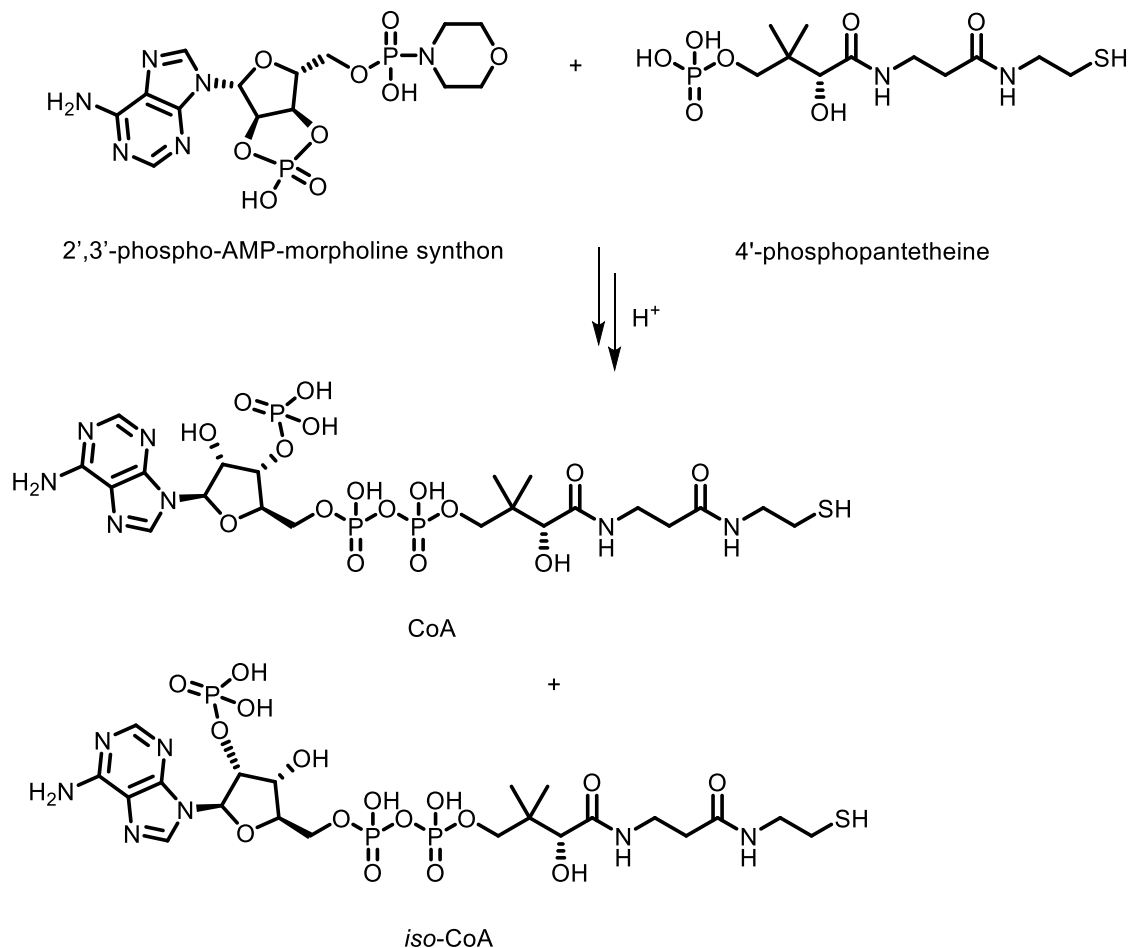
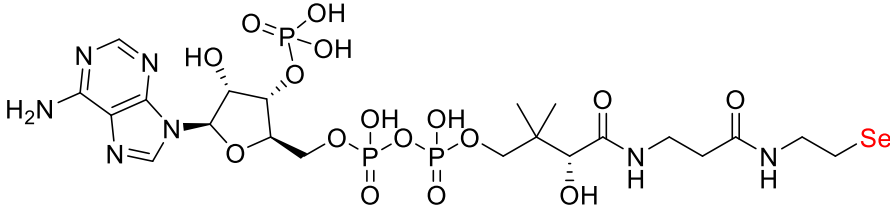
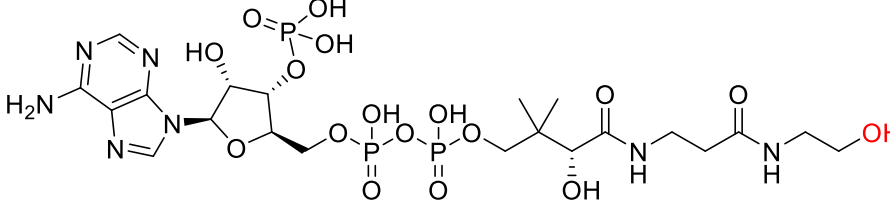
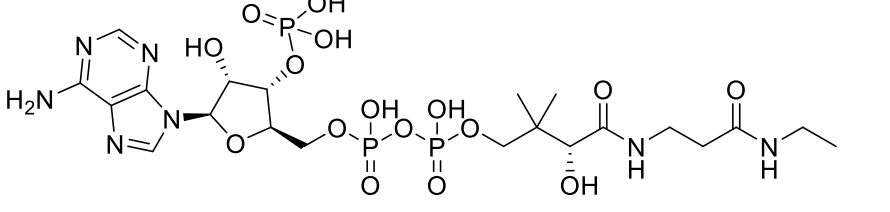
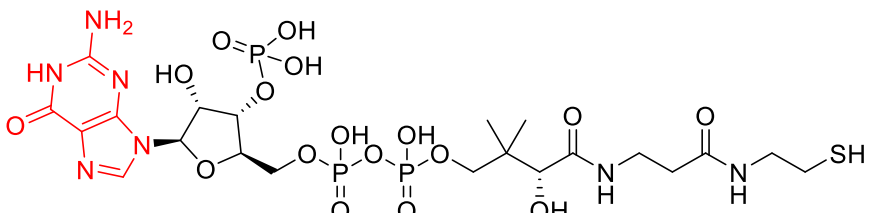


Figure 1.11 Chemical synthesis of CoA using 2',3'-phospho-AMP-morpholine synthon.

After the initial synthesis of CoA the floodgates for CoA analog synthesis and synthetic improvements were opened. The non-exhaustive table below, Table 1.1, demonstrates some of these advances in CoA analog synthesis.

Table 1.1 Non-exhaustive list of CoA analogs reported in the 1960's.

Compound (<i>substitutions shown in red</i>)	Reported year
<p>seleno-CoA</p> 	1965 ^{47}
<p>oxy-CoA</p> 	1966 ^{48}
<p>desulfo-CoA</p> 	1968 ^{49}
<p>guano-CoA</p> 	1966 ^{50}

The key to production of all of the above analogs was to synthesize a new β -aletheine moiety, shown in Figure 1.12, then use the existing CoA synthesis procedure (with minor improvements) to produce analogs of CoA^{[51](#)}. These CoA analogs of the 1960s tied together the

knowledge of synthesizing pantetheine analogs in the 1950s with the procedure of synthetic procedure of Khorana and Moffatt. In each of the initial synthesis papers, these analogs were assayed with model enzymes, such as phosphotransacetylase for their action as substrates or inhibitors^{48, 52}. The CoA analog synthesis work of this decade would serve as the roadmap for development of more sophisticated CoA analogs in the ensuing decades which would cement their use as mechanistic probes of enzyme activity.

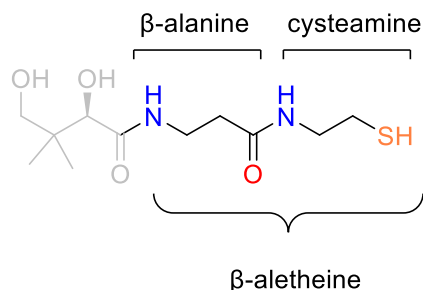


Figure 1.12 β -aletheine is composed of β -alanine and cysteamine.

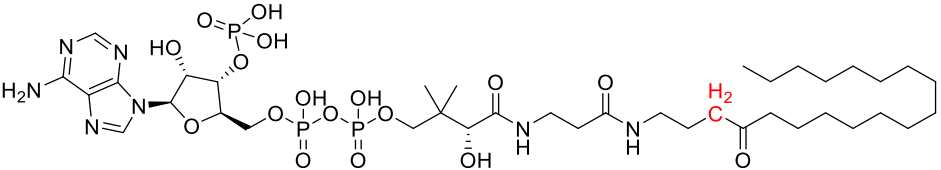
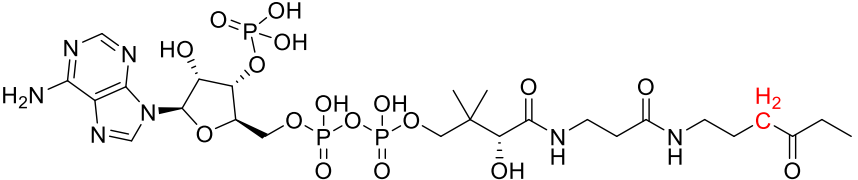
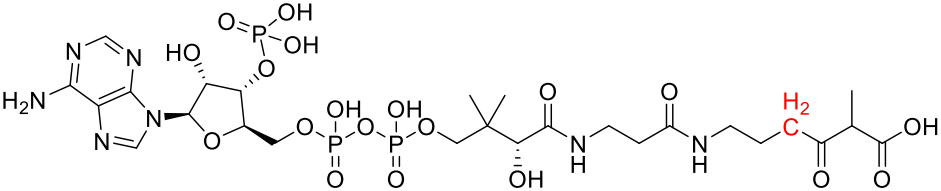
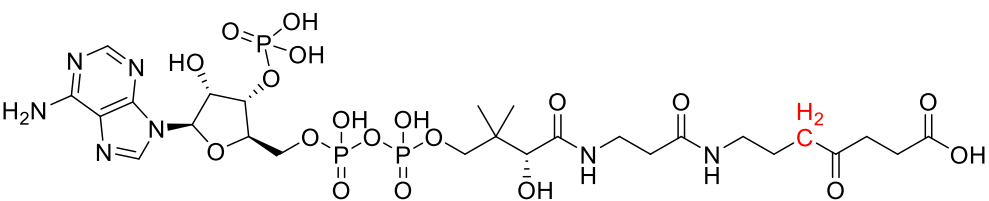
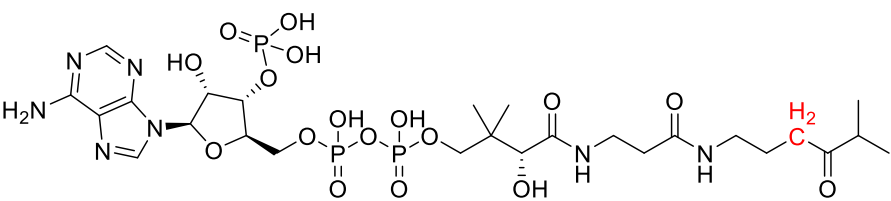
1.5.1 Acyl-CoA analogs stable to hydrolysis emerged in the 1970s with application in enzyme mechanism experiments but featured difficult synthesis procedures

In the 1970s, the method of producing CoA analogs would begin to be extended to acyl-CoA analogs, where the first syntheses of acetyl-CoA analogs were reported. The researchers led by C.J. Stewart would report the syntheses of acetyl-carba(dethia)CoA and acetyl-amino(dethia)CoA for the first time in this decade. Early studies of CoA analogs examined the importance of the role of the sulfur atom, the thioester carbonyl, and length of the acyl group with respect to enzyme catalysis. In the case of the enzyme phosphotransacetylase, it was shown that the inhibition constant (K_i) of acetyl-carba(dethia)CoA was reported as 0.36 mM⁵³. It was then found that removing the carbonyl group from the analog (producing ethyl-CoA) raised the K_i 3-fold to 1 mM. Additionally, deviations of acyl group chain length from 2-carbons raised the K_i further, as was observed for methyl-, propyl-, and butyl-CoA⁵³. Thus, the authors could conclude that acyl group length and presence/position of the acyl-carbonyl moiety are important factors in substrate recognition by phosphotransacetylase.

Using the idea of the initial acetyl-carba(dethia)CoA synthesis, groups would create other acyl-carba(dethia)CoA analogs to evaluate their propensity for serving as substrates or inhibitors

of a variety of enzymes⁵⁴. A non-comprehensive list of these analogs is presented in the table below.

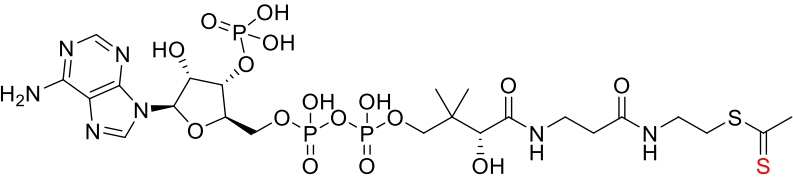
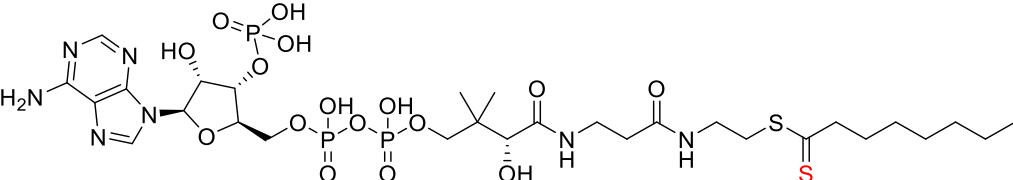
Table 1.2 Representative methylene substituted acyl-CoA analogs reported in the 1980's.

Compound (<i>substitutions shown in red</i>)	Reported year
<p>palmitoylcarba(dethia)-CoA</p> 	1981 ^{55}
<p>propionyl-carba(dethia)CoA</p> 	1986 ^{56}
<p>methylmalonyl-carba(dethia)CoA</p> 	1986 ^{56}
<p>succinyl-carba(dethia)CoA</p> 	1986 ^{56}
<p>isobutanoyl-carba(dethia)CoA</p> 	1988 ^{57}

The research group led by J. Rétey reported the complex chemical synthesis of propionyl-carba(dethia)CoA and eloquently demonstrated the ability of the enzyme transcarboxylase from *Propionibacterium shermanii* to convert this substrate analog into (2*S*)-methylmalonyl-carba(dethia)CoA. Furthermore, the authors also demonstrated the ability of methylmalonyl-CoA epimerase (MMCE) to epimerize this analog into (2*R*)-methylmalonyl-carba(dethia)CoA, which was then shown to be a substrate for methylmalonyl-CoA mutase (MCM), which produced succinyl-carba(dethia)CoA⁵⁶. Through the use of these β - and γ -keto acid analogs, nuclear magnetic resonance (NMR) experiments conducted by Rétey allowed for mechanistic characterization of MCM⁵⁸. MCM is known to be a vitamin B₁₂ dependent enzyme, and was known to perform a carbon skeleton rearrangement through a radical mechanism. The non-hydrolyzable nature of succinyl-carba(dethia)CoA and methylmalonyl-carba(dethia)CoA allowed for NMR analysis of the enzyme reaction to capture details of a 1,2 hydrogen atom shift performed by the enzyme that maintained the reaction stereospecificity⁵⁹.

During the same decade, another group took a different approach to synthesizing acyl-CoA analogs to probe enzyme mechanism. The work of V.E. Anderson and colleagues led to the synthesis of acetyl-dithio-CoA and octanoyl-dithio-CoA, which replace the carbonyl oxygen of the corresponding acyl-CoA with a sulfur atom⁶⁰. These acetyl-dithio-CoA served as a substrate for both citrate synthase and choline *O*-acetyltransferase. However, the rate of reaction was about 10-fold less than that of the natural substrate, acetyl-CoA. Additionally, the dithioester moiety provides a unique absorbance maximum at $\lambda = 306$ nm. The authors hypothesized that slow reaction rate and characteristic absorbance spectrum of acyl-dithio-CoAs would make them effective probes for detecting acyl-enzyme intermediates in reactions such as those performed by ATs. This feature of the analog would be applied nearly 20 years later, where it was determined that acetyl-dithio-CoA could not be enolized by the enzyme 3-hydroxy-3-methylglutaryl-CoA (HMG-CoA) synthase when the enzyme was mutated, preventing formation of an acyl-enzyme intermediate⁶¹. Thus, acetyl-dithio-CoA served as a mechanistic probe to confirm the existence and necessity of an acyl-enzyme intermediate for HMG-CoA synthase catalysis.

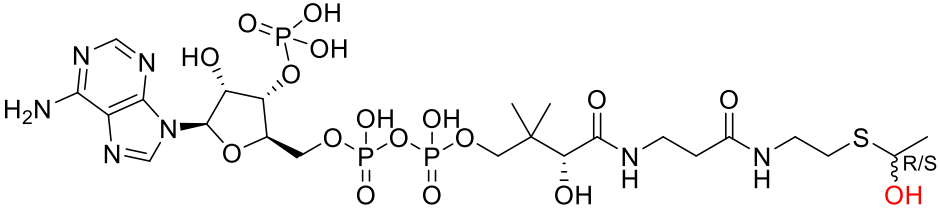
Table 1.3 Initially reported acyl-dithio-CoA analogs of the 1980's.

Compound (<i>substitutions shown in red</i>)	Reported year
<p>acetyl-dithio-CoA</p> 	1988 ⁶⁰
<p>octanoyl-dithio-CoA</p> 	1988 ⁶⁰

In the 1990s, the work of D. G. Drueckhammer's group would take development of CoA analogs used as mechanistic probes a step further by improving the upon existing CoA syntheses via chemoenzymatic synthesis, and synthesizing various reaction intermediate analogs⁶². Although it had been shown previous that purified CoA biosynthesizing enzymes, phosphopantetheine adenosyl transferase (PPAT/CoaD) and dephospho-CoA kinase (DPCK/CoaE) could be used to synthesize CoA from ¹⁴C -labelled CoA, the promiscuity of these enzymes toward unnatural substrates was unknown⁶³. This research group determined that CoaD/CoaE were able to accept diverse substrates with modified aletheine moieties, paving the way for contemporary CoA analog chemoenzymatic synthesis⁶². Also notably, Drueckhammer and colleagues synthesized a variety of acyl-CoA analogs meant to mimic intermediates of enzymatic reactions⁶⁴. As an example, this research group produced analogs that mimic the tetrahedral intermediate of acyltransfer performed by various acetyltransferases by substituting carbonyl of acetyl-CoA with a secondary alcohol in *R/S* forms⁶⁵. Using these diastereomers, the researchers found through inhibition assays that three model acetyltransferases bind the *S*-alcohol analog with significantly higher affinity than the *R*-

alcohol analog. Thus, these probes led to the discovery of previously unknown stereochemical preference for various types of acetyltransferases.

Table 1.4 Report of reaction intermediate analog, hydroxyethyl-CoA.

Compound (<i>substitutions shown in red</i>)	Reported year
<p>(<i>R/S</i>)-hydroxyethyl-CoA</p> 	1995 ⁶⁵

1.5.2 Structure-function studies of acyl-thioester analogs seek to elucidate key conformational changes

Up to this point, most mechanistic investigations of CoA utilizing enzymes had not been structural in nature. Synthetic chemists producing acyl-CoA analogs would often characterize the affinity of the analog toward enzymes, showing that it provides insight for a potential mechanistic probe⁶⁶. However, the group led by H. M. Holden and J. A. Gerlt produced a novel analog of methylmalonyl-CoA at the turn of the millennium⁶⁷. This analog removed the thioester carbonyl of methylmalonyl-CoA, leaving behind a thioether group in place. This analog, (2*S*)-carboxypropyl-CoA, was referred to as the thioether analog, and was co-crystallized with the enzyme methylmalonyl-CoA decarboxylase (MMCD) from *E. coli*. The co-crystal structure of MMCD was determined with the thioether analog bound in the active site at a resolution of 2.7 Å – relatively low for mechanistic studies, Figure 1.13. The thioether analog had its carboxylate moiety positioned to interact with the active site His-66 and Gly-110. However, modeling studies and comparison to the ligand bound structure of homologous 4-chlorobenzoyl-CoA dehalogenase did not support the positioning of the thioether analog with MMCD to be catalytically relevant. Rather, this interaction adopted by the thioether analog with His and Gly residues is likely an artifact of the missing thioester functional group, which was proposed to be coordinated by these

residues. The authors instead hypothesized that the carboxylate of methylmalonyl-CoA likely interacts with Tyr 140 in the active site to perform decarboxylation⁶⁷. A key conclusion to take away from this study is that the thioether analog may not be suitable for probing mechanism of enzymes that orient the thioester carbonyl in an oxyanion hole for catalysis.

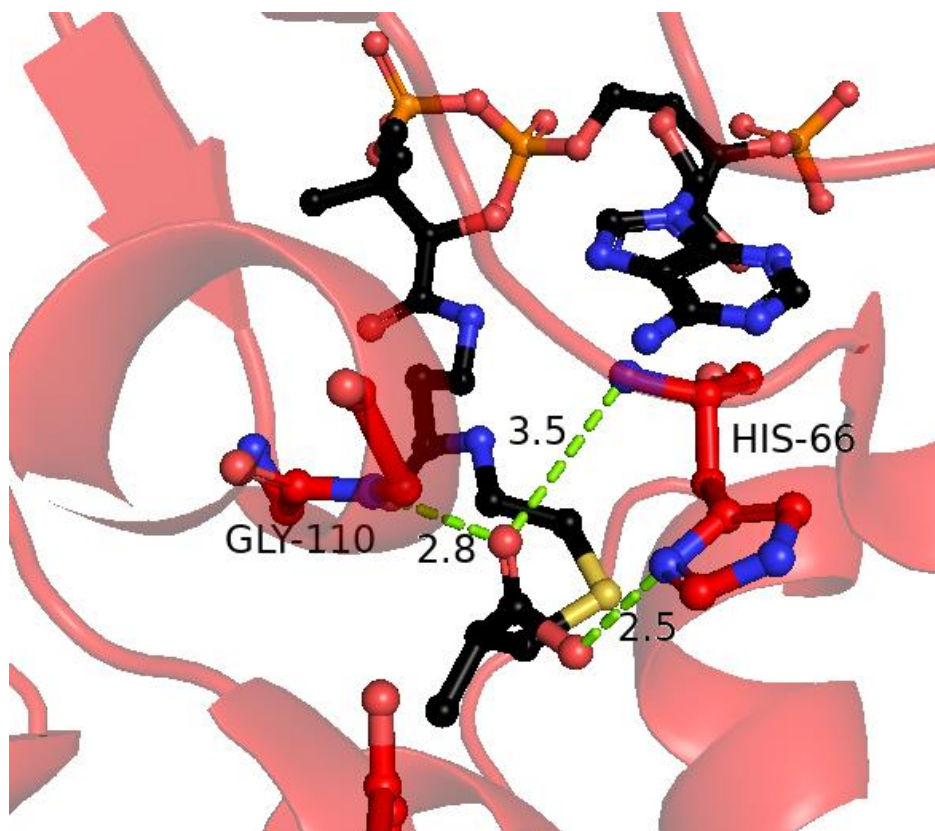


Figure 1.13 Crystal structure of *E. coli* methylmalonyl-CoA decarboxylase with (2S)-carboxypropyl-CoA (PDB: 1EF9) solved at 2.7 Å.

To provide another example in the same vein as the thioether analog from above, let's consider the work of S. Tsai and colleagues from 2018⁶⁸. In this paper, the researchers synthesized an analog of malonyl-PPANT that replaces the thioester carbonyl with an oxetane ring as probe for catalysis by daunorubicin-doxorubicin polyketide synthase (DpsC). DspC is a bifunctional AT/KS used in the synthesis the anticancer drug daunorubicin, where it uses one molecule of propionyl-CoA and malonyl-ACP to extend its polyketide chain. In this structure (PDB: 5WGC), the authors have trapped an acyl-enzyme intermediate (propionyl-Serine) with their oxetane-PPANT analog bound, mimicking the substrates in position to decarboxylate malonyl-ACP. Intuitively, the presence of the oxygen atom in the same general location as the thioester carbonyl

with the same relative molecular orbital positioning would be a quality mechanistic probe for malonyl-CoA using enzyme catalysis, Figure 1.14. However, a critical detail of this structure that is confusing is what residues form the oxyanion hole of DpsC to bind the thioester of malonyl-ACP? This is confusing as based on existing proposals of KS catalyzed Claisen condensation, we would expect the oxygen of the oxetane ring to be coordinated by an oxyanion hole, however there are no residues within range to form a polar interaction with this moiety. This disparity between the suspected location of a thioester carbonyl and the location of the oxetane ring is surprising and suggests that the oxetane-bearing malonyl-PPANT isostere is inappropriate for probing catalysis of this ketosynthase.

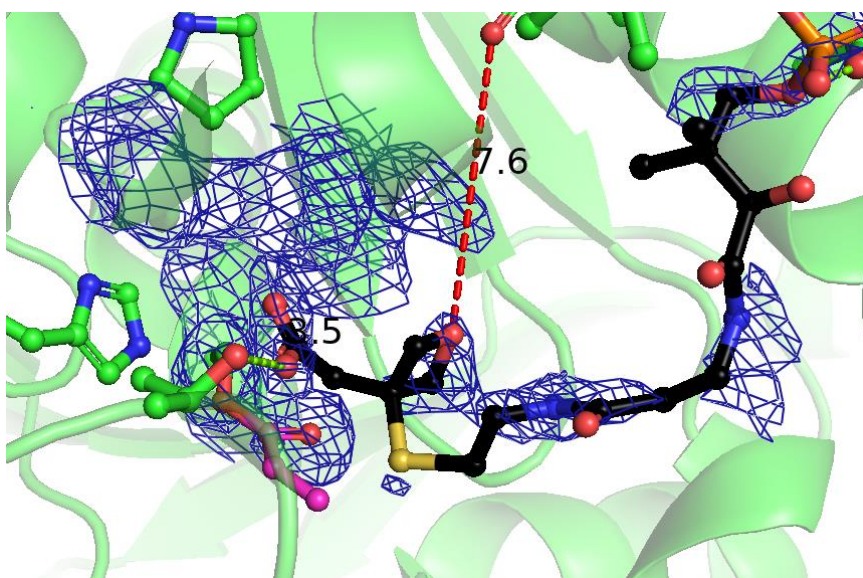


Figure 1.14 Crystal structure of *Streptomyces peucetius* DpsC with oxetane-PPANT analog bound (PDB: 5WGC) solved at 2.15 Å .

Learning from the successes and pitfalls of previous acyl-thioester analogs as mechanistic probes for enzyme catalysis, our lab, led by J. R. Lohman, reported the synthesis of sulfonate- and nitro-bearing analogs of methylmalonyl-CoA in 2019⁴⁴. These analogs feature different combinations of carboxylate and thioester substitutions for probing the catalysis of methylmalonyl-CoA using enzymes, such as MMCD. In 2019, our lab reported capture of these analogs in the active site of MMCD from *E. coli*. Unlike the previous structure of MMCD bound to the thioether analog, these structures featured the native thioester (or carbonyl-bearing analogs) situated in the oxyanion hole of MMCD formed by His-66 and Gly-110, Figure 1.15. While the

oxyanion interactions found via X-ray diffraction experiments are in line with the previously posited model for MMCD catalysis, we found that the carboxylate moiety hydrogen bonds to Thr-132, while being pressed against a hydrophobic pocket formed by several non-polar residues, Figure 1.16. This data provides support for the utility of β -carbonyl-retaining malonyl-thioester analogs in probing catalysis decarboxylating enzymes. Future studies by our group also provided evidence of the ability of these analogs to probe bifunctional AT/DC and epimerase catalysis as well^{69, 70}.

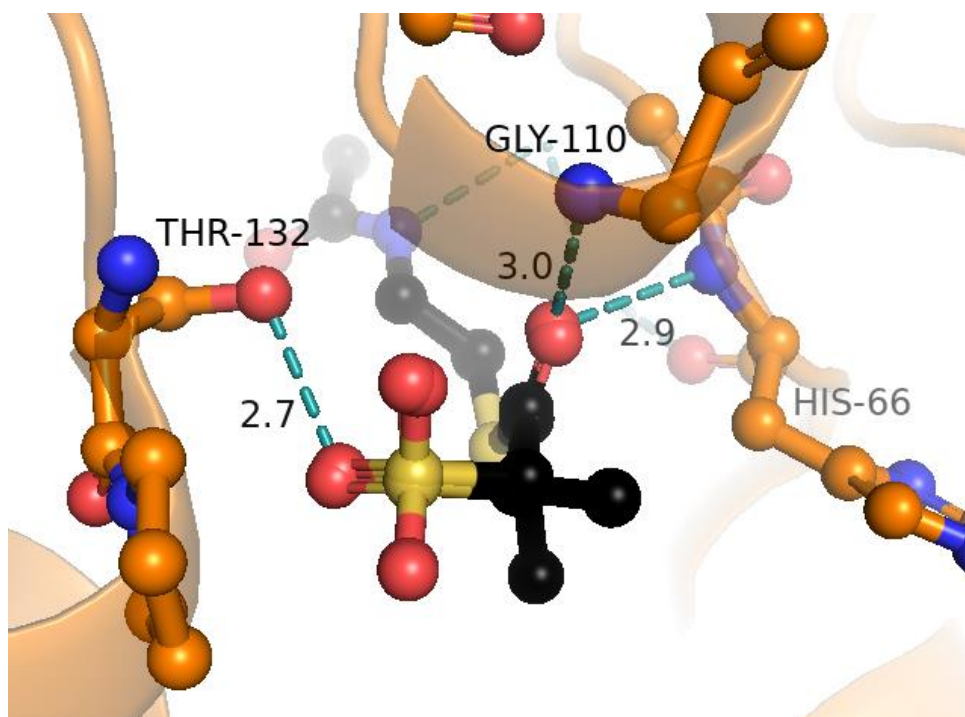


Figure 1.15 Crystal structure of *E. coli* MMCD with 2-sulfonate-propionyl-CoA bound (PDB: 6N95) solved at 1.8 Å.

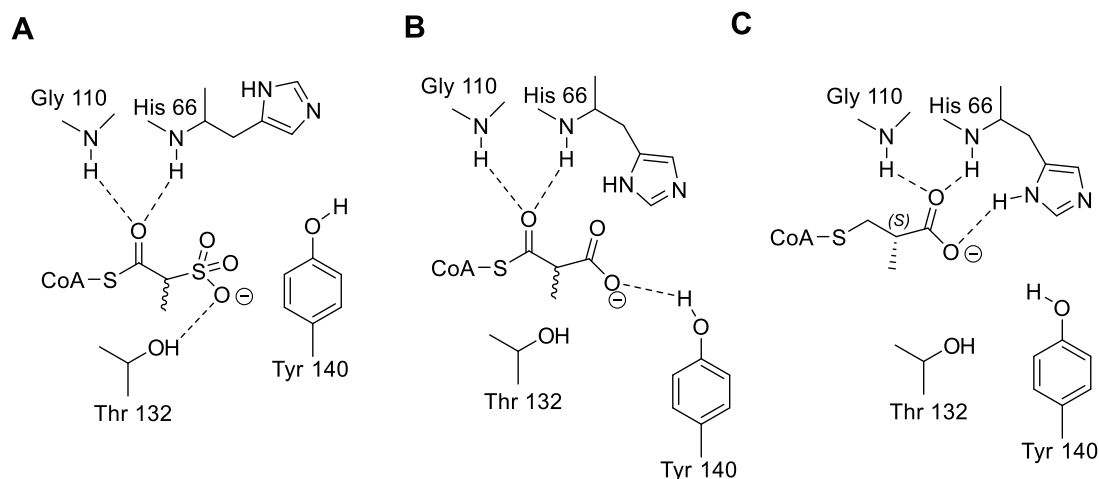


Figure 1.16 Flattened schematic displaying: A) 2-sulfonate-propionyl-CoA bound to MMCD, B) (2*R/S*)-methylmalonyl-CoA modeled with MMCD, C) (2*S*)-carboxypropyl-CoA bound to MMCD.

1.6 Our lab has applied acyl-CoA analogs as mechanistic probes to KS and carboxylase catalysis via kinetic and structure-function studies

We have seen multiple examples of the evolution of various CoA and acyl-thioester analogs employed as mechanistic probes with successes and pitfalls of various substitutions made along the way. In summary, for an acyl-thioester analog to serve as an effective mechanistic probe of an enzyme, it should deviate minimally in terms of size, charge, polarity, and function group presence from the molecule it is to mimic. Afterward, the affinity of the analog for the enzyme should approximate the K_M of the mimicked molecule. Lastly, the binding of the analog should be observed via structural/computational studies and critically evaluated for catalytic relevance. The diverse skillset required of organic synthesis, enzyme kinetics, assay development, structural techniques (e.g. X-ray diffraction, cryo-EM, or NMR), and computational work creates a complex barrier to overcome when performing mechanistic experiments. When combined with the need to multiple analogs to thoroughly approximate the reaction coordinate of the enzyme catalysis, characterizing the catalysis of a single enzyme may take decades, as seen for MMCD.

When we consider the complexity of chemistry performed by the KS enzymes of FAS and PKS, one might appreciate the difficulty in understanding how these enzymes orient the appropriate substrates and lower the activation energy to generate critical biological molecules. Understanding the details C-C bond forming catalysis of KS and carboxylases has been the subject of my graduate work. Here, I aim to convince the reader of the utility of the acyl-thioester analogs

I have synthesized as mechanistic probes that we lead to success in structure-function analysis of C-C bond forming enzymes. To reach this goal, I have synthesized several acyl-thioester analogs, assessed their stability to different enzymatic chemistries, determined the K_i of the analogs and compared them with the K_m of mimicked molecules for a given enzyme, and generated preliminary data indicating the ability of these molecules to be mechanistic probes for C-C bond forming enzymes. The information gained from my graduate work will be directly applicable to rational engineering of KS to diversify PKS products and to recognizing enzyme conformational changes when designing lead compounds for inhibition.

1.7 References

- [1] Lipmann, F. (1953) On Chemistry and Function of Coenzyme A, *Bacteriological Reviews* 17.
- [2] Strauss, T. P. B. C. K. E. (2001) The biosynthesis of coenzyme a in bacteria, *Vitamins & Hormones* 61, 157-171.
- [3] Bracher, P. J., Snyder, P. W., Bohall, B. R., and Whitesides, G. M. (2011) The Relative Rates of Thiol–Thioester Exchange and Hydrolysis for Alkyl and Aryl Thioalkanoates in Water, *Origins of Life and Evolution of Biospheres* 41, 399-412.
- [4] Leonardi, R., and Jackowski, S. (2007) Biosynthesis of Pantothenic Acid and Coenzyme A, *EcoSal Plus* 2.
- [5] Boehringer, D., Ban, N., and Leibundgut, M. (2013) 7.5-A cryo-em structure of the mycobacterial fatty acid synthase, *Journal of molecular biology* 425, 841-849.
- [6] Heath, R. J., and Rock, C. O. (1996) Inhibition of beta-ketoacyl-acyl carrier protein synthase III (FabH) by acyl-acyl carrier protein in Escherichia coli, *The Journal of biological chemistry* 271, 10996-11000.
- [7] Qiu, X., Janson, C. A., Smith, W. W., Head, M., Lonsdale, J., and Konstantinidis, A. K. (2001) Refined structures of beta-ketoacyl-acyl carrier protein synthase III, *Journal of molecular biology* 307, 341-356.
- [8] Austin, M. B., and Noel, J. P. (2003) The chalcone synthase superfamily of type III polyketide synthases, *Natural product reports* 20, 79-110.
- [9] Erb, T. J. (2011) Carboxylases in natural and synthetic microbial pathways, *Appl Environ Microbiol* 77, 8466-8477.
- [10] Tong, L. (2005) Acetyl-coenzyme A carboxylase: crucial metabolic enzyme and attractive target for drug discovery, *Cell Mol Life Sci* 62, 1784-1803.
- [11] Knowles, J. R. (1989) The mechanism of biotin-dependent enzymes, *Annual review of biochemistry* 58, 195-221.
- [12] Campbell, J. W., and John E. Cronan, J. (2001) Bacterial Fatty Acid Biosynthesis: Targets for Antibacterial Drug Discovery, *Annual review of microbiology* 55, 305-332.
- [13] Cronan, J. E., and Waldrop, G. L. (2002) Multi-subunit acetyl-CoA carboxylases, *Progress in Lipid Research* 41, 407-435.
- [14] Agency, E. C. (2021) Methyl 2-(4-(2,4-dichlorophenoxy)phenoxy)propionate, In *Substance Infocard*, European Chemicals Agency.

- [15] Freiberg, C., Brunner, N. A., Schiffer, G., Lampe, T., Pohlmann, J., Brands, M., Raabe, M., Habich, D., and Ziegelbauer, K. (2004) Identification and characterization of the first class of potent bacterial acetyl-CoA carboxylase inhibitors with antibacterial activity, *The Journal of biological chemistry* 279, 26066-26073.
- [16] Silvers, M. A., Pakhomova, S., Neau, D. B., Silvers, W. C., Anzalone, N., Taylor, C. M., and Waldrop, G. L. (2016) Crystal Structure of Carboxyltransferase from *Staphylococcus aureus* Bound to the Antibacterial Agent Moiramide B, *Biochemistry* 55, 4666-4674.
- [17] Jens Pohlmann, T. L., Mitsuyuki Shimada, Peter G. Nell, Josef Pernerstorfer, Niels Svenstrup, Nina A. Brunner, Guido Schiffer, Christoph Freiberg. (2005) Pyrrolidinedione derivatives as antibacterial agents with a novel mode of action, *Bioorganic & medicinal chemistry letters* 15, 1189-1192.
- [18] Burton, J. D., Gronwald, J. W., Keith, R. A., Somers, D. A., Gengenbach, B. G., and Wyse, D. L. (1991) Kinetics of inhibition of acetyl-coenzyme A carboxylase by sethoxydim and haloxyfop, *Pesticide Biochemistry and Physiology* 39, 100-109.
- [19] Davies, C., Heath, R. J., White, S. W., and Rock, C. O. (2000) The 1.8 Å crystal structure and active-site architecture of β -ketoacyl-acyl carrier protein synthase III (FabH) from *Escherichia coli*, *Structure* 8, 185-195.
- [20] Price, A. C., Choi, K. H., Heath, R. J., Li, Z., White, S. W., and Rock, C. O. (2001) Inhibition of beta-ketoacyl-acyl carrier protein synthases by thiolactomycin and cerulenin. Structure and mechanism, *The Journal of biological chemistry* 276, 6551-6559.
- [21] Weissman, K. J., and Leadlay, P. F. (2005) Combinatorial biosynthesis of reduced polyketides, *Nature reviews. Microbiology* 3, 925-936.
- [22] Weissman, K. J. (2009) Chapter 1 Introduction to Polyketide Biosynthesis, In *Methods in enzymology*, pp 3-16, Academic Press.
- [23] Oefner, C., Schulz, H., D'Arcy, A., and Dale, G. E. (2006) Mapping the active site of *Escherichia coli* malonyl-CoA-acyl carrier protein transacylase (FabD) by protein crystallography, *Acta crystallographica. Section D, Biological crystallography* 62, 613-618.
- [24] Park, S. R., Yoo, Y. J., Ban, Y.-H., and Yoon, Y. J. (2010) Biosynthesis of rapamycin and its regulation: past achievements and recent progress, *The Journal of antibiotics* 63, 434-441.
- [25] Wilson, M. C., and Moore, B. S. (2012) Beyond ethylmalonyl-CoA: the functional role of crotonyl-CoA carboxylase/reductase homologs in expanding polyketide diversity, *Natural product reports* 29, 72-86.
- [26] Koryakina, I., and Williams, G. J. (2011) Mutant malonyl-CoA synthetases with altered specificity for polyketide synthase extender unit generation, *Chembiochem : a European journal of chemical biology* 12, 2289-2293.
- [27] Murata, M., and Yasumoto, T. (2000) The structure elucidation and biological activities of high molecular weight algal toxins: maitotoxin, prymnesins and zooxanthellatoxins, *Natural product reports* 17, 293-314.
- [28] Organization, W. H. (2021) World Health Organization Model List of Essential Medicines - 22nd List, Geneva.
- [29] Cooper, M. A., and Shlaes, D. (2011) Fix the antibiotics pipeline, *Nature* 472, 32-32.
- [30] Sherman, D. H. (2005) The Lego-ization of polyketide biosynthesis, *Nature biotechnology* 23, 1083-1084.

- [31] Tran, L., Broadhurst, R. W., Tosin, M., Cavalli, A., and Weissman, K. J. (2010) Insights into protein-protein and enzyme-substrate interactions in modular polyketide synthases, *Chemistry & biology* 17, 705-716.
- [32] Koryakina, I., McArthur, J., Randall, S., Draelos, M. M., Musiol, E. M., Muddiman, D. C., Weber, T., and Williams, G. J. (2013) Poly specific trans-acyltransferase machinery revealed via engineered acyl-CoA synthetases, *ACS chemical biology* 8, 200-208.
- [33] Khosla, C., Herschlag, D., Cane, D. E., and Walsh, C. T. (2014) Assembly line polyketide synthases: mechanistic insights and unsolved problems, *Biochemistry* 53, 2875-2883.
- [34] Ferrer, J. L., Jez, J. M., Bowman, M. E., Dixon, R. A., and Noel, J. P. (1999) Structure of chalcone synthase and the molecular basis of plant polyketide biosynthesis, *Nat Struct Biol* 6, 775-784.
- [35] Keatinge-Clay, A. T., Shelat, A. A., Savage, D. F., Tsai, S. C., Miercke, L. J., O'Connell, J. D., 3rd, Khosla, C., and Stroud, R. M. (2003) Catalysis, specificity, and ACP docking site of *Streptomyces coelicolor* malonyl-CoA:ACP transacylase, *Structure* 11, 147-154.
- [36] Mindrebo, J. T., Patel, A., Kim, W. E., Davis, T. D., Chen, A., Bartholow, T. G., La Clair, J. J., McCammon, J. A., Noel, J. P., and Burkart, M. D. (2020) Gating mechanism of elongating beta-ketoacyl-ACP synthases, *Nature communications* 11, 1727.
- [37] Jez, J. M., Austin, M. B., Ferrer, J.-L., Bowman, M. E., Schröder, J., and Noel, J. P. (2000) Structural control of polyketide formation in plant-specific polyketide synthases, *Chemistry & biology* 7, 919-930.
- [38] Jez, J. M., and Noel, J. P. (2000) Mechanism of chalcone synthase. pKa of the catalytic cysteine and the role of the conserved histidine in a plant polyketide synthase, *The Journal of biological chemistry* 275, 39640-39646.
- [39] Austin, M. B., Bowman, M. E., Ferrer, J. L., Schroder, J., and Noel, J. P. (2004) An aldol switch discovered in stilbene synthases mediates cyclization specificity of type III polyketide synthases, *Chemistry & biology* 11, 1179-1194.
- [40] Stunkard, L. (2019) UNVEILING ENZYMATIC MECHANISMS WITH MALONYL-THIOESTER ISOSTERES, In *Biochemistry*, Purdue University, West Lafayette, IN.
- [41] Dutta, S., Whicher, J. R., Hansen, D. A., Hale, W. A., Chemler, J. A., Congdon, G. R., Narayan, A. R., Hakansson, K., Sherman, D. H., Smith, J. L., and Skinotis, G. (2014) Structure of a modular polyketide synthase, *Nature* 510, 512-517.
- [42] Whicher, J. R., Dutta, S., Hansen, D. A., Hale, W. A., Chemler, J. A., Dosey, A. M., Narayan, A. R., Hakansson, K., Sherman, D. H., Smith, J. L., and Skinotis, G. (2014) Structural rearrangements of a polyketide synthase module during its catalytic cycle, *Nature* 510, 560-564.
- [43] Lohman, J. R., Bingman, C. A., Phillips, G. N., Jr., and Shen, B. (2013) Structure of the bifunctional acyltransferase/decarboxylase LnmK from the leinamycin biosynthetic pathway revealing novel activity for a double-hot-dog fold, *Biochemistry* 52, 902-911.
- [44] Stunkard, L. M., Dixon, A. D., Huth, T. J., and Lohman, J. R. (2019) Sulfonate/Nitro Bearing Methylmalonyl-Thioester Isosteres Applied to Methylmalonyl-CoA Decarboxylase Structure-Function Studies, *Journal of the American Chemical Society* 141, 5121-5124.
- [45] Mancina, F., Smith, G. A., and Evans, P. R. (1999) Crystal structure of substrate complexes of methylmalonyl-CoA mutase, *Biochemistry* 38, 7999-8005.
- [46] Moffatt, J., and Khorana, H. (1959) The total synthesis of coenzyme A, *Journal of the American Chemical Society* 81, 1265-1265.

- [47] Günther, W. H., and Mautner, H. G. (1965) The Synthesis of Selenocoenzyme A1, 2, *Journal of the American Chemical Society* 87, 2708-2716.
- [48] Stewart, C. J., and Miller, T. L. (1965) Oxy-coenzyme A: A competitive inhibitor of coenzyme A in the phosphotransacetylase reaction, *Biochemical and biophysical research communications* 20, 433-438.
- [49] Stewart, C. J., Thomas, J. O., Ball Jr, W. J., and Aguirre, A. R. (1968) Coenzyme A analogs. III. Chemical synthesis of desulfopantetheine 4'-phosphate and its enzymic conversion to desulfo-coenzyme A, *Journal of the American Chemical Society* 90, 5000-5004.
- [50] Shimizu, M., Nagase, O., Okada, S., Abiko, Y., and Suzuki, T. (1966) Synthesis of Guano-coenzyme A, *Chemical and Pharmaceutical Bulletin* 14, 683-686.
- [51] Miller, T. L., Rowley, G. L., and Stewart, C. J. (1966) Coenzyme A Analogs. Synthesis of D-Oxypantetheine-4' Phosphate and Oxy-Coenzyme A1a,b, *Journal of the American Chemical Society* 88, 2299-2304.
- [52] Shimizu, M., Suzuki, T., Hosokawa, Y., Nagase, O., and Abiko, Y. (1970) Effect of adenine nucleotide moiety of coenzyme A on phosphotransacetylase, *Biochemical and biophysical research communications* 38, 385-392.
- [53] Stewart, C. J., and Wieland, T. (1978) Synthesis of a Carba-analog of S-Acetyl CoA, Acetyl-dethio CoA. Synthesis of a Carba-analog of S-Acetyl Coenzyme A, Acetyl-dethio Coenzyme A; an Effective Inhibitor of Citrate Synthase, *Justus Liebigs Annalen der Chemie* 1978, 57-65.
- [54] Nikawa, J., Numa, S., Shiba, T., Stewart, C. J., and Wieland, T. (1978) Carboxylation of acetyl-dethio-coenzyme A by acetyl coenzyme A carboxylase, *FEBS letters* 91, 144-148.
- [55] Ciardelli, T., Stewart, C. J., Seeliger, A., and Wieland, T. (1981) Synthesis of a carba-analog of S-palmitoyl-coenzyme A, heptadecan-2-onyldethio-CoA, and of S-Heptadecyl-CoA; effective inhibitors of citrate synthase and carnitine palmitoyltransferase, *Liebigs Annalen der Chemie* 1981, 828-841.
- [56] Michenfelder, M., and Retey, J. (1986) Methylmalonylcarba(dethia)-Coenzyme A as Substrate of the Coenzyme B12-Dependent Methylmalonyl-CoA Mutase Enzymatic Rearrangement of a β - to a γ -Keto acid, *Angewandte Chemie* 25, 366-367.
- [57] Brendelberger, G., Rétey, J., Ashworth, D. M., Reynolds, K., Willenbrock, F., and Robinson, J. A. (1988) The Enzymic Interconversion of Isobutyryl and n-Butyrylcarba(dethia)-Coenzyme A: A Coenzyme-B12-dependent Carbon Skeleton Rearrangement, *Angewandte Chemie International Edition in English* 27, 1089-1090.
- [58] Rétey. (1988) The use of carba(dethia)-coenzyme A (CH₂CoA) derivatives for mechanistic investigations, *Biofactors* 1, 267-271.
- [59] Kunz, M., and Retey, J. (2000) Evidence for a 1,2 Shift of a Hydrogen Atom in a Radical Intermediate of the Methylmalonyl-CoA Mutase Reaction, *Bioorg Chem* 28, 134-139.
- [60] Wlassics, I. D., Stille, C., and Anderson, V. E. (1988) Coenzyme A dithioesters: synthesis, characterization and reaction with citrate synthase and acetyl-CoA:choline, *Biochimica et Biophysica Acta (BBA) - Protein Structure and Molecular Enzymology* 952, 269-276.
- [61] Wang, C.-Z., Misra, I., and Miziorko, H. M. (2004) Utility of acetyldithio-CoA in detecting the influence of active site residues on substrate enolization by 3-hydroxyl-3-methylglutaryl-CoA synthase, *Journal of Biological Chemistry* 279, 40283-40288.
- [62] Martin, D. P., and Drueckhammer, D. G. (1992) Combined chemical and enzymic synthesis of coenzyme A analogs, *Journal of the American Chemical Society* 114, 7287-7288.

- [63] Stewart, C. J., and Ball, W. J. (1966) Coenzyme A Analogs. II. Enzymatic Conversion of D-Oxypanetheine 4'-Phosphate to Oxy-Coenzyme A*, *Biochemistry* 5, 3883-3886.
- [64] Martin, D. P., Bibart, R. T., and Drueckhammer, D. G. (1994) Synthesis of Novel Analogs of Acetyl Coenzyme A: Mimics of Enzyme Reaction Intermediates, *Journal of the American Chemical Society* 116, 4660-4668.
- [65] Schwartz, B., and Drueckhammer, D. G. (1996) A Stereochemical Probe of the Tetrahedral Intermediate in the Reactions of Acetyl-Coenzyme A Dependent Acetyltransferases, *Journal of the American Chemical Society* 118, 9826-9830.
- [66] Brendelberger, G., and Retey, J. (1989) Synthesis and Enzymic Conversion of Isobutanoyl-Carba(Dethia)-Coenzyme-A, *Israel J Chem* 29, 195-200.
- [67] Benning, M. M., Haller, T., Gerlt, J. A., and Holden, H. M. (2000) New reactions in the crotonase superfamily: structure of methylmalonyl CoA decarboxylase from *Escherichia coli*, *Biochemistry* 39, 4630-4639.
- [68] Ellis, B. D., Milligan, J. C., White, A. R., Duong, V., Altman, P. X., Mohammed, L. Y., Crump, M. P., Crosby, J., Luo, R., Vanderwal, C. D., and Tsai, S. C. (2018) An Oxetane-Based Polyketide Surrogate To Probe Substrate Binding in a Polyketide Synthase, *Journal of the American Chemical Society* 140, 4961-4964.
- [69] Stunkard, L. M., Kick, B. J., and Lohman, J. R. (2021) Structures of LnmK, a Bifunctional Acyltransferase/Decarboxylase, with Substrate Analogues Reveal the Basis for Selectivity and Stereospecificity, *Biochemistry* 60, 365-372.
- [70] Stunkard, L. M., Benjamin, A. B., Bower, J. B., Huth, T. J., and Lohman, J. R. (2022) Substrate Enolate Intermediate and Mimic Captured in the Active Site of *Streptomyces coelicolor* Methylmalonyl-CoA Epimerase, *Chembiochem : a European journal of chemical biology* 23, e202100487.

CHAPTER 2. DESIGN, SYNTHESIS, AND IMPROVEMENTS OF ACYL-THIOESTER ANALOGS FOR USE IN PROBING C-C BOND CATALYSIS

Contributions: Jeremy Lohman and Trevor Boram designed experiments and interpreted the resulting data. Trevor Boram carried out the majority of experiments. Lee Stunkard and Aaron Benjamin performed synthesis of some small molecules and protein expression.

Note: Literature references and chemical numbers within schemes are unique within this chapter.

2.1 Abstract

Analogues of acyl-CoAs have a long, rich history of synthesis and application to the probing of enzyme catalysis. However, the landscape of acyl-CoA analogue synthesis has greatly broadened, synthetic approaches migrating to the use of chemoenzymatic synthesis of CoA. Many useful, but laborious to synthesize acyl-CoA analogues have been reproduced here for the first time using simplified synthetic methodologies. Additionally, analogues that have been synthesized before, but have had limited use in mechanistic studies are reproduced here with the intention of applying them to structure-function studies. Lastly, the synthesis of several novel acyl-CoA analogues are reported below, such as the incorporation of a 2-acetyl-phosphonate isostere of malonyl-CoA. This chapter highlights synthetic strategies of many acyl-CoA analogues I have prepared. These analogues are expected to have a wide range of application in mechanistic studies of various acyl-CoA utilizing enzymes, outlined in subsequent chapter.

2.2 The strategy of acyl-thioester analogue design involves mimicking the enzyme catalyzed transformations from substrate to product via atom substitutions that stabilize the molecule to enzyme chemistry while having minimal changes

In Chapter 1, we learned about the rich history of CoA analogue synthesis and its applications toward probing enzyme catalysis. From previous CoA analogue mechanistic studies, we know that analogues should be similar in size, charge, and polarity to the molecule they mimic. In the case of the thioether and oxetane bearing malonyl-CoA analogues, we learned the pitfalls of using analogues that deviate notably at the thioester carbonyl as probes for C-C bond remodeling enzymes. To lead to the most meaningful mechanistic studies using substrate analogues it is recommended to

synthesize a spectrum of analogs with slightly different substitutions and confirm that all of the analogs are binding with similar affinity and orientation relative to the mimicked molecule. Even a single atom change can lead to drastic changes in enzyme-analog interaction strength, as seen below for analogs used to study the reaction of citrate synthase, Figure 2.1¹. In this figure, a single atom substitution leads to a 1000-fold decrease in citrate synthase inhibitor strength.

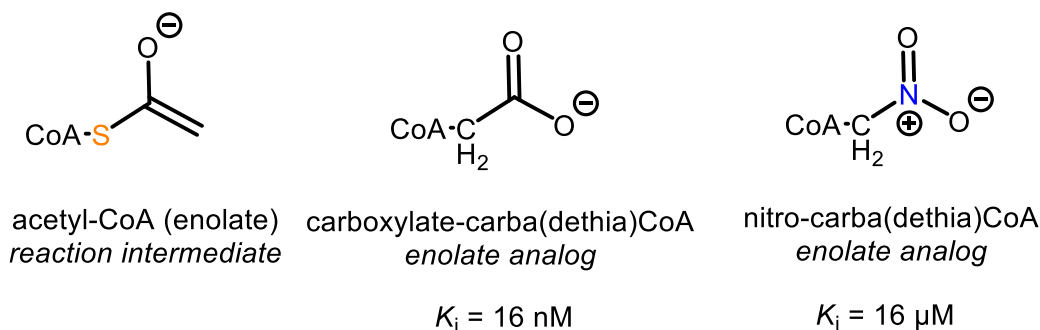


Figure 2.1 Comparison of inhibition constants of different enolate isosteres with citrate synthase.

The next consideration of analog design when probing catalysis is what molecule in the reaction is being mimicked? To illustrate this point, let's revisit KS catalysis in the below Figure 2.2.

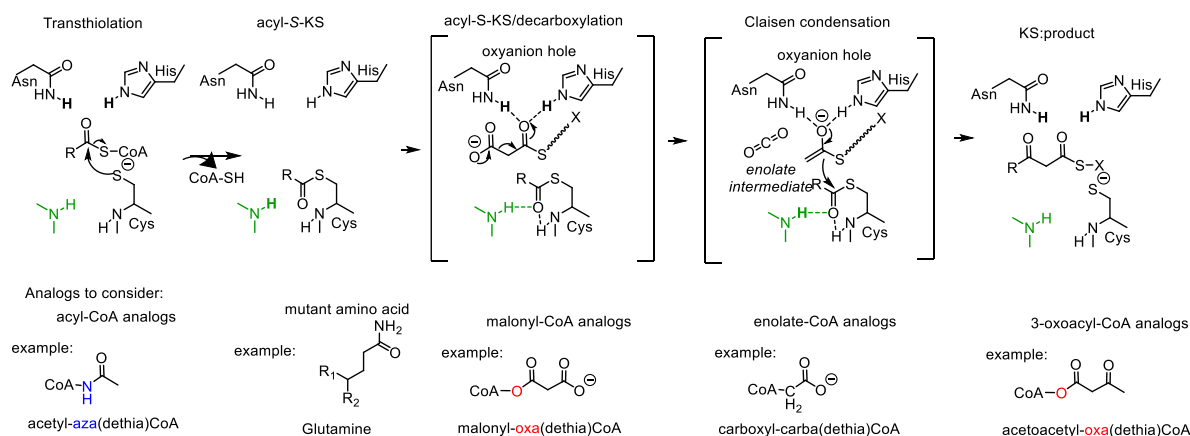


Figure 2.2 Proposed mechanism of Cys-His-Asn KS catalysis, with presentation of analogs to mimic catalytic states.

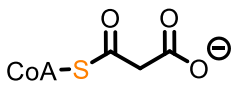
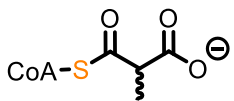
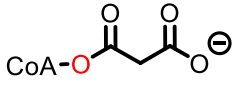
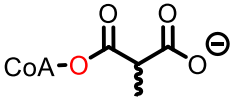
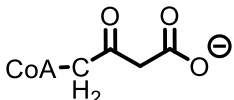
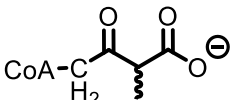
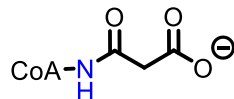
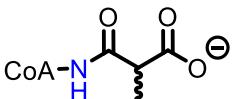
Each stage of KS catalysis can be mimicked by designing a panel of mechanistic probes resembling the ligand at each state. For example, our analogs of malonyl-CoA paired with an acyl-KS analog can allow us to make inferences about how the KS is able to lower the activation energy to

decarboxylation and orient the substrate for catalysis. With a variety of mechanistic probes, kinetic, and structure-function experiments, we can observe movement through catalytic states to propose a detailed model for KS chemistry.

2.3 Synthesis of malonyl-CoA analogs for use as mechanistic probes of C-C bond forming enzymes

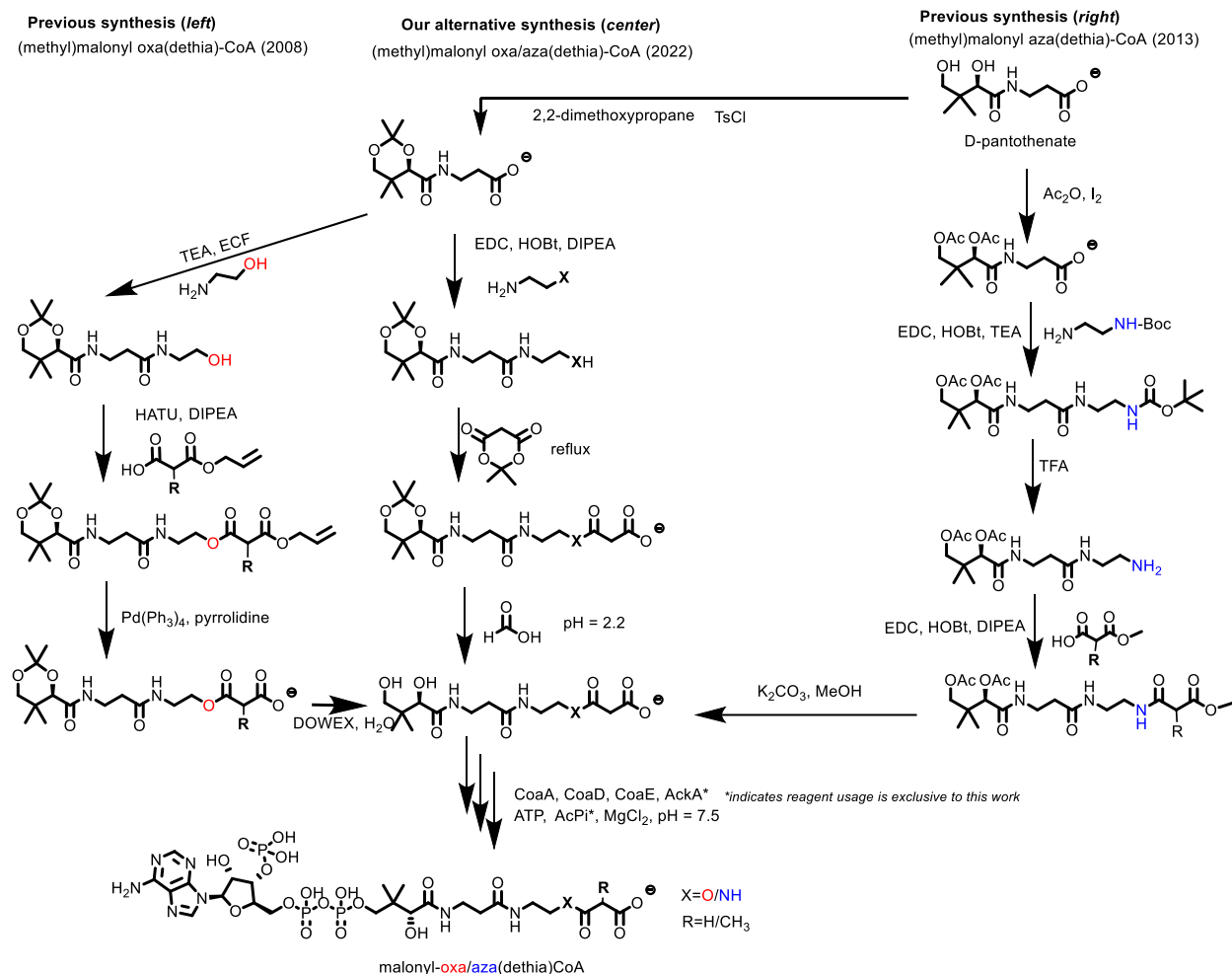
Near the end of the 2000's, the group led by Jonathan (Joe) Spencer synthesized malonyl-CoA analogs in the figure below with thioester substitutions to increase their stability to hydrolysis. The goal of these analogs was to probe the catalytic mechanism of the simple type III PKS STS by trapping various reaction intermediates and examining them via mass-spectrometry (MS)². This strategy was useful to confirm the existence of various (normally unstable) reaction intermediates. These clever analogs showed promise as mechanistic probes in structure-function studies with ketosynthases, but this potential was left unrealized by the tragic passing of Dr. Spencer in 2008. In 2013, these analogs were revisited by C. Schofield and colleagues, where the ester and ketone bearing malonyl-CoA analogs were synthesized again, as was the first (and until now only) reported synthesis of malonyl-aza(dethia)CoA³.

Table 2.1 Malonyl-CoA, methylmalonyl-CoA, and oxa, aza, and carba(dethia) thioester isosteres

sulfur substitution	malonyl-CoA and analogs	methylmalonyl-CoA and analogs
-S- (retained)	 malonyl-CoA	 methylmalonyl-CoA
-O-	 malonyl- oxa (dethia)CoA	 methylmalonyl- oxa (dethia)CoA
-CH2-	 malonyl-carba(dethia)CoA	 methylmalonyl-carba(dethia)CoA
-NH-	 malonyl- aza (dethia)CoA	 methylmalonyl- aza (dethia)CoA

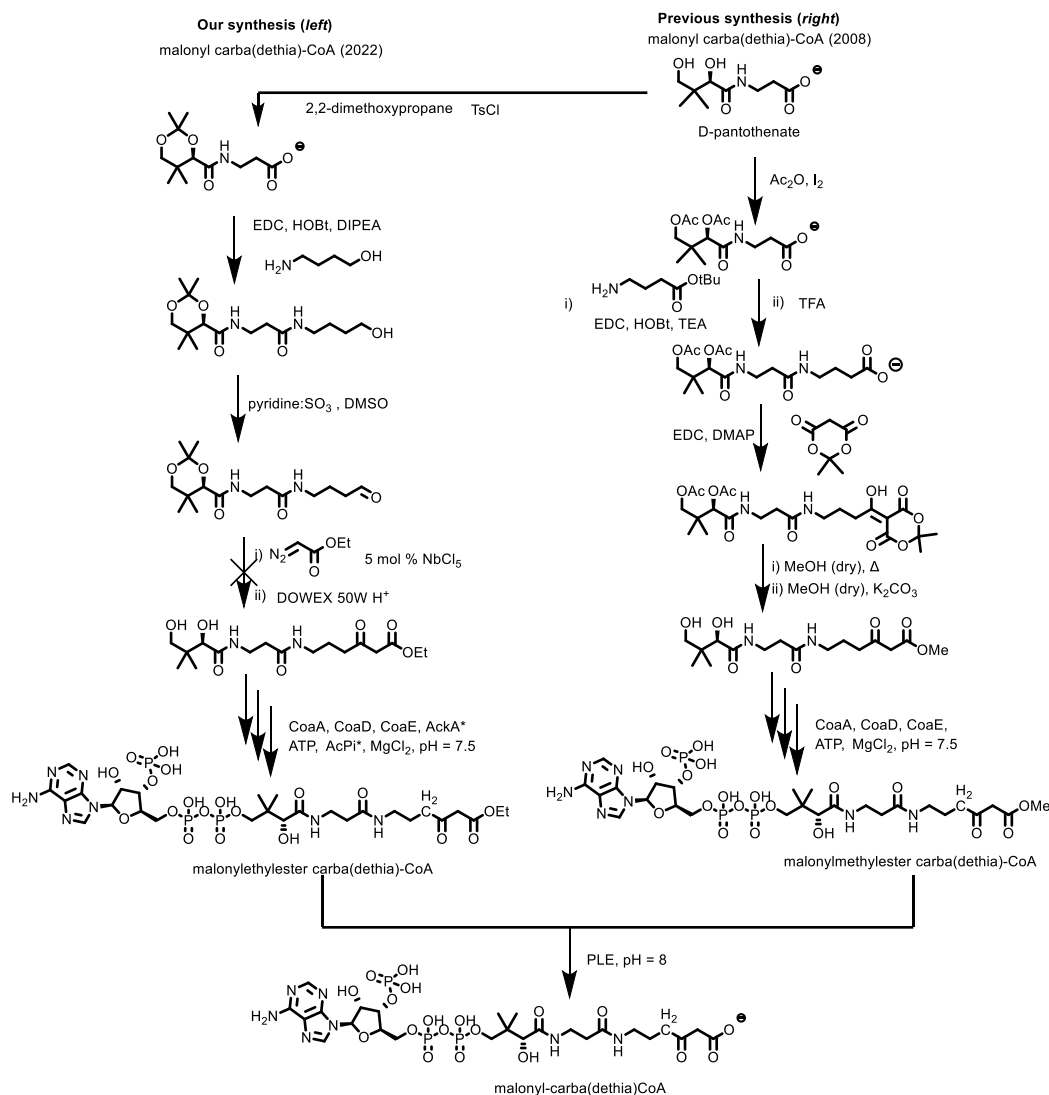
Here, we synthesize the ester and amide bearing analogs again, simplifying the synthesis of each analog by a step. In Scheme 2.1, we compare the previous reported syntheses of malonyl-oxa(dethia)CoA and malonyl-aza(dethia)CoA to our simplified synthesis for both, which reduces the number of synthesis steps to make both malonyl-oxa(dethia)CoA and malonyl-aza(dethia)CoA, while making them using the same general synthetic procedure. As is a theme in this chapter, substitution of the acyl-CoA thioester to an amide or ester minimal changes analog structure, conformation or change, while vastly increasing their stability to enzyme chemistry. Thus, we suspected amide and ester substituted malonyl-CoAs would be effective probes for malonyl-CoA using/synthesizing enzyme catalysis.

In this scheme we also illustrate how this same synthetic simplification can be used to improve upon the existing synthesis of methylmalonyl-oxa(dethia)CoA and methylmalonyl-aza(dethia)CoA. We set out to synthesize these analogs for conducting structure-function experiments with enzymes that have methylmalonyl-CoA as a substrate or product.



Scheme 2.1 Comparison of differing synthetic routes for aza(dethia) and oxa(dethia) isosteres of malonyl-CoA and (2*R/S*)-methylmalonyl-CoA.

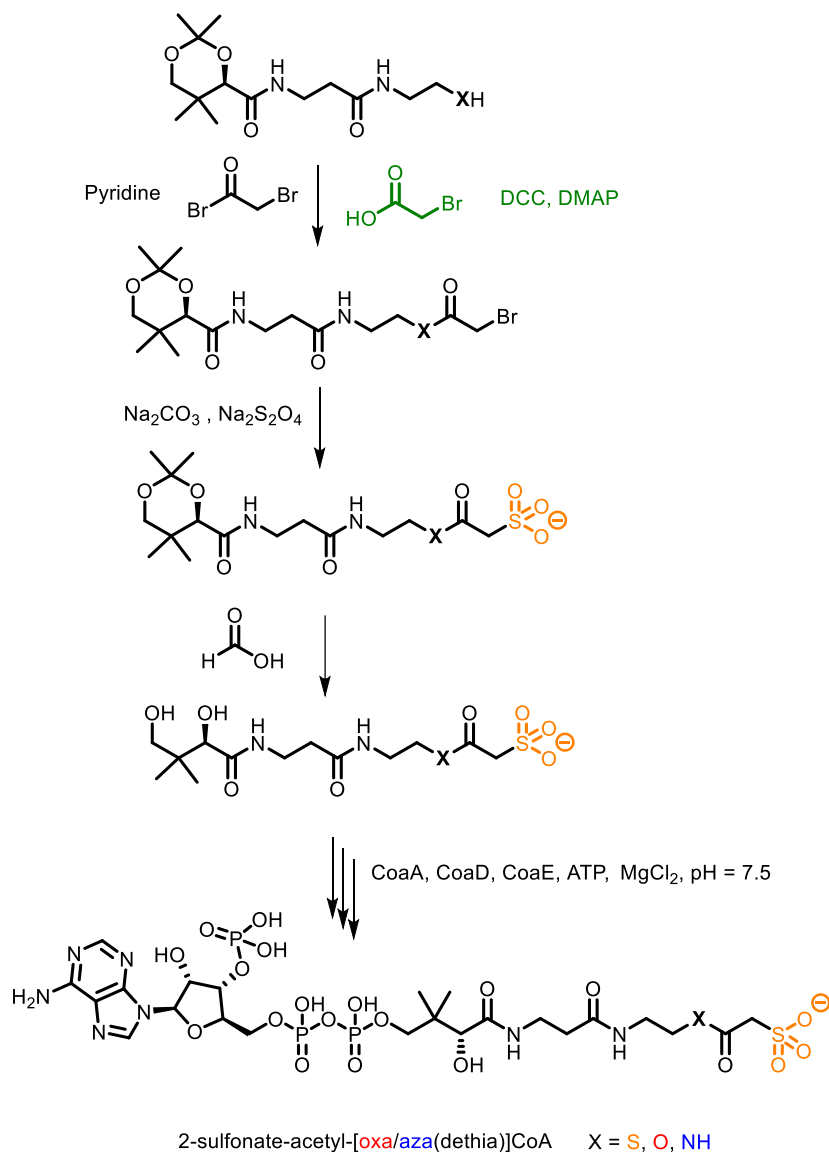
We also attempted to produce the malonyl-carba(dethia)CoA using a new procedure outlined in Scheme 2.2, which uses a formaldehyde-carba(dethia)pantetheine acetone synthon, based on previous niobium catalyzed C-C bond coupling reports⁴. The synthesis of the β -ketoester with ethyldiazoacetate leads to poor yield, thus not improving upon the existing synthesis. Unfortunately, the lack of stability of the malonyl-carba(dethia)CoA analog (which rapidly decarboxylates) limits its utility to substrate trapping and kinetic experiments, as it is not suitable for structure-function studies⁵.



Scheme 2.2 Comparison of our attempted synthetic route for malonyl-carba(dethia)CoA (left) vs. the previously reported synthesis of malonyl-carba(dethia)CoA²

To further explore malonyl-CoA analogs as probes for structure-function and kinetic experiments, we considered substitution of the carboxylate moiety for a sulfinate, sulfonate, nitro, and phosphonate moiety. We suspected that a sulfonate substitution would effectively mimic the bicarbonate model of enzyme catalyzed β -ketoacid decarboxylation. While our lab had reported synthesis of nitro and sulfonate bearing methylmalonyl-CoA analogs initially in 2019, we had difficulty achieving pure malonyl-CoA analog variants⁶. A former graduate student in the Lohman lab, Dr. Lee Stunkard, synthesized 2-sulfonoacetyl-CoA analogs, but they had low yields due to massive loss of product from the bromoacetylation step⁷. Adapting his strategy, we resynthesized

these analogs with higher yield, which is compared in Scheme 2.3. While the different synthetic steps used lead to the same intermediates, our improvements, shown in green, lead to simpler workup and higher yields.



Scheme 2.3 Synthetic improvements (*green*) for 2-sulfonate bearing isosteres of malonyl-CoA compared to their previously synthesis (*black*)⁷.

In the initial synthesis of the sulfonate-bearing isosteres of malonyl-CoA, we attempted to use sodium dithionite to convert the 2-bromoacetyl intermediate into a sulfinate isostere. Unfortunately, this species is prone to rapid oxidation under atmospheric oxygen, spontaneously converting the sulfinate into a sulfonate moiety. In theory, creating an anaerobic reaction

environment would allow for capture of the sulfinate species, but another problem we are faced with is that sodium dithionite is no more than 88% pure when prepared commercially. A common contaminant is sodium sulfite, which can react with the 2-bromoacetyl intermediate to directly produce a sulfonate. The sulfinate and sulfonate-bearing moieties are intractable. Although currently unobtainable in a pure form, the sulfinate bearing isostere would closely mimic the carboxylate of malonyl-CoA in charge and size, Figure 2.3.

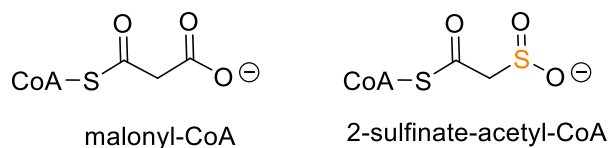
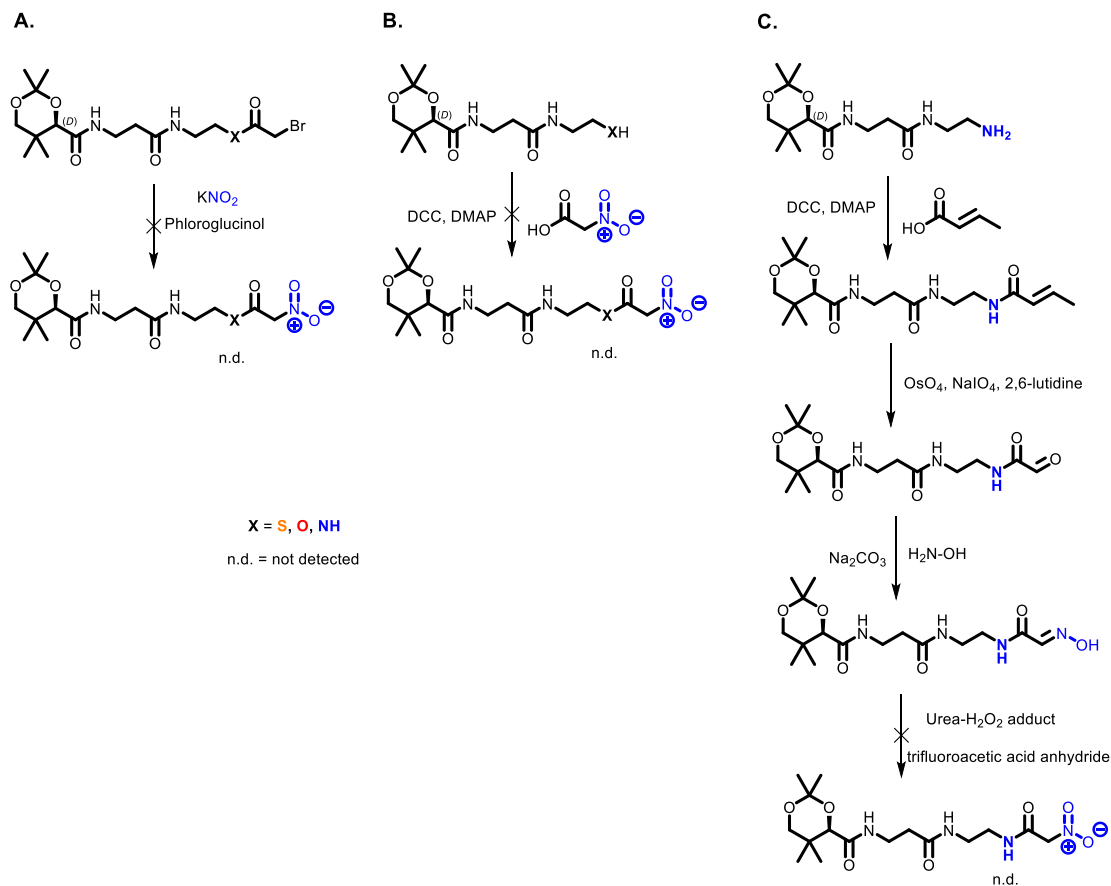


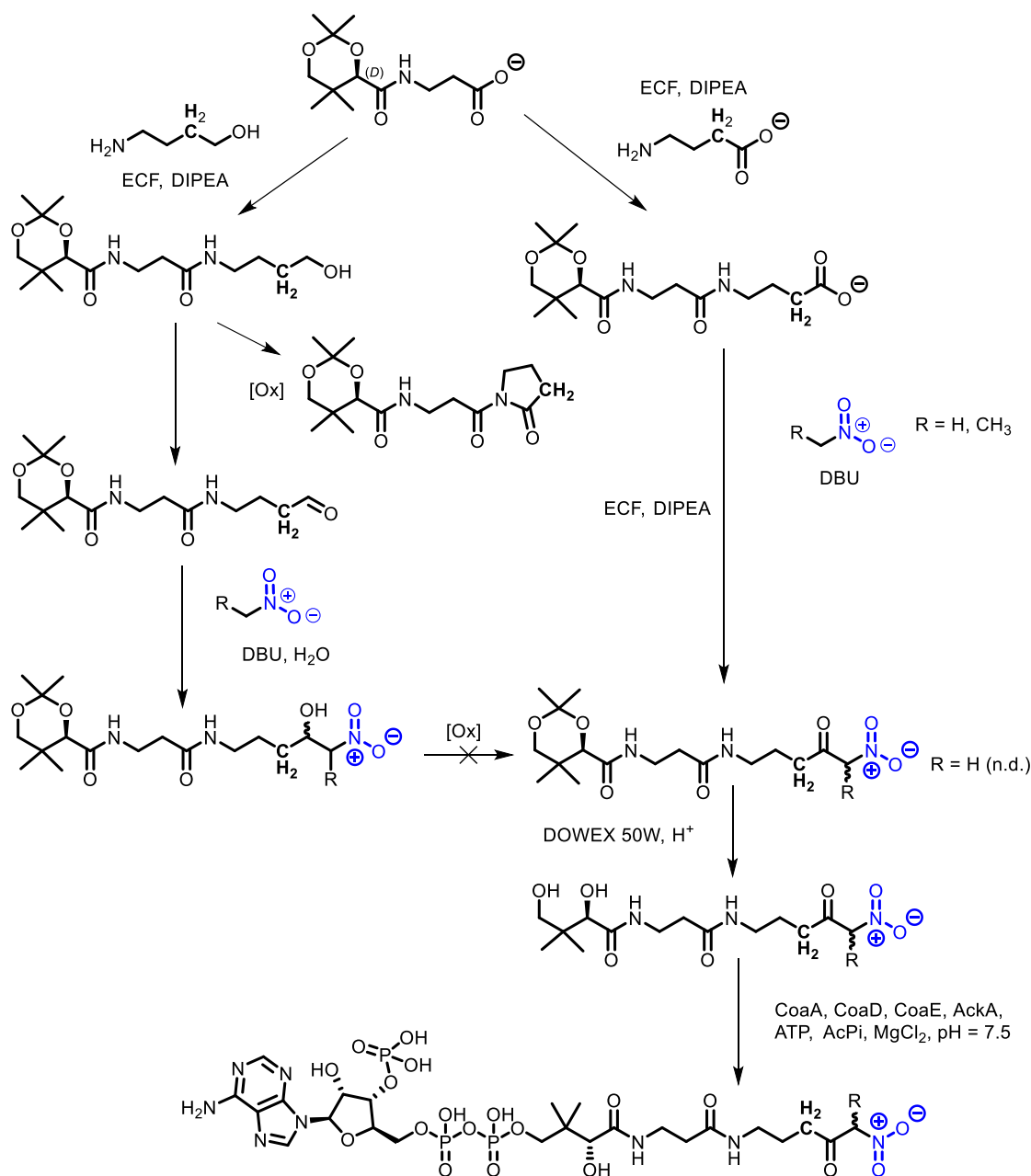
Figure 2.3 Comparison of 2-sulfinate-acetyl-CoA analog to malonyl-CoA. The single sulfur atom substitution closely mimics malonyl-CoA.

Similar to the synthesis of sulfonate-bearing analogs of methylmalonyl-CoA being applied to malonyl-CoA analogs, we attempted to apply the synthesis of nitro-bearing methylmalonyl-CoA analogs to malonyl-CoA. The original α -nitroketone synthesis applies the same method as used by Dr. Stunkard in 2019 for the synthesis of methylmalonyl-CoA nitro-bearing isosteres, Scheme 2.4 A. Both Dr. Stunkard and myself were unable to detect a product from the nitration reaction via electrospray ionization-mass spectrometry (ESI-MS)⁷. Dr. Stunkard and I also attempted a second route of producing primary α -nitroketones via a nitroacetic acid synthon, Scheme 2.4 B. Based on synthesis of nitroacetamides via nitroacetic acid, I attempted this synthesis using various carbodiimides (DCC, DIC, EDC) and a mixed anhydride method (ECF), but was never able to detect a mass-to-charge ratio (m/z) in positive or negative ionization mode that was indicative of nitro product formation. On the final attempted strategy to producing the α -nitroketone isostere of malonyl-CoA, I acylated aza(dethia)-pantetheine acetamide with a crotonyl group. I then proceeded to perform oxidative cleavage of the olefin using catalytic osmium tetroxide coupled with sodium periodate, yielding a glyoxal moiety. The glyoxal moiety was converted into an acetamido oxime group using hydroxylamine in basic conditions. This reaction was incompatible with ester and thioester-bearing substrates, which were hydrolyzed easily by hydroxylamine. This intermediate was purified and characterized by NMR spectroscopy. Afterward, several attempts were made with varying conditions to oxidize the oxime into a nitro group using trifluoroperoxyacetic acid generated *in situ* via reaction of trifluoroacetic anhydride and urea-hydrogen peroxide (UHP)

complex using the method of Ballini⁸. Alternatively, OXONE was used in place of UHP, using the method of Base and colleagues⁹. Again, conversion to nitro product was undetectable by ESI-MS, Scheme 2.4 C.



Scheme 2.4 Attempted synthesis of 2-nitroacetyl-aza(dethia)CoA via 3 routes: A) nitration of 2-bromoacetyl intermediate, B) DCC coupling of nitroacetic acid to pantetheine acetonide, C) acylation and repeated oxidation of aza(dethia)-pantetheine acetonide.



Scheme 2.5 Synthesis of (2*R/S*)-nitropropionyl-carba(dethia)CoA and attempted synthesis of 2-nitroacetyl-carba(dethia)CoA.

Not satisfied with the lack of detection of the primary α -nitroketone pantetheine acetonide product, we set out to examine the nitro forming reactions seen in Scheme 2.4 B on a test substrate. To analyze this reaction, we used benzyl alcohol as a test substrate for production of a nitroacetic ester through the same chemistry seen above. I synthesized fresh nitroacetic acid as published previously, then reacted it with benzyl alcohol¹⁰. The crude reaction was then tested via normal

phase thin-layer chromatography (TLC) against the reactant, and the reaction before addition of nitroacetic acid, Figure 2.4. The R_f of the main TLC spot from the reaction appears to have increased relative to the substrate, suggesting a potential coupling of the primary alcohol to nitroacetic acid. However, an m/z value corresponding to the anticipated product of this test reaction was not detected via ESI-MS, leaving the result of this chemistry dubious.

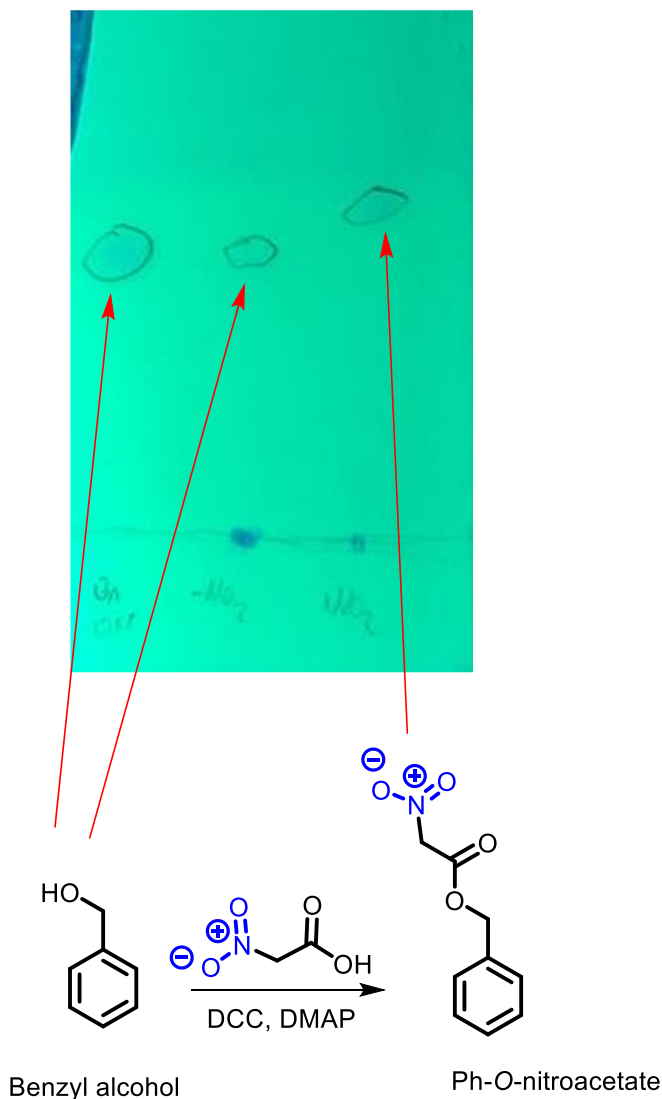
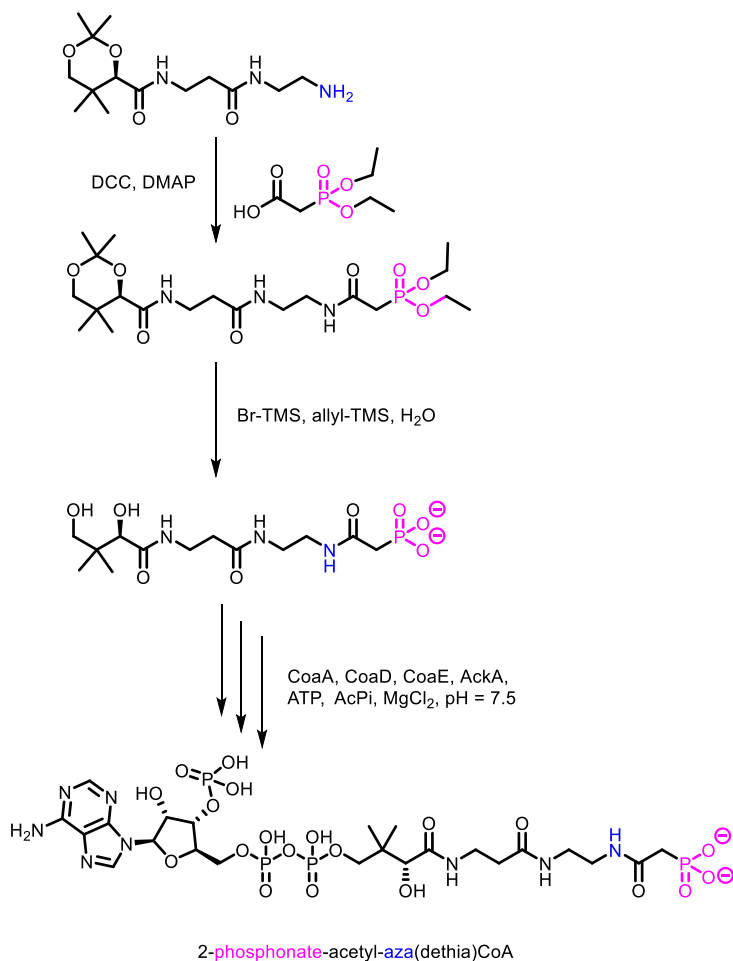


Figure 2.4 Thin-layer chromatography of different reaction states in producing phenyl-*O*-nitroacetate.

Lastly, we set out to synthesize an analog of malonyl-CoA featuring a phosphonate in lieu of the carboxylate group, while substituting the thioester to an amide moiety. This analog is expected to be stable to enzyme chemistry, but the high polarity of the phosphonate group makes

purifying the compound to be challenging. The synthesis of this analog is outlined in Scheme 2.6 below. Removal of phosphonate ethyl ester protecting groups was accomplished via McKenna reaction - careful reflux of the substrate in dichloromethane with 10-fold excess of bromotrimethylsilane (Br-TMS) with Michael acceptor allyl-TMS⁴⁴. This reaction went to completion, and simultaneous evolution of HBr removed the acetonide protecting group. The product was the incredibly polar phosphonate acetyl aza(dethia)pantetheine, which is very difficult to purify from polar reaction side products, due to its lack of retention on C18 resin, intractability from other phosphonate products on anion exchange resin, and inability to be desalted due to its low molecular weight. Instead, this material was briefly cleaned up from hydrophobic materials by washing it with ethyl acetate, then the resulting mixture was converted into a CoA product.



Scheme 2.6 Synthetic route to 2-phosphonate-acetyl-aza(dethia)CoA

The successfully synthesized malonyl-CoA and methylmalonyl-CoA analogs were examined in kinetic and structure-function experiments with model KSs, ATs, decarboxylases (DCs), and carboxylases, which will be discussed in Chapters 3 and 4.

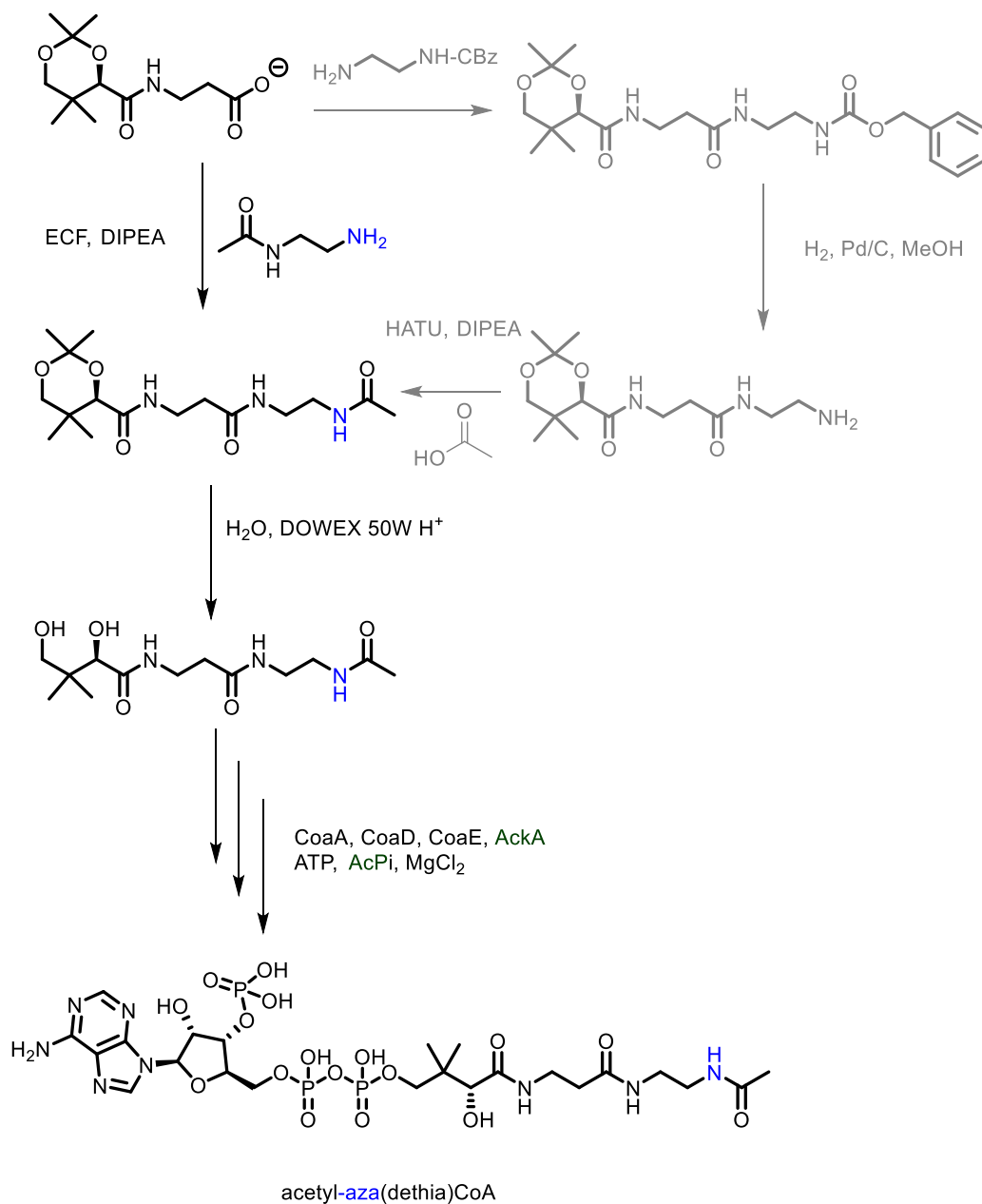
2.4 Synthesis of stable acyl-CoA, enolate, and product analogs provides a means to probe enzyme catalysis for KS, carboxylases, and related acyl-CoA using enzymes

The majority of the analogs in this section have been previously synthesized, and either feature improvements over previous syntheses or use the same method outright with new application. However, many of these analogs have never been used to study the chemistry of ketosynthase enzymes, and only feature limited previous use for probing enzyme mechanism in structure-function studies. The analogs provide a means for studying varying reaction states in acyl-CoA using enzymes. Here we revisit some of the analogs mentioned in Chapter 1 with the intention to apply them to new kinetic and structure-function studies as mechanistic probes for catalysis.

The first acyl-CoA analog we consider is acetyl-aza(dethia)CoA, which replaces the thioester function group of acetyl-CoA with an amide. Based on our knowledge of malonyl-CoA analogs, we know that substitutions to the thioester sulfur improve the stability of the linkage to hydrolysis. This analog was originally reported in 1975 in a conference abstract with a laborious chemical synthesis by C.J. Stewart's group¹². This analog would not appear again in literature until 43 years later in 2018 through the work of M.C.Y. Chang's group where it was again synthesized using a vastly improved contemporary chemoenzymatic method, Scheme 2.8¹³. Here, they would take this compound, as well as the analogous ester and ketone-bearing acetyl-CoA analogs to probe fluoroacetyl-CoA thioesterase via kinetic and structure-function experiments. We demonstrate another large improvement in acetyl-aza(dethia)CoA synthesis, where we shorten the existing scheme by 2 steps and improve the yield of these changed steps, Scheme 2.8.

Alternative synthesis (2022)

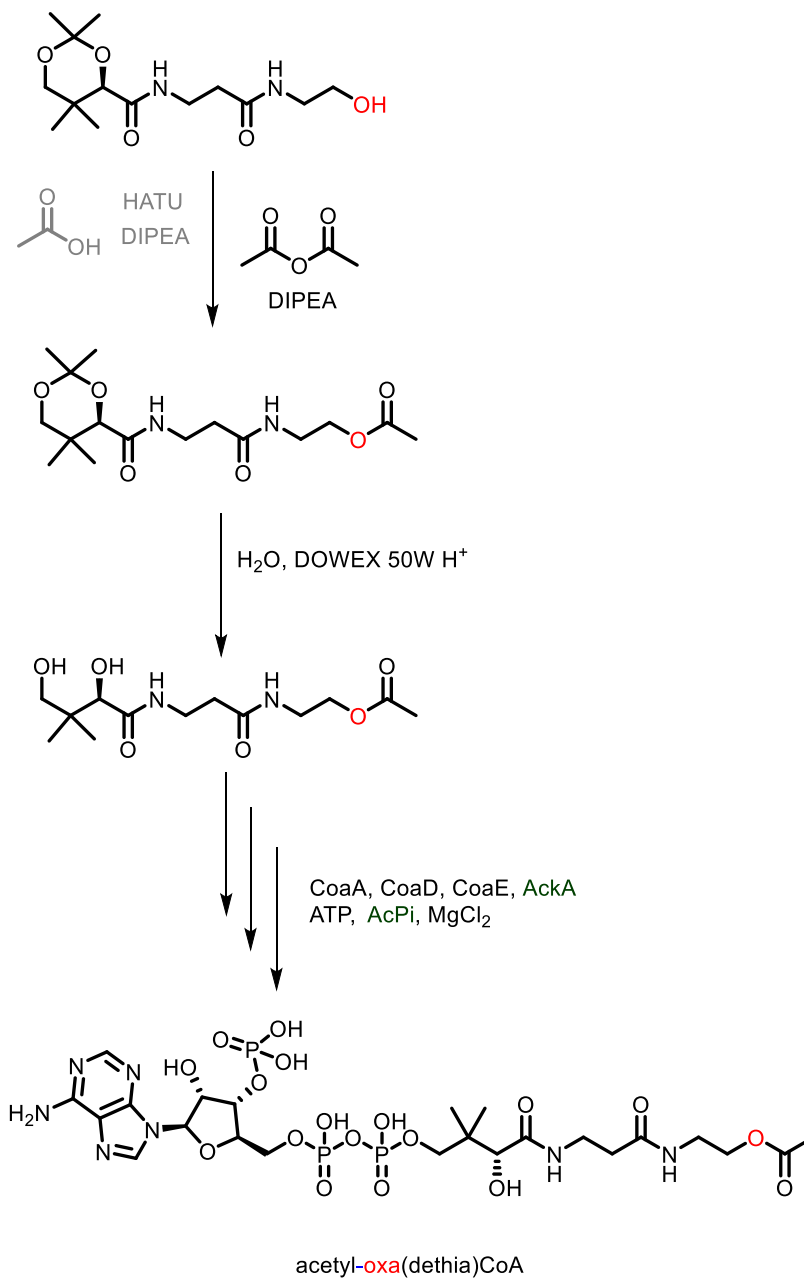
Previous synthesis (2018)



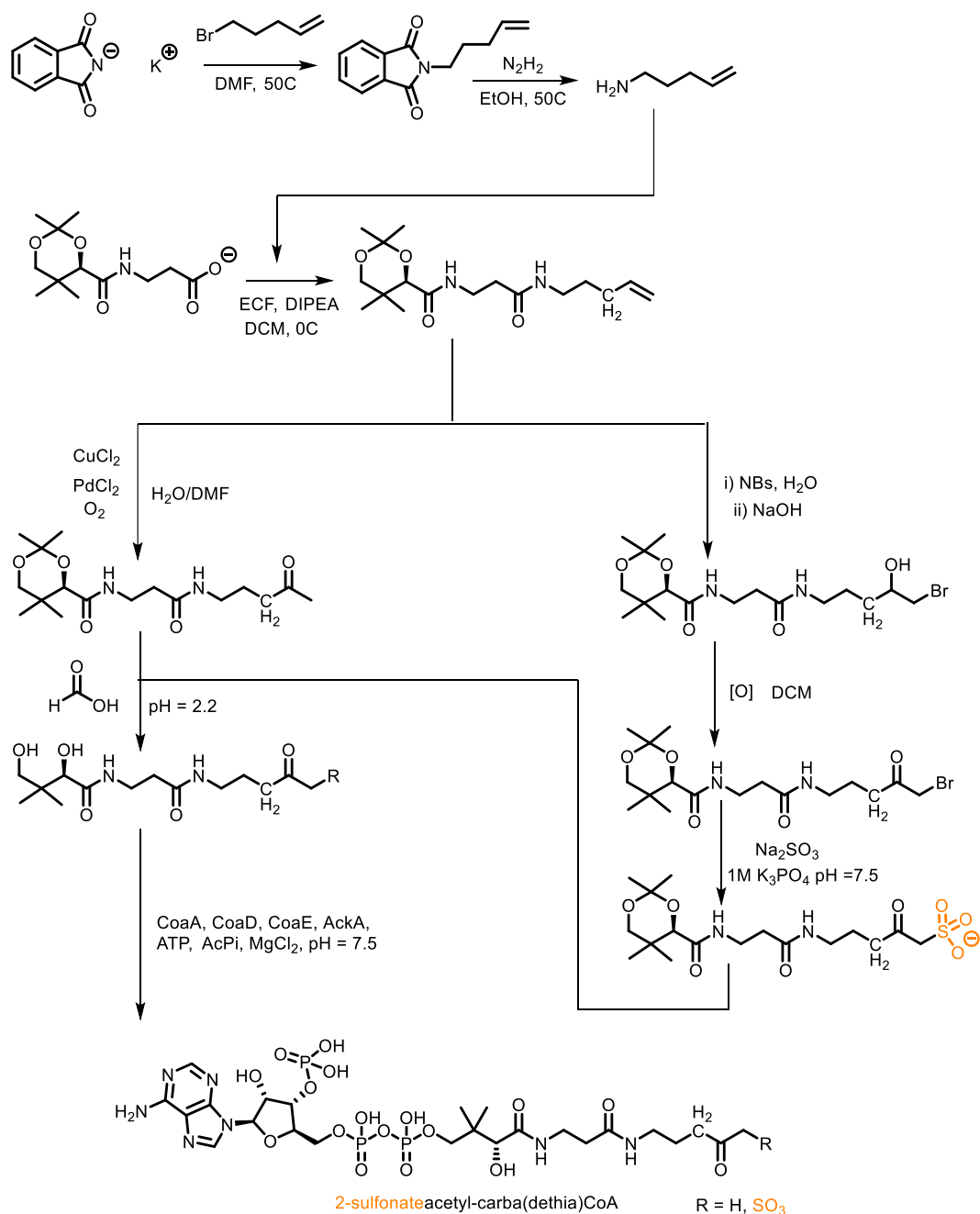
Scheme 2.7 Our synthetic route to acetyl-aza(dethia)CoA (*left*) vs. previously reported synthesis of acetyl-aza(dethia)CoA (*right*).

Similar to acetyl aza(dethia)-CoA, we also produced acetyl-oxa(dethia)CoA, this time retaining nearly the same procedure as M. Chang's research group, but improving the yield of the acetylation step by replacing acetic acid/ HATU activation for mild and volatile acetic anhydride in slightly basic conditions¹³. The resynthesized acetyl/malonyl-oxa/aza(dethia)CoA analogs will

be revisited more in-depth in their synthesis and application to studying ketosynthase catalysis in Chapter 4.



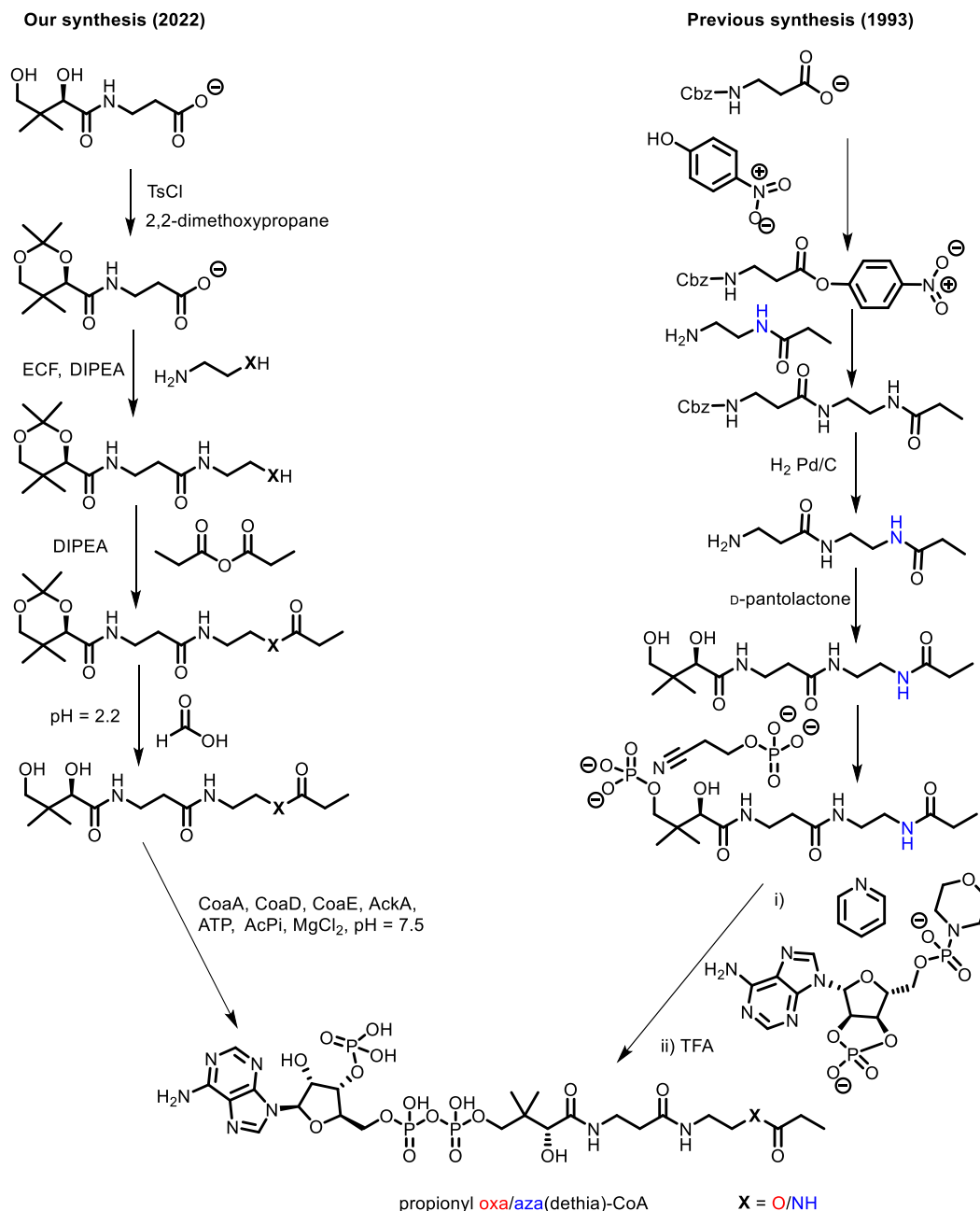
Scheme 2.8 Synthetic route and changes for acetyl-oxa(dethia)CoA. Steps exclusive to the original route are grayed out. Changes shown in the new route are shown in green text.



Scheme 2.9 New synthetic route to acetyl-carba(dethia)CoA (*left*) and novel 2-sulfonate-acetyl-carba(dethia)CoA (*right*).

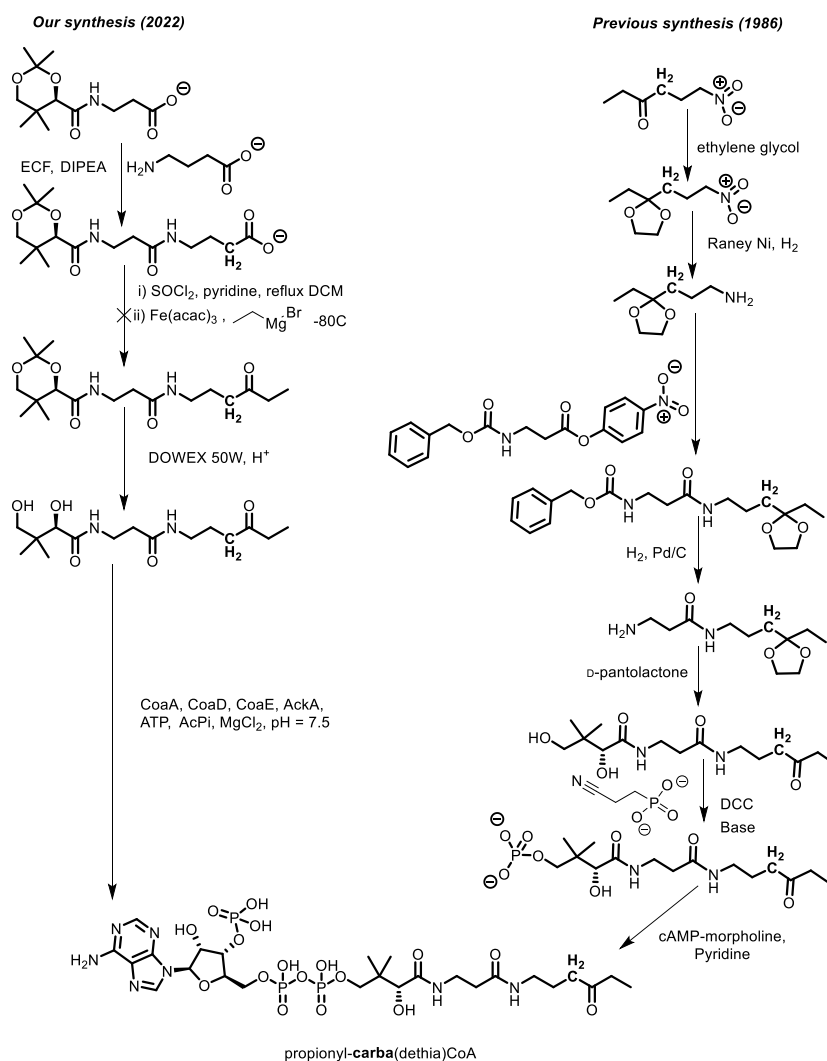
While analogs of acetyl-CoA are appropriate for studying acetyl-CoA using enzymes such as FabH, 2-PS, or ACC, other acyl-CoA analogs are needed to maintain high fidelity to the molecule being mimicked. In the case of enzymes that use propionyl-CoA (TC, PCC, or DpsC) designing stable analogs of propionyl-CoA is needed. In literature, there are few previous reports

of the synthesis of propionyl-CoA analogs, which replace the thioester with a ketone or amide¹⁴. Both of these syntheses are over 30 years old and are quite complicated. Here, we drastically improve the synthesis of propionyl-aza(dethia)CoA, while reporting the synthesis of propionyl-oxa(dethia)CoA for the first time.



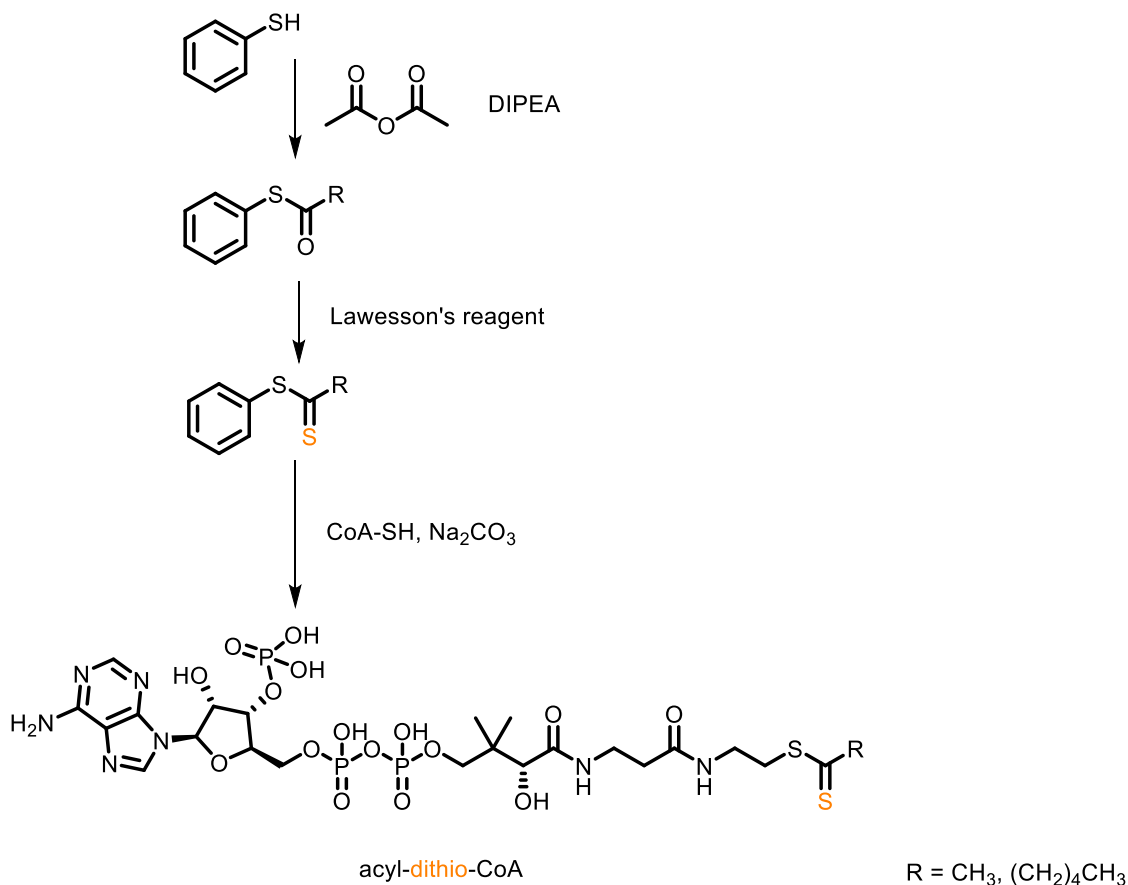
Scheme 2.10 Simplified synthesis of propionyl-aza(dethia)CoA and novel synthesis of propionyl-oxa(dethia)CoA. Our synthetic route is shown on the *left*, previous route in on the *right*¹⁵.

We additionally decided to synthesize propionyl-carba(dethia)CoA using an alternative strategy, which had not been reported in literature in over three decades. Our synthetic strategy, involved using a Grignard reagent (ethylmagnesium bromide), which acts as a carbon nucleophile to attack an pantetheine acyl chloride intermediate, leading to its alkylation. While I demonstrate this method produces product successfully, the yield is very poor as there are solvent incompatibilities between the Grignard reagent and the pantetheine substrate. Preliminary experiments in our lab suggest using a Weinreb amide functional group on a simpler aletheine substrate, then forming an amide bond with the aletheine moiety and pantothenate acetonide may be a preferable strategy.



Scheme 2.11 Simplified synthesis of propionyl-carba(dethia)CoA. Our synthetic route is shown on the *left*, previous route in on the *right*¹⁴.

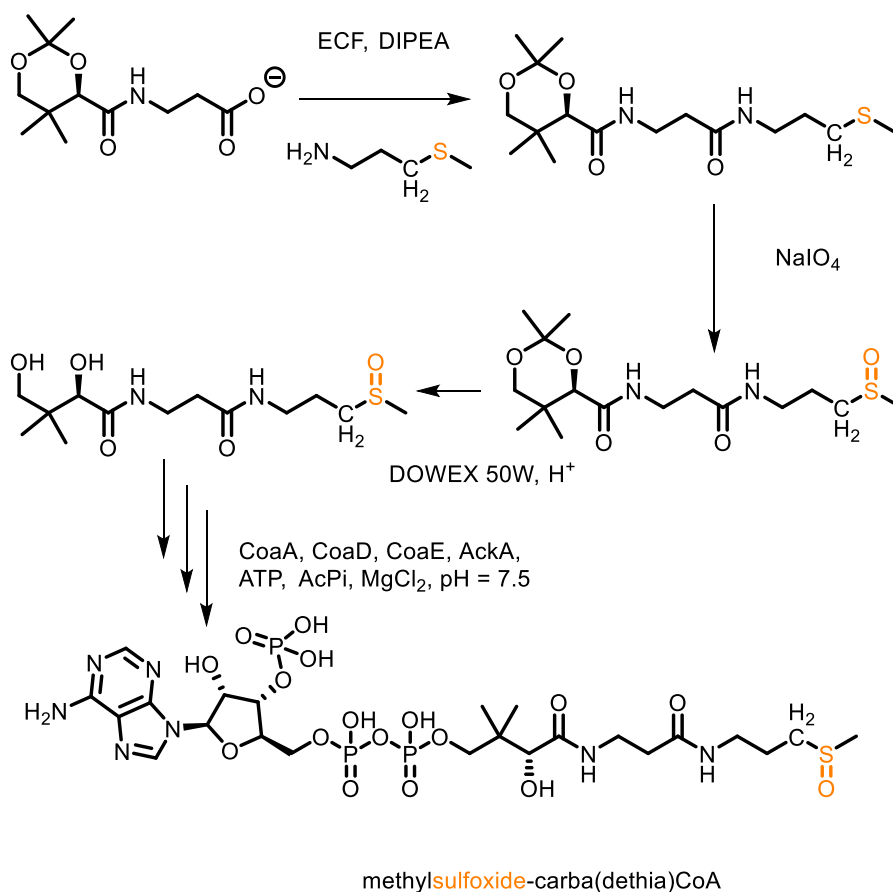
In addition to synthesis of acyl-CoA analogs with thioester sulfur substitutions, we additionally substituted the thioester carbonyl with a thiocarbonyl group. Using the same synthetic scheme as previously used by other groups, we made acetyl-dithio-CoA, and applied this chemistry to make hexanoyl-dithio-CoA for the first time, shown in Scheme 2.13⁴⁶. The acyl-dithio-CoA analogs are unique in that the thiocarbonyl group is not as electrophilic compared to a carbonyl, but the thiol of CoA is retained and is a good leaving group. These properties of the dithioester linkage allow for hydrolysis of the thiocarboxylic acid at a slow rate relative to enzyme catalyzed thioester hydrolysis. As a result, transthioylation of the acyl dithioester onto a KS catalytic cysteine may occur slowly, allowing for capture of an acyl-enzyme intermediate in structure-function studies.



Scheme 2.12 Application of previous acyl-dithio-CoA synthesis to the production of novel hexanoyl-dithio-CoA.

Like the acyl-dithio-CoA analogs, another analog type occasionally seen in literature but with minimal structure-function application are acyl-sulfoxide CoA analogs. These analogs

substitute the thioester functional group for a sulfoxide, which mimics the carbonyl in size and charge and is non-reactive to enzyme chemistry. Previously, the methylsulfoxide-carba(dethia)CoA analog has been applied to kinetic studies with the C-C bond forming enzyme citrate synthase, but has never been applied in a structure-function study to an acetyl-CoA using enzyme¹⁷. Here, we resynthesized this analog using the method reported in 2019, but improving the yield of oxidation of the thioether moiety from 25% to 70.4% using sodium periodate, Scheme 2.14¹.



Scheme 2.13 Modified synthesis of methylsulfoxide carba(dethia)-CoA. Reagents and purification strategies of this synthetic route were altered from previous work to improve the yield of this compound¹.

Many groups for the past three decades have employed the use of acyl-CoA analogs meant to mimic the enolate intermediate of C-C bond remodeling enzymes. Most of these analogs replace the thioester sulfur with a methylene group bonded to a carboxylate or amide^{17, 18}. The carboxylate

and amide linkages are proposed to mimic the enolate intermediate as the nitrogen and oxygen heteroatoms are more electron-rich and lead to partial delocalization of electron density across the function group. This partial delocalization is comparable to that seen in an enolate, which exists in resonance, Figure 2.4.

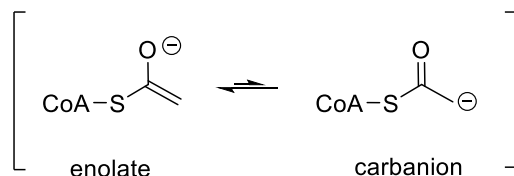
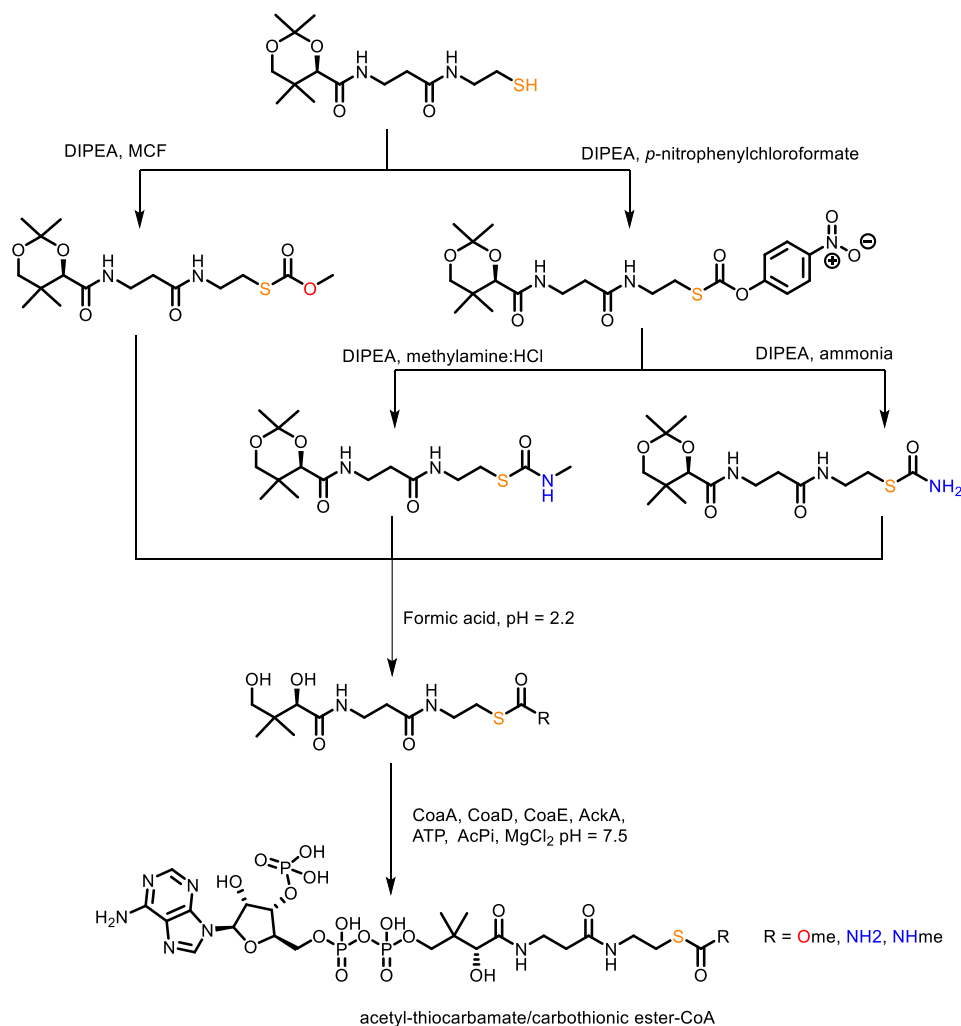
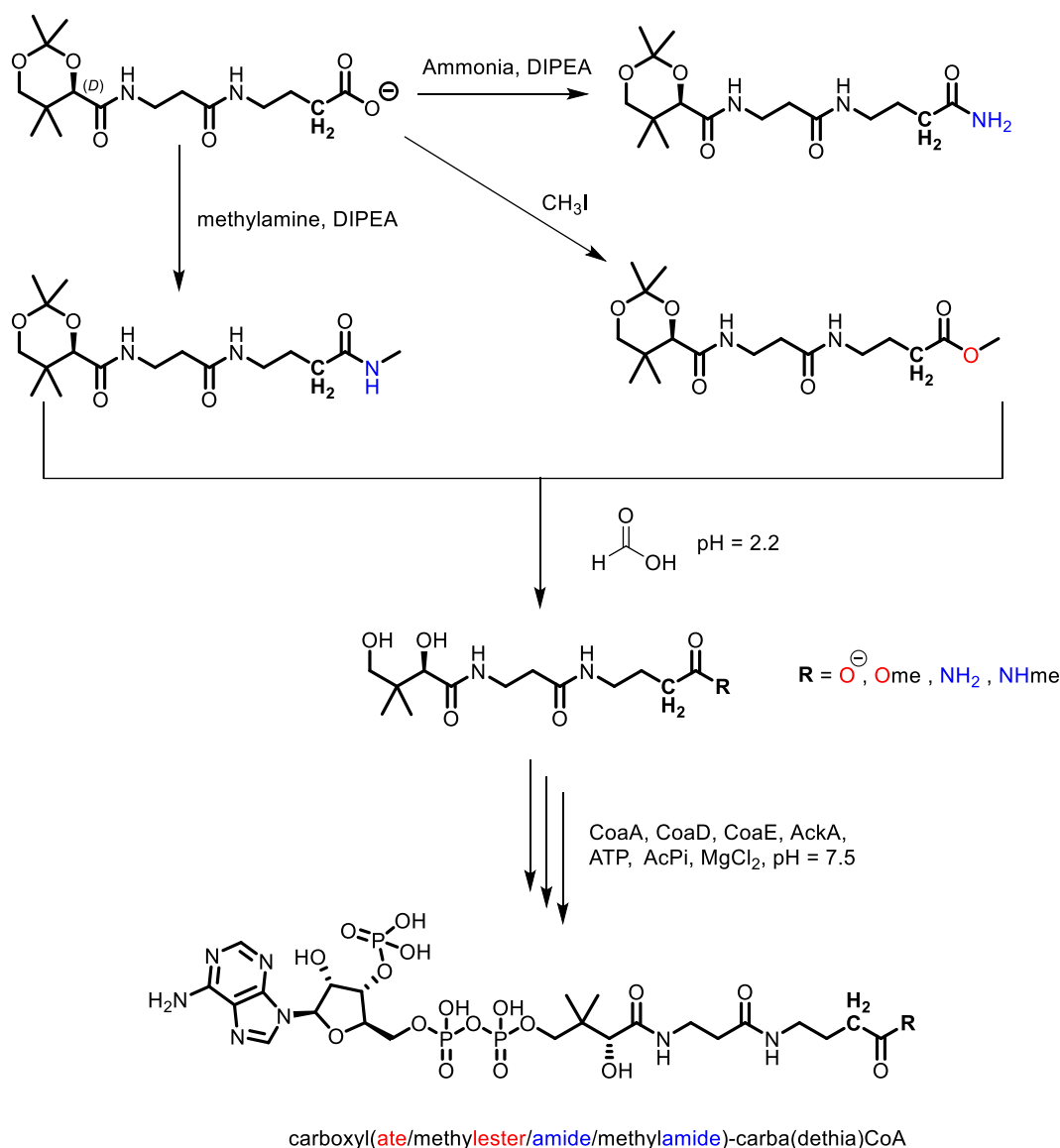


Figure 2.5 Tautomerization of an acetyl-CoA enolate intermediate.

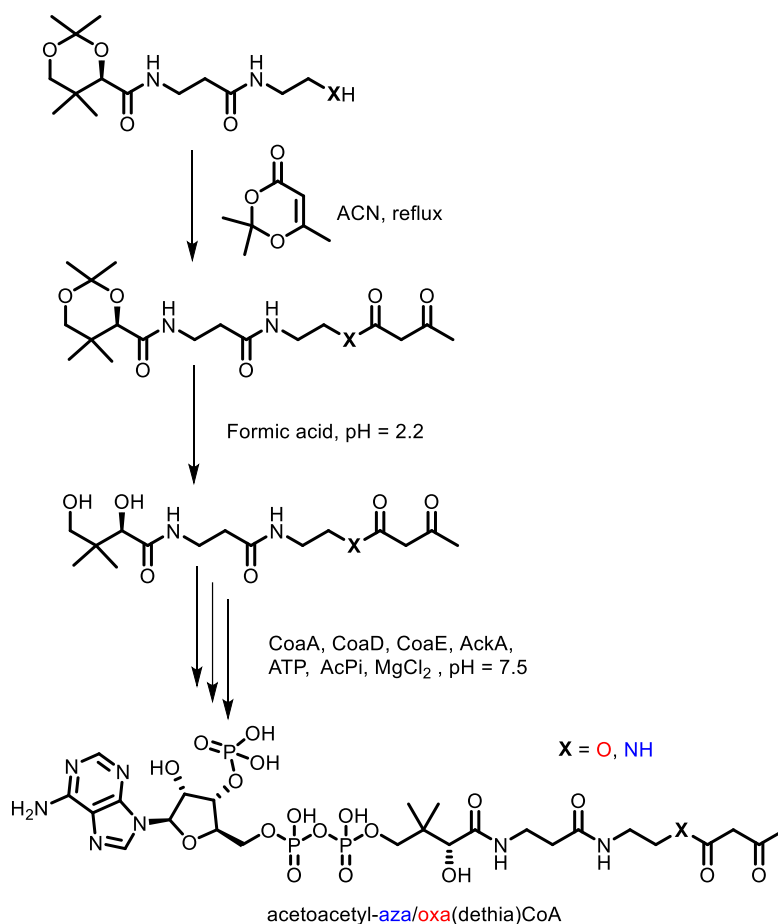


Scheme 2.14 Synthesis of thiocarbamate CoAs and a novel carbothiononic CoA ester.



Scheme 2.15 Synthetic scheme for enolate-carba(dethia)CoA analogs.

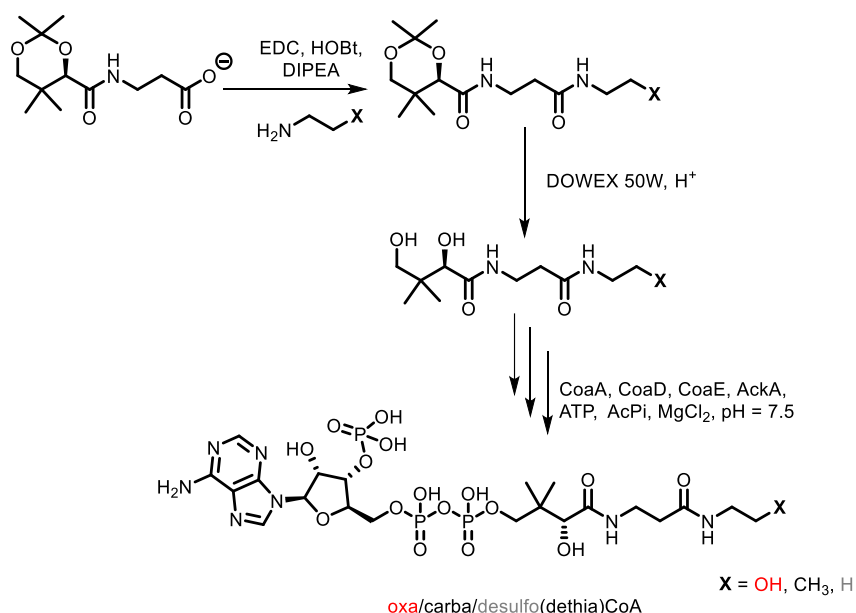
Analogues of acetoacetyl-CoA were produced as outlined below via the acetoacetylation of pantetheine acetonide isosteres, Scheme 2.16. acetoacetyl-oxa(dethia)CoA and acetoacetyl-aza(dethia)CoA were both produced rapidly using 2,2,6-trimethyl-4H-1,3-dioxin-4-one under reflux conditions. These analogues could serve as mechanistic probes to enzymes that produce acetoacetyl-CoA (such as FAS and PKS enzymes) or ones that use it as a substrate.



Scheme 2.16 Synthetic scheme for acetoacetyl-aza/oxa(dethia)CoA analogs.

2.5 Synthesis of CoA isosteres as tools for monitoring analog stability in the presence of thioester cleaving enzymes

To control for the substitution of an acyl-CoA thioester sulfur into a carba, aza, or oxa(dethia) substitution, we synthesized oxa(dethia)CoA, aza(dethia)CoA, carba(dethia)CoA, and desulfo-CoA, Scheme 2.17. The synthesis of aza(dethia)CoA proved to be more complicated than the other CoA isosteres due to its poor recognition by CoaE (*E. coli*), which is outlined in Chapter 4 of this thesis. The synthesis of the other three analogs proceeded normally via chemoenzymatic procedures detailed in Chapter 4.



Scheme 2.17 Synthesis of oxa/carba(dethia)CoA and desulfo-CoA.

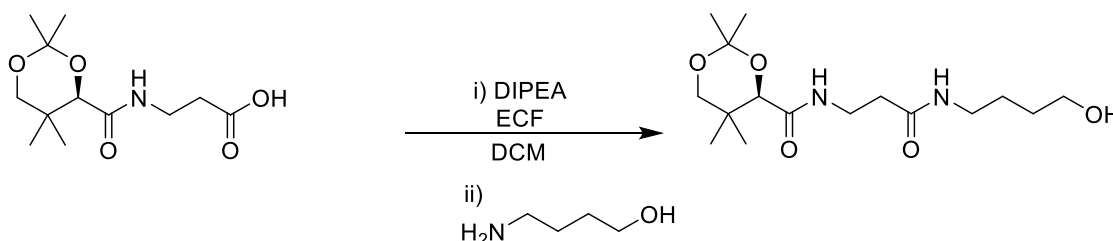
2.6 Materials and Methods

All reagents were purchased and used without additional purification from Acros, Alfa Aesar, Honeywell, Millipore-Sigma, Oakwood Chemical, TCI, or Thermo Fisher. Flash chromatography was performed on a CombiFlash Rf200 (Teledyne ISCO) with 40 gram silica columns. Solvents were dried over 4 Å molecular sieves before use. Preparative HPLC chromatography was performed on an Agilent 1100 preparative HPLC with diode array detection over a Luna 5µ C18(2) 100 Å 250 x 21.2 mm column (Phenomenex). All reactions were stirred via PTFE stir bars unless otherwise notes. Reactions and products were characterized by analytical HPLC-MS on an Agilent 1100 HPLC with diode array detection over a Luna 5 µm C18(2) 100 Å 50 x 2 mm (Phenomenex) or Luna 5 µm C18(2) 100 Å 250 x 4.6 mm (Phenomenex) with low resolution mass spectrometry (LRMS) analysis in positive and negative modes by an Agilent 1100 G1946D single quadrupole with ESI. All NMR spectra were collected on a Bruker AV500HD equipped with a 5mm BBFO Z-gradient cryoprobe in the solvents indicated. ^1H and ^{13}C NMR spectra are referenced using the signals of the residual undeuterated solvent and where applicable tetramethylsilane. All spectra were collected at 298 K. Chemical shifts are reported in parts per

million (ppm) and multiplicities are abbreviated as follows: s (singlet), d (doublet), t (triplet), q (quartet), m (multiplet), br (broad). Coupling constants (J) are reported in Hertz (Hz).

2.7 Synthetic Procedures and Results

Synthesis and characterization of malonyl/acetyl-oxa/aza(dethia)CoAs are reported in Chapter 4 of this thesis. Additionally, general procedures for the deprotection of pantetheine acetonide and the chemoenzymatic synthesis of CoA from pantetheine derivatives are outlined in Chapter 4. Pantothenic acid acetonide, aza(dethia)pantetheine, oxa(dethia)pantetheine, carboxy-carba(dethia)pantetheine acetonide, and pantetheine acetonide were synthesized as reported previously⁶. Additionally, thiomethyl-carba(dethia)pantetheine acetonide, phthalimide pentene, and pent-4-enamine were synthesized as reported previously¹.



Preparation of hydroxymethyl-carba(dethia)pantetheine acetonide via pantothenic acid acetonide.

Procedure:

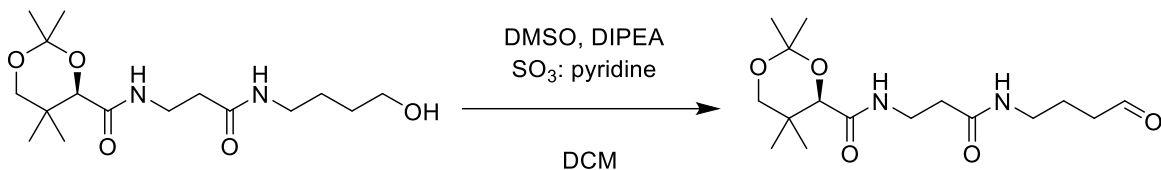
A solution of DCM containing pantethenate acetonide was mixed with DIPEA (2.5 equiv.) in a round bottom flask on ice. Ethylchloroformate (1.2 equiv.) was added slowly and the reaction was allowed to stir for 15 minutes on ice. Afterward, 2 eq. of 4-aminobutanol were dissolved in 10 ml of DCM and added dropwise to the activated carboxylic acid. The reaction was left to stir overnight, gradually warming up to room temperature. The reaction was subjected to flash chromatography (40g silica; 0 → 70% gradient of DCM → acetone over 12 column volumes) affording hydroxymethyl-carba(dethia)pantetheine acetonide.

Hydroxymethyl-carba(dethia)pantetheine acetonide:

Pantothenic acid acetonide (1000 mg, 3.85 mmol) was reacted according to the above procedure affording the pure product (clear oil, 1120 mg, 3.39 mmol, 87.9%).

¹H NMR (500 MHz, CDCl₃) δ 7.24 (d, J = 5.8 Hz, 1H), 6.96 (t, J = 6.2 Hz, 1H), 3.76 (s, 1H), 3.38 (d, J = 11.7 Hz, 1H), 3.30 (s, 1H), 3.33 – 3.20 (m, 2H), 3.15 (dq, J = 12.7, 6.2 Hz, 1H), 2.99 – 2.92 (m, 2H), 2.92 (d, J = 6.2 Hz, 1H), 2.14 (t, J = 6.7 Hz, 2H), 1.31 – 1.25 (m, 4H), 1.14 (d, J = 11.2

Hz, 6H), 0.71 (s, 3H), 0.66 (s, 3H). ^{13}C NMR (126 MHz, CDCl_3) δ 170.75, 169.39, 98.35, 77.42, 77.35, 77.16, 76.90, 76.42, 70.61, 61.01, 38.61, 34.94, 34.51, 32.23, 29.28, 28.76, 25.40, 21.48, 18.26, 18.07. MS (ESI) m/z calculated for $\text{C}_{16}\text{H}_{30}\text{N}_2\text{O}_5$ ($[\text{M}+\text{H}]^+$) 331.27, found 331.3.



Preparation of formaldehyde-carba(dethia)pantetheine acetonide via Parikh-Doering oxidation.

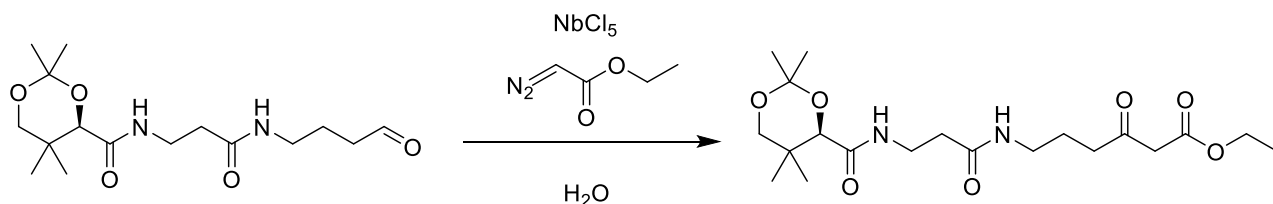
Procedure:

A solution of DCM containing hydroxymethyl-carba(dethia)pantetheine acetonide was mixed with DIPEA (5 equiv.) in a round bottom flask. DMSO (5 equiv.) was added, followed by addition of sulfur trioxide:pyridine complex (2.2 equiv.) to the stirring mixture. The reaction was left to stir for 2 hours at room temperature. The reaction was washed with saturated ammonium chloride (2 x 10 ml), then subjected to flash chromatography (40g silica; 0 \rightarrow 50% gradient of DCM \rightarrow acetone over 12 column volumes) affording formaldehyde-carba(dethia)pantetheine acetonide.

Formaldehyde-carba(dethia)pantetheine acetonide:

Hydroxymethyl-carba(dethia)pantetheine acetonide (140 mg, 0.4 mmol) was reacted according to the above procedure affording the pure product (white powder, 55.8 mg, 0.17 mmol, 42.3%).

^1H NMR (500 MHz, CDCl_3) ^{13}C NMR (126 MHz, CDCl_3) LRMS (ESI) m/z calculated for $\text{C}_{16}\text{H}_{28}\text{N}_2\text{O}_5$ ($[\text{M}+\text{H}]^+$) 329.20, found 329.2.



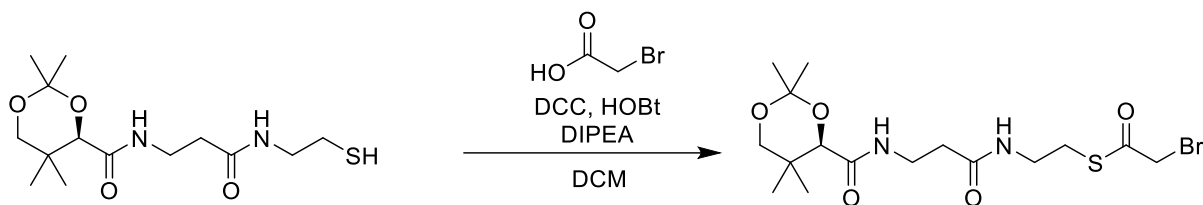
Procedure:

A solution of 6 ml of DCM containing 100 mg of formaldehyde-carba(dethia)pantetheine acetonide was mixed with niobium pentachloride (0.05 equiv.) in a round bottom flask. A 13% solution of ethyldiazoacetate (1.2 equiv.) was added dropwise. The reaction was left to stir for overnight at room temperature in the dark. The reaction was quenched by addition of 1 volume of

water (v/v). Based on HPLC peak integration, less than 10% of reactant was converted to product. The product was not purified or used in subsequent reactions.

Acetoethylacetate-carba(dethia)pantetheine acetonide:

LRMS (ESI) m/z calculated for $C_{20}H_{34}N_2O_7$ ($[M+H]^+$) 415.24, found 415.2.



Preparation of 2-bromoacetyl-pantetheine acetonide via carbodiimide activation of bromoacetic acid.

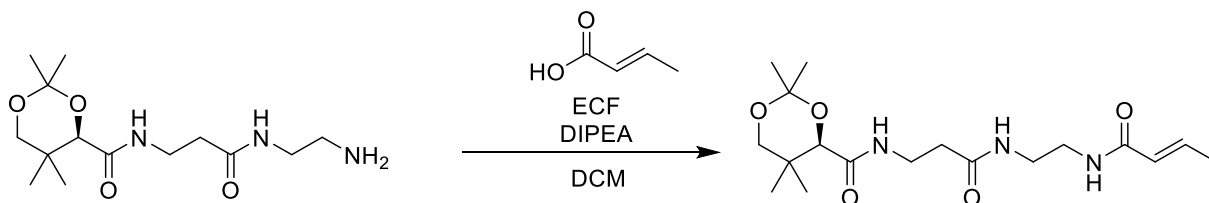
Procedure:

Pantetheine acetonide were dissolved in dichloromethane with bromoacetic acid (2 equiv.), DIPEA (3 equiv.), and HOBT (0.5 equiv.) and stirred in a round bottom flask. The reaction was initiated by addition of DCC (1.5 equiv.) and left to stir overnight at room temperature. The reaction was washed with saturated ammonium chloride (3 x 20 ml) and subjected to flash chromatography (40g silica; 0 → 50% gradient of DCM → acetone over 12 column volumes) affording 2-bromoacetyl-pantetheine acetonide.

Bromoacetyl-pantetheine acetonide:

Pantetheine acetonide (300 mg, 0.94 mmol) was reacted according to the above procedure affording bromoacetyl-pantetheine acetonide (clear oil, 261 mg, 0.60 mmol, 63.2%).

LRMS (ESI) m/z calculated for $C_{16}H_{27}N_2O_5BrS$ ($[M+H]^+$) 439.09, found 439.1, 441.1.



Preparation of (*E*)-crotonyl-aza(dethia)pantetheine acetonide via mixed anhydride method.

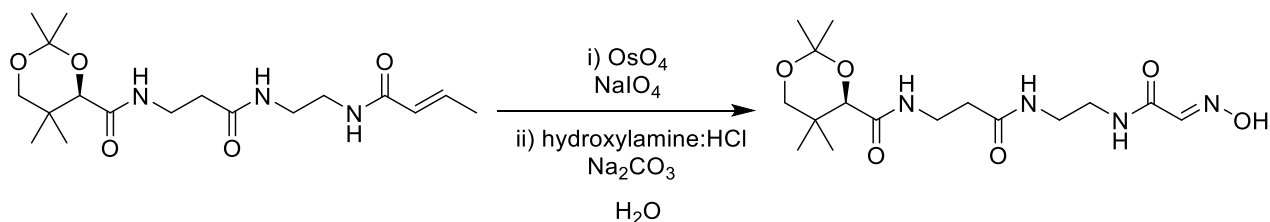
Procedure:

A solution of DCM containing *trans*-crotonic acid (1.5 equiv.) was mixed with DIPEA (2.5 equiv.) in a round bottom flask on ice. Ethylchloroformate (1.2 equiv.) was added slowly and the reaction was allowed to stir for 15 minutes on ice. Afterward, (1 equiv.) of aza(dethia)-pantetheine acetonide was dissolved in 10 ml of DCM and added dropwise to the activated carboxylic acid. The reaction was left to stir overnight, gradually warming up to room temperature. The reaction was subjected to flash chromatography (40g silica; 0 → 70% gradient of DCM → acetone over 12 column volumes) affording the (*E*)-crotonyl-aza(dethia)pantetheine acetonide.

(*E*)-crotonyl-aza(dethia)pantetheine acetonide:

Aza(dethia)pantetheine acetonide (9.6 g, 31.89 mmol) was reacted according to the above procedure affording the pure product (clear oil, 8.46 g, 22.93 mmol, 72%).

¹H NMR (500 MHz, CDCl₃) δ 7.13 (d, *J* = 5.6 Hz, 1H), 7.04 (t, *J* = 6.3 Hz, 1H), 6.78 (dq, *J* = 15.3, 6.8 Hz, 1H), 6.72 (d, *J* = 5.4 Hz, 1H), 5.81 (dq, *J* = 15.2, 1.7 Hz, 1H), 4.04 (s, 1H), 3.65 (d, *J* = 11.7 Hz, 1H), 3.59 – 3.41 (m, 2H), 3.43 – 3.30 (m, 4H), 3.24 (d, *J* = 11.7 Hz, 1H), 2.42 (t, *J* = 6.3 Hz, 2H), 1.81 (dd, *J* = 6.9, 1.7 Hz, 3H), 1.39 (s, 3H), 0.99 (s, 3H), 0.94 (s, 3H). **¹³C NMR** (126 MHz, CDCl₃) δ 172.12, 170.21, 166.95, 140.01, 124.97, 99.09, 77.32, 77.17, 77.07, 76.81, 71.38, 39.96, 39.91, 36.06, 34.94, 32.95, 29.45, 22.13, 18.88, 18.68, 17.72. LRMS (ESI) *m/z* calculated for C₁₈H₃₁N₃O₅ ([M+H]⁺) 370.23, found 370.2.



Preparation of 2-(hydroxyimino)-acetyl-aza(dethia)pantetheine acetonide via oxidative cleavage and imine formation.

Procedure:

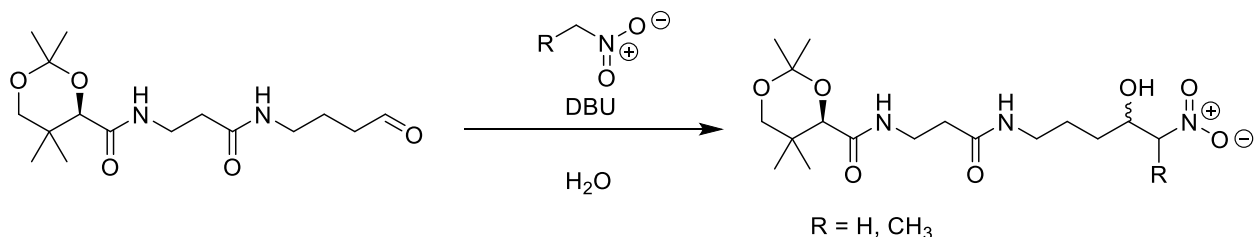
A suspension of water containing (*E*)-crotonyl-aza(dethia)pantetheine acetonide was stirred, and to it was added a 4% solution of osmium tetroxide (0.1 equiv.) in a round bottom flask. Sodium *meta*-periodate (2.2 equiv.) was added portionwise over 10 minutes and the reaction was allowed to stir for 5 hours at room temperature. Afterward, hydroxylamine:HCl (5 equiv.) and sodium

carbonate (10 equiv.) were dissolved in water, then added dropwise to the stirring glyoxal intermediate reaction, which was left to stir overnight. The reaction was subjected to flash chromatography (40g silica; 0 → 70% gradient of DCM → acetone over 12 column volumes) affording the 2-(hydroxyimino)-acetyl-aza(dethia)pantetheine acetonide.

2-(hydroxyimino)-acetyl-aza(dethia)pantetheine acetonide:

(*E*)-crotonyl-aza(dethia)pantetheine acetonide (250 mg, 0.68 mmol) was reacted according to the above procedure affording the pure product (white powder, 60 mg 0.16 mmol, 23.8%).

¹H NMR (500 MHz, MeOD) δ 4.11 (s, 1H), 3.73 (d, *J* = 11.5 Hz, 1H), 3.54 – 3.21 (m, 6H), 2.41 (t, *J* = 6.7 Hz, 2H), 1.44 (d, *J* = 4.1 Hz, 6H), 0.97 (d, *J* = 10.2 Hz, 6H). **¹³C NMR** (126 MHz, MeOD) δ 172.81, 170.87, 170.79, 163.92, 142.55, 99.00, 76.99, 70.86, 48.11, 47.94, 47.77, 47.60, 47.43, 47.26, 47.09, 38.50, 35.01, 34.84, 32.54, 28.30, 21.03, 17.99, 17.62. LRMS (ESI) *m/z* calculated for C₁₈H₃₁N₃O₅ ([*M*+*H*]⁺) 373.21, found 373.2.



Preparation of 2-nitro-hydroxyalkyl-carba(dethia)pantetheine acetonide via Henry reaction.

Procedure:

A suspension of water containing Formaldehyde-carba(dethia)pantetheine acetonide was mixed with DBU (5 equiv.) and the corresponding nitroalkane (25 equiv.) in a round bottom flask overnight. The reaction was subjected to flash chromatography (40g silica; 0 → 70% gradient of DCM → acetone over 12 column volumes) affording the 2-nitro-hydroxyalkyl-carba(dethia)pantetheine acetonide.

2-nitro-hydroxypropyl-carba(dethia)pantetheine acetonide:

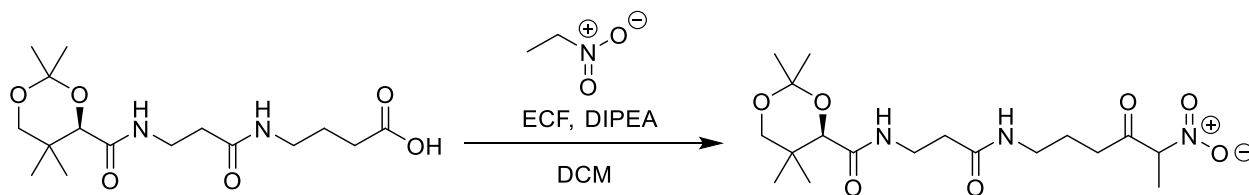
Formaldehyde-carba(dethia)pantetheine acetonide (55.8 mg, 0.17 mmol) was reacted according to the above procedure affording the pure product (orange oil, 44.1 mg, 0.11 mmol, 61%).

¹H NMR (500 MHz, CDCl₃) δ 7.07 – 7.03 (m, 1H), 6.45 (s, 0H), 4.07 (d, J = 3.8 Hz, 1H), 3.68 (d, J = 11.7 Hz, 1H), 3.52 (ddp, J = 20.4, 13.8, 6.7 Hz, 1H), 3.42 – 3.27 (m, 1H), 3.27 (d, J = 9.3 Hz, 1H), 2.63 (s, 2H), 2.55 – 2.49 (m, 1H), 2.42 (ddd, J = 20.1, 14.4, 6.7 Hz, 1H), 2.17 (d, J = 3.2 Hz, 4H), 1.99 – 1.90 (m, 1H), 1.46 (d, J = 3.4 Hz, 3H), 1.42 (s, 3H), 1.25 (s, 6H), 1.24 (s, 1H), 1.02 (d, J = 2.6 Hz, 3H), 0.96 (d, J = 2.4 Hz, 3H). **¹³C NMR** (126 MHz, CDCl₃) δ 171.50, 170.41, 99.04, 98.95, 77.45, 77.20, 77.07, 76.99, 76.94, 32.85, 29.33, 22.07, 22.02, 18.82, 18.77, 18.63. LRMS (ESI) m/z calculated for C₁₈H₃₃N₃O₇ ([M+H]⁺) 404.21, found 404.2.

2-nitro-hydroxyethyl-carba(dethia)pantetheine acetonide:

Formaldehyde-carba(dethia)pantetheine acetonide (220 mg, 0.67 mmol) was reacted according to the above procedure affording the impure product (red liquid). The product was intractable from reaction and not could be oxidized into the corresponding α-nitroketone.

LRMS (ESI) m/z calculated for C₁₇H₃₁N₃O₇ ([M+H]⁺) 390.21, found 390.2.



Preparation of 2-nitropropionyl-carba(dethia)pantetheine acetonide via mixed anhydride intermediate.

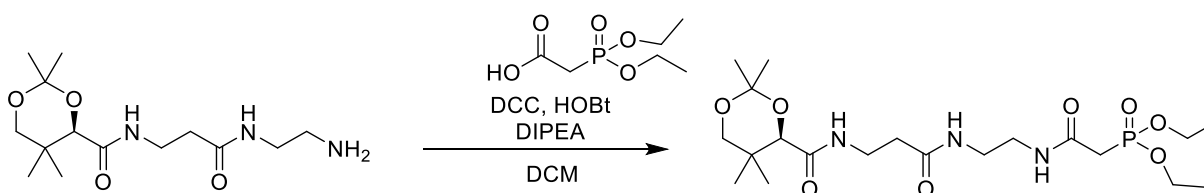
Procedure:

A solution of DCM containing carboxy-carba(dethia)pantetheine acetonide on ice was mixed with DIPEA (5 equiv.), followed by dropwise addition of ECF (1.2 equiv.), and allowed to stir for 15 minutes. Nitroethane (25 equiv.) was added dropwise to the stirring reaction, which was left to react overnight. The reaction was subjected to flash chromatography (40g silica; 0 → 60% gradient of DCM → acetone over 12 column volumes) affording the 2-nitropropionyl-carba(dethia)pantetheine acetonide.

2-nitropropionyl-carba(dethia)pantetheine acetonide:

Carboxy-carba(dethia)pantetheine acetonide (1200 mg, 3.5 mmol) was reacted according to the above procedure affording the pure product (orange oil, 240 mg, 0.6 mmol, 17%).

¹H NMR (500 MHz, CDCl₃) δ 7.07 – 7.03 (m, 1H), 6.45 (s, 1H), 4.07 (d, J = 3.8 Hz, 1H), 3.68 (d, J = 11.7 Hz, 1H), 3.52 (ddp, J = 20.4, 13.8, 6.7 Hz, 1H), 3.42 – 3.27 (m, 1H), 3.27 (d, J = 9.3 Hz, 1H), 2.63 (s, 2H), 2.55 – 2.49 (m, 1H), 2.42 (ddd, J = 20.1, 14.4, 6.7 Hz, 1H), 2.17 (d, J = 3.2 Hz, 4H), 1.99 – 1.90 (m, 1H), 1.46 (d, J = 3.4 Hz, 3H), 1.42 (s, 3H), 1.02 (d, J = 2.6 Hz, 3H), 0.96 (d, J = 2.4 Hz, 3H). **¹³C NMR** (126 MHz, CDCl₃) δ 210.88, 171.26, 170.49, 99.15, 77.28, 77.12, 77.02, 76.77, 71.39, 69.56, 53.78, 38.57, 35.84, 35.10, 32.99, 31.75, 30.95, 29.44, 29.26, 24.22, 22.14, 18.88, 18.70, 0.00. LRMS (ESI) m/z calculated for C₁₈H₃₁N₃O₇ ([M+H]⁺) 402.47, found 402.5.



Preparation of 2-(diethylphosphono)-acetyl-aza(dethia)pantetheine acetonide via carbodiimide activation of diethylphosphonoacetic acid.

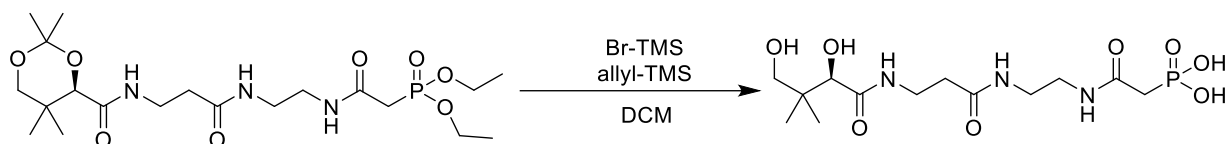
Procedure:

Aza(dethia)-pantetheine acetonide was dissolved in DCM with diethylphosphonoacetic acid (1.3 equiv.), DIPEA (3 equiv.), and HOBT (0.5 equiv.) and stirred in a round bottom flask. The reaction was initiated by addition of DCC (1.5 equiv.) and left to stir overnight at room temperature. The reaction was washed with saturated ammonium chloride (3 x 20 ml) and subjected to flash chromatography (40g silica; 0 → 40% gradient of DCM → MeOH over 12 column volumes) affording 2-(diethylphosphono)-acetyl-aza(dethia)pantetheine acetonide.

2-(diethylphosphono)-acetyl-aza(dethia)pantetheine acetonide:

Aza(dethia)pantetheine acetonide (500 mg, 1.66 mmol) was reacted according to the above procedure affording 2-(diethylphosphono)-acetyl-aza(dethia)pantetheine acetonide (clear oil, 613 mg, 1.28 mmol, 77%). **¹H NMR** (500 MHz, MeOD) δ 4.21 – 4.08 (m, 7H), 3.76 – 3.70 (m, 1H), 3.47 (ttd, J = 15.0, 8.2, 7.4, 5.8 Hz, 2H), 3.34 (s, 2H), 3.29 (s, 4H), 3.31 – 3.21 (m, 4H), 2.93 (dd,

$J = 21.6, 3.6$ Hz, 3H), 2.42 (t, $J = 6.8$ Hz, 2H), 1.93 (d, $J = 3.0$ Hz, 2H), 1.44 (d, $J = 3.9$ Hz, 6H), 1.33 (t, $J = 7.1$ Hz, 6H), 0.98 (d, $J = 9.8$ Hz, 6H). ^{13}C NMR (126 MHz, MeOD) δ 172.68, 172.20, 170.79, 170.72, 165.76, 98.98, 77.00, 70.87, 62.75, 62.70, 48.50, 48.16, 47.99, 47.82, 47.65, 47.48, 47.30, 47.13, 38.87, 38.66, 38.52, 38.44, 35.09, 34.97, 34.91, 34.84, 33.84, 32.55, 28.38, 21.27, 21.23, 21.09, 18.04, 17.69, 15.32, 15.27. LRMS (ESI) m/z calculated for $\text{C}_{20}\text{H}_{38}\text{N}_3\text{O}_8\text{P}$ ($[\text{M}+\text{H}]^+$) 480.24, found 480.2.



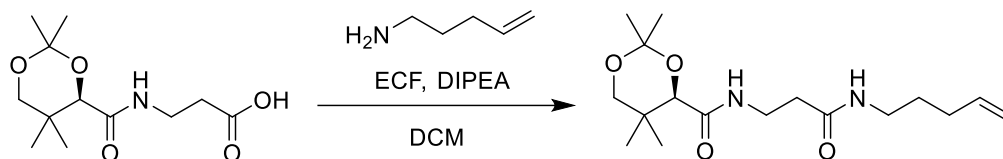
Preparation of 2-phosphonoacetyl-aza(dethia)pantetheine via McKenna reaction.

Procedure:

2-(diethylphosphono)-acetyl-aza(dethia)pantetheine acetonide was dissolved in DCM with allyl-TMS (5 equiv.) and DIPEA (2 equiv.) and stirred in a round bottom flask on a heating mantle. The reaction was initiated by addition of Br-TMS (8 equiv.) and left to stir for 6 hours at reflux. The reaction was rapidly concentrated by rotavap and quenched by addition of 20 ml of water. The reaction was then subjected to preparative RP HPLC (C18; 0 \rightarrow 10% gradient of 0.1% TFA \rightarrow ACN over 45 minutes), which was then lyophilized, affording 2-phosphonoacetyl-aza(dethia)pantetheine.

2-phosphonoacetyl-aza(dethia)pantetheine:

2-(diethylphosphono)-acetyl-aza(dethia)pantetheine acetonide (184 mg, 0.38 mmol) was reacted according to the above procedure affording 2-phosphonoacetyl-aza(dethia)pantetheine (diisopropylethylamine salt) (white powder, 88 mg, 0.23 mmol, 60.5 %). ^1H NMR (500 MHz, D_2O) δ 3.85 (d, $J = 1.1$ Hz, 1H), 3.59 (hept, $J = 6.7$ Hz, 1H), 3.42 – 3.31 (m, 3H), 3.25 (dd, $J = 11.2, 1.0$ Hz, 1H), 3.21 (dd, $J = 12.8, 6.6$ Hz, 1H), 3.19 (s, 3H), 3.15 – 3.03 (m, 1H), 2.72 – 2.69 (m, 1H), 2.66 (d, $J = 1.1$ Hz, 1H), 2.36 (t, $J = 6.5$ Hz, 2H), 1.24 – 1.17 (m, 8H), 0.80 – 0.73 (m, 6H). ^{13}C NMR (126 MHz, D_2O) δ 175.08, 174.16, 169.62, 169.57, 75.70, 68.29, 54.31, 42.50, 38.79, 38.61, 38.54, 37.64, 36.66, 35.39, 35.24, 20.43, 19.02, 17.67, 16.20, 12.09. LRMS (ESI) m/z calculated for $\text{C}_{13}\text{H}_{26}\text{N}_3\text{O}_8\text{P}$ ($[\text{M}-\text{H}]^-$) 382.13, found 382.1.



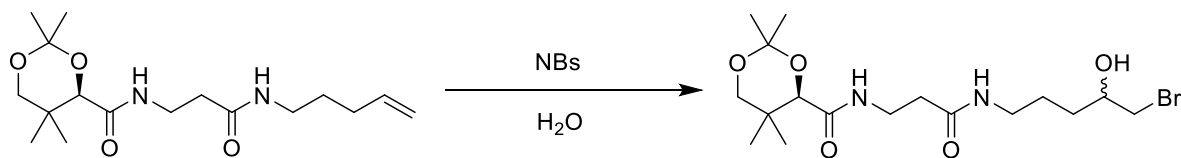
Preparation of ethene-carba(dethia)pantetheine acetonide via mixed anhydride intermediate.

Procedure:

A solution of DCM containing (1.5 equiv.) pantothenic acid acetonide on ice was mixed with DIPEA (3 equiv.), followed by dropwise addition of ECF (1.2 equiv.), and allowed to stir for 15 minutes. Pent-4-enamine (1 equiv.) was dissolved in DCM and added dropwise to the stirring reaction, which was left to react overnight. The reaction was subjected to flash chromatography (40g silica; 0 → 50% gradient of DCM → acetone over 12 column volumes) affording ethene-carba(dethia)pantetheine acetonide.

Ethene-carba(dethia)pantetheine acetonide:

Pantothenic acid acetonide (1000 mg, 11.63 mmol) was reacted according to the above procedure affording ethene-carba(dethia)pantetheine acetonide (white crystals, 1600 mg, 4.91 mmol, 42.2 %). **¹H NMR** (500 MHz, CDCl₃) δ 7.03 (t, J = 6.2 Hz, 1H), 5.99 (t, J = 5.8 Hz, 1H), 5.80 (ddt, J = 16.9, 10.2, 6.7 Hz, 1H), 5.04 (dq, J = 17.1, 1.7 Hz, 1H), 4.99 (dq, J = 10.2, 1.4 Hz, 1H), 4.08 (s, 1H), 3.69 (d, J = 11.7 Hz, 1H), 3.65 – 3.47 (m, 2H), 3.34 – 3.19 (m, 3H), 2.47 – 2.41 (m, 2H), 2.09 (tdd, J = 8.0, 6.1, 1.4 Hz, 2H), 1.61 (p, J = 7.3 Hz, 2H), 1.47 (s, 3H), 1.42 (s, 3H), 1.05 (s, 3H), 0.98 (s, 3H). **¹³C NMR** (126 MHz, CDCl₃) δ 170.83, 170.23, 137.65, 115.30, 99.09, 77.30, 77.15, 77.04, 76.79, 71.43, 39.06, 36.22, 34.91, 32.98, 31.06, 29.46, 28.72, 22.14, 18.88, 18.68. LRMS (ESI) m/z calculated for C₁₇H₃₀N₂O₄ ([M+H]⁺) 327.23, found 327.2.



Preparation of (2-bromo-hydroxyethyl)-carba(dethia)pantetheine acetonide via bromohydrin addition.

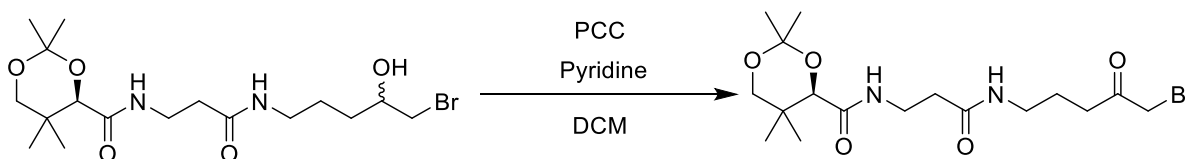
Procedure:

A suspension of water containing ethene-carba(dethia)pantetheine acetonide on ice was mixed with N-bromosuccinimide (2 equiv.) and allowed to stir for 1 hour. Afterward, the reaction was

quenched by addition of 1M NaOH to pH = 7. The reaction was subjected to flash chromatography (40g silica; 0 → 100% gradient of DCM → acetone over 12 column volumes) affording (2-bromo-hydroxyethyl)-carba(dethia)pantetheine acetonide.

(2-bromo-hydroxyethyl)-carba(dethia)pantetheine acetonide:

Ethene-carba(dethia)pantetheine acetonide (1300 mg, 3.99 mmol) was reacted according to the above procedure affording (2-bromo-hydroxyethyl)-carba(dethia)pantetheine acetonide (clear oil, 564 mg, 1.34 mmol, 33.5 %). ¹H NMR (500 MHz, CDCl₃) δ 7.03 (t, J = 6.3 Hz, 1H), 6.60 (dq, J = 12.0, 5.5 Hz, 1H), 5.26 (s, 1H), 4.02 (d, J = 1.8 Hz, 1H), 3.75 (q, J = 6.2 Hz, 1H), 3.64 (d, J = 11.7 Hz, 1H), 3.57 – 3.39 (m, 3H), 3.38 – 3.15 (m, 3H), 2.40 (td, J = 6.5, 5.4, 3.2 Hz, 2H), 1.61 (s, 1H), 1.64 – 1.55 (m, 1H), 1.42 (s, 3H), 1.38 (s, 3H), 0.98 (s, 3H), 0.92 (s, 3H). ¹³C NMR (126 MHz, CDCl₃) δ 171.15, 170.41, 170.37, 99.10, 77.35, 77.09, 76.84, 71.33, 70.65, 39.73, 39.68, 39.21, 38.70, 36.18, 35.05, 32.95, 32.07, 29.45, 29.27, 25.77, 22.13, 18.90, 18.70, 0.99. LRMS (ESI) m/z calculated for C₁₇H₃₁N₂O₅Br ([M+H]⁺) 423.25, found 423.2, 425.2.



Preparation of 2-bromoacetyl-carba(dethia)pantetheine acetonide via pyridinium chlorochromate oxidation.

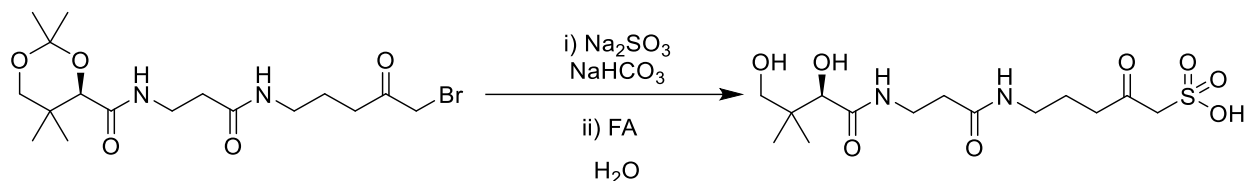
Procedure:

A solution of acetone containing (2-bromo-hydroxyethyl)-carba(dethia)pantetheine acetonide was mixed with 4 Å powdered molecular sieves (1 equiv. by m/m), followed by portionwise addition of pyridinium chlorochromate (2 equiv.) and allowed to stir for 1 hour at room temperature. Afterward, the reaction was neutralized by addition of 1M NaOH to pH = 7. The reaction was subjected to flash chromatography (24g silica; 0 → 50% gradient of DCM → acetone over 12 column volumes) affording 2-bromoacetyl-carba(dethia)pantetheine acetonide.

2-bromoacetyl-carba(dethia)pantetheine acetonide:

(2-bromo-hydroxyethyl)-carba(dethia)pantetheine acetonide (85 mg, 0.20 mmol) was reacted according to the above procedure affording 2-bromoacetyl-carba(dethia)pantetheine acetonide

(orange oil, 39 mg, 0.09 mmol, 46.4 %). **¹H NMR** (500 MHz, CDCl₃) δ 7.04, 6.37, 4.10, 4.05, 3.91, 3.67, 3.65, 3.54, 3.49, 3.27, 3.24, 2.69, 2.63, 2.62, 2.42, 2.36, 2.15, 1.44, 1.40, 1.01, 0.94. **¹³C NMR** (126 MHz, CDCl₃) δ 201.73, 171.32, 170.34, 99.11, 77.32, 77.15, 77.07, 76.81, 71.39, 38.66, 37.07, 36.95, 36.21, 34.95, 34.42, 32.97, 29.48, 29.28, 23.75, 22.16, 18.91, 18.71. LRMS (ESI) m/z calculated for C₁₇H₃₁N₂O₅Br ([M+H]⁺) 421.13, found 421.1, 423.1.



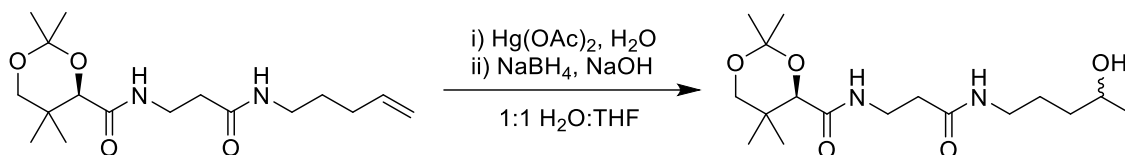
Preparation of 2-sulfonate-acetyl-carba(dethia)pantetheine via substitution reaction.

Procedure:

A suspension of water containing 2-bromoacetyl-carba(dethia)pantetheine acetonide was mixed with sodium bicarbonate (2 equiv.), followed by addition sodium sulfite (2 equiv.) and allowed to stir for overnight at room temperature. Afterward, the reaction was immediately deprotected by dropwise addition of 50% formic acid to pH = 2.0, which was left again to stir overnight. The following day, the reaction was subjected to preparative RP HPLC (C18; 0 → 20% gradient of 0.1% TFA → ACN over 45 minutes), which was then lyophilized, affording 2-sulfonate-acetyl-carba(dethia)pantetheine.

2-sulfonate-acetyl-carba(dethia)pantetheine:

2-bromoacetyl-carba(dethia)pantetheine acetonide (39 mg, 0.09 mmol) was reacted according to the above procedure affording 2-sulfonate-acetyl-carba(dethia)pantetheine (clear oil, 29 mg, 0.076 mmol, 76.8 %). **¹H NMR** (500 MHz, CDCl₃) δ 3.89 (d, J = 1.6 Hz, 1H), 3.65 (s, 0H), 3.42 (dd, J = 12.1, 5.6 Hz, 3H), 3.29 (d, J = 11.2 Hz, 1H), 3.14 – 3.03 (m, 2H), 2.71 (q, J = 7.2 Hz, 1H), 0.82 (d, J = 1.6 Hz, 3H), 0.78 (d, J = 2.0 Hz, 3H). **¹³C NMR** (126 MHz, CDCl₃) δ 204.99, 175.07, 173.20, 115.18, 75.74, 68.36, 40.34, 38.57, 38.46, 35.46, 35.29, 22.27, 20.48, 19.05. LRMS (ESI) m/z calculated for C₁₄H₂₆N₂O₈S ([M-H]⁻) 381.14, found 381.1.



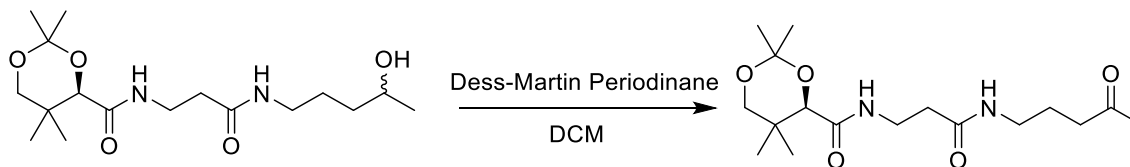
Preparation of hydroxyethyl-carba(dethia)pantetheine acetonide via oxymercuration-demercuration reaction.

Procedure:

A solution of 50% tetrahydrofuran (THF) containing ethene-carba(dethia)pantetheine acetonide was mixed with mercury (II) acetate (1.5 equiv.) and allowed to stir for 1 hour. Afterward, sodium borohydride (3 equiv.) in 3M NaOH was added to the reaction, which precipitated out elemental mercury. Mercury was removed by filtration, and the filtrate was subjected to flash chromatography (40g silica; 0 → 60% gradient of DCM → acetone over 12 column volumes) affording hydroxyethyl-carba(dethia)pantetheine acetonide.

Hydroxyethyl-carba(dethia)pantetheine acetonide:

Ethene-carba(dethia)pantetheine acetonide (130 mg, 0.40 mmol) was reacted according to the above procedure affording hydroxyethyl-carba(dethia)pantetheine acetonide (clear oil, 105 mg, 0.31 mmol, 76.54 %). **¹H NMR** (500 MHz, CDCl₃) δ 7.07 (t, J = 6.3 Hz, 1H), 6.99 (t, J = 5.6 Hz, 1H), 3.97 (s, 1H), 3.71 (h, J = 6.1 Hz, 1H), 3.62 – 3.51 (m, 2H), 3.42 (ddt, J = 31.4, 13.6, 6.7 Hz, 2H), 3.22 – 3.05 (m, 3H), 2.34 (t, J = 6.5 Hz, 2H), 1.59 – 1.44 (m, 2H), 1.37 (s, 3H), 1.33 (s, 3H), 1.08 (d, J = 6.2 Hz, 3H), 0.92 (s, 3H), 0.87 (s, 3H). **¹³C NMR** (126 MHz, CDCl₃) δ 171.25, 170.39, 170.32, 169.85, 169.11, 99.05, 98.97, 77.41, 77.16, 77.04, 76.90, 71.35, 71.28, 67.17, 62.23, 53.46, 39.42, 36.08, 35.92, 35.21, 32.88, 29.35, 25.59, 22.06, 18.83, 18.64. LRMS (ESI) m/z calculated for C₁₇H₃₂N₂O₅ ([M+H]⁺) 345.24, found 345.2.



Preparation of acetyl-carba(dethia)pantetheine acetonide via Dess-Martin Periodinane oxidation.

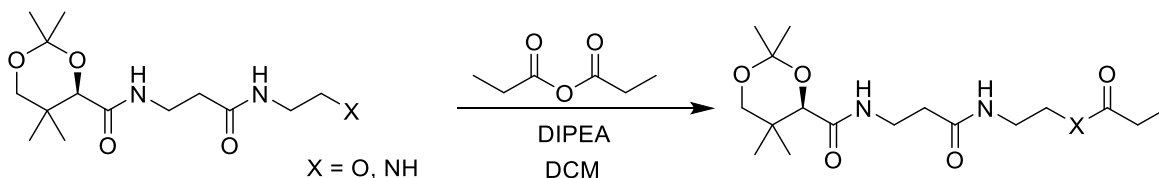
Procedure:

A solution of water containing hydroxyethyl-carba(dethia)pantetheine acetonide was mixed with Dess-Martin Periodinane (1.5 equiv.) and allowed to stir for 5 hours. Afterward, the reaction was

vacuum filtered, and washed with sodium bicarbonate (3 x 10 ml). The organic phase was subjected to flash chromatography (40g silica; 0 → 50% gradient of DCM → acetone over 12 column volumes) affording acetyl-carba(dethia)pantetheine acetonide.

Acetyl-carba(dethia)pantetheine acetonide:

Hydroxyethyl-carba(dethia)pantetheine acetonide (105 mg, 0.31 mmol) was reacted according to the above procedure affording acetyl-carba(dethia)pantetheine acetonide (clear oil, 33 mg, 0.10 mmol, 31.6 %). **¹H NMR** (500 MHz, CDCl₃) δ 7.05 (d, J = 6.5 Hz, 0H), 6.40 (d, J = 6.0 Hz, 0H), 4.04 (s, 1H), 3.65 (d, J = 11.7 Hz, 1H), 3.60 – 3.41 (m, 1H), 3.29 – 3.15 (m, 2H), 2.48 (t, J = 7.0 Hz, 1H), 2.41 (t, J = 6.3 Hz, 1H), 1.74 (p, J = 7.0 Hz, 1H), 1.43 (s, 2H), 1.39 (s, 2H), 1.00 (s, 2H), 0.94 (s, 2H), 0.91 (s, 1H). **¹³C NMR** (126 MHz, CDCl₃) δ 208.66, 171.21, 170.29, 99.09, 77.31, 77.26, 77.12, 77.06, 76.81, 71.38, 40.94, 39.01, 36.15, 36.06, 34.99, 32.95, 30.01, 29.44, 23.37, 22.11, 18.88, 18.68, 1.01. LRMS (ESI) m/z calculated for C₁₇H₃₀N₂O₅ ([M+H]⁺) 343.23, found 343.2.



Preparation of propionyl-aza/oxa(dethia)pantetheine acetonide via propionic anhydride.

General procedure:

A solution of DCM containing either oxa(dethia)pantetheine acetonide or aza(dethia)pantetheine acetonide was added DIPEA (10 equiv.) and propionic anhydride (5 equiv.) and allowed to stir for overnight. Afterward, the reaction was concentrated by rotary evaporation, then subjected to flash chromatography (40g silica; 0 → 70% gradient of DCM → acetone over 12 column volumes) affording propionyl-oxa(dethia)pantetheine acetonide or propionyl-aza(dethia)pantetheine acetonide.

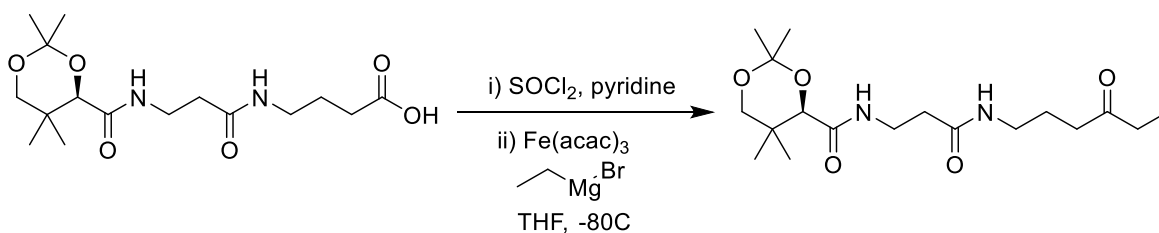
Propionyl-oxa(dethia)pantetheine acetonide:

oxa(dethia)pantetheine acetonide (400 mg, 1.32 mmol) was reacted according to the above procedure affording propionyl-oxa(dethia)pantetheine acetonide (clear oil, 357.3 mg, 1.0 mmol, 75.6 %). **¹H NMR** (500 MHz, CDCl₃) δ 7.02 (t, J = 6.4 Hz, 1H), 6.17 (d, J = 6.2 Hz, 1H), 4.15 (t,

$J = 5.4$ Hz, 2H), 4.06 (s, 1H), 3.67 (d, $J = 11.7$ Hz, 1H), 3.63 – 3.43 (m, 4H), 3.27 (d, $J = 11.7$ Hz, 1H), 2.45 (t, $J = 6.2$ Hz, 2H), 2.35 (q, $J = 7.6$ Hz, 2H), 1.41 (s, 3H), 1.14 (t, $J = 7.6$ Hz, 3H), 1.03 (s, 3H), 0.96 (s, 3H). ^{13}C NMR (126 MHz, CDCl_3) δ 174.49, 171.10, 170.25, 99.10, 77.29, 77.14, 77.03, 76.78, 71.43, 63.11, 38.74, 36.08, 34.81, 32.97, 29.46, 27.42, 22.13, 18.87, 18.69, 9.04. LRMS (ESI) m/z calculated for $\text{C}_{17}\text{H}_{30}\text{N}_2\text{O}_6$ ($[\text{M}+\text{H}]^+$) 359.22, found 359.2.

Propionyl-aza(dethia)pantetheine acetonide:

aza(dethia)pantetheine acetonide (430 mg, 1.43 mmol) was reacted according to the above procedure affording propionyl-aza(dethia)pantetheine acetonide (clear oil, 307 mg, 0.86 mmol, 60.1 %). ^1H NMR (500 MHz, CDCl_3) δ 7.45 (s, 1H), 7.01 (t, $J = 6.1$ Hz, 2H), 3.94 (s, 1H), 3.56 (d, $J = 11.6$ Hz, 1H), 3.40 (ddt, $J = 35.4, 13.5, 6.7$ Hz, 2H), 3.22 (h, $J = 2.3$ Hz, 4H), 3.14 (d, $J = 11.7$ Hz, 1H), 2.37 – 2.30 (m, 1H), 2.09 (q, $J = 7.6$ Hz, 2H), 1.31 (d, $J = 14.0$ Hz, 6H), 1.00 (td, $J = 7.6, 4.2$ Hz, 3H), 0.89 (s, 3H), 0.84 (s, 3H). ^{13}C NMR (126 MHz, CDCl_3) δ 174.98, 172.17, 170.03, 98.97, 77.46, 77.40, 77.20, 77.06, 76.95, 71.25, 39.72, 39.55, 35.68, 34.95, 32.83, 29.42, 29.33, 22.03, 18.79, 18.61, 18.28, 9.82. LRMS (ESI) m/z calculated for $\text{C}_{17}\text{H}_{31}\text{N}_3\text{O}_5$ ($[\text{M}+\text{H}]^+$) 358.24, found 358.2.



Preparation of propionyl-carba(dethia)pantetheine acetonide via Grignard Reagent.

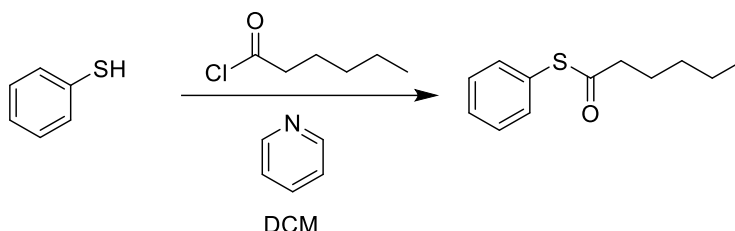
Procedure:

A solution of THF containing carboxy-carba(dethia)pantetheine acetonide was added pyridine (5 equiv.), followed by dropwise addition of thionyl chloride solution (2M in DCM) (1.5 equiv.) which was left to stir for 30 minutes at room temperature. Afterward, the reaction was placed in a dry ice/acetone bath, where Iron (III) acetoacetonate (1 equiv.) was added, followed by rapid addition of ethylmagnesium bromide solution (1M in diethylether) (1.2 equiv.). The reaction was capped and left to stir overnight, slowly warming up to room temperature. The reaction was quenched by washing with water (2 x 20 ml). The organic phase was then subjected to flash

chromatography (40g silica; 0 → 50% gradient of DCM → acetone over 12 column volumes) affording propionyl-carba(dethia)pantetheine acetonide.

Propionyl-carba(dethia)pantetheine acetonide:

Carboxy-carba(dethia)pantetheine acetonide (300 mg, 0.88 mmol) was reacted according to the above procedure affording propionyl-carba(dethia)pantetheine acetonide (orange oil, 11 mg, 0.03 mmol, 3.5 %). LRMS (ESI) m/z calculated for $C_{18}H_{32}N_2O_5$ ($[M+H]^+$) 357.23, found 357.2.



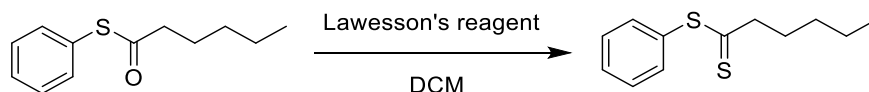
Preparation of phenylthiohexanoate via thiophenol acylation.

Procedure:

To a solution of DCM containing thiophenol and pyridine (2 equiv.) was added hexanoyl chloride (1.2 equiv.) which was left to stir for 5 hours on ice. Afterward, the reaction was subjected to flash chromatography (40g silica; 0 → 20% gradient of hexanes → EtOAc over 12 column volumes) affording phenylthiohexanoate.

Phenylthiohexanoate:

Thiophenol (500 mg, 4.54 mmol) was reacted according to the above procedure affording phenylthiohexanoate (clear oil, 858 mg, 4.13 mmol, 91%). 1H NMR (500 MHz, $CDCl_3$) δ 7.41 (s, 4H), 2.68 – 2.62 (m, 2H), 1.77 – 1.66 (m, 3H), 1.35 (tt, $J = 7.0, 2.9$ Hz, 4H), 0.95 – 0.86 (m, 3H). ^{13}C NMR (126 MHz, $CDCl_3$) δ 197.66, 134.50, 129.30, 129.16, 77.28, 77.03, 76.78, 43.71, 31.11, 25.29, 22.33, 13.88. LRMS (ESI) m/z calculated for $C_{12}H_{16}OS$ ($[M+H]^+$) 209.10, found 209.1.



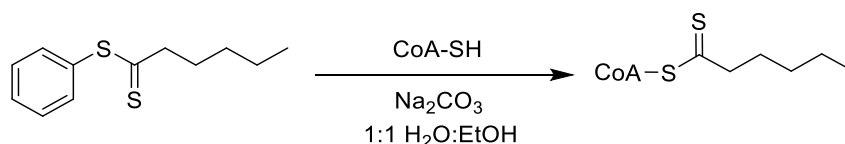
Preparation of phenyldithiohexanoate via thiophenol acylation.

Procedure:

To a solution of DCM containing phenylthiohexanoate was added Lawesson's reagent (0.7 equiv.) which was left to stir at reflux for 18 hours. Afterward, the reaction was subjected to flash chromatography (40g silica; hexanes isocratic over 12 column volumes) affording phenyldithiohexanoate.

Phenyldithiohexanoate:

Phenylthiohexanoate (858 mg, 4.13 mmol) was reacted according to the above procedure affording phenyldithiohexanoate (orange oil, 623 mg, 2.78 mmol, 67.3%). **¹H NMR** (500 MHz, CDCl₃) δ 8.44 (s, 1H), 7.49 (d, J = 7.7 Hz, 1H), 7.30 (t, J = 7.6 Hz, 1H), 7.27 – 7.20 (m, 1H), 4.00 (t, J = 2.2 Hz, 2H), 2.64 (t, J = 7.7 Hz, 2H), 1.75 (d, J = 7.5 Hz, 2H), 1.73 (s, 1H), 1.30 (ddtd, J = 15.9, 11.4, 8.6, 4.2 Hz, 5H), 0.89 (t, J = 6.8 Hz, 4H). **¹³C NMR** (126 MHz, CDCl₃) δ 207.95, 129.08, 127.52, 127.17, 77.29, 77.04, 76.78, 47.16, 45.61, 31.03, 28.99, 22.37, 13.94. LRMS (ESI) m/z calculated for C₁₂H₁₆S₂ ([M+H]⁺) 225.07, found 225.1.



Preparation of hexanoyl-dithio-CoA via transthioylation.

Procedure:

30 mg of CoA-SH were weighed and placed into a clean beaker. This material was dissolved in 50 ml of 1M Sodium bicarbonate mixed with 50 ml of ethanol. To this reaction, 200 mg of S-phenyldithiohexanoate were added. Then, to the stirring pale orange suspension were added 3 ml of ethylacetate. The reaction was covered with a larger beaker and left to stir for 30 minutes. The material was then purified away from salt and any other polar contaminants remaining via preparative reverse phase HPLC (C18) using the following gradient:

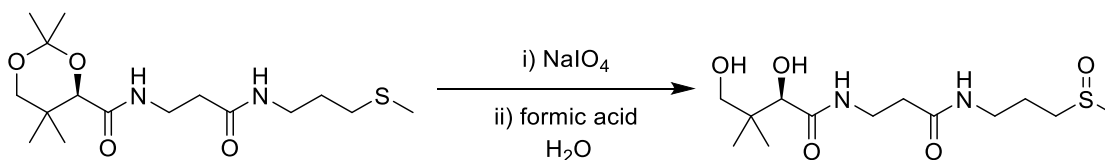
0 - 10 min, 0.1% TFA isocratic

10 - 45 min, 0.1% TFA -> 80% acetonitrile

The product fractions were pooled, neutralized to pH=7 and freeze dried.

Hexanoyl-dithio-CoA:

CoA-SH (30 mg, 0.04 mmol) was reacted according to the above procedure affording hexanoyl-dithio-CoA (orange solid, 9.4 mg, 0.01 mmol, 25%). **¹H NMR** (500 MHz, D₂O) δ 8.45 (s, 1H), 8.18 – 8.13 (m, 1H), 6.07 (dt, J = 6.9, 1.7 Hz, 1H), 4.49 (s, 1H), 3.95 – 3.90 (m, 1H), 3.74 (s, 1H), 3.47 (dd, J = 9.9, 4.8 Hz, 1H), 3.34 (dd, J = 11.9, 5.9 Hz, 4H), 3.28 (d, J = 6.4 Hz, 2H), 2.91 – 2.84 (m, 1H), 2.32 (t, J = 5.7 Hz, 2H), 1.62 (d, J = 8.1 Hz, 2H), 1.19 – 1.12 (m, 4H), 0.82 – 0.70 (m, 6H), 0.65 (q, J = 5.2, 3.5 Hz, 3H). **¹³C NMR** (126 MHz, D₂O) δ 174.70, 173.91, 163.16, 162.88, 162.60, 155.61, 152.93, 119.83, 117.51, 115.19, 112.87, 86.57, 74.36, 74.09, 51.79, 38.29, 36.93, 35.33, 35.08, 30.77, 30.02, 21.66, 20.89, 18.18, 13.19. LRMS (ESI) m/z calculated for C₂₇H₄₆N₇O₁₆P₃S₂ ([M-H]⁻) 880.16, found 880.2.



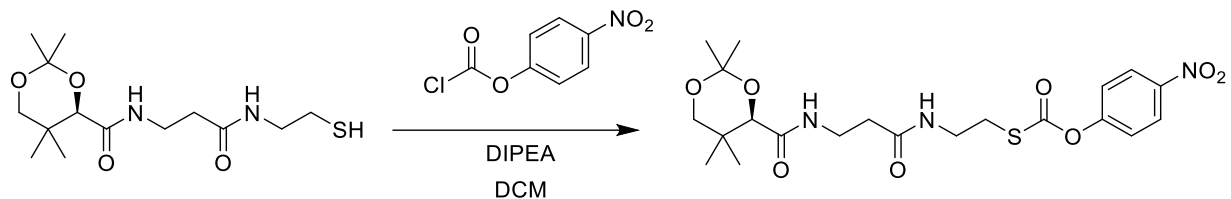
Preparation of methylsulfoxide-carba(dethia)pantetheine acetone via periodate oxidation.

Procedure:

Thiomethyl-carba(dethia)pantetheine acetonide was dissolved in 10 ml of water followed by addition of sodium meta-periodate (2 equiv.) and stirred in a round bottom flask overnight at room temperature. The reaction was subjected preparative RP HPLC (C18; 0 → 20% gradient of 0.1% TFA → ACN over 45 minutes), which was then lyophilized, affording methylsulfoxide-carba(dethia)pantetheine.

Methylsulfoxide-carba(dethia)pantetheine:

Thiomethyl-carba(dethia)pantetheine acetonide (410 mg, 1.18 mmol) was reacted according to the above procedure affording methylsulfoxide-carba(dethia)pantetheine (clear oil, 303 mg, 0.94 mmol, 79.4%). **¹H NMR** (500 MHz, D₂O) δ 4.14 (s, 1H), 3.74 (d, J = 11.9 Hz, 1H), 3.46 – 3.32 (m, 2H), 3.28 – 3.17 (m, 3H), 2.86 – 2.71 (m, 2H), 2.61 – 2.57 (m, 3H), 2.42 – 2.34 (m, 2H), 1.88 – 1.78 (m, 2H), 1.37 (t, J = 1.7 Hz, 3H), 0.87 – 0.82 (m, 6H). **¹³C NMR** (126 MHz, D₂O) δ 173.93, 171.81, 171.74, 99.83, 77.02, 70.59, 50.02, 38.01, 36.53, 35.29, 35.23, 32.32, 28.32, 21.95, 21.89, 20.91, 18.28, 18.12. LRMS (ESI) m/z calculated for C₁₃H₂₆N₂O₅S ([M+H]⁺) 323.17, found 323.2.



Preparation of *p*-nitrophenol-formate-pantetheine acetonide via acylation of pantetheine acetonide.

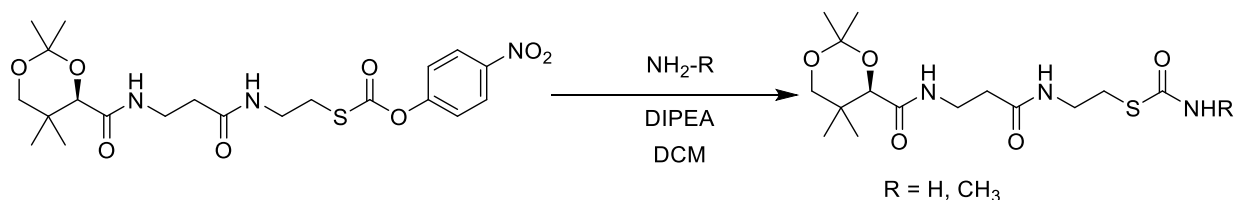
Procedure:

Pantetheine acetonide was dissolved in DCM with DIPEA (3 equiv.), followed by addition of *p*-nitrochloroformate (1.2 equiv.), which was stirred in a round bottom flask on ice overnight. The reaction was washed with saturated ammonium chloride (3 x 20 ml) and subjected to flash chromatography (40g silica; 0 → 40% gradient of DCM → acetone over 12 column volumes) affording *p*-nitrophenol-formate-pantetheine acetonide.

***p*-nitrophenol-formate-pantetheine acetonide:**

Pantetheine acetonide (190 mg, 0.60 mmol) was reacted according to the above procedure affording *p*-nitrophenol-formate-pantetheine acetonide (yellow oil, 249 mg, 0.52 mmol, 86.3%).

¹H NMR (500 MHz, CDCl₃) δ 8.31 – 8.24 (m, 2H), 7.39 – 7.32 (m, 2H), 7.02 (t, *J* = 6.3 Hz, 1H), 6.47 – 6.41 (m, 1H), 4.11 (q, *J* = 7.1 Hz, 1H), 4.08 (s, 1H), 3.70 – 3.64 (m, 1H), 3.56 (tddd, *J* = 20.3, 7.8, 6.1, 4.4 Hz, 4H), 3.27 (d, *J* = 11.7 Hz, 1H), 3.10 (t, *J* = 6.4 Hz, 2H), 2.48 (dd, *J* = 6.6, 5.8 Hz, 2H), 2.04 (s, 1H), 1.46 (s, 2H), 1.41 (d, *J* = 0.7 Hz, 3H), 1.25 (t, *J* = 7.2 Hz, 2H), 1.02 (s, 3H), 0.96 (s, 3H). **¹³C NMR** (126 MHz, CDCl₃) δ 171.35, 171.19, 170.47, 169.34, 155.46, 145.52, 125.37, 122.02, 99.14, 77.29, 77.15, 77.04, 76.78, 71.39, 60.41, 38.99, 36.16, 34.80, 32.99, 31.05, 29.48, 22.13, 18.93, 18.69, 14.20. LRMS (ESI) *m/z* calculated for C₂₁H₂₉N₃O₈S ([M+H]⁺) 484.17, found 484.2.



Preparation of formamide-pantetheine acetonide and methylformamide-pantetheine acetonide via amidation.

Procedure:

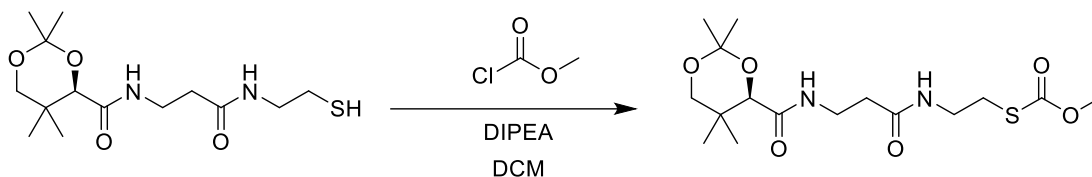
p-nitrophenol-formate-pantetheine acetonide was dissolved in DCM with DIPEA (6 equiv.), followed by addition of either ammonia solution (0.5 M in dioxane) or methylamine:HCl (3 equiv.), which was stirred in a round bottom flask on ice for 5 hours. The reaction was washed with saturated ammonium chloride (3 x 20 ml) and subjected to flash chromatography (40g silica; 0 → 100% gradient of DCM → acetone over 12 column volumes) affording formamide-pantetheine acetonide or methylformamide-pantetheine acetonide.

Formamide-pantetheine acetonide:

p-nitrophenol-formate-pantetheine acetonide (200 mg, 0.42 mmol) was reacted with ammonia according to the above procedure affording formamide-pantetheine acetonide (white powder, 80 mg, 0.22 mmol, 53%). ¹H NMR (500 MHz, CDCl₃) δ 7.03 (t, J = 6.3 Hz, 1H), 6.67 (t, J = 5.6 Hz, 1H), 5.91 (s, 2H), 4.06 (s, 1H), 3.67 (d, J = 11.7 Hz, 1H), 3.61 – 3.47 (m, 2H), 3.47 (d, J = 6.0 Hz, 1H), 3.47 – 3.39 (m, 1H), 3.27 (d, J = 11.7 Hz, 1H), 3.01 (t, J = 6.5 Hz, 2H), 2.43 (t, J = 6.3 Hz, 2H), 1.45 (s, 3H), 1.41 (s, 3H), 1.02 (s, 3H), 0.96 (s, 3H). ¹³C NMR (126 MHz, CDCl₃) δ 171.38, 170.24, 169.31, 99.11, 77.29, 77.18, 77.04, 76.79, 71.43, 40.35, 35.91, 35.05, 32.96, 29.48, 29.37, 22.15, 18.93, 18.71. LRMS (ESI) m/z calculated for C₁₅H₂₇N₃O₅S ([M+H]⁺) 362.18, found 362.2.

Methylformamide-pantetheine acetonide:

p-nitrophenol-formate-pantetheine acetonide (150 mg, 0.31 mmol) was reacted with methylamine:HCl according to the above procedure affording formamide-pantetheine acetonide (white powder, 100 mg, 0.27 mmol, 87.1%). ¹H NMR (500 MHz, CDCl₃) δ 7.04 (t, J = 6.2 Hz, 1H), 6.91 (t, J = 5.4 Hz, 1H), 6.40 (q, J = 4.8 Hz, 1H), 4.01 (s, 1H), 3.62 (d, J = 11.7 Hz, 1H), 3.56 – 3.29 (m, 5H), 3.21 (d, J = 11.7 Hz, 1H), 2.96 (t, J = 6.4 Hz, 2H), 2.80 (d, J = 4.7 Hz, 3H), 2.38 (t, J = 6.3 Hz, 2H), 1.40 (s, 3H), 0.96 (s, 3H), 0.91 (s, 3H). ¹³C NMR (126 MHz, CDCl₃) δ 171.48, 170.06, 167.76, 99.05, 77.38, 77.13, 76.87, 71.37, 40.62, 40.50, 35.66, 34.91, 32.92, 29.43, 29.10, 28.01, 22.11, 18.90, 18.69. LRMS (ESI) m/z calculated for C₁₆H₂₉N₃O₅S ([M+H]⁺) 376.19, found 376.2.



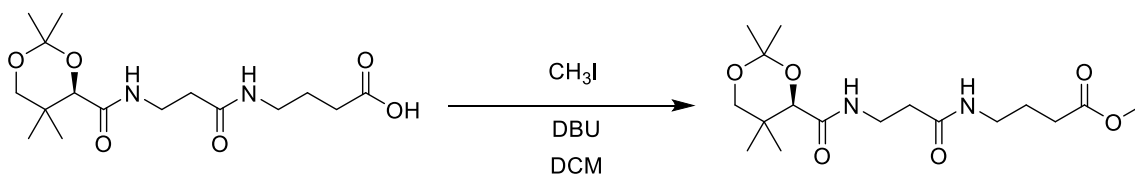
Preparation of methylformate-pantetheine acetonide via acylation of pantetheine acetonide.

Procedure:

Pantetheine acetonide was dissolved in DCM with DIPEA (3 equiv.), followed by addition of methylchloroformate (1.2 equiv.), which was stirred in a round bottom flask on ice overnight. The reaction was washed with saturated ammonium chloride (3 x 20 ml) and subjected to flash chromatography (40g silica; 0 → 40% gradient of DCM → acetone over 12 column volumes) affording methylformate-pantetheine acetonide.

Methylformate-pantetheine acetonide:

Pantetheine acetonide (150 mg, 0.47 mmol) was reacted according to the above procedure affording methylformate-pantetheine acetonide (white crystals, 158 mg, 0.42 mmol, 89%). **¹H NMR** (500 MHz, CDCl₃) δ 7.01 (t, J = 6.3 Hz, 1H), 6.30 (t, J = 5.8 Hz, 1H), 4.07 (s, 1H), 3.82 (s, 3H), 3.67 (d, J = 11.8 Hz, 1H), 3.61 – 3.40 (m, 4H), 3.27 (d, J = 11.7 Hz, 1H), 2.99 (t, J = 6.4 Hz, 2H), 2.43 (t, J = 6.2 Hz, 2H), 1.45 (s, 3H), 1.41 (s, 3H), 1.02 (s, 3H), 0.96 (s, 3H). **¹³C NMR** (126 MHz, CDCl₃) δ 171.45, 171.22, 170.19, 99.09, 77.30, 77.16, 77.04, 76.79, 71.44, 54.40, 39.52, 35.97, 34.78, 32.97, 30.56, 29.47, 22.13, 18.91, 18.69. LRMS (ESI) m/z calculated for C₁₆H₂₈N₂O₆S ([M+H]⁺) 377.18, found 377.2.



Preparation of methylformate-carba(dethia)pantetheine acetonide via methylation.

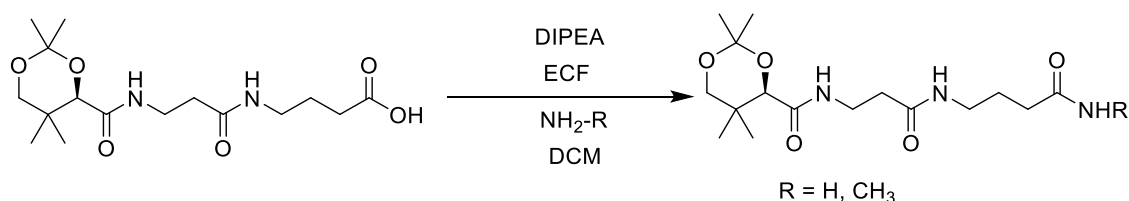
Procedure:

Carboxy-carba(dethia)pantetheine acetonide was dissolved in DCM with DBU (10 equiv.), followed by slow addition of iodomethane (10 equiv.), which was stirred in a round bottom flask on ice overnight. The reaction was quenched by washing with saturated ammonium chloride (3 x

20 ml) and subjected to flash chromatography (40g silica; 0 → 40% gradient of DCM → acetone over 12 column volumes) affording methylformate-pantetheine acetonide.

Methylformate-carba(dethia)pantetheine acetonide:

Pantetheine acetonide (300 mg, 0.88 mmol) was reacted according to the above procedure affording methylformate-carba(dethia)pantetheine acetonide (white powder, 199 mg, 0.56 mmol, 63.2%). ¹H NMR (500 MHz, CDCl₃) δ 7.02 (t, J = 6.5 Hz, 1H), 6.10 (d, J = 6.9 Hz, 1H), 5.29 (s, 2H), 4.07 (s, 1H), 3.67 (d, J = 11.6 Hz, 1H), 3.67 (s, 3H), 3.63 – 3.45 (m, 2H), 3.31 (dd, J = 13.2, 6.4 Hz, 1H), 3.28 (d, J = 2.3 Hz, 1H), 3.28 – 3.22 (m, 1H), 2.42 (t, J = 6.2 Hz, 2H), 2.36 (t, J = 7.2 Hz, 2H), 1.83 (p, J = 7.1 Hz, 2H), 1.45 (s, 3H), 1.41 (s, 3H), 1.03 (s, 3H), 0.96 (s, 3H). ¹³C NMR (126 MHz, CDCl₃) δ 173.74, 171.05, 170.23, 99.09, 77.28, 77.15, 77.03, 76.78, 71.44, 51.74, 38.96, 36.16, 34.84, 32.98, 31.45, 29.46, 24.63, 22.13, 18.87, 18.68. LRMS (ESI) m/z calculated for C₁₇H₃₀N₂O₆ ([M+H]⁺) 359.22, found 359.2.



Preparation of formamide-carba(dethia)pantetheine acetonide and methylformamide-carba(dethia)pantetheine acetonide via mixed anhydride.

Procedure:

Carboxy-carba(dethia)pantetheine acetonide was dissolved in DCM with DIPEA (6 equiv.), followed by dropwise addition of ECF while stirring on ice. The reaction was left to proceed for 15 minutes before dropwise addition of either ammonia solution (0.5 M in dioxane) or methylamine:HCl (3 equiv.), which was stirred in a round bottom flask on ice for overnight. The reaction was washed with saturated ammonium chloride (3 x 20 ml) and subjected to flash chromatography (40g silica; 0 → 100% gradient of DCM → acetone over 12 column volumes) affording formamide-carba(dethia)pantetheine acetonide or methylformamide-carba(dethia)pantetheine acetonide.

Formamide-carba(dethia)pantetheine acetonide:

Carboxy-carba(dethia)pantetheine acetonide 500 mg, 1.46 mmol) was reacted with ammonia according to the above procedure affording formamide-carba(dethia)pantetheine acetonide (white powder, 206 mg, 0.6 mmol, 41.1%). LRMS (ESI) m/z calculated for $C_{16}H_{29}N_3O_5$ ($[M+H]^+$) 344.22, found 344.2.

Methylformamide-carba(dethia)pantetheine acetonide:

Carboxy-carba(dethia)pantetheine acetonide (300 mg, 0.88 mmol) was reacted with methylamine:HCl according to the above procedure affording formamide-carba(dethia)pantetheine acetonide (white powder, 240 mg, 0.67 mmol, 76.5%). LRMS (ESI) m/z calculated for $C_{17}H_{31}N_3O_5$ ($[M+H]^+$) 358.24, found 358.2.

2.8 References

- [1] Bello, D., Rubanu, M. G., Bandaranayaka, N., Götze, J. P., Bühl, M., and O'Hagan, D. (2019) Acetyl coenzyme A analogues as rationally designed inhibitors of citrate synthase, *Chembiochem : a European journal of chemical biology* 20, 1174-1182.
- [2] Tosin, M., Spiteller, D., and Spencer, J. B. (2009) Malonyl carba(dethia)- and malonyl oxa(dethia)-coenzyme A as tools for trapping polyketide intermediates, *Chembiochem : a European journal of chemical biology* 10, 1714-1723.
- [3] Hamed, R. B., Henry, L., Gomez-Castellanos, J. R., Asghar, A., Brem, J., Claridge, T. D., and Schofield, C. J. (2013) Stereoselective preparation of lipidated carboxymethyl-proline/pipecolic acid derivatives via coupling of engineered crotonases with an alkylmalonyl-CoA synthetase, *Organic & biomolecular chemistry* 11, 8191-8196.
- [4] Yadav, J., Reddy, B. S., Eeshwaraiah, B., and Reddy, P. (2005) Niobium (V) chloride-catalyzed C-H insertion reactions of α -diazoesters: synthesis of β -keto esters, *Tetrahedron* 61, 875-878.
- [5] Tosin, M., Betancor, L., Stephens, E., Li, W. M., Spencer, J. B., and Leadlay, P. F. (2010) Synthetic chain terminators off-load intermediates from a type I polyketide synthase, *Chembiochem : a European journal of chemical biology* 11, 539-546.
- [6] Stunkard, L. M., Dixon, A. D., Huth, T. J., and Lohman, J. R. (2019) Sulfonate/Nitro Bearing Methylmalonyl-Thioester Isosteres Applied to Methylmalonyl-CoA Decarboxylase Structure-Function Studies, *Journal of the American Chemical Society* 141, 5121-5124.
- [7] Stunkard, L. (2019) UNVEILING ENZYMATIC MECHANISMS WITH MALONYL-THIOESTER ISOSTERES, In *Biochemistry*, Purdue University, West Lafayette, IN.
- [8] Ballini, R., Marcantoni, E., and Petrini, M. (1992) Synthesis of functionalized nitroalkanes by oxidation of oximes with urea-hydrogen peroxide complex and trifluoroacetic anhydride, *Tetrahedron Lett* 33, 4835-4838.
- [9] Base, D. S., and Vanajatha, G. (1998) A versatile method for the conversion of oximes to nitroalkanes, *Synthetic Commun* 28, 4531-4535.

- [10] Sylvain, C., Wagner, A., and Mioskowski, C. (1999) An efficient procedure for the esterification of nitroacetic acid: Application to the preparation of Merrifield resin-bound nitroacetate, *Tetrahedron Lett* 40, 875-878.
- [11] Justyna, K., Małolepsza, J., Kusy, D., Maniukiewicz, W., and Błażewska, K. M. (2020) The McKenna reaction—avoiding side reactions in phosphonate deprotection, *Beilstein journal of organic chemistry* 16, 1436-1446.
- [12] Stewart, C. J., Dixon, R. G., McClendon, E. M., and Swearingen, L. W. (1975) SYNTHESIS OF ACETYLAMINODESTHIO-COENZYME A, A COMPETITIVE INHIBITOR OF ACETYL-COENZYME A, *FEDERATION PROCEEDINGS* 34, 690-690.
- [13] Weeks, A. M., Wang, N., Pelton, J. G., and Chang, M. C. Y. (2018) Entropy drives selective fluorine recognition in the fluoroacetyl-CoA thioesterase from *Streptomyces cattleya*, *Proceedings of the National Academy of Sciences of the United States of America* 115, E2193-E2201.
- [14] Michenfelder, M., and Retey, J. (1986) Methylmalonylcarba(dethia)-Coenzyme A as Substrate of the Coenzyme B12-Dependent Methylmalonyl-CoA Mutase Enzymatic Rearrangement of a β - to a γ -Keto acid, *Angewandte Chemie* 25, 366-367.
- [15] Martini, H., and Rétey, J. (1993) Propionyl-Aza(dethia)coenzyme A as Pseudosubstrate of the Biotin-Containing Transcarboxylase, *Angewandte Chemie International Edition in English* 32, 278-280.
- [16] Wlassics, I. D., Stille, C., and Anderson, V. E. (1988) Coenzyme A dithioesters: synthesis, characterization and reaction with citrate synthase and acetyl-CoA:choline, *Biochimica et Biophysica Acta (BBA) - Protein Structure and Molecular Enzymology* 952, 269-276.
- [17] Mishra, P. K., and Drueckhammer, D. G. (2000) Coenzyme A Analogues and Derivatives: Synthesis and Applications as Mechanistic Probes of Coenzyme A Ester-Utilizing Enzymes, *Chemical reviews* 100, 3283-3310.
- [18] Usher, K. C., Remington, S. J., Martin, D. P., and Drueckhammer, D. G. (1994) A Very Short Hydrogen Bond Provides Only Moderate Stabilization of an Enzyme-Inhibitor Complex of Citrate Synthase, *Biochemistry* 33, 7753-7759.

CHAPTER 3. APPLICATION OF ACYL-COA ANALOGS TO MECHANISTIC AND DRUG DEVELOPMENT STUDIES WITH RESPECT TO ACYL-COA CARBOXYLASES

Contributions: Jeremy Lohman and Trevor Boram designed experiments and interpreted the resulting data. Trevor Boram carried out the majority of experiments. Lee Stunkard, Amanda Silva de Sousa, and Aaron Benjamin contributed cloning and expression of some constructs.

Note: Literature references and chemical numbers within schemes are unique within this chapter.

3.1 Abstract

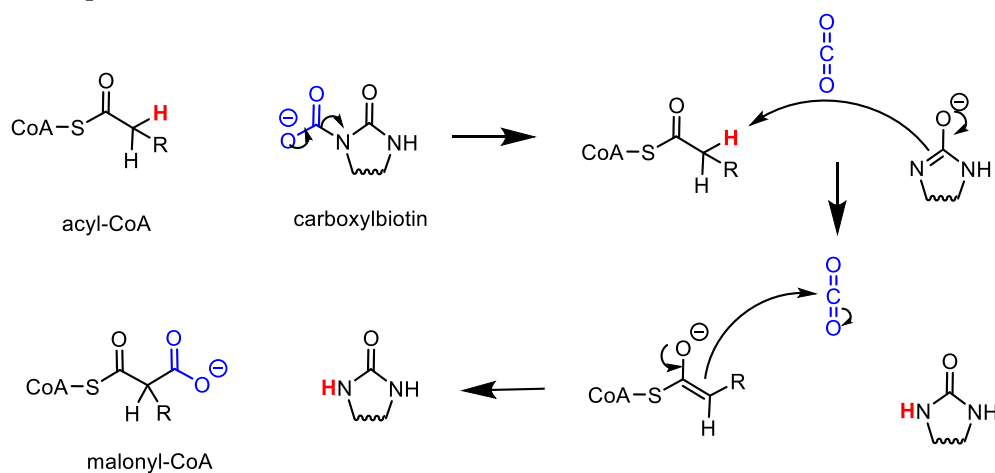
Acyl-CoA carboxylases (YCCs) are responsible for the critical role of making malonyl-CoAs through two half reactions. While the importance of malonyl-CoA is apparent from its use in making fatty acids and polyketides, there remains a great deal to be uncovered in the mechanism of YCC catalysis. Particularly, details of the second YCC half reaction, catalyzed by the carboxyltransferase reaction center are obscured due to difficulties in capturing all components of the reaction complex in structural studies. Advances in the resolving capability of cryo-EM over the past decade and synthesis of stable reactant/product analogs create new avenues for uncovering the carboxyltransferase catalytic strategy. In this chapter, I outline the application of acyl-CoA analogs to structure-function studies of various YCCs.

3.2 While the BC reaction of YCCs is largely understood and well-studied, there are still missing details obscuring understanding of the CT catalytic mechanism

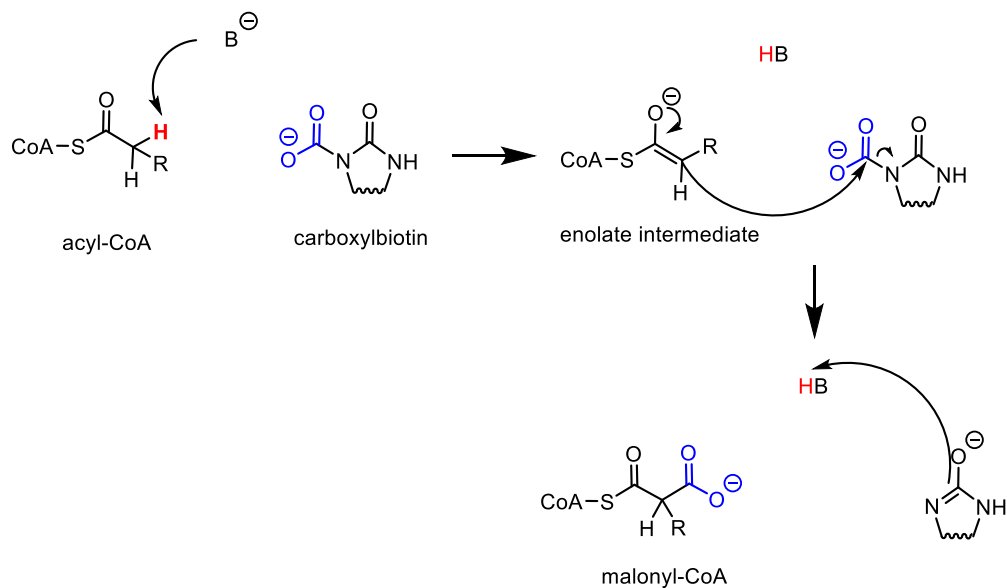
From our rudimentary discussion of YCCs in chapter 1, we learned that these biotin-dependent carboxylases ligate CO₂ to their substrates to form β -ketoacid products¹. Among these β -ketoacid products are oxaloacetate, malonyl-CoA, and (2S)-methylmalonyl-CoA, all playing roles in metabolism in fatty acid synthesis or the citric acid cycle. The mechanistic details of these biotin-dependent carboxylases have been subject to investigation for decades through a variety of kinetic, isotopic labeling, and structure-function experiments². As a result of these investigations, a vast amount of support has been provided for a proposed BC catalytic mechanism. However, providing support for catalytic details of proposed CT mechanisms has proven more challenging,

and is an important topic of investigation. In 1989, a leader in the carboxylase field, J.R. Knowles, summarized much of the work that had been done toward understanding the catalytic mechanism of biotin-dependent carboxylases, analyzing previously posited mechanisms for CT catalysis². The first mechanism which kinetic isotope effect (KIE) data did not refute features carboxylbiotin decarboxylating to yield free CO₂ and a biotin-enolate. This biotin-enolate can then act as a base to deprotonate the α -carbon of the acyl-CoA substrate, producing an acyl-CoA enolate. From here, the enolate can attack the free CO₂ to yield a malonyl-CoA product. An alternative potential mechanism proposed involves a base (provided by the CT) directly removing a proton from the α -carbon of the acyl-CoA substrate, generating the enolate form. This enolate can then attack the carboxylbiotin to generate a malonyl-CoA. Currently, there is not conclusive evidence to refute either of these mechanisms, Figure 3.1.

1. CO₂ leaves



2. Active site base attacks



B = base

HB = conjugate acid

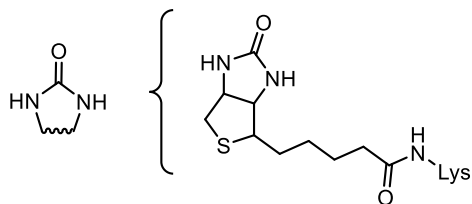


Figure 3.1 Proposed catalytic strategies of YCC CTs in the product of malonyl-CoA products

High-resolution structural data of CT domains in various YCCs is sparse, with the apo structure of the *E. coli* ACC CT being solved in 2006 at 3.2 Å³. While other CT structures improved notably on the resolution limits seen in this *E. coli* CT structure, much of the data barely approaches the resolution needed to make supported mechanistic inferences of enzyme catalysis⁴. In addition to CT resolution problems, there is a lack of catalytically relevant CT-substrate structures due to the reactivity of the substrates as well as the complexity of capturing the ternary carboxybiotin-BCCP, CT, and acyl-CoA complex crystallographically.

One of the first studied carboxylases is the transcarboxylase from *P. shermanii*, which, unlike other carboxylases, is not ATP dependent⁵. Rather, transcarboxylase moves the carboxylate of (2S)-methylmalonyl-CoA to pyruvate, yielding propionyl-CoA and oxaloacetate as the products. This reaction can proceed in either direction. Transcarboxylase does however share a similar protein organization to other carboxylases, with a BCCP tethered to biotin (1.3S subunit), a CT working on a CoA substrate (12S subunit), and a CT working on pyruvate (5S subunit)⁶. Transcarboxylase was one of the first discovered carboxylases, with notes on its reaction dating back to the 1940's, it became a model carboxylase for studying⁷.

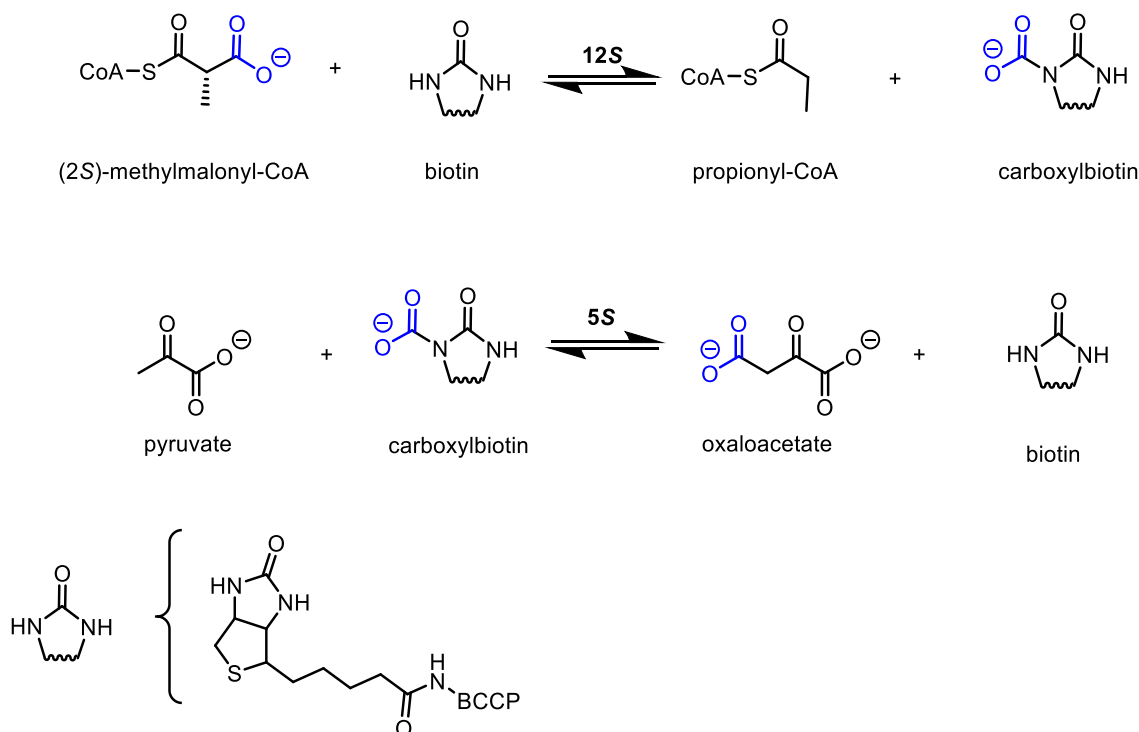


Figure 3.2 Overall reaction of *P. shermanii* transcarboxylase.

In the early 1970s, the electron microscopy (EM) structure of transcarboxylase was solved, showing that the complex consists of a core hexamer of 12S subunits, where each 12S monomer interacts with a 5S homodimer⁸. The 5S homodimeric interactions are promoted by the binding of a 1.3S subunit to interface between the 12S and 5S subunits⁹. The 12S subunit, which interconverts between propionyl-CoA and (2S)-methylmalonyl-CoA, should be expected to proceed through the same mechanism as other CTs. However, the structure-function details of this reaction are largely unknown, Figure 3.2.

In 2003, the first (and only) structure of the 12S subunit of transcarboxylase was solved (albeit the C-terminal 106 amino acids were truncated)¹⁰. Additionally, the enzyme was also solved with methylmalonyl-CoA bound with clear ligand density in the active site at a high-resolution of 1.9 Å, Figure 3.3. While initially this result seems like it should contain all critical mechanistic information we need, there is one box this structure does not check: biotin is not bound at all. Thus, we are left with the question of how does biotin participate in catalysis? More concerning from this structure – how is methylmalonyl-CoA in an orientation to decarboxylate and allow biotin to accept this CO₂ to shuttle it to the 5S subunit?

Since this structure does not include biotin, which is a substrate in catalysis, it is completely unclear how biotin could accept a CO₂, or even act as a base to deprotonate the α -carbon of methylmalonyl-CoA (proposed in CT – CO₂ *leaves* mechanism, Figure 3.1). When we consider a critical substrate is missing from the reaction that would occupy a large portion of the 12S active site, this certainly brings into question if the orientation of methylmalonyl-CoA in the active site is correct for catalysis. If we consider the second proposed CT mechanism, there should be a basic residue close enough to the substrate to remove a proton and generate an enolate intermediate. However, upon inspecting all of the residues within reasonable distance to the substrate, none of them contain appropriate functional groups or orientations to remove a proton. What is unclear is if this result indicates that biotin serves as the base to generate an enolate, or if the substrate is simply bound in the wrong orientation for catalysis due to missing biotin and BCCP interactions. An incorrect catalytic orientation is supported if we consider that enzymes that decarboxylate β -ketoacids oriented the carbonyl group in an oxyanion hole to lower the activation energy of decarboxylation. In this structure, there are no residues within a reasonable distance of the thioester carbonyl to form an oxyanion, providing evidence to why methylmalonyl-CoA has not

decarboxylated in this structure. Although the methylmalonyl-CoA substrate is intact in this crystal structure, catalytic inferences that could be made here are not sound.

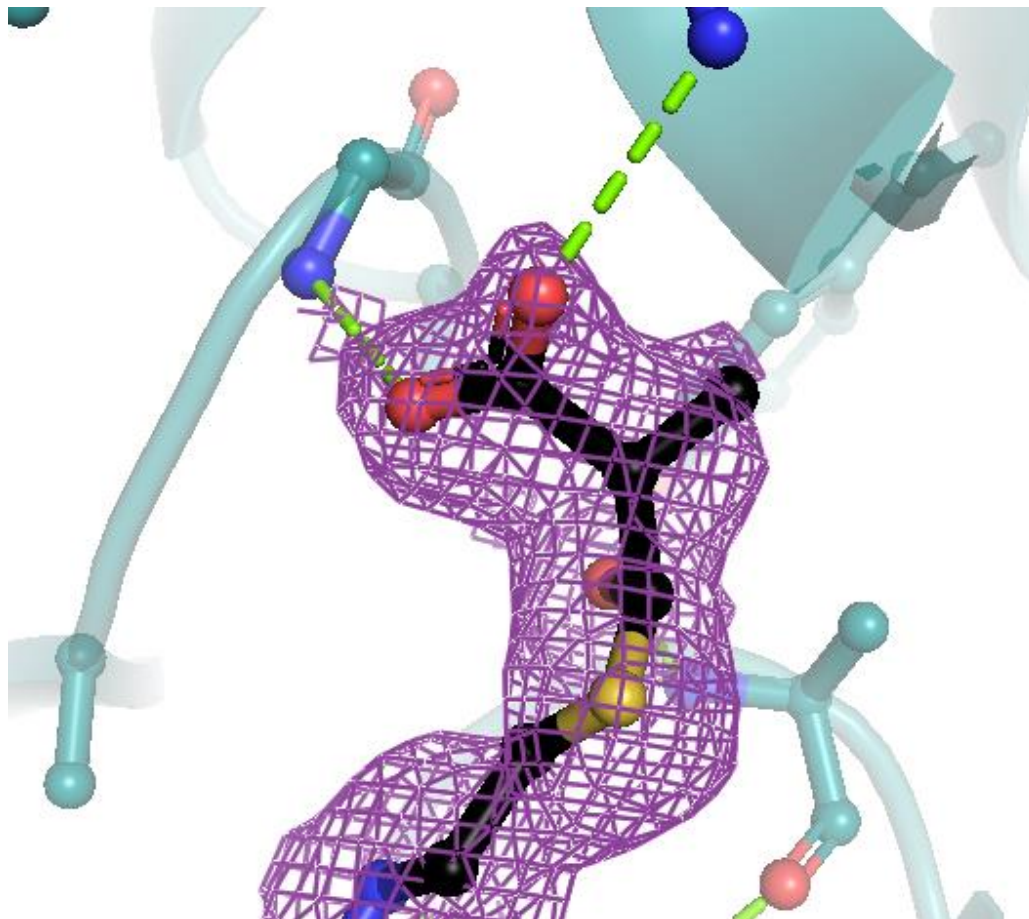


Figure 3.3 Crystal structure of *P. shermanii* transcarboxylase 12S subunit (1-507) with (2*R/S*)-methylmalonyl-CoA bound (PDB: 1ON3), solved at 1.9 Å¹⁰.

In the following year, the structure of another carboxylase CT, propionyl-CoA carboxylase (PCC) β subunit from *Streptomyces coelicolor* was solved at 2.2 Å for the first time, having both substrates - propionyl-CoA AND biotin bound in the active site¹¹. As such, the authors proposed a new, more detailed mechanism to CT catalysis, with the below flattened schematic suggesting that propionyl-CoA is situated in an oxyanion hole formed by adjacent glycine backbone amides, Figure 3.4. Additionally, this schematic shows the ureido moiety of carboxybiotin situated in an oxyanion hole, which seems logical to promote decarboxylation necessary for catalysis.

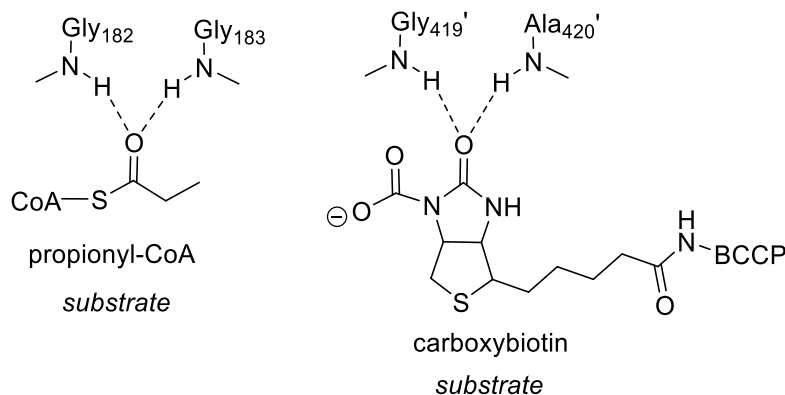


Figure 3.4 Flattened schematic displaying the inferred orientation of propionyl-CoA and carboxy-biotin bound in the active site of PCCβ from *S. coelicolor*^{[11](#)}.

However, the issue of CT catalysis remains unsolved. Like transcarboxylase before, the structure of PCCβ was missing some information necessary to understand CT catalysis. Unlike the transcarboxylase ligand density, the density of both the biotin and propionyl-CoA molecules are sparse and do not support the modeled ligands, Figure 3.5. The carbonyl of propionyl-CoA which is modeled to sit in the oxyanion hole formed by Gly 182 and Gly 183, yet there is no density for the oxygen atom. Additionally, the hydrogen-bond contact formed by the amide of G182 is 4.1 Å to the modeled carbonyl oxygen, which is unreasonable long for an H-bond. Lastly, the N'1 atom of biotin is modeled facing the α-carbon of propionyl-CoA, where it is suggested to act as a base. Without CO₂ additionally in the active site, we cannot determine if this orientation is meaningful in terms of catalysis.

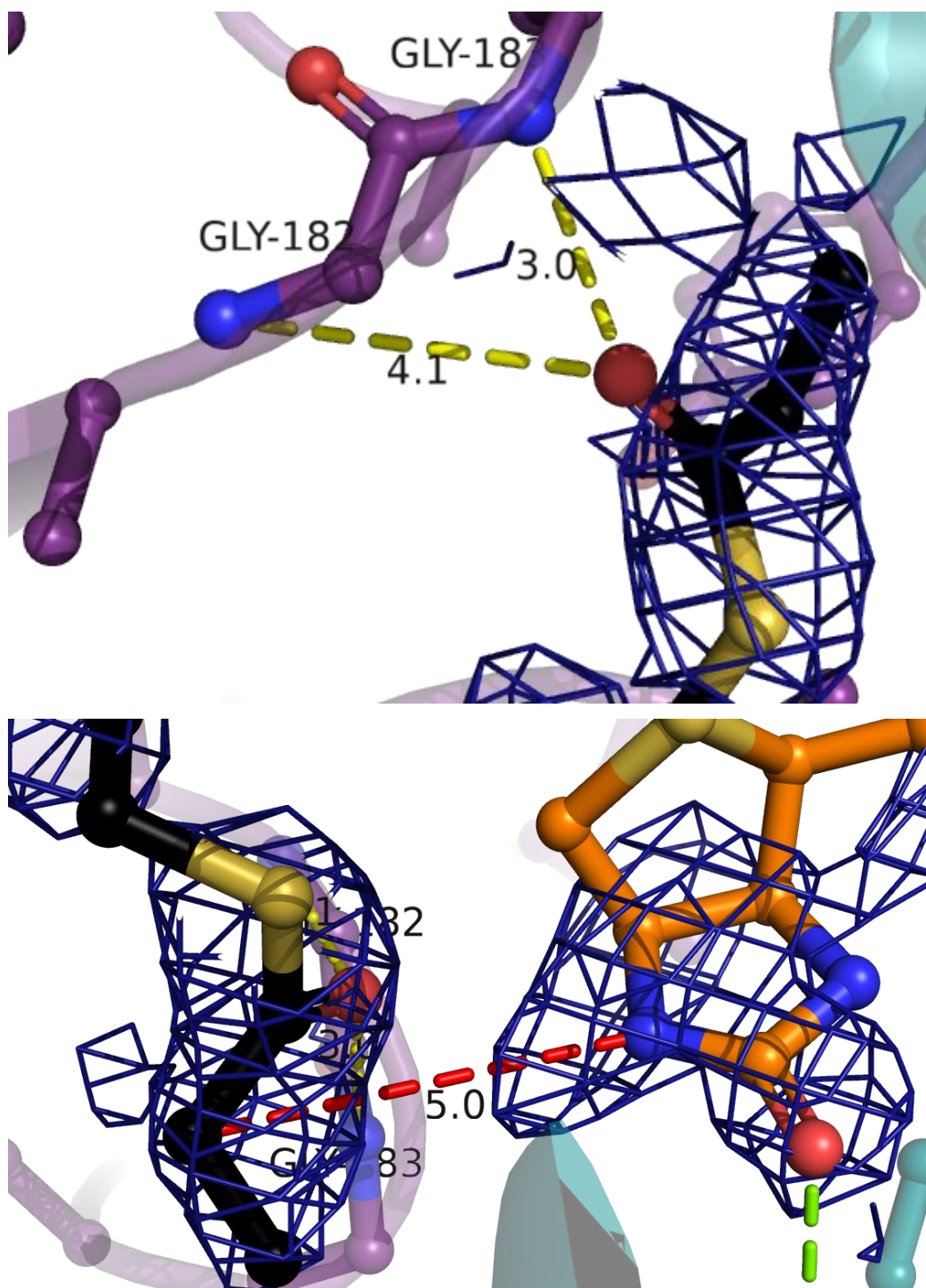


Figure 3.5 Crystal structure of PCC β from *S. coelicolor* with propionyl-CoA and biotin modeled (PDB: 1XNY) solved at 2.2 Å. Top- Display of proposed oxyanion hole with the carbonyl group of propionyl-CoA oriented for catalysis. Bottom- Display of modeled biotin and propionyl-CoA ligands in PCC β crystal structure^{[11](#)}.

Twelve years later, another notable YCC structure with ligands bound would be solved, this time of the *Saccharomyces cerevisiae* ACC1 (PDB: 5CSL)¹². This structure was determined using Cryo-EM with CoA and biotin bound in the active site, Figure 3.6. While this structure is a great achievement considering it is of the whole enzyme, it is still an incomplete picture. The resolution of this structure is 3.2 Å, which leads to a high degree of uncertainty when modeling the ligands in the proper orientation. Additionally, the ligands are incomplete, as the propionyl group of propionyl-CoA and the carboxyl group of carboxy-biotin are both missing.

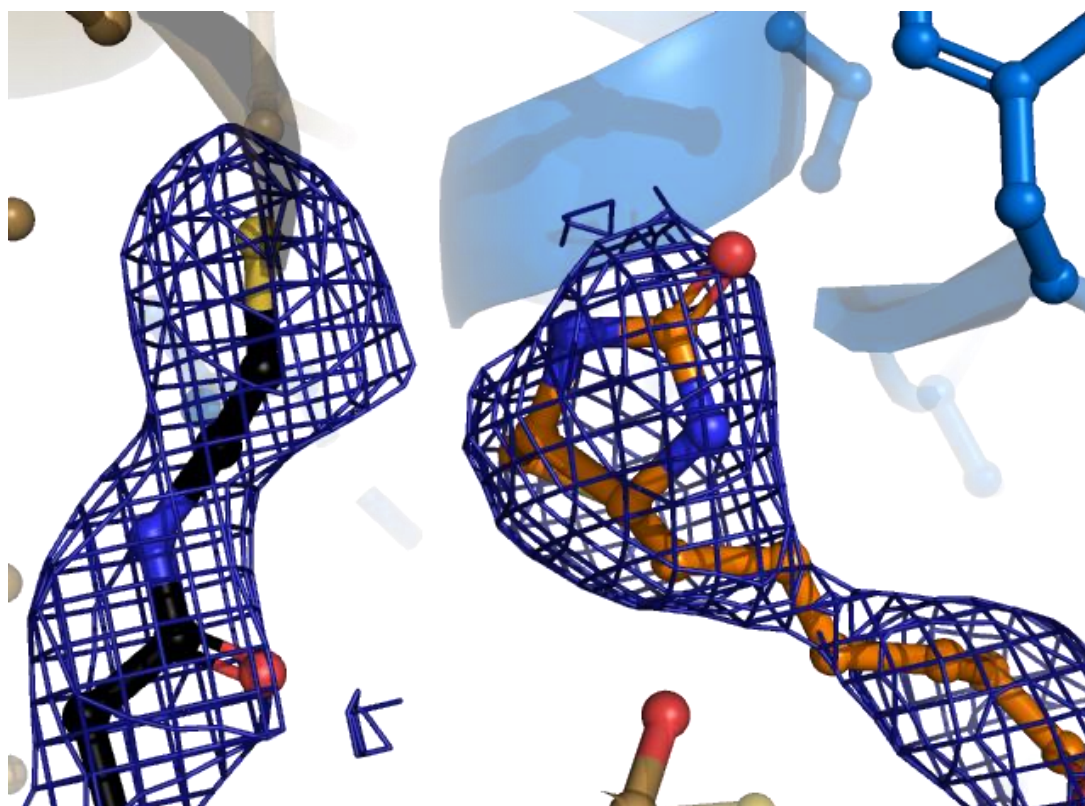


Figure 3.6 Cryo-EM structure of biotinylated-ACC1 from *S. cerevisiae* with CoA bound (PDB: 5CSL), solved at 3.2 Å¹².

Between all of these structures, we see a common theme is an inability to capture both substrates in a correctly modeled, high-resolution ternary complex. In this thesis, we attempt to co-crystallize various substrate, product, and intermediate acyl-CoA analogs with CTs to deduce the conformational changes and orientation of substrates for catalysis, Figure 3.7.

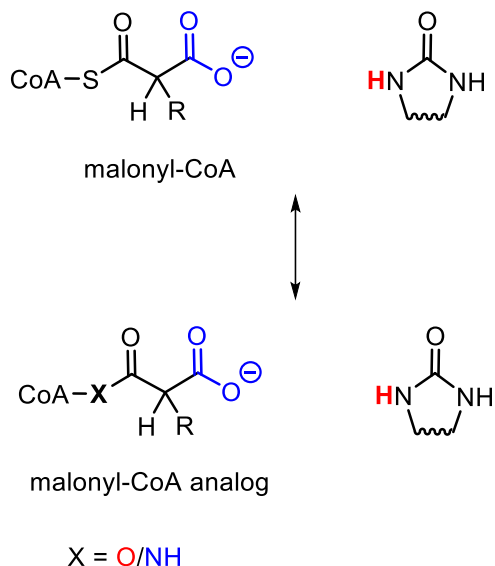


Figure 3.7 The malonyl-CoA:CT:biotin interaction could be mimicked by a stable malonyl-CoA analog, capturing the ternary complex.

3.3 Optimization of YCC production is necessary to overcome difficulty in sample production for crystallography and protein crystal diffraction quality

When attempting to determine the structure-function relationship of a YCC, biotin, and a malonyl-CoA analog, we chose to use X-ray crystallography for its ability to yield high resolution data, allowing for proper modeling of ligands. Additionally, we used a variety of YCCs, as it has been observed that differences between them may largely influence the quality of diffraction data obtained from their crystals. For example, where *Staphylococcus aureus* ACC CT had been solved to 1.8 Å, the same group solved the homologous *E. coli* ACC CT to 3.2 Å³. Therefore, we selected five representative YCCs for structure-function analysis: ACC CT from *Staphylococcus aureus*, (SaACC CT), ACC CT from *Escherichia coli* (EcACC CT), PCC CT from *Streptomyces coelicolor* (ScPCC CT), transcarboxylase 12S subunit from *Propionibacterium shermanii* (PfTC-12S), and ACC1 from *Saccharomyces cerevisiae* (ScvACC1), Figure 3.8.

YCCs all have the same core function – carboxylation, but all have different subunit organizations. This difference is a double-edged sword for the biochemist, as these differences present ample opportunity to develop drugs targeting only bacterial or plant carboxylase, while ignoring human YCCs. However, studying each enzyme biochemically comes with unique challenges in protein expression/purification, crystallization, enzyme assay development, holoenzyme reconstitution. For example, ScvACC1 is expressed as a single polypeptide, which

makes molecular cloning more laborious and crystallization efforts likely to be lower resolution. However, this enzyme can be expressed all off of one plasmid, with one purification tag, and requires no incubation of subunits to reconstitute activity. As such, with this enzyme, we decided to take a cryo-EM approach to structure-function analysis.

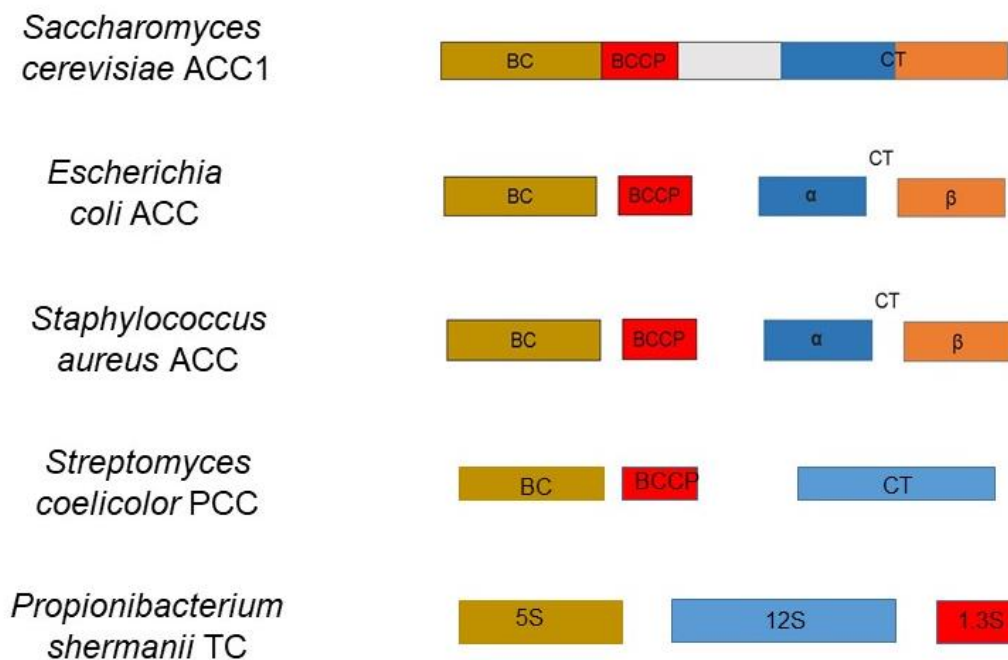


Figure 3.8 Various prokaryotic and eukaryotic YCCs were studied in mechanistic investigations in this thesis work.

Our lab was not initially trained in cryo-EM, and thus we formed a collaboration with Dr. Wen Jiang's lab at Purdue University, with postdoctoral associate, Dr. Xueyong Xu. The collaborative effort between our labs has led to promising negative stain images of ScvACC1, Figure 3.9. Based on this preliminary data, we plan to solve the structure of ScvACC1 with our nonreactive acyl-CoA analogs bound to gain insight into the conformational changes the enzyme undergoes during catalysis.

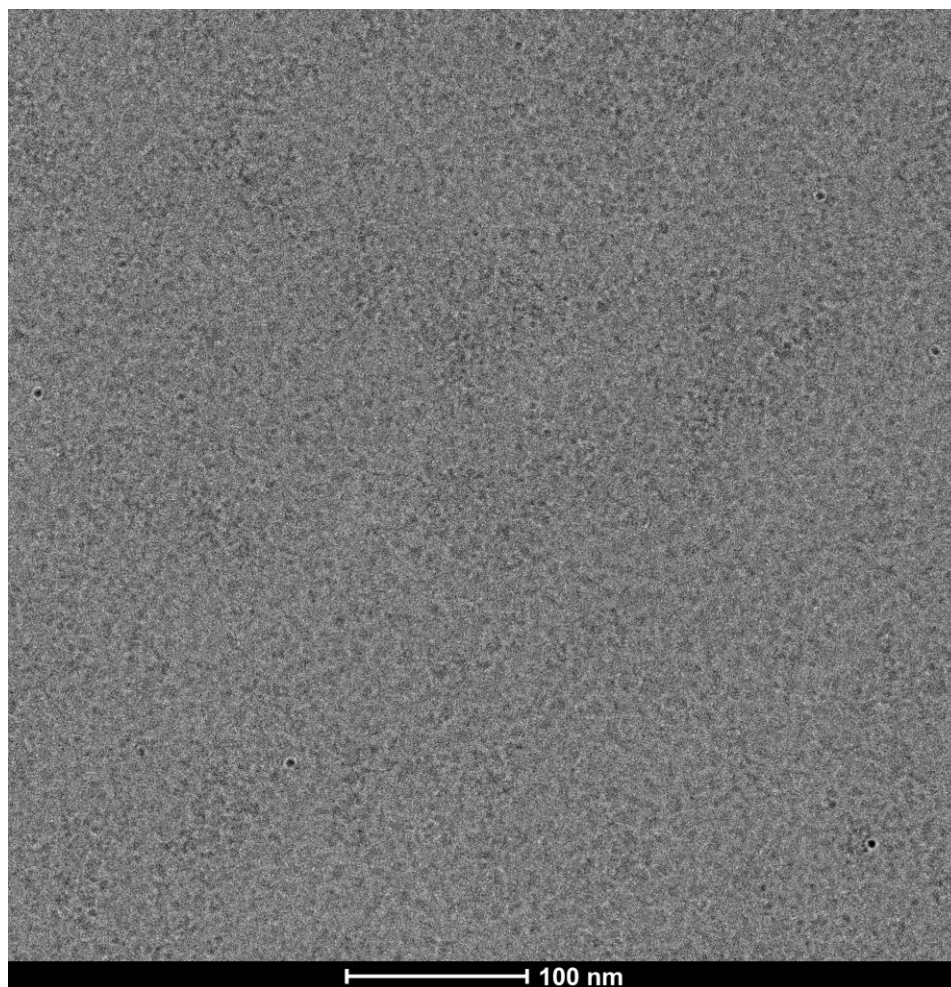


Figure 3.9 Cryo-EM negative stain of ScvACC1 in the following conditions: 1 mg/ml ACC1, 10 mM HEPES pH = 7.5, 150 mM NaCl, 20 mM sodium citrate, 0.9% glycerol

While the ScvACC1 structure may provide useful insights into overall conformational changes of the enzyme, potential higher resolution crystal structures of isolated CT components may provide more definite information of the enzyme:substrate interactions. I began my journey to capture a YCC CT crystal structure studying EcACC CT, which is formed by the gene product of the *accA* and *accD* genes. Initially, I cloned these genes on separate plasmids, and attempted to express their proteins separately, then incubate them together and correct for stoichiometry differences using size exclusion chromatography (SEC). Much of the protein was lost in this process through precipitation. I observed a notable amount of precipitation of the individually expressed CT peptides prior to mixing them together. The yields of recovered protein were further reduced due to poor cleavage by TEV protease at the His-tag cleavage site. In spite of this, we

were able to grow crystals of the enzyme, and obtain low resolution diffraction data of these crystals. Unfortunately, these crystals appeared to suffer from twinning, and we faced issues proceeding further in processing this data set.

Afterward, I generated a new construct that coexpressed accA and accD via action of a ribosome binding site between the genes. This construct featured only a single His-tag on accA, meaning less protein would need to be cleaved by TEV protease. Additionally, the coexpression of the two proteins enabled the complex to form immediately, which eliminated post-purification protein precipitation issues. Once again, we generated uniform crystals of EcACC CT produced from this construct, seen in Figure 3.10, but the crystals obtained produce very low resolution diffraction data or high resolution data with severe twinning issues, Figure 3.11.

One reason why the enzyme may diffract poorly (which had been seen in the previous EcACC CT structure) is the presence of a disordered N-terminal region. We sought to develop better diffracting crystals by truncating the flexible N-terminal residues of the AccA subunit. Thus, I next subcloned EcACC CT to remove the first 56 amino acids of EcACC. The unintended consequence of this truncation was raising the computed pI of the subunit from 5.76 to 7.9, which I suspect severely changed the stability of the protein. After protein expression, virtually all of the truncated subunit was seen in the insoluble fraction and lysate clarification.

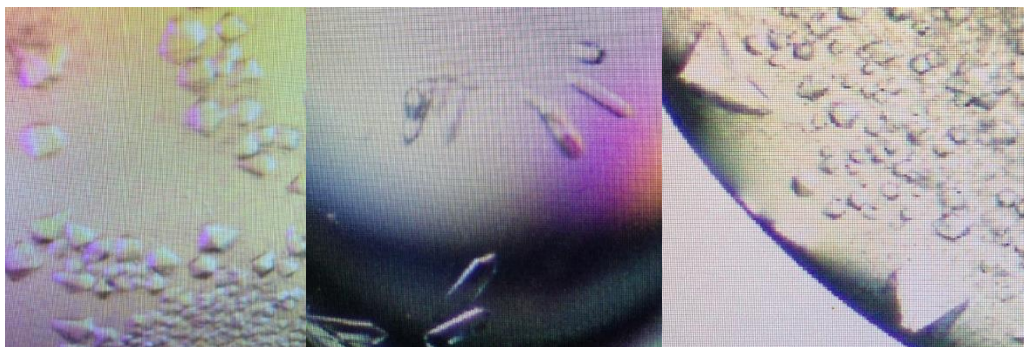


Figure 3.10 Protein crystals grown in various morphologies and sizes of *E. coli* ACC CT that led to low quality diffraction.

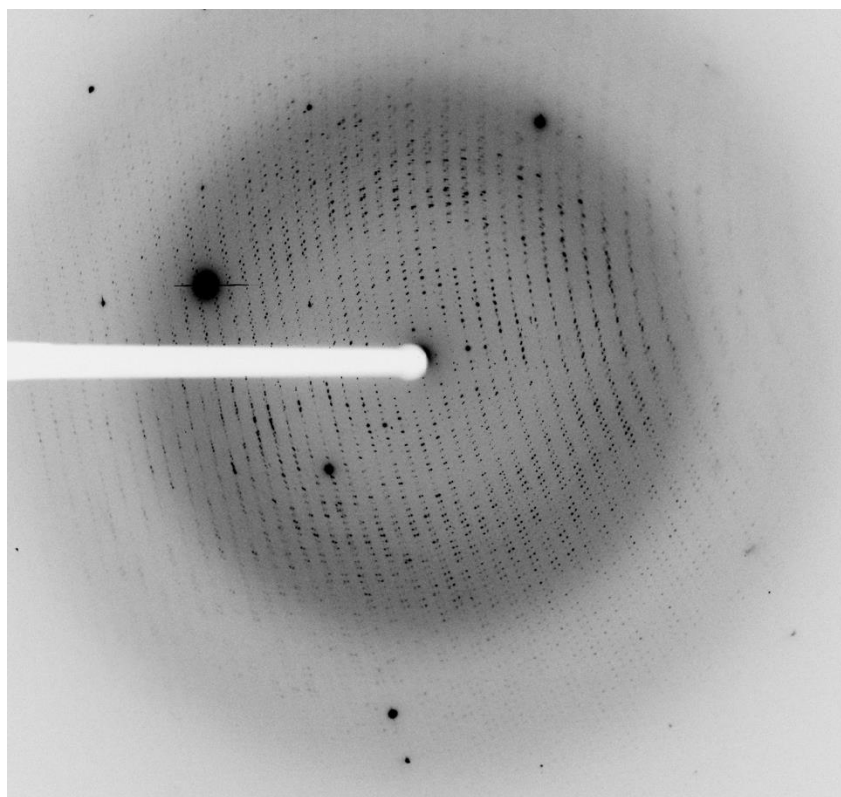


Figure 3.11 Representative X-ray diffraction image of EcACC CT crystals. Diffraction data shows severe twinning/multiple crystals.

Around this time, we decided to put EcACC CT crystallization on hold, due to existing evidence that other CTs may lead to more success in crystallography. The next such CTs we studied were ScPCC CT and SaACC CT, both of which had been solved to higher resolution than EcACC CT by other groups. Like EcACC CT, SaACC CT is encoded by an *accA* and *accD* gene, but unlike the *E. coli* ACC, SaACC CT does not feature a disordered N-terminal region. Additionally, SaACC CT genes are found next to each other in the *S. aureus* genome, and are translated together by an overlapping stop/start codon. Thus, I cloned and expressed SaACC CT together on a single plasmid, taking advantage of the overlapping stop/start system. This protein appeared to express well, but was incompletely digested by TEV protease. We suspected that the N-terminus of the protein had the opposite problem of the *E. coli* version— it had too rigid and defined of a structure which left the protease cleavage site inaccessible. Attempting to solve the problem, I cloned off of the ACC template to insert two glycine residues in between the TEV protease cleavage site and the start of SaACC CT. Unfortunately, even with the added space between the protease cut site and the body of the protein, TEV protease could still not remove the

His-tag on the protein. Additionally, I moved the His-tag from the AccD peptide to the AccA peptide of this construct, but protease cleavage was not improved. Crystallization of the His-tagged protein was not attempted due to suspicion that conformational flexibility of the large N-terminal tag would lead to low resolution diffraction data.

After the challenges faced with His-tag removal from EcACC CT and SaACC CT, I focused on producing ScPCC CT, which is produced by a single gene: *pccB*. I cloned, expressed, and purified ScPCC CT via a His-tag. This protein is known to form a homohexameric quaternary structure, and thus, features 6-His tags per ScPCC CT. However, TEV protease was able to cleave the His-tag off of the protein to yield ScPCC CT for crystallography. The construct was crystallized initially at 15 mg/ml, and rapidly produced large crystals (>0.5 mm in length), which were diffracted at the Advanced Photon Source (APS) at Argonne National Labs (ANL). These crystals yielded poor resolution, around 5 Å. It was also noted, that the crystals produced low quality diffraction spots, due to hollow-interior cores of the crystals.

Initially, we suspected that due to high stoichiometry of the ScPCC CT complex, the protein was able to form a heterogeneous population post-TEV protease cleavage of tagged and cleaved-tag ScPCC CT monomers. Thus, I cloned a variant of the protein that featured no tag, and purified it to homogeneity via ammonium sulfate fractionation, followed by anion exchange chromatography, and SEC. Purified protein was confirmed via sodium dodecyl sulfate – polyacrylamide gel electrophoresis (SDS-PAGE), Figure 3.12. The completely untagged ScPCC CT was again crystallized, again producing large, hollow crystals very rapidly. As anticipated, these crystals still experienced poor resolution diffraction. We suspected that lowering the protein concentration and reexamining crystallization conditions would slow the rate of crystal growth, thus giving them sufficient time to grow without deformed interiors. These crystals were grown at 7 mg/ml, and featured no interior deformities, but were much smaller in size, Figure 3.13. However, their diffraction improved slightly, featuring no twinning, and resolution of 3.9 Å – an improvement, but not sufficient to make mechanistic inferences, Figure 3.14.

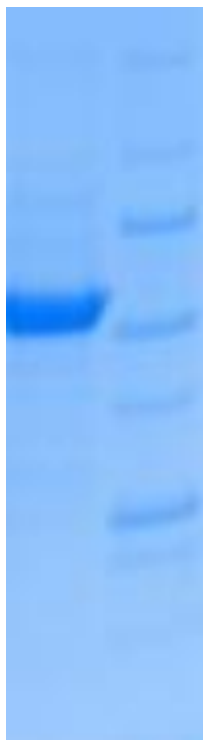


Figure 3.12 SDS-PAGE gel demonstrating the successful purification of tagless-PCC β via non-affinity chromatography methods.

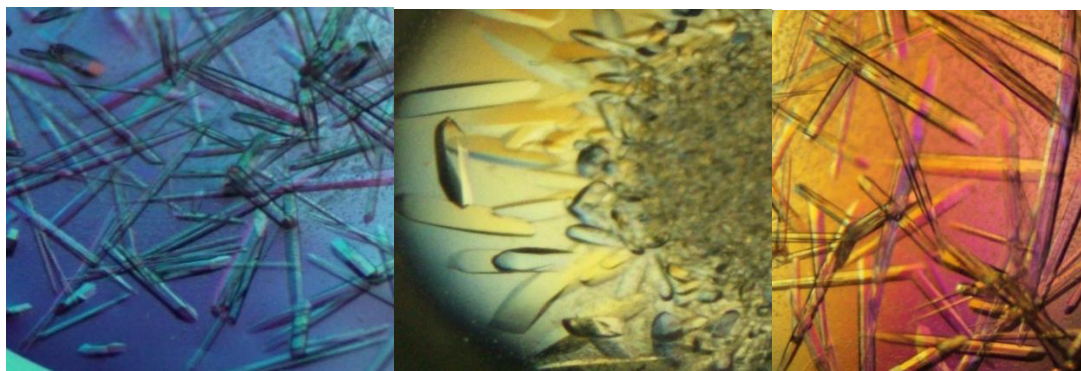


Figure 3.13 Protein crystals grown in various morphologies of *S. coelicolor* PCC β that led to low quality diffraction.

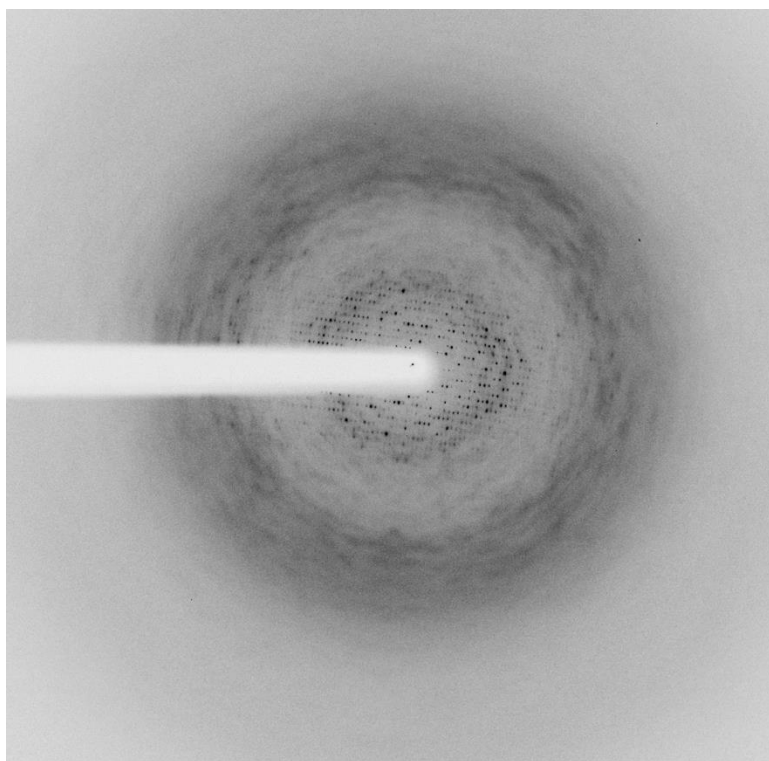


Figure 3.14 Representative X-ray diffraction image of PCC β (tagless).

PfTC 12S was the last carboxylase I studied, which (like ScPCC CT) is encoded on one gene and forms a homohexamer. Previously, a truncation of the structure of PfTC 12S had been solved to 1.9 Å, missing the C-terminal 105 amino acids. It is also known that removing this region of the protein reduces the rate of TC holoenzyme assembly. Like ScPCC CT, I expressed and purified the 12S subunit with no tag, but was unable to reconstitute its enzymatic activity based on HPLC assays. This is likely due to the inability of the enzyme to use free biotin as a substrate. Thus, I expressed the 1.3S and 5S subunits of TC, and confirmed that the 1.3S was biotinylated via MALDI-TOF mass spectrometry. I incubated these subunits together based off of existing literature, and attempted to assay TC activity again, still appearing inactive. Again I consulted the literature, and found report of PfTC 5S subunit expressed recombinantly in *E. coli* being inactive. This could be rectified by harvesting endogeneously expressed TC from *P. shermanii*, an anaerobic bacteria, which is a future goal.

3.4 Development of UV-vis assays for YCC enzymology for studying inhibitor induced futile-cycle activation

Initially, we began studying all YCC turnover via analytic HPLC activity assays, which provide extensive information about consumption and production of specific molecules, but are quite laborious and low-throughput. To simplify assay of YCCs, we decided to adopt a continuous, coupled enzyme assay for ATP dependent YCCs using the enzymes pyruvate kinase and lactate dehydrogenase (both from *Homo sapiens*). As the BC domain of a YCC hydrolyzes ATP to ADP, the reaction can be supplemented with a large excess of phosphoenolpyruvate and nicotinamide adenine dinucleotide – reduced form (NADH), which allows for monitoring decrease in UV absorbance at 340 nm as a readout, Figure 3.15.

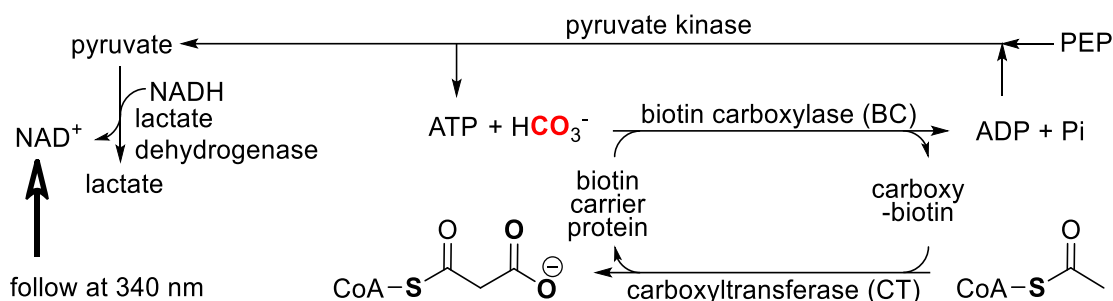


Figure 3.15 Strategy of monitoring ACC ATP turnover using a continuous, coupled UV-vis assay to look for futile cycle producing small molecules.

After purifying pyruvate kinase and lactate dehydrogenase with nickel affinity chromatography, we assayed their activity, then applied the enzymes to this assay, and were able to demonstrate that we can observe the reaction readout quickly using the above strategy.

A key reason we wanted to assay the activity of YCCs was to examine the activity of the enzyme BC half-reaction in different conditions that would not be productive for producing malonyl-CoA. This idea came from literature by Dr. J. Rétey's group, where propionyl-carba(dethia)CoA and propionyl-aza(dethia)CoA were synthesized and characterized with PfTC¹³. In these studies, the researchers found that propionyl-carba(dethia)CoA was a substrate for TC, producing (2S)-methylmalonyl-carba(dethia)CoA, but propionyl-aza(dethia)CoA was not a substrate. Interestingly, while no (2S)-methylmalonyl-aza(dethia)CoA was formed, oxaloacetate was still enzymatically turned over, suggesting that the presence of substrate to accept a carboxyl group in the CT activity site activates the reaction in the BC domain. If propionyl-aza(dethia)CoA was found to be a BC activator, this could serve as an antimetabolite to promote PCC to turnover

ATP at a rate that could limit cell growth or cause death. As such, a small molecule of high specificity and affinity for the CT active site that leads to increased BC ATP turnover may serve as a novel bacteriocidal pharmaceutical.

To test this idea, we initially performed an HPLC assay to monitor ATP turnover and malonyl-CoA formation of EcACC in the presence of acetyl-CoA, acetyl-oxa(dethia)CoA, or acetyl-aza(dethia)CoA, Figure 3.16. To more easily visualize conversion of ATP to ADP, we coupled the assay to the enzyme adenylate kinase (Adk) from *E. coli*, which converts two molecules of ADP into one molecule of ATP and one of AMP. AMP has a longer retention time on HPLC, and is retained past the solvent front, simplifying visualization. The HPLC analysis of the ACC reactions indicated that the enzyme could turnover ATP to make malonyl-CoA with acetyl-CoA as the substrate, ACC would turnover more ATP in the other cases, but fail to make any of the corresponding oxa- or aza- malonyl-CoAs. In addition, we examined the half-reaction of the BC domain on its own (without CT or acetyl-CoA) to turn over ATP and observed a large decrease in ATP turnover. Thus, we learned that the CT and its substrate occupancy is related to the ATP turnover rate of the BC domain. We can rationalize this idea as an organism should not exhaust its energy resources through ATP hydrolysis when there is no potential for a useful product to be made, such as malonyl-CoA. Non-reactive acetyl-CoA analogs exploit this feature and allow the enzyme to actively turnover ATP with no useful product formation, leading to a futile cycle.

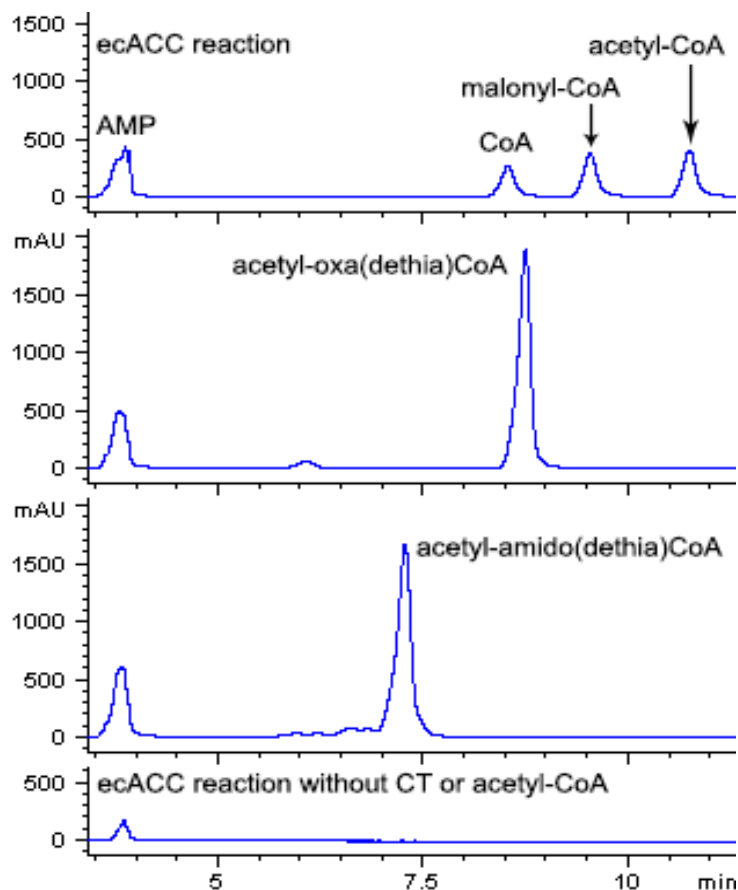


Figure 3.16 HPLC traces demonstrating nonreactive acetyl-CoA analogs lead to equivalent of increased ACC catalyzed ATP turnover relative to acetyl-CoA incubated ACC.

In the future, we would like to apply our continuous UV-vis assay to perform a high-throughput screen of a drug library with the goal of searching for molecules that induce ATP turnover in ACC, leading to a futile cycle. The structural diversity of YCCs in nature provides a means to find small molecules that exclusively target a YCC in a specific organism. Thus, a futile cycle inducer of a YCC could potential serve as an antimicrobial, herbicide, or anticancer drug.

3.5 Conclusions

From this chapter, one can appreciate the complexity of determining the catalytic details of carboxylase CTs due to the holoenzyme size, instability of the substrates/intermediates, and low affinity of BCCP:CT interactions. Structures that groups have obtained previously have all been incomplete in bringing together all of the subunits and reactants required for catalysis. Our approach of developing substrate, intermediate, and product analogs to probe enzyme catalysis is

not novel, but has never been applied to YCCs in structure-function studies. Here, we have demonstrated the ability to produce protein crystals of varying YCCs in the presence of stable product analogs. Although these crystals diffract poorly, further truncations to CT proteins being studied may produce more organized, well-diffracting crystals. In the future, we will continue to alter CT constructs, and try tagless expression to gain higher quality crystals for diffraction studies.

Additionally from this work, we have gained insight into the presence of a CT antimetabolite induced futile cycle in ACC. While we have shown that aza- and oxa- bearing isosteres of acetyl-CoA can induce futile cycles of ATP turnover in EcACC, in the future we plan to conduct a drug library screen using our high-throughput assay for futile cycle examination. Using this strategy may produce new drug leads to a biological critical, yet heavily studied enzyme.

3.6 Materials and Methods

The materials and methods section of this chapter's work are described below in detail.

3.6.1 Cloning, expression, and purification of carboxylases

Cloning of all constructs except for ScvACC1 was performed using the below primers:
EcAccA-forward: 5'- GAGAACCTCTACTTCCAAAGTCTGAATTCCTTGATTTTG -3',
EcAccA-reverse: 5'- CTCGAGGAGATTACGGATTACGCGTAACCGTAGCTCATCAGGC-3',
EcAccD-forward: 5'- GAGAACCTCTACTTCCAAAGCTGGATTGAACGAATTAAAAG -3',
EcAccD-reverse: 5'- CTCGAGGAGATTACGGATTAGGCCTCAGGTTCTGATCCGGTAC-3',
EcAccB-forward: 5'- GAGAACCTCTACTTCCAAAGTGATATTCGTAAGATTAAAAAACTG -3',
EcAccB-reverse: 5'- CTCGAGGAGATTACGGATTACTCGATGACGACCAGCGGCTCGTC-3',
EcAccC-forward: 5'- GAGAACCTCTACTTCCAAAGTCTGGATAAAATTGTTATTGCCAA-3',
EcAccC-reverse: 5'-CTCGAGGAGATTACGGATTATTTTTCCTGAAGACCGAGTTTTTCT-3',

EcBirA-forward: 5'- GAGAACCTCTACTTCCAAAGTAAGGATAACACCGTGCCACTGA -
3',

EcBirA-reverse: 5'- CTCGAGGAGATTACGGATTATTTTTCTGCACTACGCAGGGAT -3',

EcAccB rbs EcBirA forward: 5'- TAAAGaggagaATACTAGatg
AAGGATAACACCGTGCCACTGA -3',

EcAccB rbs EcBirA -reverse: 5'- catCTAGTATtctcctCTTTA
CTCGATGACGACCAGCGGCTCGTC -3',

EcAccA rbs EcAccD -forward: 5'- TAAAGaggagaATACTAGatg
AGCTGGATTGAACGAATTAAAAG-3',

EcAccA rbs EcAccD -reverse: 5 catCTAGTATtctcctCTTTA
CGCGTAACCGTAGCTCATCAGGC-3',

EcAccA D57 start -forward: 5'- TAAAGaggagaATACTAGatg
AGCTGGATTGAACGAATTAAAAG-3',

SaAccDA- forward: 5'- GAGAACCTCTACTTCCAAAGTTTTAAAGATTTTTTTAATCGAA
-3',

SaAccDA-reverse: 5'- CTCGAGGAGATTACGGATTATTCTATATAAGAACCGATATTTC -
3',

SaAccA -forward: 5'- GAGAACCTCTACTTCCAAAGTTTAGATTTTGAAAAACCACTTT-
3',

SaAccD -reverse: 5'- CTCGAGGAGATTACGGATTATTTAGTCACCTCTTGATGGATTT -
3',

SaAccA rbs SaAccD -forward: 5'- TAAAGaggagaATACTAGatg
AGCTGGATTGAACGAATTAAAAG -3',

SaAccA rbs SaAccD -reverse: 5-catCTAGTATtctcctCTTTA
TTCTATATAAGAACCGATATTTC -3',

ScPccB -forward: 5'- GAGAACCTCTACTTCCAATCCGAGCCGGAAGAGCAGCAG-3',

ScPccB -reverse: 5'- CTCGAGGAGATTACGGATTACAGGGGGATGTTGCCGTGCTTCTTC
-3',

ScPccB (no tag) -forward: 5'-
TTTAATAAGGAGATATACAATGTCCGAGCCGGAAGAGCAGCAG-3',

PfTC 12S -forward: 5'- GAGAACCTCTACTTCCAAGCTGAAAACAACAATTTGAAGCTC-3',

PfTC 12S (no tag) -forward: 5'-

TTTAATAAGGAGATATACAATGGCTGAAAACAACAATTTGAAGCTC-3',

PfTC 12S (507) -reverse: 5'-

CTCGAGGAGATTACGGATTAGCAGGGGAAGTTTCCATGCTTCTTC -3',

PfTC 12S (FL) -reverse: 5'-

CTCGAGGAGATTACGGATTAACGAATGGAATGGTTCTGCAGAGC-3',

PfTC 5S-forward: 5'- GAGAACCTCTACTTCCAAAGTCCGCGAGAAATTGAGGTTTC-3',

PfTC 5S -reverse: 5'- CTCGAGGAGATTACGGATTACGCCTGCTGAACGGTGACTTCGC -3',

PfTC 1.3S-forward: 5'-

GAGAACCTCTACTTCCAAAGTAACTGAAGGTAACAGTCAACGG-3',

PfTC 1.3S -reverse: 5'- CTCGAGGAGATTACGGATTAGCCGATCTTGATGAGACCCTGAC -3',

Genomic DNA was isolated from *Escherichia coli* (K12), *Staphylococcus aureus* MRSA (ATCC BAA-1556), *Propionibacterium freudenreichii* subsp. *Shermanii* (DSM 4902), and *Streptomyces coelicolor* (M1154) using established procedures. All inserts were PCR amplified directly from genomic DNA, except for untagged variants, which were amplified from the analogous tagged construct. All inserts were designed to overlap with the sticky ends of the linearized vector using the New England Biolabs Gibson Assembly protocol and reagent.

All inserts to be expressed with hexahistidine tags were cloned into the pRSF-TEV-Gib vector, digested at the BseR1 restriction enzyme cut site. Inserts amplified to be expressed without any tag were cloned into the pRSF-Gib-Kan vector, digested at the BseR1 restriction enzyme site.

The pRSF-TEV-Gib vector (and subsequently the pRSF-Gib-Kan vector) is derived from the previously reported pRSF-Duet vector via PCR amplification with the following primers:

TEV:GIB insert -forward: 5'-

CATGGGCAGCAGCCATCACCATCATCACCACAGCGGATCCGAGAACCTCTACTTCCAATCCGTAATCTCC -3',

TEV:GIB insert -reverse: 5'-

TCGAGGAGATTACGGATTGGAAGTAGAGGTTCTCGGATCCGCTGTGGTGATGATGGT
GATGGCTGCTGCC -3',

This was subsequently followed by digestion with the restriction enzymes NcoI and XhoI, then phosphorylation of 5' ends via T4 kinase and ligation by T4 ligase using New England Biolabs' protocol.

pRSF-Gib-Kan was produced by polymerase chain reaction (PCR) mutagenesis of the pRSF-TEV-Gib vector using the following primers:

TEV→WELQ/Δtag -forward: 5'- CAATCCGTAATCTCCTCGAGTCTG -3',

TEV→His6/Δtag -reverse: 5'- TATATCTCCTTATTAAAGTTAA -3',

All PCR products were purified by agarose gel electrophoresis using a 1% agarose gel in tris-acetate EDTA buffer (1X TAE), with GelRed for UV-vis detection and a 1 kb DNA ladder for molecular weight determination. Gels were ran at 90 V for 1 hour, before being analyzed on a transilluminator to cut out bands with the appropriate sized PCR product. Gel fragments containing PCR products were isolated using the QIAGEN - QIAquick gel extraction kit. PCR product yields ranged from 500-2000 ng of DNA. pRSF-TEV-Gib and pRSF-Gib-Kan vectors were digested by BseR1 (purchased from New England Biolabs) for 15 minutes at 37°C. The digested vector was ligated to PCR products via Gibson Assembly for 1 hour at 50°C, and subsequently transformed into chemically competent (CaCl₂ method) *E. coli* DH5α cells. Transformation was performed via a 45 second heat shock at 42°C. Outgrowth steps were performed in 350 μl of SOC buffer for 1 hour at 37°C while shaking at 220 rpm, before plating 100 μl of the culture onto LB agar plates containing 50 μg/ml of kanamycin sulfate. Plates were stored at 37°C for 18 hours, after which multiple individual colonies were grown in 5 ml LB cultures, stored in 25% glycerol, and confirmed via sequencing by the Purdue University Genomics Core. Culture glycerol stocks were stored at -80°C indefinitely. Plasmids were transformed into *E. coli* BL21 cells for subsequent protein expression.

A plasmid containing ScvACC1 coexpressed with ScvBPL1 on the pRSF-TEV-Gib vector was purchased from Genscript. Plasmids containing lactate dehydrogenase and pyruvate kinase (*Homo sapiens*) were purchased from DNASU. These plasmids were transformed into chemically competent *E. coli* DH5α and BL21 cells for later expression.

All protein expression was performed in 1L cultures of terrific broth (TB), supplemented with 50 µg/ml kanamycin sulfate and 10 mM MgCl₂. 5 ml of a saturated BL21 cell culture were added to the 1L TB solution, which was shaken at 170 rpm at 37°C until an OD₆₀₀ = 1.0 was reached. Afterward, the cultures were cooled at 18°C for 20 minutes, to which isopropyl β- d-1-thiogalactopyranoside (IPTG) was added to a final concentration of 0.5 mM. These solutions were left to shake for 18 hours. The next day, the cells were pelleted at 6,000 rpm at 4°C for 10 minutes. The cell pellets were transferred to 50 ml conical tubes and resuspended in 35 ml of lysis buffer (20 mM Tris, 300 mM NaCl, 10% Glycerol, 20 mM Imidazole pH 8.0), then frozen at -20°C indefinitely.

Protein purification of all proteins proceeded by thawing cell suspensions under running cold water for 15 minutes before adding 2 mg of lysozyme powder and 50 µl of a 2 mg/ml solution of DNase. These suspensions were then mechanically disrupted by sonication for 2 minutes with 1 second on; 1 second off pulses. Afterward, the cell lysate was clarified by centrifugation at 11,000 rpm at 4°C for 45 minutes, followed by filtration of the supernatant through a 0.45 µm syringe filter.

Hexahistidine tagged proteins were purified over a 5 ml His-Trap column using 20 column volumes of wash buffer (20 mM Tris:HCl, 40 mM Imidazole, 300 mM NaCl, pH 8.0), followed by a step gradient to 50% wash buffer and 50% elution buffer (500 mM Imidazole, 20 mM Tris:HCl, 300 mM NaCl pH 8.0) for 7 column volumes. Purified protein was analyzed by sodium dodecyl sulfate – polyacrylamide gel electrophoresis (SDS-PAGE) (Biorad). After confirmation of the molecular weight and purity of the protein eluant, the protein solution was buffer exchanged via a Superdex Hiprep 26/10 desalt column (Cytiva) into desalt buffer (10 mM Tris:HCl, 200 mM NaCl pH 8.0). Fractions were pooled for further purification by preparative SEC (Cytiva) into desalt buffer. All macromolecular chromatography was performed on an ÄKTA FPLC instrument.

Untagged proteins were purified by increasing the concentration of ammonium sulfate in solution from 0% to 50% using a 10% step size, followed by centrifugation at 11,000 rpm at 4°C for 20 minutes. Ammonium sulfate pellets were resuspended in 20 ml of desalt buffer and buffer exchanged via a Superdex Hiprep 26/10 desalt column (Cytiva) into low salt anion exchange buffer (50 mM Tris:HCl, 50 mM NaCl pH 8.5). The desalted protein fractions were analyzed via SDS-PAGE and fractions containing the an appropriate molecular weight band were further

purified. Anion exchange chromatography was performed using a 5 ml quaternary ammonium fast flow column (Cytiva), using a linear gradient of Buffer A (50 mM Tris:HCl, 50 mM NaCl pH 8.5) to Buffer B (50 mM Tris:HCl, 1 M NaCl pH 8.5) over 30 column volumes. Fractions were analyzed again by SDS-PAGE gel, and pooled for further purification by preparative SEC over a Superdex 26/100 200 pg. preparative size exclusion column (Cytiva) into desalt buffer. Pure protein was then examined by SDS-PAGE.

All proteins were concentrated via centrifuge concentrators with 30,000 Da molecular weight cutoff values at 4°C to concentrations between 20-30 mg/ml. Purified proteins were frozen in 40 µl droplets on liquid nitrogen and stored indefinitely at -80°C.

3.6.2 Crystallization and diffraction of EcACC CT and ScPCC CT

EcACC CT and ScPCC CT were examined in a sitting-drop crystallization screen, that examined 384 conditions at the 0.5 µl scale at room temperature, set up with a Mosquito (SPTlabtech, Melbourne, Australia). This screen used EcACC CT at 15 mg/mL stored in desalt buffer (20 mM Tris:HCl at pH 8.0 and 200 mM NaCl), with 1 mg/ml biotin and 5 mM 2-sulfonateacetyl-oxa(dethia)CoA as ligands. For ScPCC CT, crystals were screened at both 7 mg/ml and 20 mg/ml (stored in desalt buffer), with 1 mg/ml biotin and malonyl-aza(dethia)CoA as ligands. Initial conditions that led to ScPCC CT crystals were produced in 4 µl hanging drop trays over 1.0 mL wells with mother liquor conditions: A) 0.17 M ammonium acetate, 0.085 M Sodium acetate:HCl pH = 4.6, 26% PEG 3350 and 15% glycerol; B) 0.1 M Bis-Tris:HCl pH = 6.5 and 20% PEG 3350; C) 0.11 M sodium citrate and 20% PEG 3350 with 5% isopropanol. EcACC CT crystals were also produced in hanging drop trays with mother liquor conditions: A) 0.15 M sodium citrate, 1% PEG 400, 18% PEG 3350, 22% isopropanol; B) 0.1 M sodium citrate, 19% PEG 3350, 21% glycerol. Crystals grown for 3-5 days were looped using 0.15, 0.3, and 0.6 mm Litholoops and transferred immediately to liquid nitrogen. Diffraction experiments were conducted at the LS-CAT beamline 21-ID-F. Diffraction intensities were analyzed using the HKL2000 suite ^[12].

3.6.3 HPLC assay, UV-vis assay, and futile cycle development for EcACC

All EcACC UV-vis assays were conducted in a 1.2 ml semimicro quartz cuvette (Starna Cells) in 1 ml reactions using Cary Win UV 100 spectrophotometer. Reactions were setup with

100 mM bis-tris propane:HCl (pH 7.5), 20 mM KCl, 7 mM MgCl₂, 0.1 mM ATP, 0.025 mM acetyl-CoA, 40 mM sodium bicarbonate, 1 mM phosphoenolpyruvate, 0.4 mM NADH, 1 μ M lactate dehydrogenase, 1 μ M pyruvate kinase, and 1 μ M of EcACC (holoenzyme). Reactions were initiated by addition of EcACC holoenzyme, which was prepared by incubation of 50 μ M of each EcACC subunit. Reactions were continuously monitored at 340 nm for 1 hour at 23°C. An extinction coefficient of 6.220 mM⁻¹cm⁻¹ at 340 nm was used to determine concentration change of NADH over time. For futile cycle assays, acetyl-CoA was omitted from the reaction and replaced with an equivalent concentration of acetyl-oxa(dethia)CoA or acetyl-aza(dethia)-CoA.

HPLC assays were performed on an Agilent 1100 instrument and prepared as UV-vis assays were with the following modifications. NADH, phosphoenolpyruvate, pyruvate kinase, and lactate dehydrogenase were all omitted from the reaction. Also the concentration of acetyl-CoA (or acetyl-CoA analog) was increased from 0.025 mM to 0.25 mM. Additionally, the 1 ml reaction was prepared in a microcentrifuge tube instead of a quartz cuvette. Lastly, discrete 100 μ l time points were taken from the reaction at 0 min, 1 min, 5 min, 10 min, 30 min, and 1 hr after addition of enzyme. All time points were quenched by rapid mixing of the reaction aliquot with 50 μ l of 50% FA. The reaction time points were examined by analytical HPLC using a C18 column (Phenomenex) and a gradient of pure Buffer A (0.1% TFA in water) to 25% Buffer B (acetonitrile) over the course of 20 minutes. UV was monitored continuously using a diode array detector (DAD).

3.7 References

- [1] Dimroth, P., Guchhait, R. B., Stoll, E., and Lane, M. D. (1970) Enzymatic Carboxylation of Biotin: Molecular and Catalytic Properties of a Component Enzyme of Acetyl CoA Carboxylase, *Proceedings of the National Academy of Sciences* 67, 1353-1360.
- [2] Knowles, J. R. (1989) The mechanism of biotin-dependent enzymes, *Annual review of biochemistry* 58, 195-221.
- [3] Bilder, P., Lightle, S., Bainbridge, G., Ohren, J., Finzel, B., Sun, F., Holley, S., Al-Kassim, L., Spessard, C., Melnick, M., Newcomer, M., and Waldrop, G. L. (2006) The structure of the carboxyltransferase component of acetyl-coA carboxylase reveals a zinc-binding motif unique to the bacterial enzyme, *Biochemistry* 45, 1712-1722.
- [4] Tong, L. (2013) Structure and function of biotin-dependent carboxylases, *Cell Mol Life Sci* 70, 863-891.
- [5] Wood, H. G., and Stjernholm, R. (1961) Transcarboxylase. II. Purification and properties of methylmalonyl-oxaloacetic transcarboxylase, *Proceedings of the National Academy of Sciences of the United States of America* 47, 289-303.

- [6] Wood, H. G., Chiao, J. P., and Poto, E. M. (1977) A new large form of transcarboxylase with six outer subunits and twelve biotinyl carboxyl carrier subunits, *The Journal of biological chemistry* 252, 1490-1499.
- [7] Wood, H. G. (1946) The fixation of carbon dioxide and the interrelationships of the tricarboxylic acid cycle, *Physiological Reviews* 26, 198-246.
- [8] Green, N. M., Valentine, R. C., Wrigley, N. G., Ahmad, F., Jacobson, B., and Wood, H. G. (1972) Transcarboxylase: XI. Electron microscopy and subunit structure, *Journal of Biological Chemistry* 247, 6284-6298.
- [9] Xie, Y., Shenoy, B. C., Magner, W. J., Hejlik, D. P., and Samols, D. (1993) Purification and characterization of the recombinant 5 S subunit of transcarboxylase from *Escherichia coli*, *Protein expression and purification* 4, 456-464.
- [10] Hall, P. R., Wang, Y. F., Rivera-Hainaj, R. E., Zheng, X., Pustai-Carey, M., Carey, P. R., and Yee, V. C. (2003) Transcarboxylase 12S crystal structure: hexamer assembly and substrate binding to a multienzyme core, *EMBO J* 22, 2334-2347.
- [11] Diacovich, L., Mitchell, D. L., Pham, H., Gago, G., Melgar, M. M., Khosla, C., Gramajo, H., and Tsai, S. C. (2004) Crystal structure of the beta-subunit of acyl-CoA carboxylase: structure-based engineering of substrate specificity, *Biochemistry* 43, 14027-14036.
- [12] Wei, J., and Tong, L. (2015) Crystal structure of the 500-kDa yeast acetyl-CoA carboxylase holoenzyme dimer, *Nature* 526, 723-727.
- [13] Martini, H., and Rétey, J. (1993) Propionyl-Aza(dethia)coenzyme A as Pseudosubstrate of the Biotin-Containing Transcarboxylase, *Angewandte Chemie International Edition in English* 32, 278-280.

CHAPTER 4. APPLICATION OF ACYL-COA ANALOGS TO MECHANISTIC STUDIES WITH KETOSYNTHASES

Contributions: Jeremy Lohman and Trevor Boram designed experiments and interpreted the resulting data. Trevor Boram carried out the majority of experiments. Lee Stunkard, Amanda Silva de Sousa, and Aaron Benjamin contributed synthesis, kinetics, cloning and expression of some constructs. Note: Literature references and chemical numbers within schemes are unique within this chapter.

4.1 Abstract

Fatty acid biosynthetic enzymes exploit the reactivity of acyl- and malonyl-thioesters for catalysis. Here we synthesize acetyl/malonyl-CoA analogs with ester or amides in place of the thioester and characterize their behavior as substrates or inhibitors of the *E. coli* FabH ketosynthase. The acetyl- and malonyl-oxa(dethia)CoA analogs undergo extremely slow hydrolysis in the presence of FabH or C112Q mutant, which mimics the acyl-enzyme intermediate. Decarboxylation of malonyl-oxa(dethia)CoA by FabH or C112Q mutant was not detected. The amide analogs were completely stable to enzyme activity as expected. In enzyme assays, acetyl-oxa(dethia)CoA is surprisingly somewhat activating, while acetyl-aza(dethia)CoA is a moderate inhibitor. The malonyl-oxa/aza(dethia)CoAs are all relatively poor inhibitors. Considering that malonyl-CoA is an extremely poor substrate for FabH compared to malonyl-S-acyl carrier protein and that these substrate analogs are stable, the analogs are promising for structure-function studies to uncover the basis of FabH cooperativity and acyl carrier protein interactions. Furthermore, we determine the reaction rates of each substrate alone, informing us about the fundamental catalytic traits of FabH.

4.2 Synthesis and Application of Acyl-CoA analogs to FabH may serve as effective mechanistic probes

Acyl-CoA analogs have been used in a relatively small number of enzyme structure-function studies, where the analogs can clarify roles of catalytic residues¹. These acyl-CoA analogs have the relatively labile thioester substituted with esters/amides/ketones to examine acyl-transfer

catalysis, or the acyl-thioester is substituted by acyl-enolate isosteres to examine carbon-carbon bond forming enzymes. The thioester bond of malonyl-CoA is considered to be especially labile compared to acetyl-CoA². Thus, stable malonyl-thioester analogs are desired for use in structure-function studies³⁻⁵. Other uses for stable malonyl-CoA analogs include off-loading polyketide synthase metabolic intermediates, or as probes of enzymes like carboxymethylproline synthase, where the analogs can participate as slow substrates⁶⁻⁸. To determine suitability of stable acetyl/malonyl-thioester analogs in fatty acid and polyketide synthase structure-function studies or as inhibitor warheads, we report alternative syntheses of acetyl-oxa(dethia)CoA/acetyl-aza(dethia)CoA (**1/2**), malonyl-oxa(dethia)CoA/malonyl-aza(dethia)CoA (**3/4**) and their reactivity with *Escherichia coli* FabH, a ketosynthase (KS) initiating fatty acid biosynthesis, Figure 4.1. We also determine the inhibition constants of **1-4**, oxa(dethia)CoA (**5**) and aza(dethia)CoA (**6**) against FabH using a continuous spectrophotometric assay applicable to other KS.

Carbon-carbon bonds in fatty acids are generated by condensation of acyl-thioesters and malonyl-thioesters, carried by either CoA or an acyl carrier protein (ACP)⁹. In *E. coli* and related bacteria the first fatty acid carbon-carbon bond formed is between acetyl-CoA and malonyl-S-ACP by FabH, which is likely rate limiting in vivo, Figure 4.1A¹⁰. Inhibition of FabH with thiolactomycin in vivo leads to overall growth inhibition, revealing FabH and homologs are valid drug targets^{11, 12}. Thus, a better understanding of FabH catalysis might inform drug discovery efforts¹³.

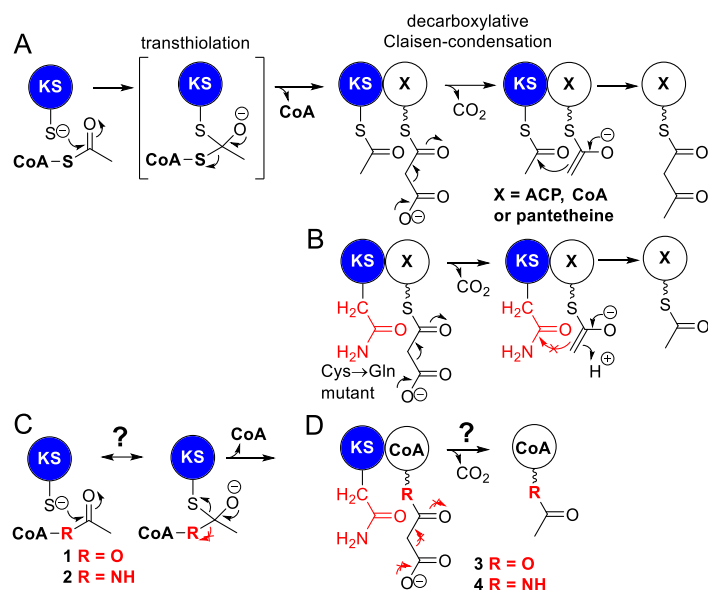
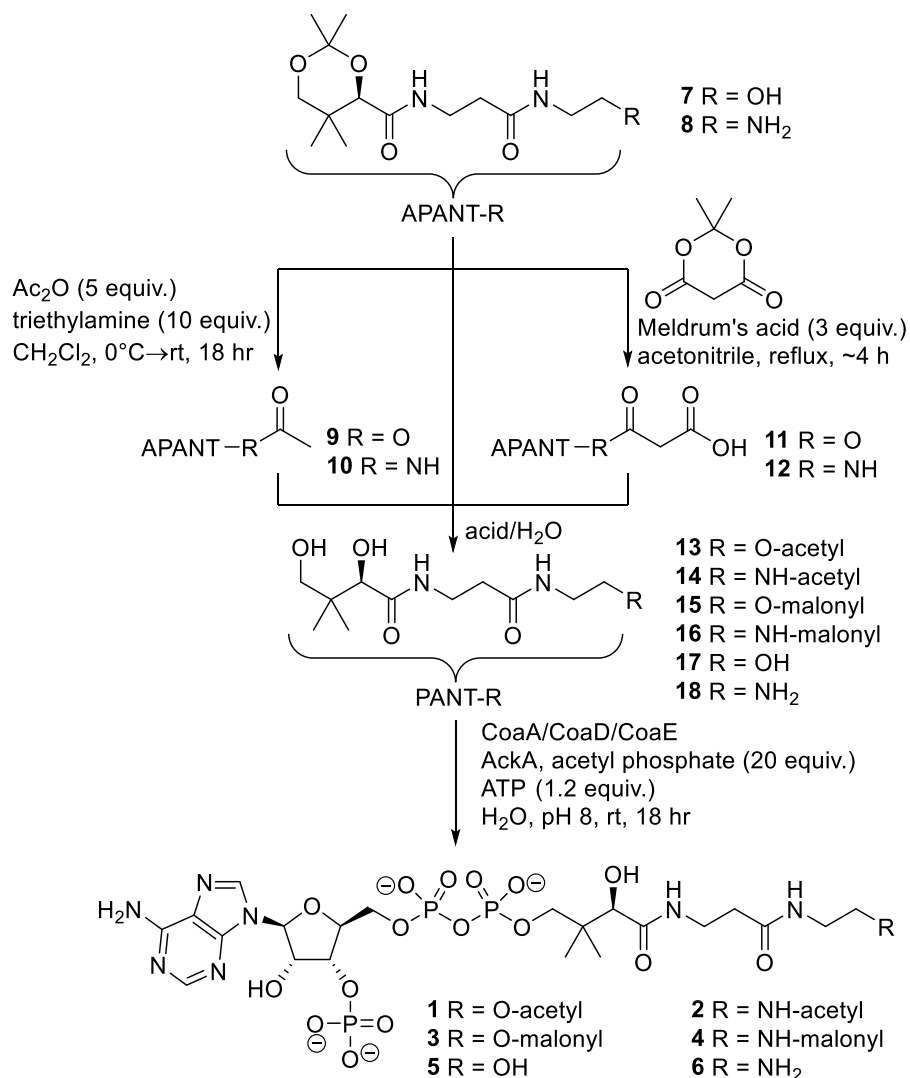


Figure 4.1 Initiation of fatty acid biosynthesis and potential substrate analogs. A) FabH activity. B) FabH C→Q mutant decarboxylation activity. C) FabH transthiolation reaction prevented by stable acetyl-CoA analogs. D) Decarboxylation reaction of FabH C→Q prevented or slowed by stable malonyl-thioester analogs.

It is known that FabH transfers the acetyl group of acetyl-CoA onto its active site cysteine followed by decarboxylation of malonyl-S-ACP forming an enolate intermediate that reacts with acetyl-S-FabH generating acetoacetyl-S-ACP^{11, 14-17}. Mutation of the FabH active site cysteine to a glutamine is expected to generate a malonyl-S-ACP decarboxylase, similar to other β -ketoacyl-ACP synthases, Figure 4.1B¹⁸. Studies probing FabH catalysis with CoA mixed disulfides revealed negative cooperativity between the active sites of the dimer¹⁹. We expect that substrate analogs combined with structural biology can reveal the details of negative cooperativity, conformational changes and decarboxylation mechanism, but a first step is synthesis and characterization of substrate analog:enzyme affinity and stability.

We synthesized the extremely polar acetyl-CoA and malonyl-CoA analogs using the strategy in Scheme 4.1, similar to our previous synthesis of methylmalonyl-CoA analogs²⁰. Acetonide protected oxa(dethia)pantetheine (**7**) and aza(dethia)pantetheine (**8**) were generated as previously published²⁰. The acetonide pantetheine analogs **7/8** were treated with acetic anhydride and triethylamine to give acetyl-oxa(dethia)pantetheine acetonide (**9**) and acetyl-aza(dethia)pantetheine acetonide (**10**), respectively. Malonyl-oxa(dethia)pantetheine acetonide (**11**) and malonyl-aza(dethia)pantetheine acetonide (**12**) were generated through heating **7/8** with

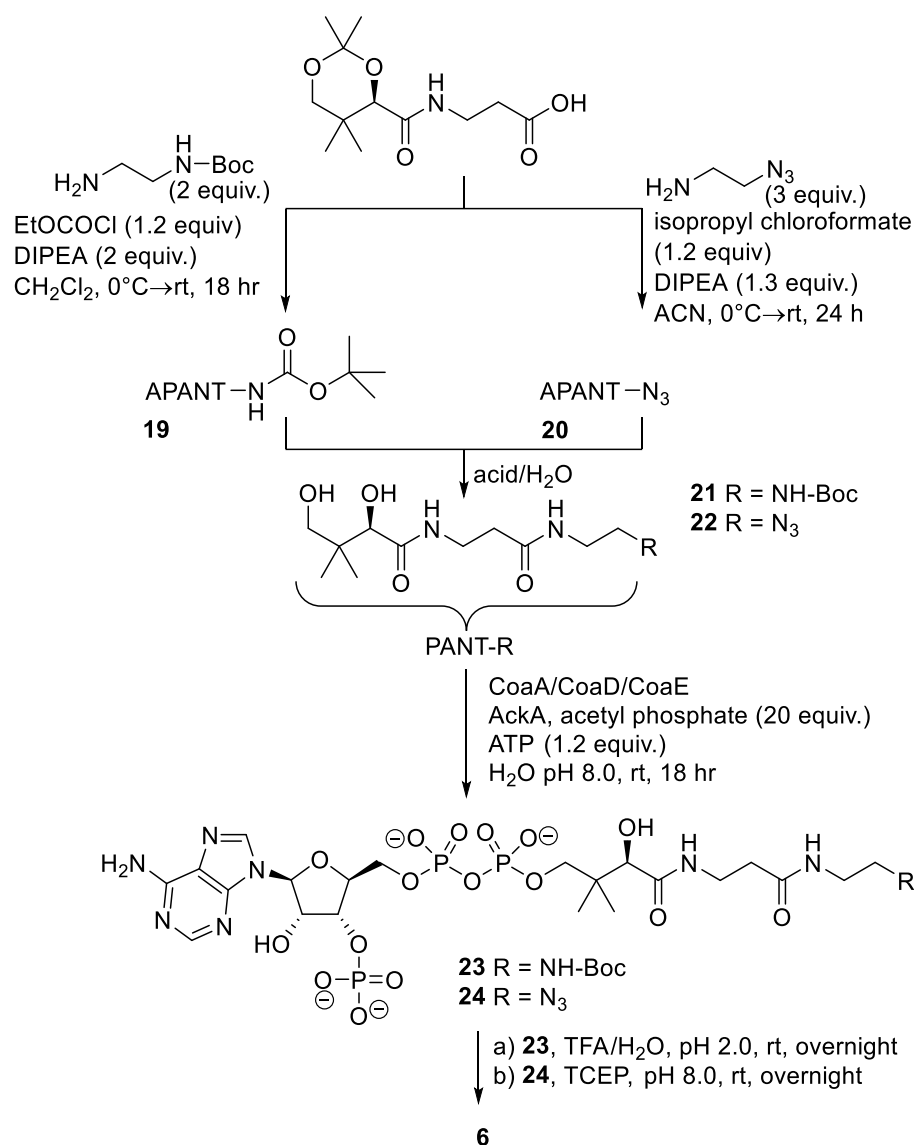
Meldrum's acid for 4 hours, respectively. Decarboxylation of **11/12** to **9/10** was detected if the reactions were left refluxing for extended times. The acetonides **7-12** were deprotected with formic acid in water and chemoenzymatically converted to the CoA analogs **1-5** using an acetate kinase ATP regeneration system. The deprotection of esters **9** and **11** required careful addition of formic acid to a pH of 2.2 and careful neutralization to avoid ester hydrolysis.



Scheme 4.1 Synthesis of acetyl- and malonyl-oxa/aza(dethia)CoA analogs.

The product standard aza(dethia)CoA (**6**) was a challenge to generate using our workflow due to side reactions or limited turnover during chemoenzymatic preparation. If the ATP regeneration system was used with aza(dethia)pantetheine (**14**), a large amount of **2** was generated due to acetylation by acetyl phosphate as an expected side product. If an excess of ATP is used

rather than the ATP regeneration system **6** can be generated in small quantities but the major product is 3'-dephospho-aza(dethia)CoA, which appears to be a very poor substrate for *E. coli* CoaE. Therefore, we turned to alternative routes for **6**, Scheme 4.2. Starting with *N*-Boc-ethylenediamine and pantothenic acid acetonide, we produced intermediate **19** using mixed anhydride coupling. We generated the azide intermediate **20** using previously published methods²¹. Selective acetonide deprotection of **19** to *N*-Boc-aza(dethia)pantetheine (**21**) and **20** to azide(dethia)pantetheine (**22**) was achieved with careful application of formic acid. The *N*-protected pantetheines were converted to CoAs chemoenzymatically yielding **23** and **24**. The final deprotection of **23** to **6** using TFA was possible with careful monitoring. The conversion of **24** to **6** was examined with a few reducing reagents with TCEP being superior to the reagents triphenylphosphine, tributylphosphine, tris(hydroxymethyl)phosphine, or borohydride. We confirmed the identity of **6** through comparison of products by HPLC, HRMS and NMR.



Scheme 4.2 Alternative synthetic routes of aza(dethia)CoA using different amine protecting strategies.

Our synthesis of the malonyl-CoA analogs **3/4** via Meldrum's acid used fewer steps than previous methods and gave high yields before purification as judged by analytical LCMS⁶⁻⁸. Furthermore, our strategy of using Meldrum's acid is likely applicable to 2-substituted analogs for use with polyketide synthase enzymes. All of the analogs **1-6** are completely stable overnight in buffer at pH 6, 7 and 8 used for the subsequent enzymology.

To establish our FabH enzyme is active we performed HPLC assays with acetyl-CoA and malonyl-CoA, Figure 4.2. We chose malonyl-CoA rather than malonyl-S-ACP for a few reasons.

First to avoid the need for coupled enzyme assays with FabD to generate malonyl-S-ACP, since FabD is also expected to be inhibited by the malonyl-CoA analogs. In addition we needed to avoid generating ACPs with substrate analogs attached for use in the enzyme assays. Another reason is that malonyl-CoA has been used as a FabH substrate in drug screening platforms or in other studies with FabH homologs, but is incompletely characterized as a substrate²²⁻²⁵. One complication of our HPLC assay is that the substrate acetyl-CoA peak overlaps with the product, acetoacetyl-CoA, although the acetoacetyl-CoA peak is distinctly broader, Figure 4.2, panel A. Nevertheless, the disappearance of malonyl-CoA and appearance of CoA can be easily monitored to provide kinetics, Figure 4.2, panels J and K. In these HPLC assays with 10 μ M FabH and equimolar acetyl-CoA and malonyl-CoA at 125 or 250 μ M at pH 8, the initial rates were 0.33 ± 0.01 and 0.61 ± 0.02 min^{-1} respectively, suggesting FabH was still not saturated even at these high concentrations. FabH activity increased slightly from pH 6.3 to 7.3 and 8.1, Table 4.1.

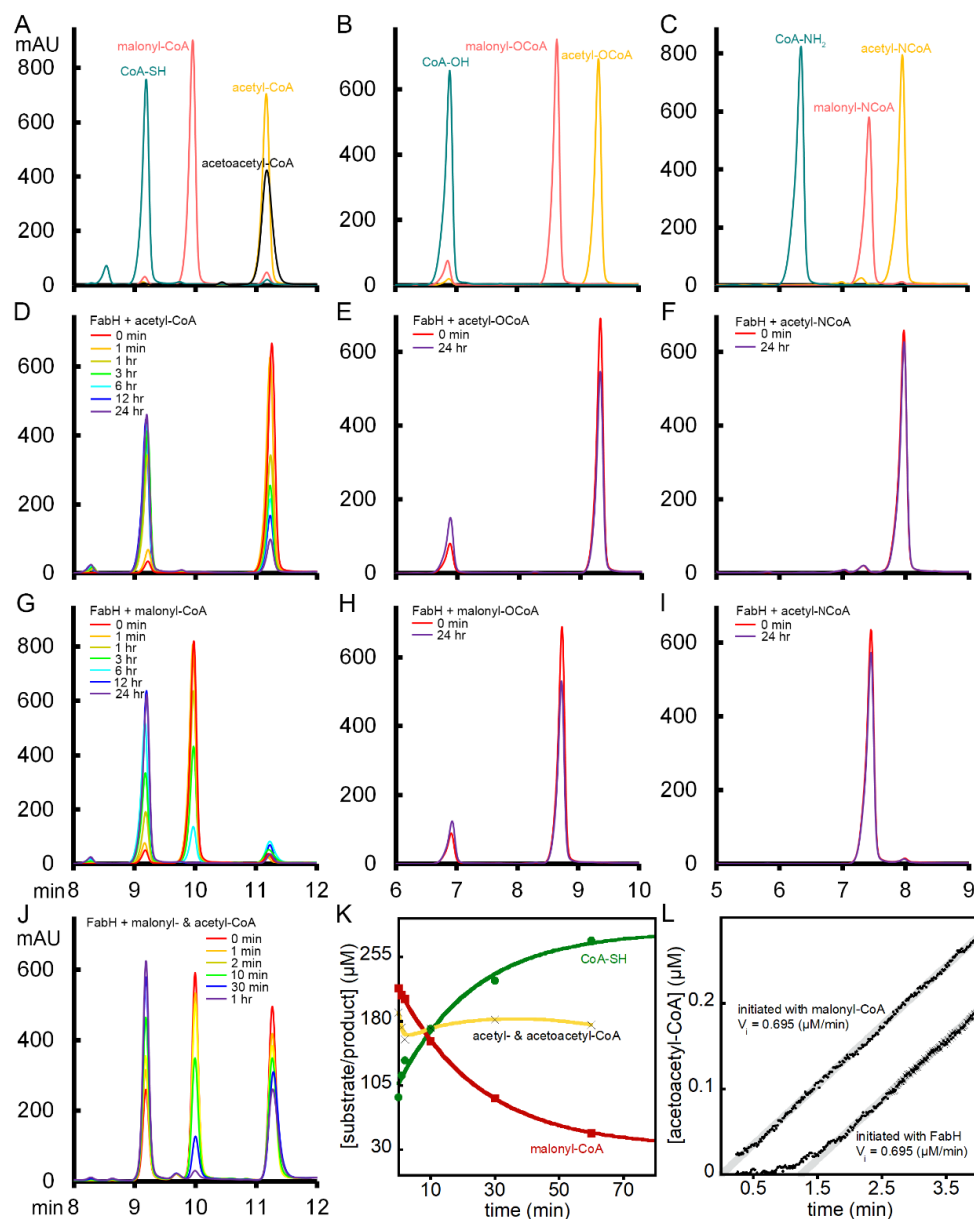


Figure 4.2 Analyses of FabH activity with substrates and analogs at pH 8.1. HPLC traces for A) acyl- and Coenzyme A standards, B) **1, 3, 5**, C) **2, 4, 6** standard HPLC traces for D-I) stability of 250 μM acetyl- or malonyl-CoA and analogs with 10 μM FabH over 24 hours at pH 8.1, D) acetyl-CoA, E) **1**, F) **2**, G) malonyl-CoA, H) **3**, I) **4**. J) HPLC traces for 10 μM FabH with 250 μM each acetyl- and malonyl-CoA at pH 8.1. K) Representative kinetic analysis of HPLC data from panel J) with malonyl-CoA (red squares and line) use and CoA (green circles and line) production fit to exponential decay or increase, with the acetyl-CoA substrate and acetoacetyl-CoA (black Xs and gold line) product peaks integrated together and shown with a smoothed trend line for visualization. Notice that the CoA production line and acetyl-CoA/acetoacetyl-CoA has a burst phase, while malonyl-CoA does not. L) Representative UV-Vis assay for acetoacetyl-CoA production by 0.5 μM FabH with 30 μM acetyl-CoA and 125 μM malonyl-CoA, initiating the reaction with either FabH or malonyl-CoA. Notice that there is a significant lag phase when the reaction is initiated with FabH as compared to malonyl-CoA.

In order to determine the reactivity or inhibition behavior of FabH with acetyl- and malonyl-CoA analogs, we first explored their stability in the presence of FabH, Figure 4.2, panels D-I. Our synthesis of the standards oxa and aza(dethia)CoA, allowed us to confirm the presence or absence of the hydrolysis products and acetyl-oxa/aza(dethia)CoA and decarboxylation products. The reactions of acetyl-CoA and malonyl-CoA alone varied greatly with pH in the presence of FabH, while the oxa(dethia) analogs were relatively unreactive and aza(dethia) analogs were completely stable over 24 hours. Surprisingly, at pH 8.1 FabH displayed biphasic acetyl-CoA hydrolysis, which we could attribute to transfer of the acetyl-group from CoA to DTT in a fast phase, with a slow phase that is likely due to hydrolysis of the acyl-enzyme intermediate. FabH generates some acetoacetyl-CoA via de-carboxylation of malonyl-CoA to acetyl-CoA at pH 6.3 and 7.3, whereas hydrolysis dominates at pH 8.1, Figure 4.2, panel G. However, the background rate of decarboxylation was much slower than in the overall reaction, suggesting formation of the acyl-enzyme intermediate generates a state of FabH that is more competent for decarboxylation.

The C112Q mutation is expected to generate a FabH locked into an acyl-enzyme intermediate state primed for decarboxylation, Figure 4.1B. The stability of malonyl-CoA and analogs was tested with the FabH C112Q mutant. Again, while malonyl-CoA was relatively rapidly converted to CoA or acetyl-CoA in a pH dependent fashion, malonyl-oxa(dethia)CoA was relatively unreactive and malonyl-aza(dethia)CoA was completely stable over 24 hours, Figure 4.3. The rate of malonyl-CoA decarboxylation by FabH C112Q was 2-5 fold slower than the rate of malonyl-CoA decarboxylative Claisen condensation by the wild-type enzyme, Table 4.1. However, FabH C112Q decarboxylation of malonyl-CoA was 10-20 times faster than wild-type in the absence of acetyl-CoA. The hydrolysis of malonyl-CoA and acetyl-CoA by FabH C112Q was unexpected but only $1/10^{\text{th}}$ the rate of decarboxylation. Upon reflection, the lack of an electrophile or appropriate proton donor in the active site is expected for FabH C112Q, thus water is likely to fulfill that role, accounting for the lower rate of decarboxylation and hydrolytic activity.

Table 4.1 Rates of FabH or C112Q mutant reactivity with substrates and analogs.

reactants → products	pH	FabH wt (rates in min ⁻¹)			FabH C112Q (rates in min ⁻¹)		
		6.3	7.3	8.1	6.3	7.3	8.1
acetyl-CoA & malonyl-CoA → acetoacetyl-CoA		0.503 ± 0.001	0.565 ± 0.008	0.610 ± 0.020			
acetyl-CoA → CoA		0.010 ± 0.003	0.058 ± 0.009	0.019 ± 0.008	0.0033 ± 0.0003	0.0230 ± 0.0040	0.0270 ± 0.0050
malonyl-CoA → acetyl-CoA or acetoacetyl-CoA		0.006 ± 0.005	0.024 ± 0.001	0.008 ± 0.001	0.1270 ± 0.0090	0.2600 ± 0.0300	0.1210 ± 0.0090
malonyl-CoA → CoA		0.023 ± 0.007	0.072 ± 0.009	0.069 ± 0.007	0.0036 ± 0.0003	0.0148 ± 0.0003	0.0187 ± 0.0005
acetyl-oxa(dethia)CoA → oxa(dethia)CoA				0.003			0.001
malonyl-oxa(dethia)CoA → oxa(dethia)CoA				0.001			0.001

* reactions determined by HPLC analysis have 250 μM substrate or analog and 10 μM FabH wt or FabH C112Q.

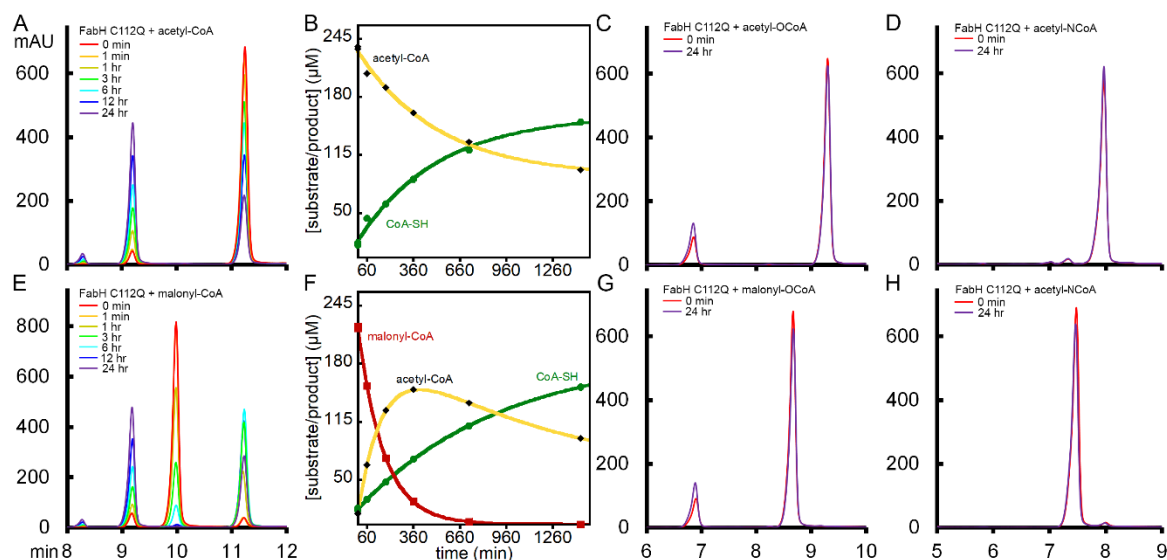


Figure 4.3 Analyses of FabH C112Q activity with substrates and analogs at pH 8.1. HPLC traces for A/C/D/E/G/H) stability of 250 μM acetyl- or malonyl-CoA and analogs with 10 μM FabH over 24 hours at pH 8.1, A) acetyl-CoA, C) 1, D) 2, E) malonyl-CoA, G) 3, H) 4. B) Kinetic analysis of HPLC data from panel A) with the acetyl-CoA substrate (gold Xs and line) and hydrolysis product CoA (green circles and line) fit to exponential decay or increase. F) Kinetic analysis of HPLC data from panel E) with the malonyl-CoA (red squares and line) substrate and acetyl-CoA (gold Xs and line) product or hydrolysis product CoA (green circles and line) fit to exponential decay or increase.

Since there was some activity with the acetyl-oxa(dethia)CoA analog, we assayed it with malonyl-CoA and wild-type FabH. FabH with acetyl-oxa(dethia)CoA and malonyl-CoA is expected to generate acetoacetyl-CoA, however the same amount of acetoacetyl-CoA was generated whether or not acetyl-oxa(dethia)CoA was added, indicating the reaction is minimal when compared to the background rate of malonyl-CoA decarboxylation to acetyl-CoA. Thus, we can conclude that the ester and amide analogs of acetyl- and malonyl-CoA are stable to the

enzymatic activity of FabH on the timeframe of biophysical experiments, leading us to characterize the analogs as inhibitors.

In order to obtain inhibition constants, we used a continuous UV-Vis assay for the production of acetoacetyl-CoA. Previously a UV-Vis assay based on 5,5'-dithiobis(2-nitrobenzoic acid) (DTNB, Ellman's reagent) as a probe of CoA production was used to examine the inhibition of FabH by small molecules²⁵. However, we found that incubation of FabH with DTNB resulted in precipitation of the protein, which decreased accuracy and repeatability. FabH precipitation was likely avoided with the use of 10% DMSO in the previous DTNB assay, or not a problem since it was an endpoint assay. Rather, we chose to follow the production of acetoacetyl-CoA, which has a reasonable extinction coefficient at 302 nm of $17.7 \text{ mM}^{-1} \text{ cm}^{-1}$ in the presence of 50 mM Mg^{2+} at pH 8.0 and has been previously described for FabH at pH 7 where the extinction coefficient is lower^{24, 26}. Comparison of FabH enzymatic reactions in the presence and absence of Mg^{2+} followed by HPLC revealed no inhibition by 50 mM Mg^{2+} . In our UV-Vis assays, with equimolar acetyl-CoA and malonyl-CoA, we again could not saturate the enzyme, but could determine a $k_{\text{cat}}/K_{\text{M}}$ of $1.87 \pm 0.05 \text{ nM}^{-1} \cdot \text{min}^{-1}$, Figure 4.1A.

We observed a significant lag-phase if the reactions were started with FabH, which was eliminated by starting the reactions with malonyl-CoA, Figure 4.2 panel L, which we attributed to hysteresis of FabH. This suggests conversion of the enzyme from the ground state to an active state takes place in the presence of acetyl-CoA. Such hysteresis is likely difficult to observe in the discontinuous radioactivity based assays previously used. The lack of a burst phase for production of acetoacetyl-CoA with acetyl-CoA preincubated FabH indicates C-C bond formation is the slow step with malonyl-CoA as a substrate. This observation is further supported by the HPLC assays where there appears to be a burst phase of acetyl-CoA conversion to CoA but not for malonyl-CoA consumption.

In previous reports at pH 7.0 with malonyl-S-ACP as an acceptor, the observed k_{cat} values are on the order of $2\text{-}3 \text{ s}^{-1}$, with an apparent K_{M} of 5 μM for malonyl-ACP and 40 μM for acetyl-CoA, approximate $k_{\text{cat}}/K_{\text{M}}$ of $24 \text{ }\mu\text{M}^{-1} \cdot \text{min}^{-1}$ and $3 \text{ }\mu\text{M}^{-1} \cdot \text{min}^{-1}$ respectively^{27, 28}. This indicates malonyl-CoA is a comparatively very poor substrate compared to malonyl-S-ACP. To determine the importance of the malonyl-CoA nucleotide, we explored FabH catalysis with malonyl-S-pantetheine, see supplemental information for synthesis. Surprisingly, malonyl-S-pantetheine is an even poorer substrate than malonyl-CoA with a $k_{\text{cat}}/K_{\text{M}}$ that is 20 times lower, further

demonstrating the importance of the ACP for FabH catalysis. As such, we did not attempt to determine inhibition constants for the acetyl- and malonyl-pantetheine substrate analogs. We expect follow up studies comparing structures of FabH in the presence of malonyl-CoA and malonyl-S-ACP analogs will reveal how the significant substrate specificity is determined, but these studies need to be guided by knowledge of analog behavior with the enzyme.

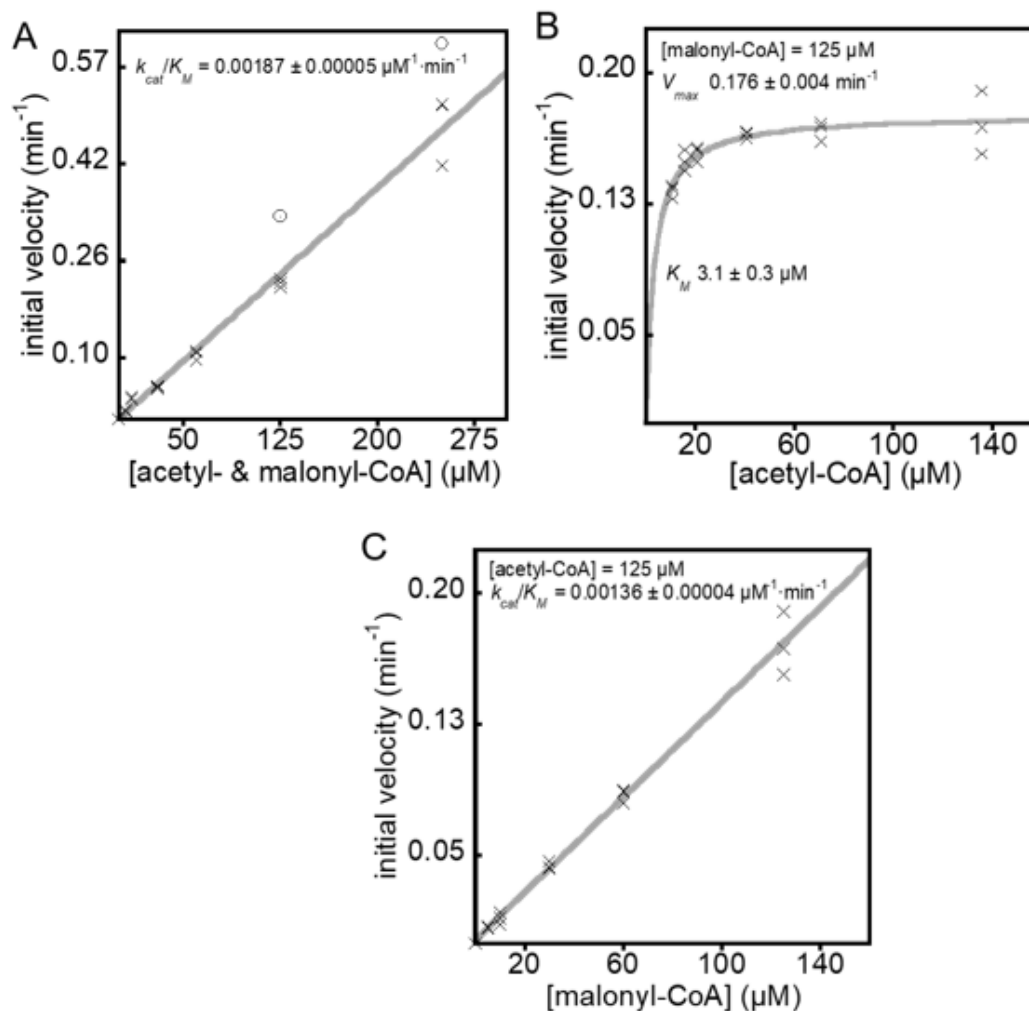


Figure 4.4 Kinetic analysis of FabH activity with acetyl- and malonyl-CoA. Panel A) is varying both substrates at the same concentration, Xs are data points for UV-Vis assay monitoring formation of acetoacetyl-CoA and circles are from the HPLC assay for the disappearance of malonyl-CoA. Panel B) varying acetyl-CoA while holding malonyl-CoA at 125 μM. Panel C) varying malonyl-CoA while holding malonyl-CoA at 125 μM.

Our initial assay used equimolar acetyl-CoA and malonyl-CoA, which likely only reported on the k_{cat}/K_M of the rate limiting substrate. We attempted to find the K_M of acetyl-CoA with

malonyl-CoA as the acceptor. If we hold the malonyl-CoA concentration at 125 μM and vary acetyl-CoA, we find an apparent K_M of $3.1 \pm 0.3 \mu\text{M}$ and V_{max} of $0.176 \pm 0.004 \text{ min}^{-1}$ for acetyl-CoA, Figure 4.4. A confounding factor for determination of the apparent K_M was contamination of commercial malonyl-CoA with between $\sim 9\%$ acetyl-CoA, preventing us from going lower in acetyl-CoA concentration. We have accounted for the acetyl-CoA concentration coming from stocks of malonyl-CoA in our calculations. Holding acetyl-CoA constant at 125 μM and varying acetyl-CoA up to 250 μM we find that there is no saturation. Nevertheless, we have kinetic values necessary to determine inhibition by the analogs.

Based on the UV-Vis assays in the presence of 50 μM acetyl- and malonyl-CoA with 150 μM acetyl-oxa(dethia)CoA we found no inhibition and unexpectedly, some slight activation. This suggests acetyl-oxa(dethia)CoA sufficiently mimics acetyl-CoA as far as promoting FabH activation. Conversely, acetyl-aza(dethia)CoA was a mild inhibitor with a K_i of 33 μM , see Table 4.2 for inhibition constants. The replacement of the relatively non-polar CoA thioester sulfur with an oxygen generates a substrate analog with two hydrogen bond acceptors, while an amide generates a hydrogen bond donor. The more polar ester and amide likely need to be desolvated to enter the active site compared to the thioester, explaining the weak inhibition. The thioester is expected to generate a tetrahedral intermediate en route to the acyl-enzyme intermediate. Specific deprotonation of the active site cysteine and protonation of the leaving CoA thiolate would be expected to speed up the reaction. However, since our analogs are poor inhibitors and substrates, it suggests the FabH active site does not strongly interact with the CoA thioester sulfur during catalysis and does not likely protonate the thiolate leaving group upon acyl transfer to the active site cysteine.

Table 4.2 Inhibition constants of substrate and product analogs

Substrate or Product analog	K_i (mM)
1 acetyl-oxa(dethia)CoA	slight activation
2 acetyl-aza(dethia)CoA	0.0328 ± 0.005
3 malonyl-oxa(dethia)CoA	1.1 ± 0.2
4 malonyl-aza(dethia)CoA	2.2 ± 0.4
5 oxa(dethia)CoA	0.9 ± 0.2
6 aza(dethia)CoA	1.2 ± 0.3
CoA	0.090 ± 0.04

In order to confirm the lack of interaction of FabH with the CoA product, we determined product inhibition constants. We found that CoA is a reasonable inhibitor with a K_i of 90 μM , while, oxa(dethia)CoA inhibits with a K_i of 900 μM and aza(dethia)CoA inhibits with a K_i of 1200 μM . This weak inhibition by the CoA product analogs again confirms these analogs don't strongly interact with any of the catalytic states. We would like to note that in our HPLC assays, the commercial acetyl- and malonyl-CoA stocks had a significant amount of Coenzyme A contamination, such that the concentration may contribute to lowering the overall activity observed, Figure 4.2 panels J and K. Substrates with much lower Coenzyme contamination were used for the individual substrate studies and in the UV-Vis assay.

The malonyl-CoA substrate analogs are also poor inhibitors, Table 4.2, but not especially so when considering the fact that malonyl-CoA is also poor substrate. Previous experiments using malonyl-CoA as a substrate at 5 mM suggests the k_{cat} is roughly 3 min^{-1} ,²⁴ combined with our k_{cat}/K_M , we can estimate the K_M to be 1.7 mM. Since the k_{cat}/K_M for malonyl-S-ACP is 16000 times larger than malonyl-CoA, and K_M for malonyl-S-ACP is about 340 times lower than malonyl-CoA, we expect appending the malonyl-thioester isosteres to the ACP will also engender them with tighter binding on the same order of magnitude.

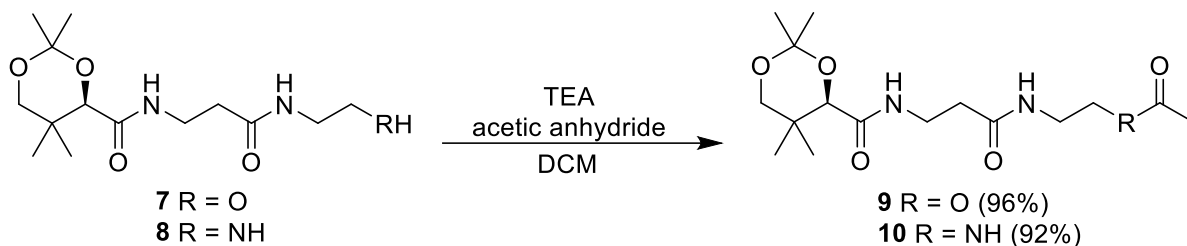
There are two previous reports of malonyl- and methylmalonyl-aza(dethia)CoA synthesis and use in enzyme assays^{7, 8}. In both cases the material was tested for the ability to undergo decarboxylative Claisen condensation or decarboxylative Michael addition. We here demonstrate again that the malonyl-aza(dethia)CoA is stable in the presence of an enzyme. The β -keto acid decarboxylation would normally be enabled by the formation of an enolate intermediate, however amide resonance competes with enolate formation. The malonyl-oxa(dethia)CoA analog also likely behaves similar to the amino analog with regard to ester resonance competing with enolate formation. For example, if we consider the methyl-group pKa of acetyl-CoA and analogs (pKa ~21 for the thioester, ~26 for the ester and ~28 for the amide)²⁹ stabilization of the enolate during decarboxylation by FabH is appropriately 5 orders of magnitude more difficult for the ester and 7 for the amide compared to the thioester. A slight decrease in binding affinity on the other hand reveals why the analogs are stable and likely promising isosteres for structure-function studies in experiments that take hours to days like NMR and crystallography.

In a previous study of fluoroacetyl-CoA hydrolase, the acetyl-CoA oxa/aza analogs were generated and compared with the corresponding fluorinated analogs as sub-strates³⁰. In those

studies, the aza analogs were completely stable, whereas the oxa analogs were substrates at very low rates. In our study, we found that the oxa analogs undergo minor hydrolysis. Together these studies reveal the usefulness of acyl-CoA thioester isosteres for studying enzyme function.

In conclusion, we have demonstrated an alternative route to malonyl-CoA analogs where the thioester has been replaced with an ester or amide. These analogs were found to be generally stable over a 24-hour time course with FabH, an enzyme which performs acyl transfer and decarboxylative Claisen-condensation. Furthermore, in the course of investigating the stability of substrate stability in the presence of FabH, we have revealed some interesting aspects of FabH catalysis, especially hysteresis. Previous reports of FabH reactivity with CoA disulfides revealed that there was likely a disordered conformation of FabH in the absence of acetyl-CoA along with negative cooperativity between the FabH active sites of the dimer, however the structural basis was not apparent in crystal structures¹⁹. We expect careful examination of FabH catalysis with the UV-Vis assay used here and malonyl-S-ACP will reveal deeper insights into previously suggested FabH negative cooperativity.

4.3 Synthetic Procedures and Characterization Data



Preparation of 9/10 via 7/8:

General procedure

A solution of DCM containing **7/8** was mixed with TEA in a round bottom flask on ice. Acetic anhydride was added slowly and the reaction was left stirring overnight at room temperature. The reaction was mixed with silica, the solvent removed, and subjected to flash chromatography (0 → 100% gradient of DCM → acetone with six column volumes of acetone at the end of the gradient) affording **9/10**.

Acetyl-oxa(dethia)-pantetheine acetonide (**9**):

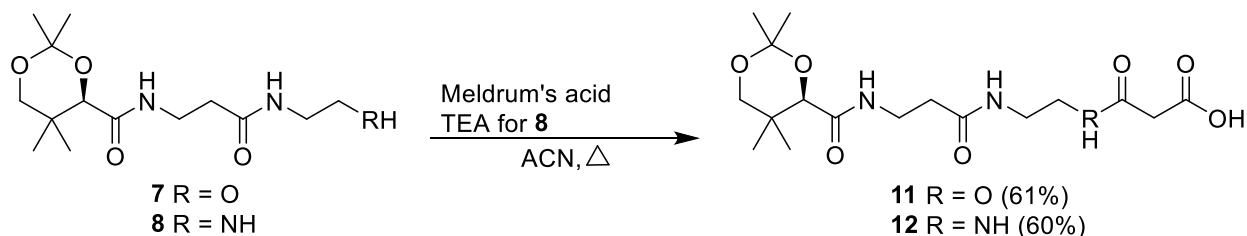
7 (1.0 g, 3.31 mmol) was reacted with acetic anhydride (1 mL, 10.6 mmol) in DCM with TEA (4 mL, 23.0 mmol) according to the general procedure above affording **7** (transparent oil that solidifies on standing, 1.1 g, 3.19 mmol 96%).

¹H NMR (500 MHz, CDCl₃) δ 6.97 (t, J = 6.3 Hz, 1H), 6.83 (t, J = 5.8 Hz, 1H), 3.97 (t, J = 5.6 Hz, 2H), 3.90 (s, 1H), 3.52 (d, J = 11.7 Hz, 1H), 3.47 – 3.23 (m, 4H), 3.11 (d, J = 11.7 Hz, 1H), 2.31 (t, J = 6.3 Hz, 2H), 1.90 (s, 3H), 1.28 (d, J = 15.7, 6H), 0.83 (d, J = 27.5, 6H). **¹³C NMR** (126 MHz, CDCl₃) δ 171.28, 170.83, 169.99, 98.93, 77.5, 71.22, 62.97, 38.35, 35.62, 34.77, 32.80, 29.31, 22.01, 20.74, 18.76, 18.57. LRMS (ESI) *m/z* calculated for C₁₆H₂₈N₂O₆ ([M+H]⁺) 345.41, found 345.0.

Acetyl-aza(dethia)-pantetheine acetonide (**10**):

8 (1.0 grams, 3.32 mmol) was reacted with acetic anhydride (1 mL, 10.6 mmol) in DCM with TEA (4 mL, 28.7 mmol) according to the general procedure above affording **10** (transparent oil that solidifies on standing, 1.05 g, 3.06 mmol 92%).

¹H NMR (500 MHz, CDCl₃) δ 7.04 (t, J = 6.2 Hz, 1H), 6.94 (d, J = 5.0 Hz, 1H), 6.61 (s, 1H), 4.05 (s, 1H), 3.67 (d, J = 11.7 Hz, 1H), 3.61 – 3.44 (m, 2H), 3.42 – 3.30 (m, 4H), 3.26 (d, J = 11.7 Hz, 1H), 2.44 (t, J = 6.3 Hz, 2H), 1.97 (s, 3H), 1.43 (d, J = 18.5 Hz, 6H), 0.98 (d, J = 28.7 Hz, 6H). **¹³C NMR** (126 MHz, CDCl₃) δ 172.09, 171.23, 170.33, 99.12, 77.17, 71.38, 40.06, 39.91, 36.2, 34.95, 32.96, 29.48, 23.2, 22.13, 18.88, 18.7. LRMS (ESI) *m/z* calculated for C₁₆H₂₉N₃O₅ ([M+H]⁺) 344.42, found 344.0.



Preparation of **9-10** via **5-6**:

General procedure

A solution of ACN containing **7/8** and Meldrum's acid was refluxed over approximately 4 hours. Every 20 min the reaction was monitored via LCMS and if **7** or **8** remained, 1.5-2 equivalents of

Meldrum's acid was added until no starting material remained. The reaction was mixed with silica, the solvent removed and subjected to flash chromatography (0 → 100% gradient of DCM → acetone for **11** and DCM → MeOH for **12**) affording **11/12**.

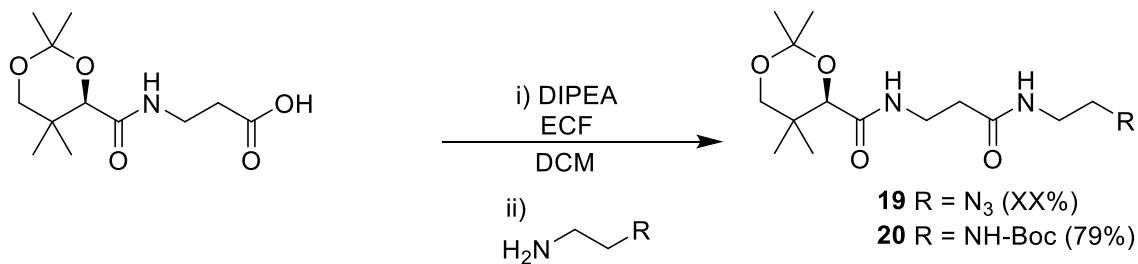
Malonyl-oxa(dethia)-pantetheine acetonide (11**):**

7 (303 mg, 1.0 mmol) was reacted with four additions of Meldrum's acid (240 mg, 1.67 mmol) according to the general procedure above affording **11** (slight yellow oil, 237 mg, 0.61 mmol 61%). ¹H NMR (500 MHz, CDCl₃) δ 7.19 (t, J = 6.4 Hz, 1H), 6.78 (t, J = 5.8 Hz, 1H), 4.27 (t, J = 5.2 Hz, 2H), 4.10 (s, 1H), 3.68 (d, J = 11.7 Hz, 1H), 3.63 – 3.45 (m, 4H), 3.42 (s, 2H), 3.28 (d, J = 11.7 Hz, 1H), 2.45 (t, J = 6.8 Hz, 2H), 1.44 (d, J = 21.0 Hz, 6H), 0.98 (d, J = 25.4 Hz, 6H). ¹³C NMR (126 MHz, CDCl₃) δ 171.43, 171.28, 168.94, 166.81, 99.28, 77.04, 71.31, 63.66, 41.52, 38.18, 35.96, 35.62, 33.03, 29.4, 22.06, 18.84, 18.7. MS (ESI) m/z calculated for C₁₇H₂₈N₂O₈ ([M-H]⁻) 387.42, found 387.0.

Malonyl-aza(dethia)-pantetheine acetonide (12**):**

8 (361.7 mg, 1.2 mmol) was reacted with four additions of Meldrum's acid (280 mg, 1.94 mmol) in acetonitrile with TEA (0.7 ml, 5 mmol) according to the general procedure above affording **12** as the TEA salt (slight yellow oil, 351 mg, 0.72 mmol 60%).

¹H NMR (500 MHz, CDCl₃) δ 8.26 (s, 1H), 7.35 (s, 1H), 7.14 (t, J = 6.2 Hz, 1H), 4.04 (s, 1H), 3.65 (d, J = 11.7 Hz, 1H), 3.49 (m, 2H), 3.40 – 3.30 (m, 4H), 3.28 – 3.22 (m, 5H), 3.10 (q, J = 7.3 Hz, 6H), 2.42 (t, J = 6.4 Hz, 2H), 1.94 (s, 2H), 1.42 (d, J = 18.9 Hz, 6H), 1.29 (t, J = 7.3 Hz, 9H), 0.96 (d, J = 21.7 Hz, 6H). ¹³C NMR (126 MHz, CDCl₃) δ 172.16, 171.96, 170.27, 169.23, 99.11, 77.15, 71.39, 45.61, 42.35, 39.26, 35.78, 35.13, 32.95, 29.44, 22.98, 22.14, 18.89, 18.71, 8.54. MS (ESI) m/z calculated for C₁₇H₂₈N₂O₈ ([M-H]⁻) 386.43, found 386.0.



Preparation of **19/20** via pantothenic acid acetonide

General procedure

A solution of DCM containing **19/20** was mixed with DIPEA (2 equiv.) in a round bottom flask on ice. Ethylchloroformate (1.2 equiv.) was added slowly and the reaction was allowed to stir for 15 minutes on ice. Afterward, 2 eq. of either N-Boc ethylenediamine (**19**) or 2-azidoethylamine (**20**) were dissolved in 10 ml of DCM and added dropwise to the activated carboxylic acid. The reaction was left to stir overnight, warming up to room temperature. The reaction was subjected to flash chromatography (40g silica; 0 → 50% gradient of DCM → acetone over ten column volumes) affording **19/20**.

Boc-aza(dethia)-pantetheine acetonide (19):

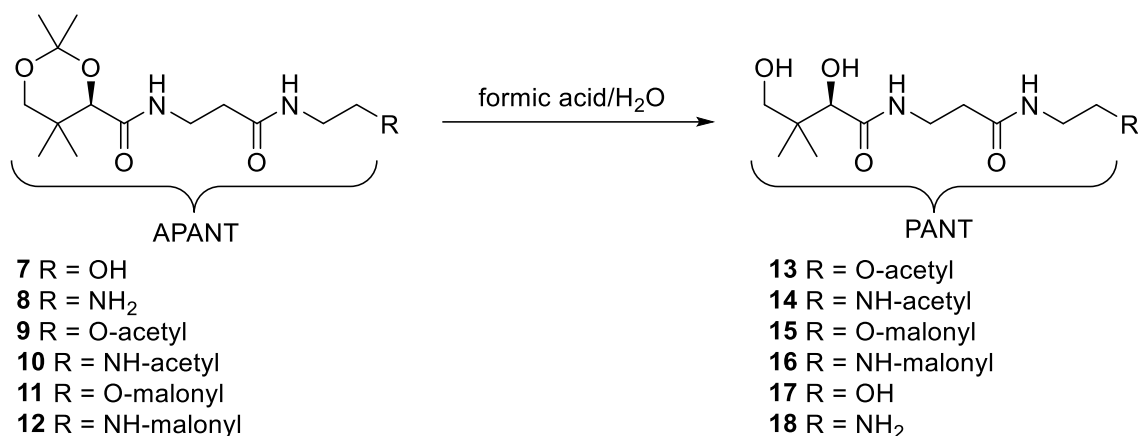
Pantothenic acid acetonide (1000 mg, 4.24 mmol) was reacted according to the general procedure above affording **20** (white powder, 1220 mg, 2.98 mmol 79%).

¹H NMR (500 MHz, CDCl₃) δ 7.04 (d, J = 6.8 Hz, 1H), 6.47 (s, 1H), 4.97 (s, 1H), 4.08 (s, 1H), 3.68 (d, J = 11.7 Hz, 1H), 3.62 – 3.47 (m, 2H), 3.43 – 3.29 (m, 2H), 3.27 (dd, J = 11.3, 6.6 Hz, 3H), 2.44 (t, J = 6.1 Hz, 2H), 1.46 (s, 3H), 1.44 (s, 9H), 1.42 (s, 3H), 1.04 (s, 3H), 0.97 (s, 3H). **¹³C NMR** (126 MHz, CDCl₃) δ 171.58, 170.21, 99.10, 71.45, 40.72, 40.29, 36.14, 34.81, 32.97, 29.49, 28.37, 22.14, 18.89, 18.71. MS (ESI) m/z calculated for C₁₉H₃₅N₃O₆ ([M+H]⁺) 402.26, found 402.3.

Azido(dethia)-pantetheine acetonide (20):

Pantothenic acid acetonide (1000 mg, 3.85 mmol) was reacted according to the general procedure above affording **20** (white powder, 970 mg, 2.98 mmol, 77.4%).

¹H NMR (500 MHz, CDCl₃) δ 7.04 (t, J = 6.3 Hz, 1H), 6.54 (d, J = 5.7 Hz, 1H), 4.08 (s, 1H), 3.68 (d, J = 11.7 Hz, 1H), 3.59 (dt, J = 13.9, 6.2 Hz, 1H), 3.54 (q, J = 6.2, 5.5 Hz, 1H), 3.54 – 3.45 (m, 1H), 3.47 – 3.43 (m, 1H), 3.45 – 3.40 (m, 2H), 3.43 – 3.35 (m, 1H), 3.28 (d, J = 11.7 Hz, 1H), 2.48 (t, J = 6.2 Hz, 2H), 1.46 (s, 3H), 1.42 (s, 3H), 1.04 (s, 3H), 0.97 (s, 3H). **¹³C NMR** (126 MHz, CDCl₃) δ 171.33, 170.30, 99.09, 77.13, 71.40, 50.72, 38.89, 36.02, 34.74, 32.96, 29.46, 22.11, 18.86, 18.67, 18.65. MS (ESI) m/z calculated for C₁₄H₂₅N₅O₄ ([M+H]⁺) 328.39, found 328.2.



Preparation of 13-18 via 7-12:

General procedure

One of **7-12** was added to 10 mL of water and enough methanol added to solubilize the material, which was then acidified to pH 2.2 with formic acid. The reaction was monitored by LCMS until complete, around 8 hours. The solution was placed under a stream of air to remove some formic acid and methanol, then frozen and lyophilized affording **13-18**.

Acetyl-oxa(dethia)-pantetheine (**13**):

9 (500 mg, 1.45 mmol) was used as starting material to afford **11** (white powder, 435 mg, 1.43 mmol 98%).

¹H NMR (500 MHz, D₂O) δ 8.35 (s, 2H), 4.05 (t, *J* = 5.3 Hz, 2H), 3.87 (s, 1H), 3.47 – 3.36 (m, 5H), 3.27 (d, *J* = 11.3 Hz, 1H), 2.39 (t, *J* = 6.5 Hz, 2H), 1.99 (s, 3H), 0.79 (d, *J* = 17.7 Hz, 6H). **¹³C NMR** (126 MHz, D₂O) δ 175.06, 174.26, 174.09, 170.94, 75.73, 68.36, 63.42, 38.58, 38.23, 35.40, 35.24, 20.49, 20.35, 19.07. LRMS (ESI) *m/z* calculated for C₁₃H₂₄N₂O₆ ([M+H]⁺) 305.34, found 305.0.

Acetyl-aza(dethia)-pantetheine (**14**):

10 (500 mg, 1.46 mmol) was used as starting material to afford **14** (white crystals, 428 mg, 1.41 mmol 97%).

¹H NMR (500 MHz, D₂O) δ 8.17 (s, 0H), 3.84 (s, 1H), 3.43 – 3.30 (m, 3H), 3.28 – 3.19 (m, 2H), 3.16 (s, 4H), 3.07 (q, *J* = 7.3 Hz, 4H), 2.35 (t, *J* = 6.6 Hz, 2H), 1.85 (s, 3H), 1.15 (t, *J* = 7.3 Hz, 6H), 0.85 (d, *J* = 12.7 Hz, 1H), 0.78 (s, 3H), 0.75 (s, 3H). **¹³C NMR** (126 MHz, D₂O) δ 175.02,

174.24, 174.03, 119.84, 117.52, 115.20, 75.73, 68.33, 46.62, 38.63, 38.59, 35.40, 35.27, 21.89, 20.47, 19.09. LRMS (ESI) m/z calculated for $C_{13}H_{25}N_3O_5$ ($[M+H]^+$) 304.36, found 304.0.

Malonyl-oxa(dethia)-pantetheine (15):

11 (111.5 mg, 0.29 mmol) was used as starting material to afford **15** (white powder, 95.5 mg, 0.27 mmol 93%).

1H NMR (500 MHz, D_2O) δ 3.86 (d, J = 3.5 Hz, 1H), 3.53 (m, J = 6.3, 5.5, 0.9 Hz, 2H), 3.50 – 3.29 (m, 4H), 3.29 – 3.25 (m, 1H), 2.40 (t, J = 6.5 Hz, 2H), 0.80 (d, J = 2.7 Hz, 4H), 0.77 (d, J = 2.4 Hz, 4H). **^{13}C NMR** (126 MHz, D_2O) δ 176.16, 175.12, 174.15, 172.35, 75.73, 68.32, 59.85, 38.54, 35.69, 35.42, 20.43, 19.02. MS (ESI) m/z calculated for $C_{14}H_{24}N_2O_8$ ($[M-H]^-$) 347.35, found 347.0.

Malonyl-aza(dethia)-pantetheine (16):

12 (108.6 mg, 0.29 mmol) was used as starting material to afford **16** (oil, 94.5 mg, 0.27 mmol 97%).

1H NMR (500 MHz, D_2O) δ 3.89 (s, 1H), 3.46 – 3.35 (m, 3H), 3.32 – 3.15 (m, 7H), 2.40 (t, J = 6.5 Hz, 2H), 0.82 (s, 3H), 0.79 (s, 3H). **^{13}C NMR** (126 MHz, D_2O) δ 175.18, 175.10, 174.18, 171.08, 75.77, 68.36, 45.24, 38.68, 38.64, 38.59, 35.46, 35.34, 20.53, 19.11. MS (ESI) m/z calculated for $C_{16}H_{28}N_2O_6$ ($[M-H]^-$) 346.37, found 346.0.

oxa(dethia)-pantetheine (17):

7 (111.5 mg, 0.29 mmol) was used as starting material to afford **13** (oil, 95.5 mg, 0.27 mmol 95.5%).

1H NMR (500 MHz, D_2O) δ 3.86 (d, J = 3.5 Hz, 1H), 3.53 (m, J = 6.3, 5.5, 0.9 Hz, 2H), 3.50 – 3.29 (m, 4H), 3.29 – 3.25 (m, 1H), 2.40 (t, J = 6.5 Hz, 2H), 0.80 (d, J = 2.7 Hz, 4H), 0.77 (d, J = 2.4 Hz, 4H). **^{13}C NMR** (126 MHz, D_2O) δ 176.16, 175.12, 174.15, 172.35, 75.73, 68.32, 59.85, 38.54, 35.69, 35.42, 20.43, 19.02. MS (ESI) m/z calculated for $C_{14}H_{24}N_2O_8$ ($[M-H]^-$) 347.35, found 347.0.

aza(dethia)-pantetheine (18):

8 (108.6 mg, 0.29 mmol) was used as starting material to afford **14** (oil, 94.5 mg, 0.27 mmol 97%).

¹H NMR (500 MHz, D₂O) δ 3.89 (s, 1H), 3.46 – 3.35 (m, 3H), 3.32 – 3.15 (m, 7H), 2.40 (t, J = 6.5 Hz, 2H), 0.82 (s, 3H), 0.79 (s, 3H). **¹³C NMR** (126 MHz, D₂O) δ 175.18, 175.10, 174.18, 171.08, 75.77, 68.36, 45.24, 38.68, 38.64, 38.59, 35.46, 35.34, 20.53, 19.11. MS (ESI) *m/z* calculated for C₁₆H₂₈N₂O₆ ([M-H]⁻) 346.37, found 346.0.

Boc-aza(dethia)-pantetheine (21):

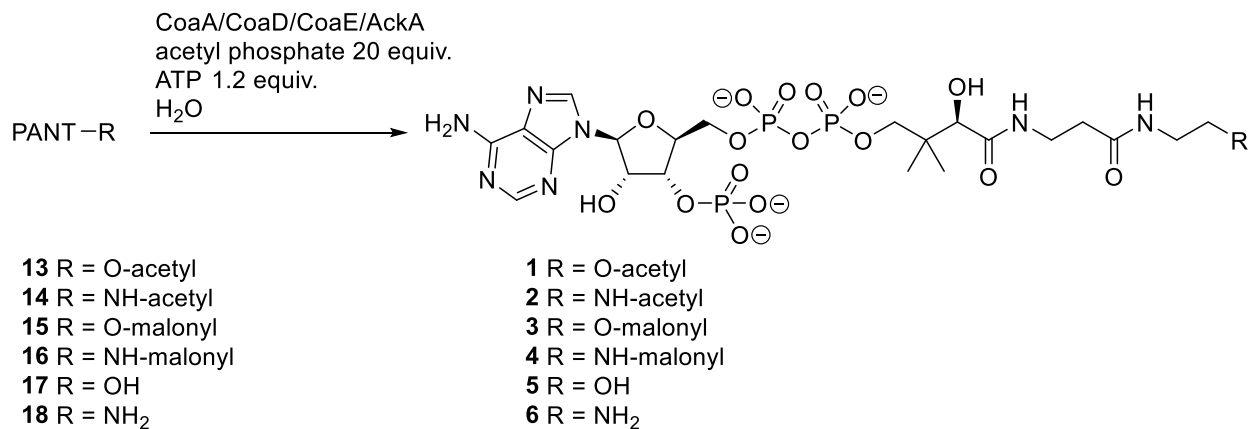
19 (81 mg, 0.20 mmol) was reacted according to the general procedure above affording **21** (white powder, 49 mg, 0.14 mmol 67.2 %).

¹H NMR (500 MHz, D₂O) δ 3.80 (s, 1H), 3.38 – 3.28 (m, 3H), 3.20 (d, J = 11.2 Hz, 1H), 3.08 (dd, J = 6.7, 4.9 Hz, 2H), 3.00 (dd, J = 6.7, 4.8 Hz, 2H), 2.30 (t, J = 6.6 Hz, 2H), 1.24 (s, 9H), 0.72 (d, J = 18.1 Hz, 6H). **¹³C NMR** (126 MHz, D₂O) δ 175.04, 173.99, 158.13, 80.87, 75.62, 68.23, 39.14, 38.49, 35.40, 35.29, 27.56, 20.39, 18.95, 12.70. MS (ESI) *m/z* calculated for C₁₆H₃₁N₃O₆ ([M+H]⁺) 362.23, found 362.2.

Azido(dethia)-pantetheine (22):

Pantothenic acid acetonide (149 mg, 0.46 mmol) was reacted according to the general procedure above affording **20** (white powder, 114 mg, 0.40 mmol 87.2%).

¹H NMR (500 MHz, D₂O) δ 3.89 (s, 1H), 3.50 – 3.37 (m, 3H), 3.37 – 3.27 (m, 5H), 2.43 (t, J = 6.5 Hz, 2H), 0.82 (d, J = 17.3 Hz, 6H). **¹³C NMR** (126 MHz, D₂O) δ 175.12, 174.22, 75.72, 75.48, 68.32, 49.90, 38.65, 38.55, 35.33, 35.20, 20.42, 19.01. MS (ESI) *m/z* calculated for C₁₁H₂₁N₅O₄ ([M+H]⁺) 288.17, found 288.2.



Chemoenzymatic preparation of 1-8:

General procedure

A solution containing 100 mM Triethanolamine (pH 7.5), 10 mM MgCl₂, 50 mM NaCl, 100 mM acetyl-phosphate, and 6 mM ATP was used to dissolve the **13-18** at a final concentration of 5.5 mM, between 20-100 mL total. Then CoaA and AckA were added to final concentrations of 2.7 μ M and 1 μ M respectively, and the reaction allowed to mix at room temperature for 1 hours. Then CoaD and CoaE were added to a final concentration of 5.6 μ M and 13.1 μ M, respectively, and allowed to mix at room temperature overnight. The reaction was quenched with by dropwise addition of 50% TFA to a final pH of 2.2, precipitating the protein out of solution, which was removed by centrifugation (4500 RPM at room temperature for 10 minutes), followed by passage through a 0.2 μ m syringe filter. Reverse phase HPLC (C18) was used to purify the final products using isocratic 0.1% TFA in water for 0-10 minutes, followed by 0 \rightarrow 15% gradient of 0.1% TFA in water \rightarrow ACN from 10-45 minutes. Pure fractions were pooled and lyophilized.

Acetyl-oxa(dethia)-CoA (**1**):

13 (200 mg, 0.25 mmol) was used as starting material to afford **1** (off white powder, 492 mg, 0.62 mmol 94%).

¹H NMR (500 MHz, D₂O) δ 8.41 (s, 1H), 8.10 (s, 1H), 6.04 (d, J = 6.5 Hz, 1H), 4.71 (d, 1H), 4.46 (q, J = 2.7 Hz, 1H), 4.13 (m, 2H), 3.99 (t, J = 5.2 Hz, 2H), 3.87 (s, 1H), 3.70 (m, 1H), 3.43 (m, 1H), 3.32 (m, 4H), 2.37 – 2.26 (m, 3H), 1.94 (s, 3H), 0.74 (s, 3H), 0.61 (s, 3H). **¹³C NMR** (126 MHz, D₂O) δ 174.68, 174.23, 174.06, 155.53, 152.86, 149.25, 139.82, 118.48, 86.52, 83.90, 74.16, 74.05, 73.47, 71.85, 65.64, 63.34, 61.26, 59.41, 38.25, 38.17, 35.36, 35.26, 20.74, 20.30, 18.02. MS (ESI) m/z calculated for C₂₃H₃₈N₇O₁₈P₃ ([M-H]⁻) 792.14, found 792.1.

Acetyl-aza(dethia)-CoA (**2**):

14 (200 mg, 0.25 mmol) was used as starting material to afford **2** (off white powder, 484 mg, 0.61 mmol 92%).

¹H NMR (500 MHz, D₂O) δ 8.58 – 8.51 (m, 1H), 8.34 (s, 1H), 6.12 (dd, J = 5.7, 2.1 Hz, 1H), 4.84 – 4.77 (m, 2H), 4.53 – 4.49 (m, 1H), 4.18 (d, J = 7.9 Hz, 1H), 3.98 (d, J = 7.5 Hz, 1H), 3.92 (dd, J = 2.0, 1.0 Hz, 1H), 3.82 – 3.75 (m, 1H), 3.62 (dt, J = 2.1, 1.1 Hz, 5H), 3.58 – 3.52 (m, 1H), 3.41 – 3.35 (m, 2H), 3.32 (dt, J = 10.8, 3.2 Hz, 1H), 3.30 – 3.11 (m, 8H), 3.11 – 3.05 (m, 1H), 2.62 – 2.53

(m, 1H), 2.36 (td, J = 6.8, 6.4, 2.1 Hz, 2H), 2.16 – 2.07 (m, 1H), 1.99 (ddt, J = 14.9, 2.0, 1.0 Hz, 1H), 1.90 – 1.82 (m, 6H), 1.25 – 1.03 (m, 5H), 0.97 (dddd, J = 8.2, 7.2, 2.0, 1.0 Hz, 1H), 0.88 – 0.82 (m, 3H), 0.74 (d, J = 2.2 Hz, 3H). **¹³C NMR** (126 MHz, D₂O) δ 174.72, 174.40, 174.17, 163.06, 162.78, 158.92, 149.86, 148.47, 144.69, 142.48, 118.54, 117.44, 115.12, 87.51, 83.37, 74.22, 73.84, 72.04, 65.12, 61.76, 61.42, 59.30, 46.65, 44.49, 44.37, 39.59, 39.14, 38.67, 38.59, 38.30, 37.15, 35.43, 35.36, 25.77, 22.08, 21.85, 21.81, 21.54, 20.75, 18.29, 13.79, 12.62, 11.63, 8.20. MS (ESI) m/z calculated for C₂₃H₃₉N₈O₁₇P₃ ([M-H]⁻) 791.15, found 791.1.

Malonyl-oxa(dethia)-CoA (3):

15 (50 mg, 0.14 mmol) was used as starting material to afford **3** (off white powder, 112 mg, 0.13 mmol 93%).

¹H NMR (500 MHz, D₂O) δ 8.58 (s, 3H), 8.34 (s, 3H), 6.12 (d, J = 5.5 Hz, 3H), 4.78 (s, 6H), 4.51 (s, 2H), 4.17 (s, 4H), 4.13 (t, J = 5.0 Hz, 2H), 3.93 (d, J = 2.0 Hz, 3H), 3.77 (dd, J = 10.1, 4.4 Hz, 3H), 3.62 (s, 10H), 3.56 – 3.48 (m, 9H), 3.38 (q, J = 4.7, 3.0 Hz, 8H), 3.19 (t, J = 5.5 Hz, 6H), 2.62 – 2.52 (m, 2H), 2.38 (q, J = 8.3, 7.5 Hz, 7H), 2.16 – 2.07 (m, 2H), 0.84 (s, 9H), 0.73 (s, 9H). **¹³C NMR** (126 MHz, D₂O) δ 174.76, 174.18, 171.52, 144.72, 142.49, 87.44, 74.18, 73.97, 71.88, 61.41, 59.85, 59.28, 41.43, 38.28, 35.44, 35.35, 20.82, 18.18. MS (ESI) m/z calculated for C₂₄H₃₈N₇O₂₀P₃ ([M-H]⁻) 836.14, found 836.1.

Malonyl-aza(dethia)-CoA (4):

16 (49 mg, 0.14 mmol) was used as starting material to afford **4**.

¹H NMR (500 MHz, D₂O) δ 8.51 – 8.47 (m, 1H), 8.31 – 8.27 (m, 1H), 6.06 (dt, J = 6.0, 1.0 Hz, 1H), 4.83 – 4.71 (m, 2H), 4.48 (s, 1H), 4.15 (p, J = 14.3, 13.1 Hz, 2H), 3.90 – 3.85 (m, 1H), 3.84 – 3.73 (m, 2H), 3.53 (dd, J = 9.8, 4.4 Hz, 1H), 3.37 – 3.28 (m, 3H), 3.27 – 3.19 (m, 1H), 3.20 (d, J = 4.5 Hz, 1H), 3.21 – 3.13 (m, 3H), 2.32 (t, J = 6.6 Hz, 2H), 0.81 (s, 3H), 0.73 – 0.69 (s, 3H). **¹³C NMR** (126 MHz, D₂O) δ 174.67, 174.16, 171.57, 168.94, 149.73, 148.36, 144.71, 142.38, 118.39, 87.45, 83.20, 74.34, 74.30, 74.19, 73.78, 73.74, 72.14, 72.09, 65.13, 55.23, 54.94, 41.89, 38.72, 38.43, 38.34, 38.28, 35.39, 35.31, 20.68, 18.30. MS (ESI) m/z calculated for C₂₄H₃₉N₈O₁₉P₃ ([M-H]⁻) 835.14, found 835.1.

Oxa(dethia)-CoA (5):

15 (18 mg, 0.14 mmol) was used as starting material to afford **3** (off white powder, 112 mg, 0.13 mmol 93%).

¹H NMR (500 MHz, D₂O) δ 8.58 (s, 3H), 8.34 (s, 3H), 6.12 (d, J = 5.5 Hz, 3H), 4.78 (s, 6H), 4.51 (s, 2H), 4.17 (s, 4H), 4.13 (t, J = 5.0 Hz, 2H), 3.93 (d, J = 2.0 Hz, 3H), 3.77 (dd, J = 10.1, 4.4 Hz, 3H), 3.62 (s, 10H), 3.56 – 3.48 (m, 9H), 3.38 (q, J = 4.7, 3.0 Hz, 8H), 3.19 (t, J = 5.5 Hz, 6H), 2.62 – 2.52 (m, 2H), 2.38 (q, J = 8.3, 7.5 Hz, 7H), 2.16 – 2.07 (m, 2H), 0.84 (s, 9H), 0.73 (s, 9H). **¹³C NMR** (126 MHz, D₂O) δ 174.76, 174.18, 171.52, 144.72, 142.49, 87.44, 74.18, 73.97, 71.88, 61.41, 59.85, 59.28, 41.43, 38.28, 35.44, 35.35, 20.82, 18.18. MS (ESI) m/z calculated for C₂₁H₃₆N₇O₁₇P₃ ([M-H]⁻) 750.14, found 750.0.

Aza(dethia)-CoA (6):

16 (50 mg, 0.14 mmol) was used as starting material to afford **4** (off white powder, 108.5 mg, 0.13 mmol 90%).

¹H NMR (500 MHz, D₂O) δ 8.39 (s, 1H), 8.10 (dd, J = 10.8, 0.7 Hz, 1H), 6.00 (dd, J = 20.1, 6.3 Hz, 1H), 4.46 – 4.41 (m, 1H), 4.11 – 4.05 (m, 2H), 3.85 (s, 1H), 3.69 – 3.60 (m, 2H), 3.59 (s, 6H), 3.58 – 3.52 (m, 1H), 3.39 (dd, J = 9.8, 5.0 Hz, 1H), 3.35 – 3.24 (m, 3H), 3.23 – 3.09 (m, 5H), 3.09 – 2.96 (m, 3H), 2.38 – 2.21 (m, 4H), 2.02 – 1.93 (m, 1H), 1.23 – 1.05 (m, 6H), 0.72 (d, J = 9.6 Hz, 3H), 0.61 (d, J = 29.7 Hz, 3H). **¹³C NMR** (126 MHz, D₂O) δ 175.15, 174.63, 174.05, 171.49, 155.54, 152.84, 149.30, 139.83, 118.54, 86.47, 74.06, 73.70, 71.82, 65.60, 61.31, 59.31, 54.28, 46.52, 45.19, 42.48, 38.59, 38.51, 38.22, 38.16, 35.37, 35.30, 28.68, 20.74, 18.49, 17.96, 17.69, 16.23, 12.10, 8.18. MS (ESI) m/z calculated for C₂₄H₃₉N₈O₁₉P₃ ([M-H]⁻) 749.14, found 749.1.

4.4 Cloning and mutagenesis of FabH and AckA from *Escherichia coli*

A modified pRSF-Duet1 vector with a Gibson cloning site was used, which leads to the overexpression of proteins with an N-terminal sequence of MGSSHHHHHHSGSENLYFQ, which is cleaved by TEV protease and will be referred to as pRSF-TEV/GIB. Briefly, pRSF-TEV/GIB was digested with BseRI and purified by gel electrophoresis, mixed with with PCR fragments described below, and treated with Gibson Assembly Master Mix (New England Biolabs). The assembled vector were cloned into *E. coli* DH5 α , and the resulting isolated plasmid sequences confirmed by sequencing. The *ackA* and *fabH* genes were amplified by PCR from *E. coli* DH5 α

genomic DNA (or from plasmids containing the genes) using the following primers (overlapping regions with pRSF-TEV/GIB underlined, extra codons are in bold):

AckA-forward: 5'-GAGAACCTCTACTTCCAA **AG**TTCGAGTAAGTTAGTACTGG-3'

AckA-reverse: 5'-CTCGAGGAGATTACGGATTATCAGGCAGTCAGGCGGCTC-3'

FabH-forward: 5'- GAGAACCTCTACTTCCAA**AG**TATGTATACGAAGATTATTGGTAC-3',

FabH+GG-forward:

5'-GAGAACCTCTACTTCCAA**AGTGGTGGT**CAATTTGCATTTGTGTTCC-3',

FabH-reverse: 5'-CTCGAGGAGATTACGGATT**AG**AAACGAACCAGCGCGGAGCCC-3',

Plasmids containing the appropriate genes were isolated and confirmed by DNA sequencing, yielding expression plasmids for AckA (pRSF-TEV/GIB-*ackA*), FabH (pRSF-TEV/GIB-*fabH*), and FabH+GG (pRSF-TEV/GIB-GG*fabH*). Extra N-terminal glycines were added to FabH in order to yield protein that was cleavable by TEV protease. Expression plasmids for CoaA/D/E were previously described.

The mutant FabH+GG C112Q was generated by PCR mutagenesis with the following primers:

FabH-C112Q forward: 5'-GGCTGCTGCAACGTCAAATG-3',

FabH-C112X reverse: 5'-GCAGCAGCCcagGCAGGTTTCAC-3',

The PCR product was treated with polynucleotide kinase, T4 DNA ligase and transformed into *E. coli* DH5 α . Plasmids containing were isolated and the mutation confirmed by DNA sequencing, yielding expression plasmid for FabH+GG C112Q (pRSF-TEV/GIB-GG*fabHC112Q*).

4.5 Enzyme expression and purification

Expression plasmids for FabH, FabH C112Q, and AckA were transformed into *E. coli* BL21 (DE3), and the resultant recombinant strains were grown overnight in 50 mL of LB and 50 μ g/mL kanamycin. A 5 mL aliquot of the overnight culture was used to inoculate 1 L of TB containing 10 mM MgCl₂ and 50 μ g/mL kanamycin, which was incubated at 37 °C while being shaken at 180 rpm. Once the OD₆₀₀ reached 1.0, the temperature was reduced to 18 °C. Once the cultures reached thermal equilibrium, gene expression was induced by the addition of isopropyl β -

D-thiogalactopyranoside with a final concentration of 0.5 mM, with incubation for an additional 18 hours. *E. coli* cells were harvested by centrifugation at 6000 rpm at 4 °C for 10 min.

E. coli cell pellets, carrying FabH, FabH C112Q, and AckA were re-suspended in lysis buffer [2 µg/mL DNase, 1 µg/mL lysozyme, 300 mM NaCl, 20 mM imidazole, 10% glycerol, and 20 mM Tris-HCl (pH 8.0)], sonicated (60 × 1 s on ice), and clarified by centrifugation at 11000 rpm at 4 °C for 30 min. The supernatant was passed through a 0.45 µm filter, applied to a 5 mL HisTrap HP column (GE Healthcare), and washed with lysis buffer using an Äkta pure fast-performance liquid chromatography system (GE Healthcare). Wash buffer [300 mM NaCl, 40 mM imidazole and 20 mM Tris-HCl (pH 8.0)] was used to remove additional contaminants, and proteins were eluted with wash buffer containing 500 mM imidazole. At this point the purity of FabH, FabH C112Q, and AckA from the fractions was analyzed by sodium dodecyl sulfate–polyacrylamide gel electrophoresis (SDS–PAGE). Pure fractions were pooled and cleaved using TEV protease to remove the hexahistidine tag except for AckA. All three were then buffer-exchanged into 20 mM Tris-HCl (pH 8.0), 200 mM NaCl, and 1 mM DTT, concentrated, and frozen in small aliquots on liquid nitrogen followed by stored at –80 °C.

4.6 FabH enzymatic assay procedures

The stability or activity assays (containing either acetyl-CoA or malonyl-CoA exclusively) were performed in a 1 ml reaction mixture which contained 100 mM bis-tris propane buffer at pH 8.0, 10 mM MgCl₂, 10 µM enzyme (FabH or FabH C112Q), and 250 µM of **1-4** (stability assays) or acetyl-CoA/malonyl-CoA (activity assays). Reaction mixtures were incubated at 25 °C, 100 µL aliquots taken at times 0 min, 1 min, 1 hour, 3 hours, 6 hours, 12 hours, and 24 hours (only 0 min and 24 hour time points were used for stability assays of **1-4**), quenched by rapid mixing in 50 µL of 25% FA (v/v) to precipitate the protein. Centrifugation at 13000 rpm at 25 °C for 2 minutes was used to pellet the protein and the supernatant was analyzed via the procedure outlined below.

General procedure for interpretation of HPLC stability and activity assays. Acyl-CoA, CoA, and **1-6** were identified using HPLC with detection at 254 nm over a 250 x 4.6 mm C18(2) column. The analytes were separated with a 2 → 25% gradient of 0.1% TFA in water → ACN over 20 min. Peak areas of assays containing **1-6**, malonyl-CoA, acetyl-CoA, and CoA were integrated, concentration determined, and plotted over time using KaleidaGraph (Synergy Software).

E. coli FabH kinetic parameters were determined using a continuous spectroscopic UV-vis assay. All assays were performed using an Agilent Cary 100 UV-vis spectrophotometer in a semimicro quartz cuvette (Starna Cells). 100 mM bis-tris propane:HCl (pH 8.0), 50 mM MgCl₂, 10 mM KCl, 5 mM tris(2-carboxylethyl)phosphine (TCEP), 50 mM NaCl, 50 μM acetyl-CoA, 50 μM malonyl-CoA, and 1 μM FabH. Inhibition assays added 0 or 150 μM inhibitor (300 μM inhibitor was used in lieu of 150 μM for malonyl-CoA analogs). All reactions were conducted at 25°C for 10 minutes. Reactions were initiated by addition of malonyl-CoA followed by 10 second rapid mixing via pipette, then quickly closing the instrument door to collect data and set a baseline. Production of acetoacetyl-CoA enol by FabH was monitored at 302 nm (calculated $\epsilon_{302} = 17.7 \text{ mM}^{-1} \cdot \text{cm}^{-1}$). All reactions were conducted in triplicate.

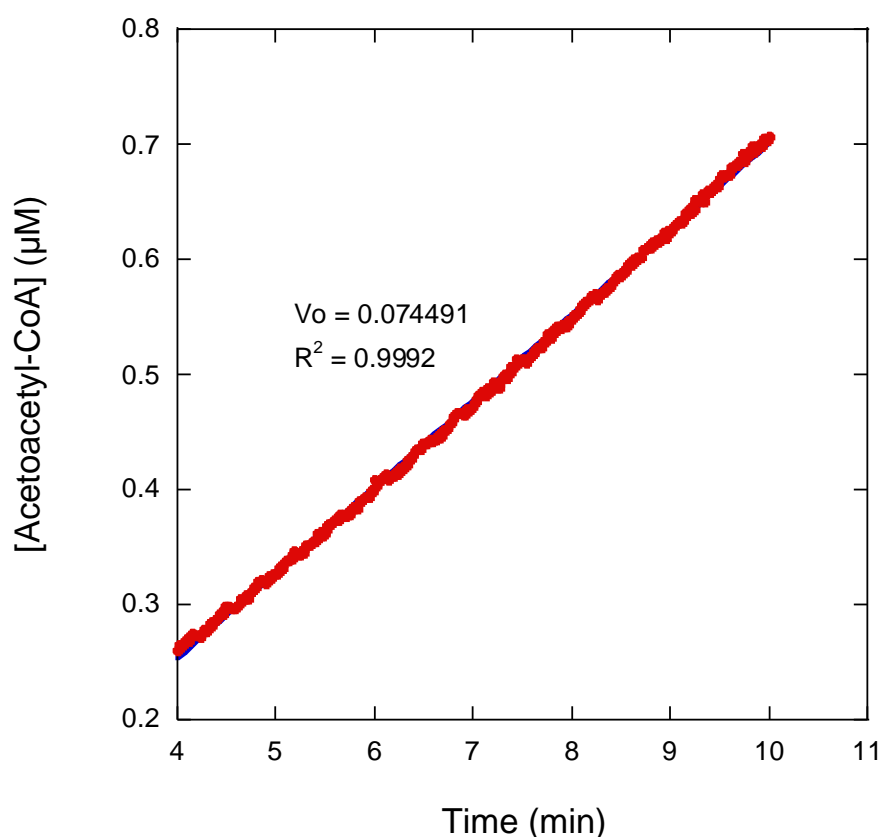


Figure 4.5 Representative plot, fitting, and determination of initial rates of FabH with varying malonyl-CoA and acetyl-CoA concentrations. [E] = 0.5 μM, [acetyl-CoA] = 15 μM, [malonyl-CoA] = 125 μM.

4.7 References

- [1] Mishra, P. K., and Drueckhammer, D. G. (2000) Coenzyme A Analogues and Derivatives: Synthesis and Applications as Mechanistic Probes of Coenzyme A Ester-Utilizing Enzymes, *Chemical reviews* 100, 3283-3310.
- [2] Kulkarni, R. A., Worth, A. J., Zengeya, T. T., Shrimp, J. H., Garlick, J. M., Roberts, A. M., Montgomery, D. C., Sourbier, C., Gibbs, B. K., Mesaros, C., Tsai, Y. C., Das, S., Chan, K. C., Zhou, M., Andresson, T., Weissman, A. M., Linehan, W. M., Blair, I. A., Snyder, N. W., and Meier, J. L. (2017) Discovering Targets of Non-enzymatic Acylation by Thioester Reactivity Profiling, *Cell Chem Biol* 24, 231-242.
- [3] Benning, M. M., Haller, T., Gerlt, J. A., and Holden, H. M. (2000) New reactions in the crotonase superfamily: structure of methylmalonyl CoA decarboxylase from *Escherichia coli*, *Biochemistry* 39, 4630-4639.
- [4] Ellis, B. D., Milligan, J. C., White, A. R., Duong, V., Altman, P. X., Mohammed, L. Y., Crump, M. P., Crosby, J., Luo, R., Vanderwal, C. D., and Tsai, S. C. (2018) An Oxetane-Based Polyketide Surrogate To Probe Substrate Binding in a Polyketide Synthase, *Journal of the American Chemical Society* 140, 4961-4964.
- [5] Mancía, F., Smith, G. A., and Evans, P. R. (1999) Crystal structure of substrate complexes of methylmalonyl-CoA mutase, *Biochemistry* 38, 7999-8005.
- [6] Tosin, M., Spiteller, D., and Spencer, J. B. (2009) Malonyl carba(dethia)- and malonyl oxa(dethia)-coenzyme A as tools for trapping polyketide intermediates, *Chembiochem : a European journal of chemical biology* 10, 1714-1723.
- [7] Tosin, M., Betancor, L., Stephens, E., Li, W. M., Spencer, J. B., and Leadlay, P. F. (2010) Synthetic chain terminators off-load intermediates from a type I polyketide synthase, *Chembiochem : a European journal of chemical biology* 11, 539-546.
- [8] Hamed, R. B., Henry, L., Gomez-Castellanos, J. R., Asghar, A., Brem, J., Claridge, T. D., and Schofield, C. J. (2013) Stereoselective preparation of lipidated carboxymethyl-proline/pipecolic acid derivatives via coupling of engineered crotonases with an alkylmalonyl-CoA synthetase, *Organic & biomolecular chemistry* 11, 8191-8196.
- [9] White, S. W., Zheng, J., Zhang, Y. M., and Rock. (2005) The structural biology of type II fatty acid biosynthesis, *Annual review of biochemistry* 74, 791-831.
- [10] Jackowski, S., and Rock, C. O. (1987) Acetoacetyl-acyl carrier protein synthase, a potential regulator of fatty acid biosynthesis in bacteria, *Journal of Biological Chemistry* 262, 7927-7931.
- [11] Jackowski, S., Murphy, C. M., Cronan, J. E., and Rock, C. O. (1989) Acetoacetyl-acyl carrier protein synthase: A target for the antibiotic thiolactomycin, *Journal of Biological Chemistry* 264, 7624-7629.
- [12] Price, A. C., Choi, K. H., Heath, R. J., Li, Z., White, S. W., and Rock, C. O. (2001) Inhibition of beta-ketoacyl-acyl carrier protein synthases by thiolactomycin and cerulenin. Structure and mechanism, *The Journal of biological chemistry* 276, 6551-6559.
- [13] Pérez-Castillo, Y., Froeyen, M., Nowé, A., and Cabrera-Pérez, M. Á. (2014) Bacterial FabH: Towards the Discovery of New Broad-Spectrum Antibiotics, 131-158.
- [14] Williamson, I. P., and Wakil, S. J. (1966) Studies on the Mechanism of Fatty Acid Synthesis: XVII. PREPARATION AND GENERAL PROPERTIES OF ACETYL COENZYME A AND MALONYL COENZYME A-ACYL CARRIER PROTEIN TRANSACYLASES, *Journal of Biological Chemistry* 241, 2326-2332.

- [15] Alberts, A. W., Majerus, P. W., Talamo, B., and Vagelos, P. R. (1964) Acyl-Carrier Protein. II. Intermediary Reactions of Fatty Acid Synthesis, *Biochemistry* 3, 1563-1571.
- [16] Tsay, J. T., Oh, W., Larson, T. J., Jackowski, S., and Rock, C. O. (1992) Isolation and characterization of the beta-ketoacyl-acyl carrier protein synthase III gene (fabH) from *Escherichia coli* K-12, *The Journal of biological chemistry* 267, 6807-6814.
- [17] Davies, C., Heath, R. J., White, S. W., and Rock, C. O. (2000) The 1.8 Å crystal structure and active-site architecture of β -ketoacyl-acyl carrier protein synthase III (FabH) from *Escherichia coli*, *Structure* 8, 185-195.
- [18] Witkowski, A., Joshi, A. K., Lindqvist, Y., and Smith, S. (1999) Conversion of a β -Ketoacyl Synthase to a Malonyl Decarboxylase by Replacement of the Active-Site Cysteine with Glutamine[†], *Biochemistry* 38, 11643-11650.
- [19] Alhamadsheh, M. M., Musayev, F., Komissarov, A. A., Sachdeva, S., Wright, H. T., Scarsdale, N., Florova, G., and Reynolds, K. A. (2007) Alkyl-CoA disulfides as inhibitors and mechanistic probes for FabH enzymes, *Chemistry & biology* 14, 513-524.
- [20] Stunkard, L. M., Dixon, A. D., Huth, T. J., and Lohman, J. R. (2019) Sulfonate/Nitro Bearing Methylmalonyl-Thioester Isosteres Applied to Methylmalonyl-CoA Decarboxylase Structure-Function Studies, *Journal of the American Chemical Society* 141, 5121-5124.
- [21] Meier, J. L., and Burkart, M. D. (2009) Chapter 9 Synthetic Probes for Polyketide and Nonribosomal Peptide Biosynthetic Enzymes, In *Complex Enzymes in Microbial Natural Product Biosynthesis, Part A: Overview Articles and Peptides*, pp 219-254.
- [22] Hou, J., Zheng, H., Tzou, W. S., Cooper, D. R., Chruszcz, M., Chordia, M. D., Kwon, K., Grabowski, M., and Minor, W. (2018) Differences in substrate specificity of *V. cholerae* FabH enzymes suggest new approaches for the development of novel antibiotics and biofuels, *The FEBS journal* 285, 2900-2921.
- [23] Sachdeva, S., Musayev, F. N., Alhamadsheh, M. M., Scarsdale, J. N., Wright, H. T., and Reynolds, K. A. (2008) Separate entrance and exit portals for ligand traffic in *Mycobacterium tuberculosis* FabH, *Chemistry & biology* 15, 402-412.
- [24] Zhang, Y. M., Rao, M. S., Heath, R. J., Price, A. C., Olson, A. J., Rock, C. O., and White, S. W. (2001) Identification and analysis of the acyl carrier protein (ACP) docking site on beta-ketoacyl-ACP synthase III, *The Journal of biological chemistry* 276, 8231-8238.
- [25] Ekstrom, A. G., Wang, J. T., Bella, J., and Campopiano, D. J. (2018) Non-invasive (19)F NMR analysis of a protein-templated N-acylhydrazone dynamic combinatorial library, *Organic & biomolecular chemistry* 16, 8144-8149.
- [26] Stern, J. R. (1956) OPTICAL PROPERTIES OF ACETOACETYL-X-COENZYME A AND ITS METAL CHELATES, *Journal of Biological Chemistry* 221, 33-44.
- [27] Heath, R. J., and Rock, C. O. (1996) Inhibition of beta-ketoacyl-acyl carrier protein synthase III (FabH) by acyl-acyl carrier protein in *Escherichia coli*, *The Journal of biological chemistry* 271, 10996-11000.
- [28] Khandekar, S. S., Konstantinidis, A. K., Silverman, C., Janson, C. A., McNulty, D. E., Nwagwu, S., Van Aller, G. S., Doyle, M. L., Kane, J. F., Qiu, X., and Lonsdale, J. (2000) Expression, purification, and crystallization of the *Escherichia coli* selenomethionyl beta-ketoacyl-acyl carrier protein synthase III, *Biochemical and biophysical research communications* 270, 100-107.
- [29] Amyes, T. L., and Richard, J. P. (2017) Substituent Effects on Carbon Acidity in Aqueous Solution and at Enzyme Active Sites, *Synlett* 28, 2407-2421.

- [30] Weeks, A. M., Wang, N., Pelton, J. G., and Chang, M. C. Y. (2018) Entropy drives selective fluorine recognition in the fluoroacetyl-CoA thioesterase from *Streptomyces cattleya*, *Proceedings of the National Academy of Sciences of the United States of America* 115, E2193-E2201.

CHAPTER 5. CONCLUDING REMARKS

5.1 Analogs of acyl-thioesters have broader implications in the study of enzymes that are not C-C bond forming

Returning to the initial ideas posited in the beginning of this thesis, the reader is reminded that acyl-CoA analogs have seen broad application toward a variety of enzymes, such as phosphotransacetylase, DpsC, MMCD, MCM, and MMCE¹⁻⁵. All of these enzymes perform completely different chemistry on similar acyl-thioester substrates. With a diverse panel of analogs in hand, we can probe the catalytic mechanism of any enzyme that has an acyl-thioester substrate, intermediate, or product. While C-C bond forming enzymes are critical in the incorporation of different extender units in PKS biosynthesis and extension of catenated chains in FAS, Figures 1.2 and 1.7 show that they are just once piece of a complicated puzzle. Other researchers in the PKS field have shown the importance of further understanding of the protein-protein interactions in modular PKS assembly lines for effective engineering of PKS products^{6, 7}. However, the major takeaway from this work is that our panel of tools is broadly applicable, and we have demonstrated proof of principle of their power in probing C-C bond forming enzyme catalysis.

In future work, we plan to expand the scope of our analog applicability by loading acyl-CoA analogs onto various ACPs, which are often greatly preferred enzyme substrates mimics over the corresponding acyl-CoAs⁸. As observed in the case of FabH in Chapter 4, malonyl-CoA (and its aza- / oxa-bearing analogs) bind to the enzyme with very low affinity compared to malonyl-ACP. Using the enzyme Sfp from *Bacillus subtilis*, we can load our analogs onto a variety of ACPs (*crypto*-ACPs), seen in Figure 5.1, appropriate for targeting many type I PKS and FAS enzymes in cryo-EM studies^{9, 10}. We have had challenges confirming the phosphopantetheinylation activity of Sfp on ACP, due to lack of a detection strategy for determine the amount of ACP labeled. Missing protein-protein interactions between the acyl-carrier protein and the ketosynthase, seen in our FabH kinetic studies allows for the inference of the importance of this interaction in enzyme-substrate affinity.

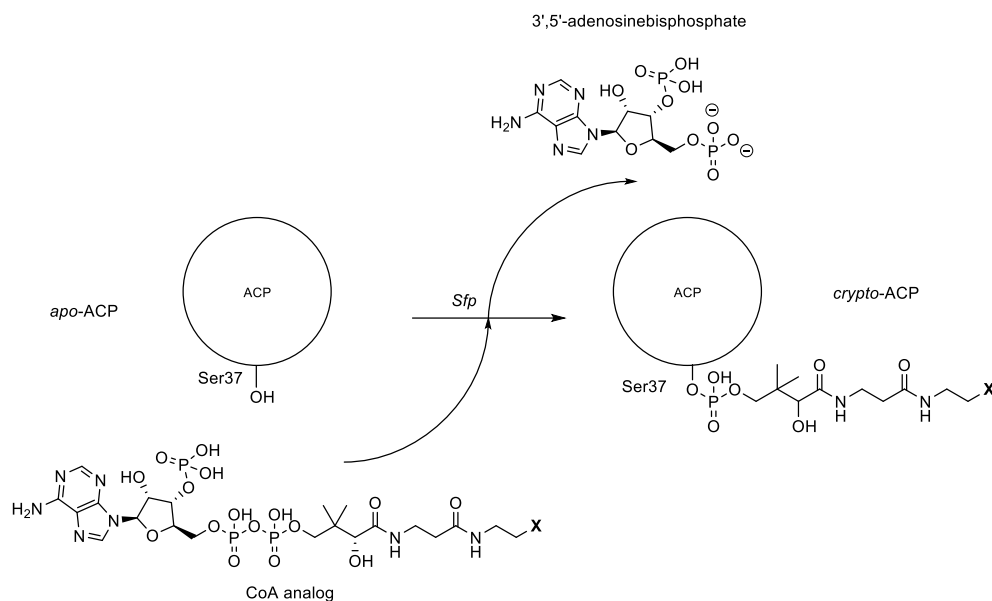


Figure 5.1 Preparation of *crypto*-ACPs from acyl-CoA analogs using Sfp catalysis.

A current interest of the lab is the synthesis and purification of diastereomers of acyl-CoAs and their analogs for kinetic and structure-functions studies. For example, the AT/DC enzyme LnmK will only accept (2*R*)-methylmalonyl-CoA as a substrate. Thus, within racemic mixtures of substrates and analogs, the enzyme will only bind half of the material, with the other half potentially affecting the activity of the enzyme in an unknown manner. We can exploit the activity and stereospecificity of different acyl-CoA synthesizing enzymes to producing stereochemically pure acyl-CoAs. PCCβ is known to only produce (2*S*)-methylmalonyl-CoA as a product, which is the only accepted substrate of various PKS. Similarly, MatB is known to only synthesize (2*R*)-methylmalonyl-CoA, the substrate of LnmK, Figure 5.2. The enzyme MMCE, which interconverts between the R/S absolute configurations of methylmalonyl-CoA could be assayed in a coupled enzyme assay with LnmK and (2*S*-¹⁴C)-methylmalonyl-CoA via NMR spectroscopy.

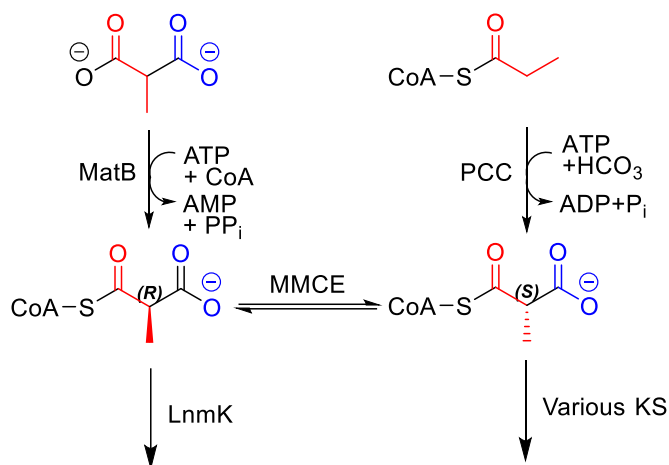


Figure 5.2 Proposed enzymatic synthesis of stereospecific methylmalonyl-CoA for kinetic characterization of LnmK and KS enzymes with stereochemical substrate preference.

5.2 Concluding remarks

In summary, we have developed a panel of new acyl-CoA analogs to be used as mechanistic probes for acyl-thioester enzyme catalysis. Additionally, we resynthesized and improved on the synthesis of several existing analogs and applied them for the first time as probes to a ketosynthase enzyme. We have also performed structure-function studies of these analogs with various carboxylase and ketosynthase enzymes using a combination of X-ray diffraction and cryo-EM experiments. This work outlines a general strategy of how one can synthesize various acyl-thioester analogs to kinetically and structurally characterize enzyme-ligand relationships in order to gain insight into catalytic mechanism. We also provide a stern reminder of the importance of critically analyzing structure-function studies with analogs to assess their relevance in the context of enzyme catalysis. Through mechanistic characterization of enzymes involved in the assembly line-like catalysis of PKS and FAS enzymes, we anticipate new insights into engineering these enzymes will be revealed from greater understanding of conformational changes, protein-protein interactions, and substrate orientation in the active site.

The implications of PKS engineering are great within the context of rapid derivatization of natural products, resulting in seemingly endless combinatorial variations of already successful pharmaceutical molecules. Thorough understanding of the protein-protein interactions between PKS components, conformational changes associated with catalysis, and substrate orientation can rationally guide PKS engineering. However, attempts at investigating these topics through

structure-function studies have been hampered by the reactivity of acyl-thioester and β -ketoacid substrates. In this thesis, we have synthesized a panel of acyl-CoA analogs to mimic substrates, products, and intermediates of PKS catalysis. Furthermore, we have determined inhibition constants of these analogs with a model KS (FabH) and conducted preliminary structure-function studies with these analogs and model C-C bond forming enzymes. Follow up work determining structure-function relationships of individual and complexed PKS enzymes can lead to mechanistic inferences, which will provide insight into rational engineering of PKS pathways. For example, determination of enzyme conformation and orientation of a malonyl-thioester in the binding pocket of a KS that accepts only malonyl-ACP may reveal a bulky residue (i.e. phenylalanine) sterically hindering entry of α -substituted malonyl-thioesters. Using this knowledge, if researchers wanted this KS to perform chemistry on a hydroxymalonyl-ACP substrate, incorporating a new hydroxyl group into the polyketide product, they could mutate phenylalanine into a smaller hydrophobic amino acid (i.e. valine), then test if the KS can accept the new substrate.

To emphasize the importance of this work further, the analogs synthesized in Chapters 2 and 4 of this thesis are not limited to studying C-C bond forming enzymes. As demonstrated in Chapter 1, acyl-CoA analogs have been kinetically characterized with many enzymes of all different classes. With the massive pool of enzymes estimated to use acyl-thioester substrates, the utility of acyl-thioester analogs as mechanistic probes in structure-functions studies is boundless. Future studies may gain insight from these structure-function studies to rationally engineer PKS and other enzymes to produce diverse libraries of natural product derivatives. These natural product derivatives will serve as important pharmaceutical leads in the future.

5.3 References

- [1] Ellis, B. D., Milligan, J. C., White, A. R., Duong, V., Altman, P. X., Mohammed, L. Y., Crump, M. P., Crosby, J., Luo, R., Vanderwal, C. D., and Tsai, S. C. (2018) An Oxetane-Based Polyketide Surrogate To Probe Substrate Binding in a Polyketide Synthase, *Journal of the American Chemical Society* 140, 4961-4964.
- [2] Stewart, C. J., and Miller, T. L. (1965) Oxy-coenzyme A: A competitive inhibitor of coenzyme A in the phosphotransacetylase reaction, *Biochemical and biophysical research communications* 20, 433-438.
- [3] Stunkard, L. M., Dixon, A. D., Huth, T. J., and Lohman, J. R. (2019) Sulfonate/Nitro Bearing Methylmalonyl-Thioester Isosteres Applied to Methylmalonyl-CoA Decarboxylase Structure-Function Studies, *Journal of the American Chemical Society* 141, 5121-5124.

- [4] Stunkard, L. M., Benjamin, A. B., Bower, J. B., Huth, T. J., and Lohman, J. R. (2022) Substrate Enolate Intermediate and Mimic Captured in the Active Site of *Streptomyces coelicolor* Methylmalonyl-CoA Epimerase, *Chembiochem : a European journal of chemical biology* 23, e202100487.
- [5] Hull, W. E., Michenfelder, M., and Retey, J. (1988) The error in the cryptic stereospecificity of methylmalonyl-CoA mutase. The use of carba-(dethia)-coenzyme A substrate analogues gives new insight into the enzyme mechanism, *European Journal of Biochemistry* 173, 191-201.
- [6] Khosla, C., Herschlag, D., Cane, D. E., and Walsh, C. T. (2014) Assembly line polyketide synthases: mechanistic insights and unsolved problems, *Biochemistry* 53, 2875-2883.
- [7] Wong, F. T., Chen, A. Y., Cane, D. E., and Khosla, C. (2010) Protein-protein recognition between acyltransferases and acyl carrier proteins in multimodular polyketide synthases, *Biochemistry* 49, 95-102.
- [8] Heath, R. J., and Rock, C. O. (1996) Inhibition of beta-ketoacyl-acyl carrier protein synthase III (FabH) by acyl-acyl carrier protein in *Escherichia coli*, *The Journal of biological chemistry* 271, 10996-11000.
- [9] Quadri, L. E., Weinreb, P. H., Lei, M., Nakano, M. M., Zuber, P., and Walsh, C. T. (1998) Characterization of Sfp, a *Bacillus subtilis* phosphopantetheinyl transferase for peptidyl carrier protein domains in peptide synthetases, *Biochemistry* 37, 1585-1595.
- [10] Mindrebo, J. T., Chen, A., Kim, W. E., Re, R. N., Davis, T. D., Noel, J. P., and Burkart, M. D. (2021) Structure and Mechanistic Analyses of the Gating Mechanism of Elongating Ketosynthases, *ACS Catalysis* 11, 6787-6799.